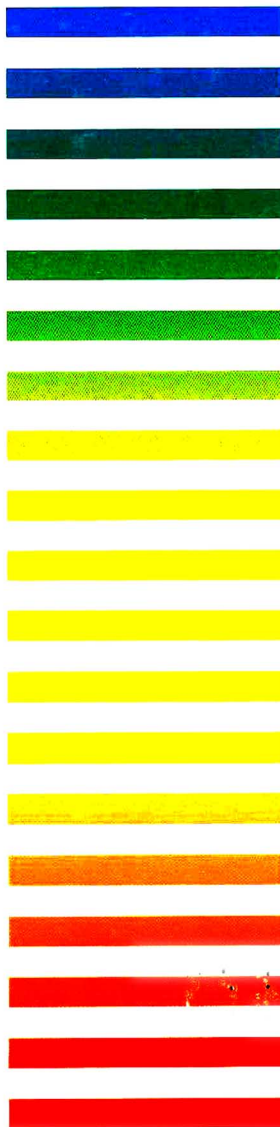




VOL. 647 NO. 2 SEPTEMBER 24, 1993

9th Montreux Symp. on LC-MS,
SFC-MS, CZE-MS and MS-MS
Montreux, November 4-6, 1992
Part II

JOURNAL OF
CHROMATOGRAPHY
INCLUDING ELECTROPHORESIS AND OTHER SEPARATION METHODS



SYMPOSIUM VOLUMES

EDITORS

E. Heftmann (Orinda, CA)
Z. Deyl (Prague)

EDITORIAL BOARD

E. Bayer (Tübingen)
S.R. Binder (Hercules, CA)
S.C. Churms (Rondebosch)
J.C. Fetzer (Richmond, CA)
E. Gelpi (Barcelona)
K.M. Gooding (Lafayette, IN)
S. Hara (Tokyo)
P. Helboe (Brønshøj)
W. Lindner (Graz)
T.M. Phillips (Washington, DC)
S. Terabe (Hyogo)
H.F. Walton (Boulder, CO)
M. Wilchek (Rehovot)

JOURNAL OF CHROMATOGRAPHY

INCLUDING ELECTROPHORESIS AND OTHER SEPARATION METHODS

Scope. The *Journal of Chromatography* publishes papers on all aspects of **chromatography, electrophoresis** and related methods. Contributions consist mainly of research papers dealing with chromatographic theory, instrumental developments and their applications. The section *Biomedical Applications*, which is under separate editorship, deals with the following aspects: developments in and applications of chromatographic and electrophoretic techniques related to clinical diagnosis or alterations during medical treatment; screening and profiling of body fluids or tissues related to the analysis of active substances and to metabolic disorders; drug level monitoring and pharmacokinetic studies; clinical toxicology; forensic medicine; veterinary medicine; occupational medicine; results from basic medical research with direct consequences in clinical practice. In *Symposium volumes*, which are under separate editorship, proceedings of symposia on chromatography, electrophoresis and related methods are published.

Submission of Papers. The preferred medium of submission is on disk with accompanying manuscript (see *Electronic manuscripts* in the Instructions to Authors, which can be obtained from the publisher, Elsevier Science Publishers B.V., P.O. Box 330, 1000 AH Amsterdam, Netherlands). Manuscripts (in English; four copies are required) should be submitted to: Editorial Office of *Journal of Chromatography*, P.O. Box 681, 1000 AR Amsterdam, Netherlands, Telefax (+31-20) 5862 304, or to: The Editor of *Journal of Chromatography, Biomedical Applications*, P.O. Box 681, 1000 AR Amsterdam, Netherlands. Review articles are invited or proposed in writing to the Editors who welcome suggestions for subjects. An outline of the proposed review should first be forwarded to the Editors for preliminary discussion prior to preparation. Submission of an article is understood to imply that the article is original and unpublished and is not being considered for publication elsewhere. For copyright regulations, see below.

Publication. The *Journal of Chromatography* (incl. *Biomedical Applications*) has 40 volumes in 1993. The subscription prices for 1993 are:

J. Chromatogr. (incl. *Cum. Indexes, Vols. 601-650*) + *Biomed. Appl.* (Vols. 612-651):
Dfl. 8520.00 plus Dfl. 1320.00 (p.p.h.) (total ca. US\$ 5466.75)

J. Chromatogr. (incl. *Cum Indexes, Vols. 601-650*) only (Vols. 623-651):
Dfl. 7047.00 plus Dfl. 957.00 (p.p.h.) (total ca. US\$ 4446.75)

Biomed. Appl. only (Vols. 612-622):
Dfl. 2783.00 plus Dfl. 363.00 (p.p.h.) (total ca. US\$ 1747.75).

Subscription Orders. The Dutch guilder price is definitive. The US\$ price is subject to exchange-rate fluctuations and is given as a guide. Subscriptions are accepted on a prepaid basis only, unless different terms have been previously agreed upon. Subscriptions orders can be entered only by calendar year (Jan.-Dec.) and should be sent to Elsevier Science Publishers, Journal Department, P.O. Box 211, 1000 AE Amsterdam, Netherlands, Tel. (+31-20) 5803 642, Telefax (+31-20) 5803 598, or to your usual subscription agent. Postage and handling charges include surface delivery except to the following countries where air delivery via SAL (Surface Air Lift) mail is ensured: Argentina, Australia, Brazil, Canada, China, Hong Kong, India, Israel, Japan*, Malaysia, Mexico, New Zealand, Pakistan, Singapore, South Africa, South Korea, Taiwan, Thailand, USA. *For Japan air delivery (SAL) requires 25% additional charge of the normal postage and handling charge. For all other countries airmail rates are available upon request. Claims for missing issues must be made within six months of our publication (mailing) date, otherwise such claims cannot be honoured free of charge. Back volumes of the *Journal of Chromatography* (Vols. 1-611) are available at Dfl. 230.00 (plus postage). Customers in the USA and Canada wishing information on this and other Elsevier journals, please contact Journal Information Center, Elsevier Science Publishing Co. Inc., 655 Avenue of the Americas, New York, NY 10010, USA, Tel. (+1-212) 633 3750, Telefax (+1-212) 633 3764.

Abstracts/Contents Lists published in Analytical Abstracts, Biochemical Abstracts, Biological Abstracts, Chemical Abstracts, Chemical Titles, Chromatography Abstracts, Current Awareness in Biological Sciences (CABS), Current Contents/Life Sciences, Current Contents/Physical, Chemical & Earth Sciences, Deep-Sea Research/Part B: Oceanographic Literature Review, Excerpta Medica, Index Medicus, Mass Spectrometry Bulletin, PASCAL-CNRS, Referativnyi Zhurnal, Research Alert and Science Citation Index.

US Mailing Notice. *Journal of Chromatography* (ISSN 0021-9673) is published weekly (total 52 issues) by Elsevier Science Publishers (Sara Burgerhartstraat 25, P.O. Box 211, 1000 AE Amsterdam, Netherlands). Annual subscription price in the USA US\$ 4446.75 (subject to change), including air speed delivery. Second class postage paid at Jamaica, NY 11431. **USA**

POSTMASTERS: Send address changes to *Journal of Chromatography*, Publications Expediting, Inc., 200 Meacham Avenue, Elmont, NY 11003. Airfreight and mailing in the USA by Publications Expediting.

See inside back cover for Publication Schedule, Information for Authors and information on Advertisements.

© 1993 ELSEVIER SCIENCE PUBLISHERS B.V. All rights reserved.

0021-9673/93/\$06.00

No part of this publication may be reproduced, stored in a retrieval system or transmitted in any form or by any means, electronic, mechanical, photocopying, recording or otherwise, without the prior written permission of the publisher, Elsevier Science Publishers B.V., Copyright and Permissions Department, P.O. Box 521, 1000 AM Amsterdam, Netherlands.

Upon acceptance of an article by the journal, the author(s) will be asked to transfer copyright of the article to the publisher. The transfer will ensure the widest possible dissemination of information.

Special regulations for readers in the USA. This journal has been registered with the Copyright Clearance Center, Inc. Consent is given for copying of articles for personal or internal use, or for the personal use of specific clients. This consent is given on the condition that the copier pays through the Center the per-copy fee stated in the code on the first page of each article for copying beyond that permitted by Sections 107 or 108 of the US Copyright Law. The appropriate fee should be forwarded with a copy of the first page of the article to the Copyright Clearance Center, Inc., 27 Congress Street, Salem, MA 01970, USA. If no code appears in an article, the author has not given broad consent to copy and permission to copy must be obtained directly from the author. All articles published prior to 1980 may be copied for a per-copy fee of US\$ 2.25, also payable through the Center. This consent does not extend to other kinds of copying, such as for general distribution, resale, advertising and promotion purposes, or for creating new collective works. Special written permission must be obtained from the publisher for such copying.

No responsibility is assumed by the Publisher for any injury and/or damage to persons or property, as a matter of products liability, negligence or otherwise, or from any use or operation of any methods, products, instructions or ideas contained in the materials herein. Because of rapid advances in the medical sciences, the Publisher recommends that independent verification of diagnoses and drug dosages should be made.

Although all advertising material is expected to conform to ethical (medical) standards, inclusion in this publication does not constitute a guarantee or endorsement of the quality or value of such product or of the claims made of it by its manufacturer.

This issue is printed on acid-free paper.

Printed in the Netherlands

For Contents see p. I.

CONTENTS

9TH MONTREUX SYMPOSIUM ON LIQUID CHROMATOGRAPHY-MASS SPECTROMETRY, SUPERCRITICAL FLUID CHROMATOGRAPHY-MASS SPECTROMETRY, CAPILLARY ZONE ELECTROPHORESIS-MASS SPECTROMETRY AND TANDEM MASS SPECTROMETRY, MONTREUX, NOVEMBER 4-6, 1992

LC-MS

Applications (continued)

- Thermospray liquid chromatographic-mass spectrometric analysis of crude plant extracts containing phenolic and terpene glycosides
by J.L. Wolfender, M. Maillard and K. Hostettmann (Lausanne, Switzerland) 183
- Liquid chromatographic-UV detection and liquid chromatographic-thermospray mass spectrometric analysis of *Chironia* (Gentianaceae) species. Rapid method for the screening of polyphenols in crude plant extracts
by J.L. Wolfender and K. Hostettmann (Lausanne, Switzerland) 191
- Determination of mesocarb metabolites by high-performance liquid chromatography with UV detection and with mass spectrometry using a particle-beam interface
by R. Ventura, T. Nadal, P. Alcalde and J. Segura (Barcelona, Spain) 203
- Evaluation of liquid chromatography-thermospray mass spectrometry in the determination of some phenylglycidyl ether-2'-deoxynucleoside adducts
by F. Lemière (Antwerp, Belgium), E.L. Esmans (Wilrijk, Belgium), W. Van Dongen (Antwerp, Belgium), E. Van den Eeckhout (Ghent, Belgium) and H. Van Onckelen (Wilrijk, Belgium) 211
- Surfactants: non-biodegradable, significant pollutants in sewage treatment plant effluents. Separation, identification and determination by liquid chromatography, flow-injection analysis-mass spectrometry and tandem mass spectrometry
by H.F. Schröder (Aachen, Germany) 219
- Thermospray mass spectral studies of pesticides. Temperature and salt concentration effects on the ion abundances in thermospray mass spectra
by D. Volmer, A. Preiss, K. Levsen and G. Wünsch (Hannover, Germany) 235
- Development of a high-performance liquid chromatographic-mass spectrometric technique, with an ionspray interface, for the determination of platelet-activating factor (PAF) and lyso-PAF in biological samples
by L. Silvestro and R. Da Col (Turin, Italy), E. Scappaticci and D. Libertucci (Turin, Italy) and L. Biancone and G. Camussi (Naples, Italy) 261
- Determination of quaternary amine pesticides by thermospray mass spectrometry
by D. Barceló and G. Durand (Barcelona, Spain) and R.J. Vreeken (Lausanne, Switzerland) 271
- Electrospray mass spectrometry of neutral and acidic oligosaccharides: methylated cyclodextrins and identification of unknowns derived from fruit material
by A.P. Tinke, R.A.M. van der Hoeven, W.M.A. Niessen and J. van der Greef (Leiden, Netherlands) and J.P. Vincken and H.A. Schols (Wageningen, Netherlands) 279
- Characterization of the chemical structure of sulphated glycosaminoglycans after enzymatic digestion. Application of liquid chromatography-mass spectrometry with an atmospheric pressure interface
by R. Da Col and L. Silvestro (Turin, Italy), A. Naggi and G. Torri (Milan, Italy), C. Baiocchi (Turin, Italy), D. Moltrasio and A. Cedro (Villaguardia, Italy) and I. Viano (Turin, Italy) 289
- Rapid analysis of enzymatic digests of a bacterial protease of the subtilisin type and a "bio-engineered" variant by high-performance liquid chromatography-frit fast atom bombardment mass spectrometry
by W.D. van Dongen and C. Versluis (Utrecht, Netherlands), P.D. van Wassenaar (Vlaardingen, Netherlands) and C.G. de Koster, W. Heerma and J. Haverkamp (Utrecht, Netherlands) 301
- Application of liquid chromatography-thermospray mass spectrometry to the analysis of polyester oligomers
by A. Guarini, G. Guglielmetti and R. Po (Novara, Italy) 311
- Recent progress in high-performance anion-exchange chromatography-thermospray mass spectrometry of oligosaccharides
by W.M.A. Niessen, R.A.M. van der Hoeven and J. van der Greef (Leiden, Netherlands), H.A. Schols and A.G.J. Voragen (Wageningen, Netherlands) and C. Bruggink (Breda, Netherlands) 319

OTHER COMBINATIONS WITH MS

Fast screening method for eight phenoxyacid herbicides and bentazone in water. Optimization procedures for flow-injection analysis–thermospray tandem mass spectrometry by R.B. Geerdink and P.G.M. Kienhuis (Leylstad, Netherlands) and U.A.Th. Brinkman (Amsterdam, Netherlands)	329
Determination of chlorinated pesticides by capillary supercritical fluid chromatography–mass spectrometry with positive and negative-ion detection by A. Jablonska and M. Hansen (Oslo, Norway), D. Ekeberg (Ås, Norway) and E. Lundanes (Oslo, Norway)	341
Packed-column supercritical fluid chromatography coupled with electrospray ionization mass spectrometry by F. Sadoun and H. Virelizier (Gif-sur-Yvette, France) and P.J. Arpino (Paris, France)	351
Capillary zone electrophoresis–ionspray mass spectrometry of a synthetic drug–protein conjugate mixture by R. Kostianen, E.J.F. Franssen and A.P. Bruins (Groningen, Netherlands)	361
Off-line coupling of capillary electrophoresis with matrix-assisted laser desorption mass spectrometry by P.A. van Veelen and U.R. Tjaden (Leiden, Netherlands), J. van der Greef (Zeist and Leiden, Netherlands) and A. Ingendoh and F. Hillenkamp (Münster, Germany)	367
Pseudo-electrochromatography–negative-ion electrospray mass spectrometry of aromatic glucuronides and food colours by M. Hugener, A.P. Tinke, W.M.A. Niessen, U.R. Tjaden and J. van der Greef (Leiden, Netherlands)	375
AUTHOR INDEX	387

CHROMSYMP. 2778

Liquid chromatographic–thermospray mass spectrometric analysis of crude plant extracts containing phenolic and terpene glycosides

J.L. Wolfender, M. Maillard and K. Hostettmann*

Institut de Pharmacognosie et Phytochimie, École de Pharmacie, Université de Lausanne, CH-1015 Lausanne (Switzerland)

ABSTRACT

In crude plant extracts, constituents of biological or pharmaceutical interest often exist in the form of glycosides. Mass spectral investigations of these metabolites require soft ionization techniques such as desorption chemical ionization (D/CI) or fast atom bombardment if information on molecular mass or sugar sequence is desired. Thermospray (TSP) provides mass spectra similar to those obtained with positive-ion D/CI-MS using NH_3 and thus is potentially applicable to on-line analyses for these compounds and can be applied to plant extract analysis. Extracts of Gentianaceae species (containing secoiridoids and xanthone mono- and diglycosides), Polygalaceae (containing flavonol di- and triglycosides), Pedaliaceae (containing iridoids, phenylpropanoid glycosides) and Leguminosae (containing triterpene glycosides) have been screened by LC–TSP-MS. The plant extracts were analysed under standard LC–TSP-MS conditions on reversed-phase columns using methanol–water or acetonitrile–water gradients. Good optimization of the temperature of the source and the vaporizer was crucial for the observation of pseudo-molecular ions of glycosides.

INTRODUCTION

Natural products often exist in the form of glycosides and these conjugates may or may not occur together with their respective aglycones in the plants. Glycosides are thermally labile, polar and non-volatile compounds. Mass spectra investigation requires soft ionization techniques such as desorption chemical ionization (D/CI) or fast atom bombardment (FAB) [1,2], if information on molecular masses or sugar sequences is desired. These off-line techniques, however, require preliminary isolation and purification of the compounds. The development of LC–MS in the early 1980s now allows MS analysis to be coupled on-line with analytical HPLC separation. Hence it is possible to analyse many classes

of non-volatile compounds without isolation from their biological matrices. The two pioneering techniques of moving belt (MB) and direct liquid introduction (DLI) have been widely replaced by thermospray (TSP) [3] and, more recently, by the atmospheric pressure ionization (API) technique [4], whereas continuous-flow (CF)-FAB and Frit-FAB [5] have not gained popularity owing to their technical complexity.

LC–TSP-MS using ammonium acetate as buffer provides mass spectra nearly identical with those obtained with D/CI-MS using NH_3 and thus is potentially applicable to the on-line measurement of glycosides containing up to three sugar units [2,6]. TSP allows the use of high flow-rates, and standard reversed-phase HPLC conditions (4 mm I.D. column, gradient capability flow-rate, 1–2 ml/min) are compatible with this interface. Parameters developed for routine HPLC–UV analysis of crude plant extracts are thus straightforwardly applicable to

* Corresponding author.

LC-TSP-MS. Only the use of non-volatile buffers has to be avoided.

LC-TSP-MS has been widely used for bio-environmental investigations, but surprisingly few examples of glycoside analyses of crude plant extracts are known [7,8]. In the context of our studies on the active principles of higher plants [9] and in our search for more rapid and powerful methods for plant extract screening [10], conditions have been established for the TSP-MS analysis of different types of naturally occurring glycosides.

LC-TSP-MS analyses were performed on extracts containing secoiridoids, xanthone mono- and diglycosides (Gentianaceae), flavonol di- and triglycosides (Polygalaceae), iridoids and phenylpropanoid glycosides (Pedaliaceae) and saponins (Leguminosae). In all these examples, the correct tuning of TSP for the observation of molecular ion species was of great importance.

EXPERIMENTAL

Chemicals

HPLC-grade water was prepared by distillation on a Buchi (Flawil, Switzerland) Fontavapor 210 distillation instrument and passed through a 0.50- μ m filter (Millipore, Bedford, MA, USA). HPLC-grade acetonitrile and methanol from Maechler (Reinach, Basle, Switzerland) was passed through a 0.45- μ m filter. Ammonium acetate and trifluoroacetic acid (TFA) were obtained from Merck (Darmstadt, Germany) and diaminoethane from Fluka (Buchs, Switzerland).

HPLC conditions

Separations were performed on different RP-18, RP-8 or DIOL columns. Gradients of acetonitrile–water or methanol–water (1 ml/min) were used. In some instances, to avoid the tailing of phenolic compounds, 0.05–0.1% of trifluoroacetic acid was added to the solvents, giving a pH of 3.

LC-TSP-MS analyses

A Finnigan MAT (San Jose, CA, USA) TSQ-700 triple quadrupole instrument equipped with a TSP 2 interface was used for the data acquisi-

tion and processing. Depending on the type of compounds to be analysed and the eluent composition, the temperature of the TSP source block was set to 220–300°C and the vaporizer to 90–110°C. The electron multiplier voltage was 1800 V, dynode voltage 15 kV and the filament and discharge were off in all instances. Usually full-scan spectra from m/z 150 to 800 in the positive-ion (PI) mode were recorded (scan time 12 s). Concerning the LC part, the eluent delivery was provided by an HPLC 600-MS pump (Waters, Bedford, MA, USA) equipped with a gradient controller. The UV trace was recorded on-line with a Waters 490-MS programmable multi-wavelength detector. Postcolumn addition of buffer (0.5 M ammonium acetate) was effected with a Waters 590-MS programmable HPLC pump (0.2 ml/min).

Samples

Extracts were prepared from the dried plant material by maceration at room temperature with methanol. Solutions to be analysed were usually prepared by dissolving 30 mg of extract in 1 ml of a methanol–water mixture. The injected volumes varied from 10 to 20 μ l.

RESULTS

The plant extracts were separated under standard HPLC conditions (RP-8 or RP-18, methanol–water or acetonitrile–water gradients at 1–1.5 ml/min, 0.05 or 0.1% TFA for suppression of tailing). To avoid any alteration of the chromatographic conditions, buffer [0.5 M aqueous ammonium acetate or diaminoethane (0.2 ml/min)] was added postcolumn. The HPLC separation was followed by the use of an on-line multi-wavelength detector. Details of HPLC conditions for each extract are given in the figure captions.

TSP tuning

As glycosides are thermolabile compounds, the ability to observe their molecular ions is a function of temperatures set for the TSP interface. With polyphenolic diglycosides, the observation of pseudo-molecular ions is, for example, greatly dependent on the vaporizer tempera-

ture. In order to reveal these pseudo-molecular ions, the parameters [11] of the TSP interface were tuned in the positive-ion mode with a solution of rutin (M_r 610) (0.16 mM), a common flavonoid diglycoside, in acetonitrile–water (50:50). Measurement of ion intensities at various temperatures of the vaporizer (50–110°C) (source block temperature 250°C) showed that the best ion intensities for the observation of the pseudo-molecular ion $[M + H]^+$ were obtained with a setting of 90°C (Fig. 1). The intensity plot of the ion at m/z 465 is not indicated in Fig. 1 but is similar to that of $[M + H]^+$, showing also a maximum intensity at 90°C. Nevertheless, the intensity of these two ions remained low in comparison with the corresponding fragment ion of the aglycone $[A + H]^+$, which was the base peak of the spectrum (Fig. 1). For vaporizer temperatures below 75°C or higher than 100°C detection of the molecular ion was almost impossible and only the aglycone ion $[A + H]^+$ which was still of high intensity at these temperatures was observed. This point is of crucial

importance when extracts are screened for unknown compounds, as the relative pseudo-molecular ion intensities of glycosides are weak if the vaporizer is badly tuned and peaks due to glycosides could be wrongly attributed to aglycones.

The mass spectra of rutin were also recorded at different repeller potential values (0–200 V) but only a small influence on the ion intensities was observed and only extreme values below 20 V or higher than 160 V induced an important decrease in ion intensities. An increase in buffer concentration (higher than 0.1 M) in the eluent and the use of the filament- or discharge-on mode were found to have no significant influence on the ionization of glycosides. The source block temperature was set between 200 and 300°C, depending on the eluent composition.

These optimized tuning parameters are theoretically applicable only for this specific flavonoid. However, these parameters provide a good starting point for studying other related compounds in crude plant extracts. For this purpose,

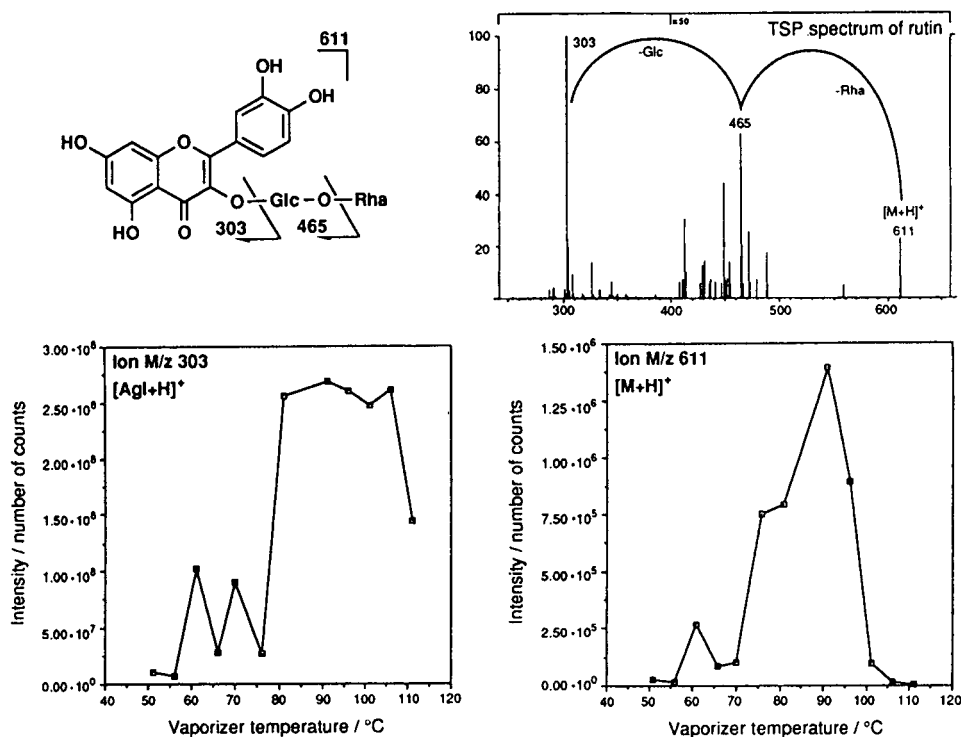


Fig. 1. Influence of vaporizer temperature on the aglycone $[Agl + H]^+$ and pseudo-molecular ions $[M + H]^+$ of rutin.

the optimization of the parameters is usually improved by performing several injections of the extract, varying slightly the starting parameters (obtained with pure products) and looking at the aspect of the total ion current trace.

Extract analysis

The mass spectra obtained for naturally occurring glycosides after injection of crude plant extracts were similar to those obtained by loop injection of the pure products if the peak resolution of the HPLC separation was good enough. Most of the extracts required a solvent gradient to ensure a good separation of the great variety of their metabolites. When subjected to reversed-phase HPLC, glycosides eluted faster than their corresponding aglycones in an extract. Some examples of TSP-MS analyses for naturally occurring glycosides in plant extracts are described below.

Iridoid and secoiridoid glycosides

Iridoids and secoiridoids represent a large and still expanding group of cyclopentane[c]pyran monoterpenoids. They are found as natural

constituents in a large number of plant families, usually, but not invariably, as glucosides. They also often exist as coumaroyl, caffeoyl, sinapoyl, feruloyl or diphenyl esters. Ionization of these compounds by conventional methods is difficult owing to their high lability [12]. To illustrate the use of TSP with iridoids and secoiridoids, two examples of plant extract analyses have been selected.

A methanolic extract of *Sesamum angolense* Welw. (Pedaliaceae) [13] was separated on an RP-8 column with an acetonitrile–water (0.05% TFA) gradient system (Fig. 2). The temperature of the TSP vaporizer was set to 110°C and the source block to 220°C. The total ion trace recorded was in good accordance with the UV trace (220 nm). The spectra of iridoids **1** (phlomiol) and **2** (sesamoside) showed intense $[M + NH_4]^+$ pseudo-molecular ions and weak $[M + H]^+$ ions. Intense fragments at m/z 180 ($[Glc + NH_4^+ - H_2O]$) and m/z 198 ($[Glc + NH_4^+]$) were recorded in both spectra, characteristic of the presence of a hexose residue, glucose in this instance. Ions at m/z 259 (**1**) and 240 (**2**) corresponded to dehydrated aglycone

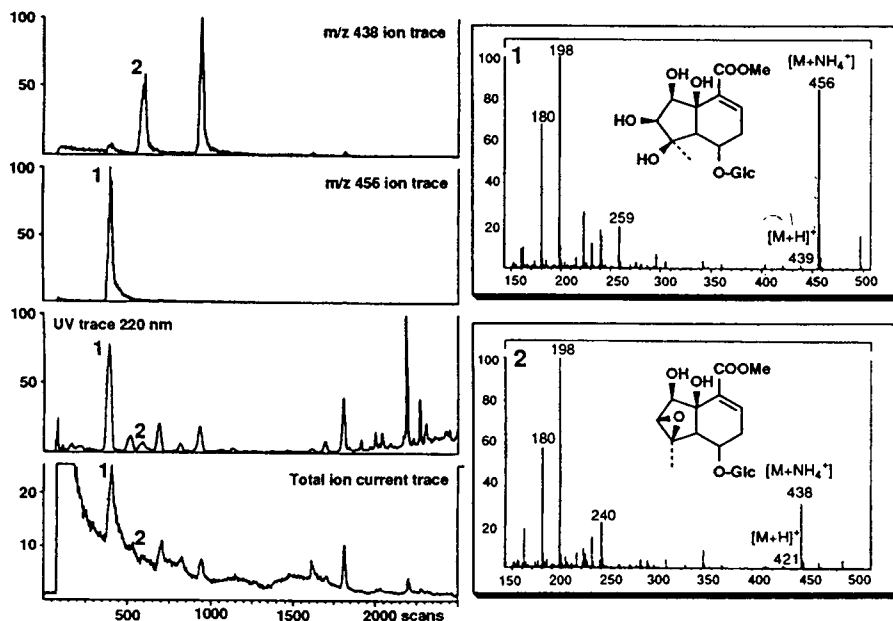


Fig. 2. LC-TSP-MS of the root methanolic extract of *Sesamum angolense* (Pedaliaceae), and TSP mass spectra of phlomiol (**1**) and sesamoside (**2**). HPLC: column, RP-8 Nucleosil ($5 \mu\text{m}$, $125 \times 4 \text{ mm}$ I.D.); gradient, $\text{CH}_3\text{CN}-\text{H}_2\text{O}$ (0.05% TFA) 2:98 \rightarrow 7:93 in 30 min and 7:93 \rightarrow 37:63 in 30 min (1 ml/min). TSP: vaporizer, 110°C; source, 220°C; ammonium acetate buffer (0.5 M, 0.2 ml/min); PI mode.

moieties. Spectra recorded on-line with LC–TSP–MS were comparable to those obtained by D/CI of the corresponding pure products using NH_3 in the positive-ion mode [13]. However, the intensities of fragments corresponding to the aglycone ion adducts were greater with D/CI.

A dimeric secoiridoid, lisianthioside (**3**), has been found in the root methanolic extract of *Lisianthus seemanii* Robyns et Elias (Gentianaceae) [14]. The LC–TSP–MS analysis of the crude extract was carried out on a RP-18 column with an acetonitrile–water (0.05% TFA) gradient system. The total ion trace recorded for the whole chromatogram showed a very intense response for this metabolite, which was the main compound of the extract. The spectrum (Fig. 3A) recorded with ammonium acetate as buffer exhibited an intense pseudo-molecular ion at m/z 734 and an important fragment at m/z 359. This information was insufficient for the attribu-

tion of the pseudo-molecular ion at m/z 734 to $[\text{M} + \text{NH}_4^+]$ or $[\text{M} + \text{NH}_4^+ - \text{H}_2\text{O}]$, as no $[\text{M} + \text{H}]^+$ ion was present. Therefore, a second TSP–MS analysis of the extract was carried out with another buffer to confirm the molecular mass of the secoiridoid. Diaminoethane (0.5 M, 0.2 ml/min), which has a higher proton affinity than ammonium acetate, was used. This buffer is known to produce only $[\text{M} + 61]^+$ ($[\text{M} + (\text{H}_2\text{N}(\text{CH}_2)_2\text{NH}_3)^+]$) pseudo-molecular ion adducts [15]. The spectrum (Fig. 3B) recorded on-line under the same conditions as with the diamine buffer exhibited an important pseudo-molecular ion $[\text{M} + 61]^+$ at m/z 777, confirming the molecular mass to be 716 u. The intense fragment ion at m/z 359 (A) corresponded to a protonated entity with half the mass of the parent molecule. Compound **3** was therefore certainly a dimer (2×359 u). The ion of m/z 359 was found to be the pseudo-molecular ion ($[\text{M} + \text{H}]^+$) of sweroside, another secoiridoid common in the Gentianaceae, also present in the extract. On the basis of these results, **3** was formulated as a dimer of sweroside; the full structural determination of this novel type of secoiridoid was confirmed after isolation of the pure substance [14].

This example shows that it is often helpful to have different types of pseudo-molecular ion adducts to ensure the on-line molecular mass determination of unknown metabolites.

To our knowledge, diaminoethane or other diamines [15] are the only alternative buffers to ammonium acetate which have been used in TSP analyses for glycosides. Further, it appears that diamines usually give adducts with compounds which form $[\text{M} + \text{NH}_4^+]$ ions with ammonium acetate.

Phenolic and polyphenolic glycosides

Simple phenolic compounds such as phenylpropanoid glycosides are found, for example, in plants of the Pedaliaceae family. The TSP–MS analysis of the methanol extract of the aerial parts of *Rogeria adenophylla* J. Gay ex. Del. (Pedaliaceae) (Fig. 4) showed the presence of verbascoside (**4**), a phenylpropanoid derivative. Different pseudo-molecular ion adducts were recorded for this compound: an $[\text{M} + \text{H}]^+$ ion

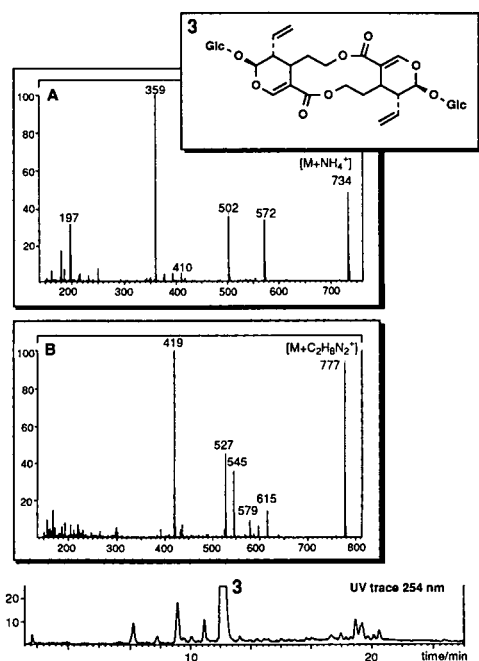


Fig. 3. TSP mass spectra of lisianthioside (**3**; molecular mass 716) recorded from the root methanolic extract of *Lisianthus seemanii* (Gentianaceae). HPLC: column, RP-18 Novapak (4 μm , 150×3.9 mm I.D.); gradient, $\text{CH}_3\text{CN}-\text{H}_2\text{O}$ (0.05% TFA) 5:95 \rightarrow 70:30 in 50 min (1 ml/min). TSP: vaporizer, 100°C; source, 250°C. (A) Ammonium acetate buffer (0.5 M, 0.2 ml/min); (B) diaminoethane buffer (0.5 M, 0.2 ml/min); PI mode.

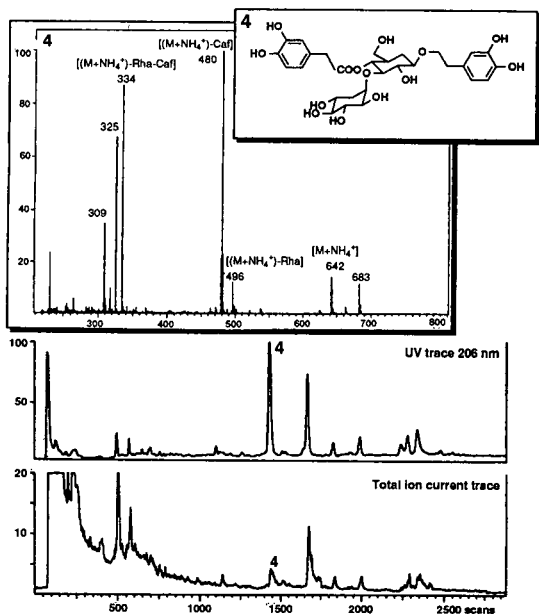


Fig. 4. LC-TSP-MS of the root methanolic extract of *Rogeria adenophylla* (Pedaliaceae) and spectrum of verbasin (4). HPLC: column, RP-8 Nucleosil ($5\ \mu\text{m}$, $125 \times 4\ \text{mm}$ I.D.); gradient, $\text{CH}_3\text{CN}-\text{H}_2\text{O}$ (0.05% TFA) 0:100 (5 min), 0:100 \rightarrow 10:90 in 5 min and 10:90 \rightarrow 25:75 in 50 min (1 ml/min). TSP: vaporizer, 110°C ; source, 280°C ; ammonium acetate buffer (0.5 M, 0.2 ml/min); PI mode.

(m/z 625) and two intense ions at m/z 642 [$\text{M} + \text{NH}_4^+$] and 683 [$\text{M} + \text{CH}_3\text{CN} + \text{NH}_4^+$], confirming the molecular mass to be 624 u. The TSP mass spectrum also exhibited important significant fragment ions due to the loss of a rhamnosyl unit (m/z 496), a caffeoyl unit (m/z 480) or consecutive losses of both moieties (m/z 334). The spectrum obtained was similar to the D/CI (NH_3 positive-ion mode) of the corresponding pure product, with the exception of the sodium adduct ions [16].

Polyphenols (including flavonoids) have long been recognized as one of the largest and most widespread classes of plant constituents, occurring throughout the higher and lower plants [17]. They occur as O- or C-glycosides with various numbers of sugar units. Xanthones are found mainly in two families (Gentianaceae and Polygalaceae) [18], where they exist as aglycones and mono- or diglycosides.

The TSP mass spectra of these compounds were recorded from different plant extracts. To

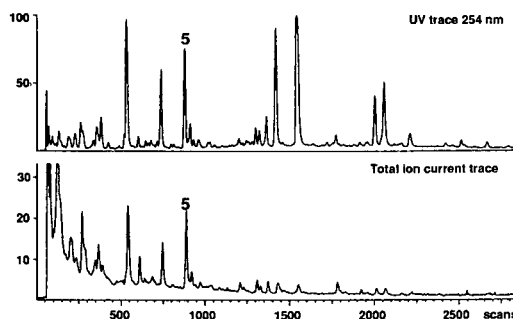


Fig. 5. UV trace (254 nm) and total ion current trace of the methanolic extract of *Gentiana dasyantha* (Gentianaceae). HPLC: column, RP-18 Novapak ($4\ \mu\text{m}$, $150 \times 3.9\ \text{mm}$ I.D.); gradient, $\text{CH}_3\text{CN}-\text{H}_2\text{O}$ (0.1% TFA) 10:90 \rightarrow 50:50 in 60 min (1 ml/min). TSP: vaporizer, 100°C ; source, 250°C . TSP mass spectrum of bellidifolin-8-O-glucoside (5) is shown in Fig. 6.

illustrate their ionization, the TSP spectra of mono-, di- and tri-O-glycosidic polyphenols is discussed here (Fig. 6).

The TSP mass spectrum of 1,5-hydroxy-3-methoxy-8-O-glucosylxanthone (bellidifolin-8-O-glucoside) (5) was recorded in the crude methanolic extract of *Gentiana dasyantha* Gilg. [19] (Fig. 5) (Gentianaceae), whereas the spectrum of 3,5-dimethoxy-1-O-[xylosyl-(1 \rightarrow 6)-glucosyl]xanthone (6) was recorded in the root methanolic extract of *Chironia krebsii* Griseb. [20], another Gentianaceous plant (chromatograms in Figs. 2 and 3 in ref. 21). The spectrum of the flavonoid triglycoside 3-O-(O-apiosyl-(1 \rightarrow 2)-O-rhamnosyl-(1 \rightarrow 6)-galactosyl]kaempferol (7) was obtained from the methanolic extract of *Monnina sylvatica* Schlecht. et Cham. (Polygalaceae) [22]. The xanthone monoglycoside 5 exhibited a single intense pseudo-molecular ion ($[\text{M} + \text{H}]^+$) and a fragment corresponding to the protonated aglycone moiety $[\text{A} + \text{H}]^+$, which was the base peak of the spectrum (Fig. 6). The xanthone diglycoside 6 showed a less intense protonated pseudo-molecular ion at m/z 567. A very weak signal at m/z 435 ($[\text{M} + \text{H} - 132]^+$) was characteristic of the loss of the xylosyl terminal sugar unit. As with 5, the base peak of the spectrum consisted of the aglycone fragment (Fig. 6). The triglycosidic flavonoid 7 presented only a very weak $[\text{M} + \text{H}]^+$ ion and two adducts ($[\text{M} + \text{Na}^+]$ and $[\text{M} + \text{CH}_3\text{CN} + \text{NH}_4^+]$), hardly discernible from the

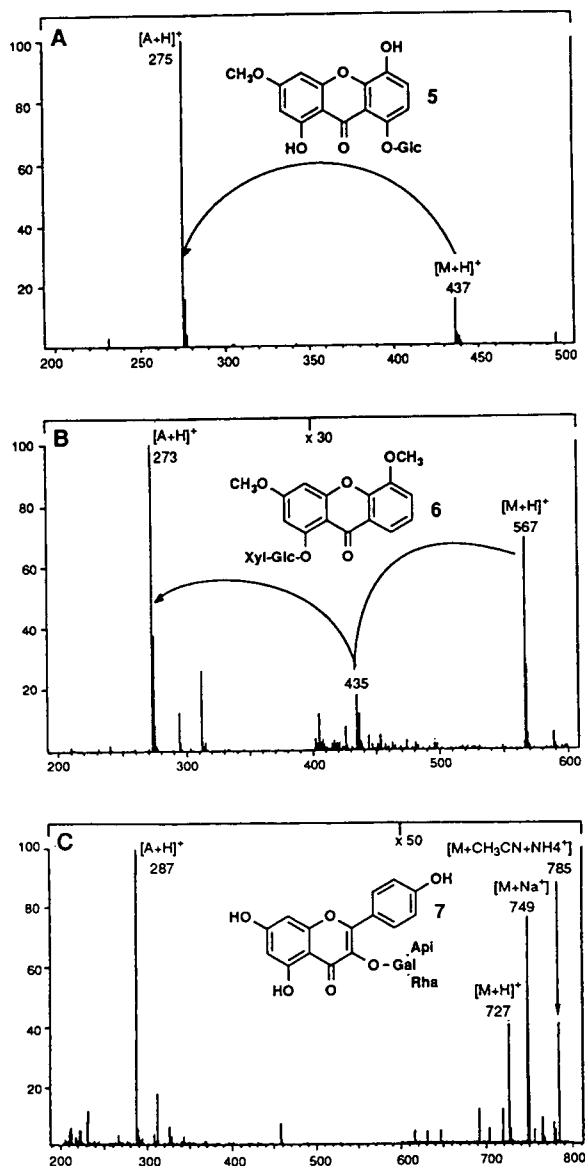


Fig. 6. Mass spectra of polyphenol glycosides. (A) TSP mass spectrum of bellidifolin-8-O-glucoside (5) recorded from the methanolic extract of *Gentiana dasyantha* (Gentianaceae). HPLC: column, RP-18 Novapak ($4\ \mu\text{m}$, $150 \times 3.9\ \text{mm}$ I.D.); gradient, $\text{CH}_3\text{CN}-\text{H}_2\text{O}$ (0.1% TFA) 10:90 \rightarrow 50:50 in 60 min (1 ml/min). TSP: vaporizer, 100°C ; Source, 250°C . (B) TSP mass spectrum of the xanthone 6 recorded from the methanolic root extract of *C. krebsii* (Gentianaceae). HPLC: column, RP-18 Novapak ($4\ \mu\text{m}$, $150 \times 3.9\ \text{mm}$ I.D.); gradient, $\text{CH}_3\text{CN}-\text{H}_2\text{O}$ (0.1% TFA) 5:95 \rightarrow 70:30 in 50 min (1 ml/min). TSP: vaporizer, 100°C ; source, 280°C . (C) TSP mass spectrum of 7 recorded from the methanolic extract of *Momina sylvatica* (Polygalaceae). HPLC: column, LiChrosorb DIOL ($7\ \mu\text{m}$, $250 \times 4.6\ \text{mm}$ I.D.); water (1 ml/min). TSP: vaporizer, 95°C ; source, 270°C .

background noise and no fragments corresponding to the intermediate ions of the glycosidic unit were observed (Fig. 6). Ammonium adducts were not recorded for polyphenolic glycosides except for very polar triglycosides, but some salt adducts can occur.

Examples of mono- and diglycosidic flavonoids are not shown here but similar types of ions to those observed for xanthenes are obtained [7].

Triterpene glycosides

Triterpene glycosides occur commonly in higher plants. The TSP mass spectra obtained usually gave molecular mass and sugar sequence information for glycosides up to three sugar units [23].

CONCLUSIONS

LC-TSP-MS is very suitable for on-line analyses for various naturally occurring glycosides encountered in crude plant extracts. Owing to the thermal instability of glycosides, the TSP interface needs to be properly tuned in order to obtain all the structural information desired. While the technique permits an unambiguous molecular mass determination of mono- and diglycosides, the observation of triglycoside parent ions is difficult, particularly with polyphenols. Other "softer" ionization techniques are then required (e.g., CF-FAB or Frit-FAB) to record higher molecular mass ions [24]. The spectra obtained on-line by LC-TSP-MS using ammonium acetate as buffer in the positive-ion mode are usually comparable to the D/CI (NH_3) mass spectra of the corresponding pure products. However, salt adducts which do not appear in the D/CI mass spectra may occur in the TSP mass spectra.

Iridoids, secoiridoids and simple phenol glycosides are well ionized by TSP and usually form intense $[\text{M} + \text{NH}_4]^+$ ions, which may constitute the base peak of the spectra.

Polyphenol glycosides usually exhibit small but clearly discernible protonated pseudo-molecular ions for compounds with up to two sugar residues. The intensity of the molecular ion decreases with increase in the number of sugar

residues and the base peak of the spectra is the protonated aglycone ion.

The on-line detection of unknown compounds in crude plant extracts is possible with TSP, but often requires different techniques to confirm the results obtained. Hence the use of other buffers to confirm the molecular mass determination, the use of alternative on-line detection methods (such as photodiode-array detection to characterize the type of constituents by their UV spectra) and chemotaxonomic considerations are necessary for structure elucidation of unknown metabolites.

As TSP is compatible with high flow-rates and has a large field of ionization, it is a promising tool for the HPLC phytochemical screening of plants. As a "soft" ionization technique, it is not limited to stable, volatile compounds but is also an excellent tool for the mass spectrometric investigation of moderately volatile thermolabile compounds such as glycosides.

ACKNOWLEDGEMENT

Financial support was provided by the Swiss National Science Foundation.

REFERENCES

- 1 B. Domon and K. Hostettmann, *Phytochemistry*, 24 (1985) 575.
- 2 J.L. Wolfender, M. Maillard, A. Marston and K. Hostettmann, *Phytochem. Anal.*, 3 (1992) 193.
- 3 C.R. Blackley and M.L. Vestal, *Anal. Chem.*, 7 (1983) 750.
- 4 A.P. Bruins, *Methodol. Surv. Biochem. Anal.*, 18 (1988) 339.

- 5 M. Caprioli, *Trends Anal. Chem.*, 7 (1988) 328–333.
- 6 D. Schaufelberger, B. Domon and K. Hostettmann, *Planta Med.*, 50 (1984) 398.
- 7 E. Schroeder and I. Mefort, *Biol. Mass. Spectrom.*, 20 (1991) 11.
- 8 J. Iida, M. Ono, K. Inoue, T. Fujita, *Chem. Pharm. Bull.*, 39 (1991) 2057.
- 9 M. Hamburger and K. Hostettmann, *Phytochemistry*, 30 (1991) 3864.
- 10 K. Hostettmann, B. Domon, D. Schaufelberger and M. Hostettmann, *J. Chromatogr.*, 283 (1984) 137.
- 11 A.L. Vergey, C.G. Edmonds, I.A.S. Lewis and M.L. Vestal, *Liquid Chromatography/Mass Spectrometry*, Plenum Press, New York, 1989.
- 12 P. Junior, *Planta Med.*, 56 (1990) 1.
- 13 O. Potterat, J.D. Msonthi and K. Hostettmann, *Phytochemistry*, 27 (1988) 2677.
- 14 M. Hamburger, M. Hostettmann, H. Stoeckli-Evans, P.N. Solis, M.P. Gupta and K. Hostettmann, *Helv. Chim. Acta*, 73 (1990) 1845.
- 15 H.D. Chace and P.S. Callery, *Biol. Mass. Spectrom.*, 21 (1992) 125.
- 16 O. Potterat, *Ph.D. Thesis*, University of Lausanne, Lausanne, 1991.
- 17 J.B. Harbone, *The Flavonoids: Advances in Research Since 1980*, Chapman and Hall, London, 1988.
- 18 K. Hostettmann and M. Hostettmann, *Methods Plant Biochem.*, 1 (1989) 493.
- 19 M.C. Recio, I. Slacanin, M. Hostettmann, A. Marston and K. Hostettmann, *Bull. Liais. Groupe Polyphénols (Strasbourg)*, 15 (1990) 25.
- 20 J.L. Wolfender, M. Hamburger, J.D. Msonthi and K. Hostettmann, *Phytochemistry*, 30 (1991) 3625.
- 21 J.L. Wolfender and K. Hostettmann, *J. Chromatogr.*, 647 (1993) 191.
- 22 A. Bashir, M. Hamburger, M.P. Gupta, P.N. Solis and K. Hostettmann, *Phytochemistry*, 30 (1991) 3781.
- 23 M.P. Maillard and K. Hostettmann, *J. Chromatogr.*, 647 (1993) 137.
- 24 M. Hattori, Y. Kawata, N. Kakiuchi, K. Matsuura, T. Tomimori and T. Namba, *Chem. Pharm. Bull.*, 36 (1988) 4467.

Liquid chromatographic–UV detection and liquid chromatographic–thermospray mass spectrometric analysis of *Chironia* (Gentianaceae) species

A rapid method for the screening of polyphenols in crude plant extracts

J.L. Wolfender and K. Hostettmann*

Institut de Pharmacognosie et Phytochimie, École de Pharmacie, Université de Lausanne, CH-1015 Lausanne (Switzerland)

ABSTRACT

The use of liquid chromatography–thermospray mass spectrometry (LC–TSP–MS) and liquid chromatography coupled with UV photodiode-array detection (LC–UV) in the analysis of crude plant extracts provides important structural information on metabolites directly in their biological matrices. In the LC analysis of polyphenols (such as xanthenes), shift reagents can be added postcolumn and UV spectra recorded on-line. Information on the position of free hydroxyl groups can be obtained by adding reagents such as AlCl₃, weak and strong bases and boric acid. Thus, for certain polyphenols, the combination of LC–UV with postcolumn addition of shift reagents and LC–MS permits a full on-line structural determination involving no time-consuming isolation process. To illustrate this qualitative analytical approach, crude extracts of different Gentianaceae (*Chironia* species) were submitted to LC–TSP–MS and LC–UV measurements with postcolumn addition of shift reagents. This method permitted the identification of a large number of xanthenes which are of pharmaceutical interest as potential inhibitors of monoaminoxidases.

INTRODUCTION

Species of the Gentianaceae family are known to contain secoiridoids and xanthenes [1–3]. The latter class of substance is of special interest as it includes strong inhibitors of monoaminoxidase (MAO) [4,5]. Further, xanthenes are useful chemotaxonomic markers [5]. In the course of an investigation of tropical and subtropical Gentianaceae [6,7], we have collected several *Chironia* species. The genus *Chironia* L. is distributed mainly in South Africa, but several species range northward into tropical Africa and Madagascar [8]. A first phytochemical study of

the roots and leaves of *C. krebsii* has afforded eighteen xanthenes (1–18) [7] (Fig. 1) and three secoiridoids, swertiamarin (19), gentiopicroside (20) and sweroside (21). The xanthenes are currently being tested for their inhibitory activities on monoaminoxidases A and B.

For a rapid qualitative survey of the xanthenes in other species and for identification of minor xanthenes, different extracts of four *Chironia* species, namely *C. krebsii* Griseb., *C. palustris* Burch., *C. pupurascens* Verdoorn and *C. baccifera* L., have been screened by liquid chromatography with UV photodiode-array detection (LC–UV) with postcolumn addition of shift reagents [9,10] and by LC with thermospray mass spectrometric detection (LC–TSP–MS) [11].

* Corresponding author.

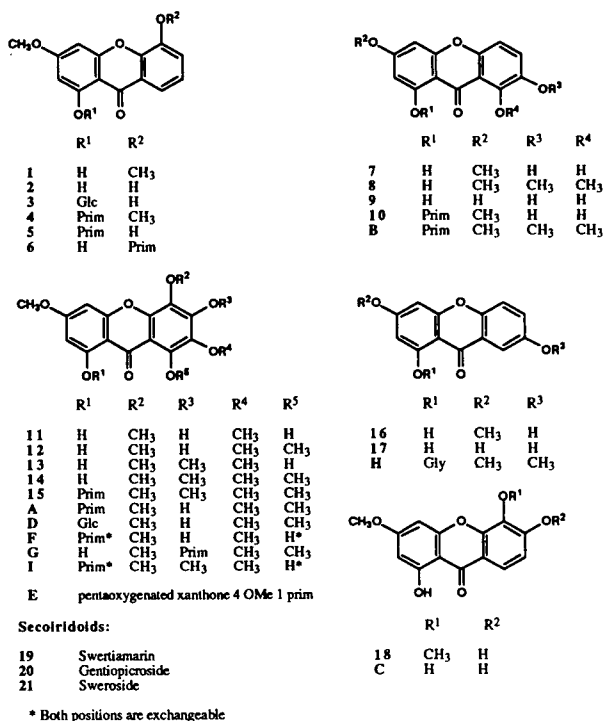


Fig. 1. Compounds found in *Chironia* species. Compounds 1–21 were isolated from *C. krebsii*. Xanthenes A–I were identified only from MS and UV data obtained on-line. Glc = glucose; Gly = undefined glycoside; Prim = primeverose [$=\beta$ -D-xylopyranosyl-(1 \rightarrow 6)- β -D-glucopyranoside].

The separation of the xanthenes directly from a crude plant extract was achieved by reversed-phase LC using an acetonitrile–water gradient system. The same LC conditions were used for the LC–UV and LC–MS investigations.

Xanthenes present characteristic UV spectra with four bands of decreasing intensity [12]. These spectra are easily recorded during the LC separation of a crude plant extract, on-line with the aid of a photodiode array detector (220–450 nm). The UV spectra depend on the substitution pattern of the polyphenols. The location of free hydroxyl groups on a xanthone nucleus can be established with the aid of classical shift reagents [13]. These reagents induce a shift of the absorption maxima and their applications to structure elucidation of flavonoids and xanthenes have been extensively described [13, 14]. In this work, reagents were added to the eluate using a post-

column derivatization system [9,10]. As the separations were achieved in an acidic acetonitrile–water system, the shift reagents usually used in methanol solutions required some adaptations.

LC–TSP–MS is a soft ionization technique [11] that mainly forms adduct ions such as $[M + H]^+$ with molecules. These adduct molecular ions allow a rapid determination of the molecular mass of a component directly after its elution from the LC column. The use of LC–TSP–MS has already provided on-line molecular mass information in the analysis of polyphenols and polyphenol glycosides such as flavonoids [15]. Xanthenes, which are closely related to flavones, can be ionized under nearly identical conditions, with ammonium acetate as buffer and in the positive ion and filament-off modes.

This paper presents the results obtained by LC–UV with postcolumn addition of shift reagents and LC–TSP–MS in the analysis of crude extracts of Gentianaceae. The combination of structural information obtained by the two on-line detection methods is discussed.

EXPERIMENTAL

Chemicals

HPLC-grade water was prepared by distillation on a Buchi (Flawil, Switzerland) Fontavapor 210 distillation instrument and passed through a 0.50- μ m filter (Millipore, Bedford, MA, USA). HPLC-grade acetonitrile from Maechler (Reinach, Basle, Switzerland) was passed through a 0.45- μ m filter. Boric acid, sodium acetate, ammonium acetate and trifluoroacetic acid (TFA) were obtained from Merck (Darmstadt, Germany) and aluminium chloride, sodium hydroxide and potassium hydroxide from Fluka (Buchs, Switzerland).

LC conditions

Separations were performed on a Nova-Pak RP-18 (4 μ m) column (150 \times 3.9 mm I.D.) from Waters (Bedford, MA, USA), equipped with a Nova-Pak Guard precolumn. A gradient of acetonitrile–water from 5:95 to 70:30 in 50 min (1 ml/min) was used. To avoid the tailing of phenolic compounds, 0.05% of trifluoroacetic

acid was added to the solvents, leading to a pH of 3.

Shift reagents

For comparison purposes, classical shift reagents were prepared according to the standard procedure [13]. The reagents used in the post-column derivatization system were as follows (Table I): weak base, 0.5 M aqueous sodium acetate solution (basified with a 0.01 M NaOH solution to pH 8); strong base, 0.3 M aqueous potassium hydroxide solution; 0.3 M aqueous aluminium chloride solution (with this reagent, the reaction coil was heated to 90°C and the eluent was previously neutralized with 0.02 M NaOH solution); boric acid, a methanol–water (1:1) solution containing 0.7 M boric acid and 0.1 M sodium acetate. All the reagent solutions were filtered through a 0.50- μ m filter (Millipore, Bedford, MA, USA).

LC–UV analyses

Eluent delivery was provided by an LC-9A HPLC pump (Shimadzu, Tokyo, Japan) equipped with an FCV-9AL low-pressure mixing valve and a Model 7125 injection valve with a 20- μ l loop (Rheodyne, Cotati, CA, USA). Post-column addition of the bases (for neutralization of the mobile phase) and of the shift reagents was achieved with two M-6000 pumps (Waters). Neutralization of the mobile phase was effected

in an Upchurch (Oak Harbor, WA, USA) mixing tree and reaction with the shift reagent was carried out in a 10- μ l Visco mixer (Lee, Westbrook, CO, USA) followed by a reaction coil. UV spectra were recorded with an HP-1040A photodiode-array detector 1040A and the data were processed on an HP-1090 Chemstation (Hewlett-Packard, Palo Alto, CA, USA) (see Fig. 4).

LC–MS analyses

A Finnigan MAT (San Jose, CA, USA) TSQ-700 triple quadrupole instrument equipped with a TSP 2 interface was used for data acquisition and processing. The temperatures of the TSP were source block 280°C, vaporizer 100°C and aerosol 280–300°C (beginning–end of gradient). The electron multiplier voltage was 1800 V, dynode 15 kV and the filament and discharge were off. Full-scan spectra from m/z 150 and 800 in the positive ion mode were obtained (scan time 1.2 s). Concerning the LC part, the eluent delivery was provided by a 600-MS pump HPLC (Waters) equipped with a gradient controller. The UV trace was recorded on-line with a Water 490-MS programmable multi-wavelength detector. Postcolumn addition of buffer (0.5 M ammonium acetate) was achieved with a Waters 590-MS programmable HPLC pump (0.2 ml/min) using a simple tee junction (Waters).

TABLE I
CONDITIONS FOR POSTCOLUMN ADDITION OF SHIFT REAGENTS

Shift reagent	Pump 1 ^a	Flow-rate (ml/min)	pH	Pump 2 ^a	Flow-rate (ml/min)	pH	Temperature (°C)
Eluent	H ₂ O	0.2	3	H ₂ O	0.4	3	Room
NaOAc	NaOAc (0.5 M)	0.4	7	NaOH (0.01 M)	0.3	8	Room
KOH	H ₂ O	0.2	3	KOH (0.3 M)	0.4	14	Room
AlCl ₃	NaOH (0.02 M)	0.2	7	AlCl ₃ (0.3 M)	0.4	3.5	90
AlCl ₃ ^b , acid	H ₂ O	0.2	3	AlCl ₃ (0.3 M)	0.4	2.5	90
H ₃ BO ₃ –NaOAc	NaOH	0.2	6	H ₃ BO ₃ (0.7 M)–NaOAc (0.1 M)	0.4	7	Room

^a For pumps 1 and 2, see Fig. 4.

^b 0.1% TFA in the mobile phase.

Samples

The dried plant material was extracted at room temperature with solvents of increasing polarity (dichloromethane and methanol). Aerial parts and roots of the following plants of the Gentianaceae family were used: *Chironia krebsii* Griseb., collected in Malawi, *Chironia pupurascens* Verdoorn and *Chironia palustris* Burch, collected in Zimbabwe, and *Chironia baccifera* L., collected in South Africa. Solutions to be analysed were prepared by dissolving 30 mg of the root methanolic extract in 1 ml of methanol–water (1:1). The injection volume was 20 μ l.

RESULTS

Reversed-phase LC on RP-18 columns with methanol–water or acetonitrile–water containing acetic acid, phosphoric acid or formic acid has been successfully applied to analyses for polar polyphenols such as xanthone glycosides and xanthone aglycones [12, 16]. A linear gradient of an acetonitrile–water system, containing trifluoroacetic acid to avoid peak tailing (pH 3), was developed to achieve the separation of the different xanthone aglycones and glycosides which were found in the crude root methanolic and dichloromethane extracts of the *Chironia* species (Fig. 2).

LC–UV Photodiode array detection

The use of a photodiode-array detector permits the measurement of the whole UV spectrum (220–450 nm) of each peak of the chromatogram. The attribution of the peaks to xanthenes (1–18) and secoiridoids (19–21) was unambiguous, the xanthenes usually exhibiting a UV spectrum consisting of four bands of decreasing intensity (200–400 nm), while the secoiridoids exhibit only one band (230–240 nm). The number of bands and the general aspects of the UV spectra of xanthenes (UV spectra 1–18 in Fig. 2) allowed a first attribution of the type of oxygenation pattern encountered [12,14]. The comparison of the chromatogram of the methanolic extract of the roots with the corresponding dichloromethane extract permitted the localization of xanthone aglycones and xanthone glycosides (Fig. 2). Indeed, the extraction with

dichloromethane permitted the selective acquisition of the polyphenolic aglycones only, owing to their low polarity. The peaks observed for the xanthone aglycones corresponded to the slower running peaks in the chromatogram (Fig. 2).

LC–MS thermospray detection

In order to obtain more information on the molecular masses, the crude formulae and the sugar sequence (glycosides) of the xanthenes, LC–TSP–MS analysis of the extracts was carried out. The same LC conditions as for the LC–UV analysis were used (see Experimental). The ammonium acetate buffer (0.5 M) was added postcolumn (0.2 ml/min) to avoid modification of the chromatographic conditions. In order to obtain the optimum intensities of ions for both xanthone aglycones and glycosides, the parameters of the TSP interface were tuned with a solution of rutin (M_r 610), a flavonoid diglycoside. The vaporizer temperature range for observation of the $[M + H]^+$ ion of rutin was narrow and the optimum intensity was found for a setting of the vaporizer of 100°C with the source block at 280°C. Nevertheless, even at this temperature the $[M + H]^+$ ion was weak, and the major ion was the aglycone moiety $[A + H]^+$. The influence of the change in the composition of the eluent during in the gradient (5–70% acetonitrile) and the presence of trifluoroacetic acid in the mobile phase was found to be negligible. No improvement was observed by using the filament-on or discharge-on mode, and the analysis was finally carried out in the filament-off mode.

Under these conditions, all the peaks recorded in the UV trace (254 nm) of the different extracts gave a clearly discernible MS response in the total ion current trace (TIC) (Fig. 3). As the molar absorptivities ϵ of the xanthenes were of the same order of magnitude [7], comparison of the UV chromatogram with the TIC trace showed a poor MS response for some compounds. Indeed, the total ion current response for highly hydroxylated xanthenes with high melting point, such as **9** (1,3,7,8-tetrahydroxanthone, m.p. >335°C [7]), was found to be very weak compared with the UV trace of the corresponding peak. The relationship between the

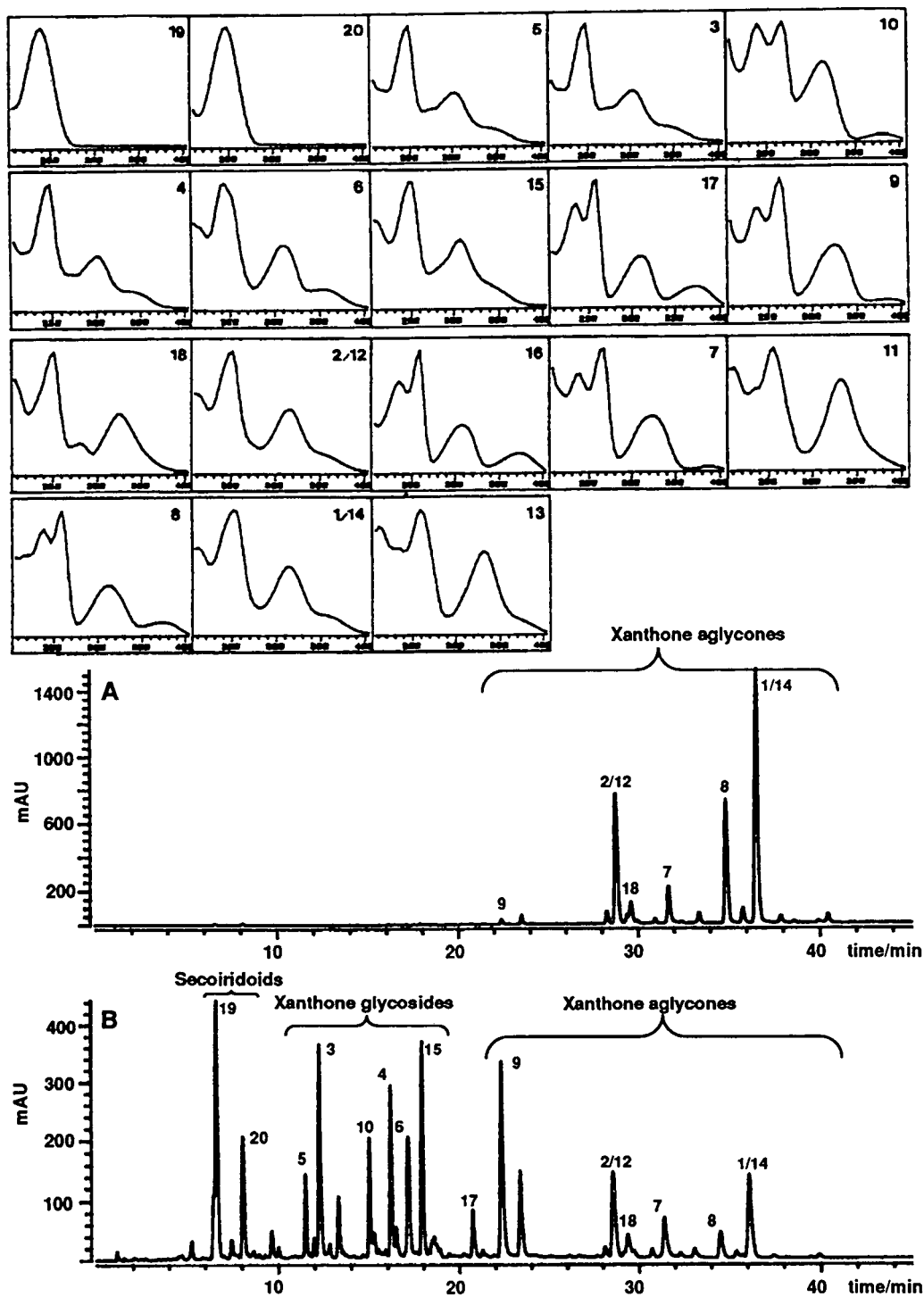


Fig. 2. Comparison of the LC-UV traces of (A) the root dichloromethane and (B) the root methanolic extracts of *C. krebsii*. The UV spectra displayed were recorded from chromatogram B. UV traces were recorded at 254 nm. UV spectra were recorded from 200 to 400 nm. For identities of the peaks, see Fig. 1.

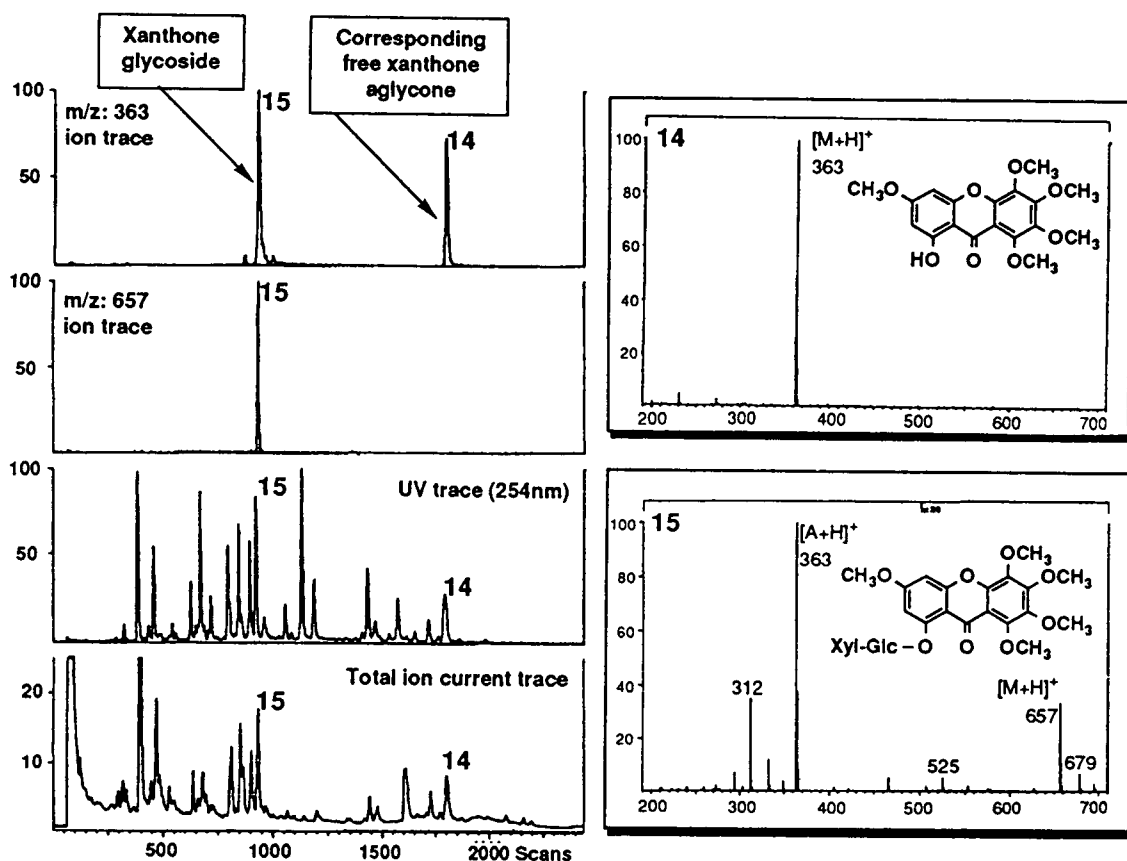


Fig. 3. LC-TSP-MS analysis of the root methanolic extract of *C. krebsii*. The ion trace for m/z 657 displayed corresponds to the pseudo-molecular ion $[M+H]^+$ of xanthone 15. The ion at m/z 363 is the main fragment of 15 and corresponds to the pseudo-molecular ion of its corresponding free aglycone 14 also present in the extract.

TIC intensity and melting point was investigated by injecting equal amounts ($2.5 \mu\text{g}$) of xanthenes with melting points varying from 158 to $>335^\circ\text{C}$ (1, 173°C ; 2, 272°C ; 7, 226°C ; 8, 158°C ; 9, $>335^\circ\text{C}$). Under the conditions used for LC-TSP-MS analysis of the extracts, the TIC for a non-volatile compound such as 9 (m.p. $>335^\circ\text{C}$) was about 30 000 times lower than for a more volatile xanthone such as 8 (m.p. 158°C). In the same way, the MS responses of xanthenes 1, 2 and 7 were dependent on their melting points. Hence LC-TSP-MS alone cannot be used for direct semi-quantitative determination of xanthenes.

The TSP mass spectra of the xanthone aglycones recorded on-line from the liquid chromatogram exhibited only the $[M+H]^+$ ions as main peak; the molecular mass determination was thus unambiguous (see Figs. 3 and 5). For

simple xanthenes, the number of hydroxyl and methoxyl substituents was deduced by subtracting the molecular mass of the xanthone nucleus (M_r 196) from that of the aglycones.

The TSP mass spectra of xanthone glycosides usually show two weak ions corresponding to the $[M+H]^+$ and $[M+Na]^+$ adducts, and a main peak corresponding to the protonated aglycone moiety $[A+H]^+$ (see Figs. 3 and 6). In the case of diglycosides, a weak intermediate fragment due to the loss of a first sugar unit was observed (see Fig. 6). These results were in good agreement with those obtained for flavonoid glycosides [15]. The mass spectra of the xanthone diglycosides found in the *Chironia* species presented a first loss of 132 u corresponding to a pentose residue, followed by a loss of 162 u (hexose residue) leading to the aglycone ion $[A+H]^+$. These two losses were attributable to

a primeverose moiety, a β -D-xylopyranosyl-(1 \rightarrow 6)- β -D-glucopyranoside disaccharide unit often encountered in the Gentianaceae family [2,16]. The monoglycosidic xanthenes presented $[M + H]^+$ ions more intense than the diglycoside ions and exhibited only a loss of 162 u, attributed to be a glucosyl moiety. The structures were confirmed by a full determination of the main isolated glycosides [7].

These first LC–UV and LC–TSP–MS results afforded the molecular mass, the number of methoxyl and hydroxyl groups, the number of sugars and an idea about the substitution pattern of the xanthenes found in the extracts of the *Chironia* species. In order to obtain more precise structural information on the position of the free hydroxyl groups on the xanthone nucleus, LC–UV with postcolumn addition of shift reagents for polyphenols was performed.

LC–UV photodiode-array detection with postcolumn addition of shift reagents

The use of these shift reagents played an important role in the characterization of phenolic compounds, and application of such reagents to flavonoids [13] and xanthenes [12] have been extensively described. A weak base (sodium acetate) deprotonates only the more acidic phenolic groups, whereas a strong base (sodium methanolate) reacts with all phenolic groups. Aluminium chloride in neutral solution forms complexes with *ortho*-dihydroxyl groups and/or with keto functions having a hydroxyl group in an α - or *peri*-position. The former complexes are unstable when HCl is added. *ortho*-Dihydroxyl groups also form a chelate complex with boric acid. For flavonoids and xanthenes, all these reactions are in general carried out in methanol. They provide useful information about the type of flavonoid or xanthone and the oxidation pattern and the location of free hydroxyl groups.

The method employed for the postcolumn addition of shift reagents is based on the work of Hostettmann *et al.* [9] and the improvement described by Mueller-Harvey and Blackwell [10]. The experimental set-up is shown in Fig. 4. The method presented here was adapted for the use of an acidic acetonitrile–water eluent system. The shift reagents, KOH, AlCl_3 and H_3BO_3 , were prepared as described by Hostettmann *et*

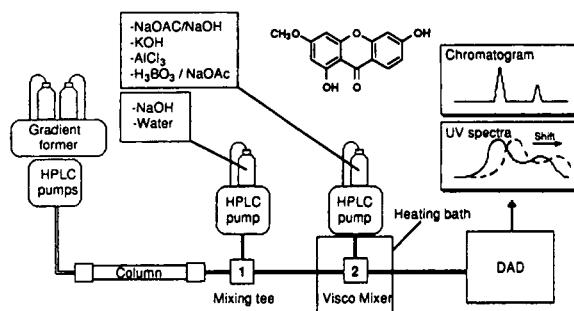


Fig. 4. Experimental set-up used for postcolumn addition of the shift reagents.

al. [9]. However, the use of Na_2HPO_4 as a weak base was found to be incompatible with the acetonitrile–water system for reasons of solubility. Even at lower concentrations than those proposed by Hostettmann *et al.* [9], Na_2HPO_4 precipitated in the eluent, producing pressure instability and plugging. Na_2HPO_4 was therefore replaced with sodium acetate (0.5 M, 0.4 ml/min). As this weak base is not strong enough to deprotonate acidic phenolic groups in an aqueous solvent system, NaOH was added in a second HPLC pump (0.01 M, 0.3 ml/min) to obtain a pH of 8 (Table I, Fig. 4).

The location of *ortho*-dihydroxyl groups is not always possible in an acetonitrile–water system with the use of NaOAc – H_3BO_3 reagent [9]. However, the use of AlCl_3 in the acidic mobile phase (pH 3, 0.1% TFA) showed similar shifts to those observed for pure compounds having an *ortho*-dihydroxyl group with the classical AlCl_3 –HCl [13] reagent in methanol. Hence the comparison of on-line AlCl_3 UV spectra at pH 7 and 3 allows the detection of the labile *ortho*-dihydroxyl complexes.

All the shift reagents were tested with an artificial mixture of previously isolated xanthenes (1, 2, 5, 7, 9, 11 and 12) [7], eluted under the same chromatographic conditions as those used for the extracts. The optimum concentration, flow rate and temperature are presented in Table I.

Examples of structural information obtained on-line

The structural information obtained on-line by the combination of LC–UV, LC–TSP–MS and

LC–UV with postcolumn addition of shift reagents is illustrated by two examples (Figs. 5 and 6).

The first example shows the structure determi-

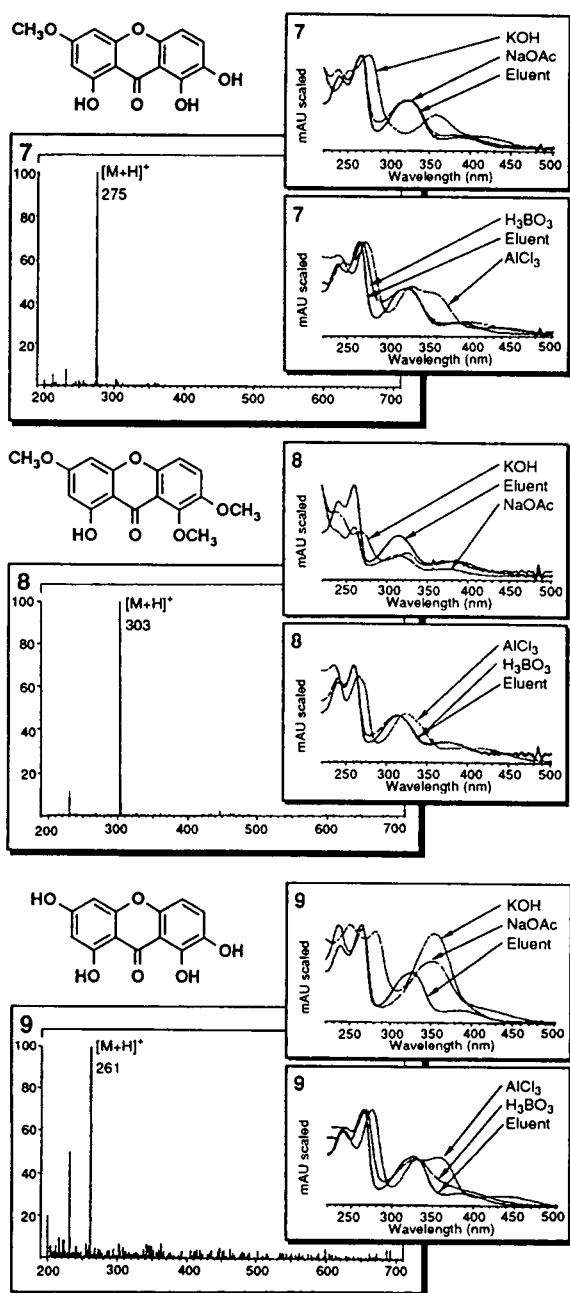


Fig. 5. Summary of all structural information obtained on-line for three 1,3,7,8-tetra-substituted xanthone aglycones. Mass and UV spectra of 7, 8 and 9 were recorded from the liquid chromatogram of *C. krebsii*.

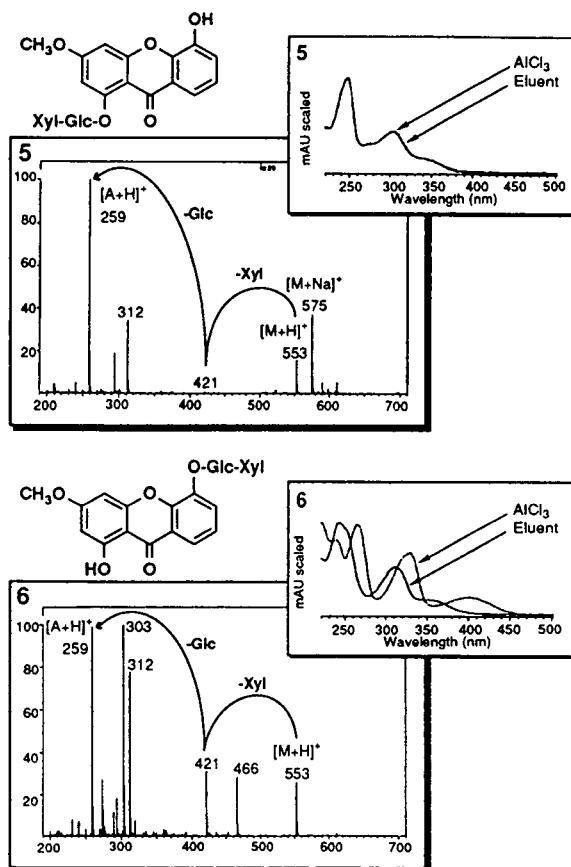


Fig. 6. Differentiation of two isomeric xanthone diglycosides. The TSP mass spectra of 5 and 6 are comparable, and both xanthenes have a molecular mass of 552. The only difference between them is shown by the AlCl_3 spectrum, proving the difference in the position of attachment of the disaccharide unit in 5 and 6. Mass and UV spectra of 5 and 6 were recorded from the liquid chromatogram of *C. krebsii*.

nation of three xanthone aglycones (7–9) in the LC–UV analysis of the root methanolic extract of *C. krebsii*. These xanthenes presented nearly the same UV spectra (Fig. 2). According to Kaldas [16], the UV spectra of 7–9 with four absorption maxima and a higher intensity of band II (Table II) is characteristic of tetraoxygenated 1,3,7,8-xanthenes with a free hydroxyl in position 1. The TSP mass spectra recorded on-line permit the molecular mass determination and the assignment of the number and the type of substituents of 7 (M_r 274: 3 OH, 1 OMe), 8 (M_r 302: 1 OH, 3 OMe) and 9 (M_r 260: 4 OH)

TABLE II
ON-LINE STRUCTURAL INFORMATION FOR COMPOUNDS 1–18

Abbreviations: Al = AlCl₃ in neutralized mobile phase; KO = KOH; Na = NaOAc; Bo = H₃BO₃-NaOAc; AlH = AlCl₃ in acidic mobile phase; I–IV = UV absorption maxima bands with the wavelength in nm and in parentheses the relative intensity in %, according to ref. 17; ckrm = *C. krebsii* root methanolic extract; cbm = *C. baccifera* root methanolic extract; ckad = *C. krebsii* aerial part dichloromethane extract; the TSP-MS values are the mass (in a.m.u.) of the ions [M + H]⁺ and [A + H]⁺; nd = not detected.

Compound	Mixture	TSP-MS		Shifted UV spectra					UV spectra					Extract
		M + H	A + H	Al	KO	Na	Bo	AlH	I	II	II'	III	IV	
1	1 + 14		273	+	+	-	-	-	251(100)			315(52)	359(13)	ckrm
2	2 + 12		259	+	+	-	-	-	251(100)			315(49)	359(11)	ckrm
3	3 + ?	421	259	+	+	+	+	-	239(100)	265(87)		315(63)	379(12)	ckrm
4		567	263	-	-	-	-	-	247(100)	269(32)		303(43)	339(14)sh	ckrm
5		553	259	-	+	-	-	-	247(100)	275(28)		303(41)	341(12)sh	ckrm
6		553	259	+	+	-	-	-	241(100)	260(90)sh		311(51)	349(16)	ckrm
7			275	+	+	-	-	+	238(75)	265(100)		323(44)	387(10)	ckrm
8			303	+	+	-	-	-	239(80)	259(100)		314(40)	373(10)	ckrm
9			261	+	+	+	+	+	237(79)	263(100)		325(51)	385(11)	ckrm
10		569	275	+	+	-	+	-	239(100)	267(100)		313(68)	379(13)	ckrm
11			335	+	+	+	-	-	254(100)			329(61)		ckrm
12	12 + 2		349	+	+	-	-	-	251(100)			315(49)	359(11)	ckrm
13			349	nd	nd	nd	nd	nd	235(63)	261(100)		331(71)	373(13)sh	ckad
14	14 + 1		363	+	+	-	-	-	251(100)			315(52)	359(13)	ckrm
15		657	363	-	-	-	-	-	250(100)			308(15)	347(15)sh	ckrm
16	sh		259	+	+	nd	nd	-	247(100)		277(23)	319(50)		ckrm
17			245	+	+	+	+	-	235(81)	258(100)		312(47)	372(17)	ckrm
18			289	+	+	+	+	-	246(100)		277(25)	319(50)		ckrm

(Fig. 5). The shifted UV spectra recorded on-line for **9** confirmed this compound to be a 1,3,7,8-tetrahydroxyxanthone. Indeed, the shift observed with the NaOAc spectrum indicated an acidic phenol in position 3. The presence of a free hydroxyl in positions 1 and 8 was characterized by the substantial shift recorded with AlCl₃ and finally the presence of an *ortho*-dihydroxyl group was confirmed by the shift due to the complexation of boric acid (Fig. 5). Xanthone **7** exhibited the same shifts as those recorded for **9**, except that the NaOAc spectra remained unchanged in this instance, indicating the presence of a methoxyl instead of a hydroxyl group in position 3. The structure of **7** was thus attributable to a 1,7,8-trihydroxy-3-methoxyxanthone. The KOH spectra of **8** show a large decrease in the band intensity and only a very small shift, indicating no free hydroxyl group, with the exception of a chelated one. This was confirmed

by the shift measured with AlCl₃. The NaOAc and H₃BO₃ spectra remained unchanged, confirming the structure of **8** as a 1-hydroxy-3,7,8-trimethoxyxanthone (Fig. 5).

The second example shows the differentiation and structural determination of two isomeric xanthone glycosides. Compounds **5** and **6** (Fig. 2) exhibited nearly the same UV spectra, indicating the same oxygenation pattern (probably 1,3,5-) [17]. The TSP mass spectra of both **5** and **6** were comparable: they both exhibited an [M + H]⁺ ion at *m/z* 553 and presented a consecutive loss of 132 and 162 u, leading to their respective aglycone ions [A + H]⁺ at *m/z* 259 (Fig. 6). The mass of the aglycone ions was characteristic of a xanthone with one methoxyl and two hydroxyl groups and the presence of a pentose and hexose moiety was due to a primeverosyl residue. No shift was observed for either compound with the weak base (Table II), indicating no free hydroxyl

TABLE III
ON-LINE STRUCTURAL INFORMATION OF COMPOUNDS A–I

Abbreviations as in Table II; cparm = *C. palustris* root methanolic extract; cpurm = *C. pupurascens* root methanolic extract.

Compound	TSP-MS		Shifted UV spectra					UV spectra					Extract
	M + H	A + H	Al	KO	Na	Bo	AlH	I	II	II'	III	IV	
A	643	349	–	+	+	–	–	248(100)		283(27)sh	311(52)		cpurm
B	597	303	–	–	–	–	–	243(100)	251(49)sh		305(51)	355(18)sh	cpurm
C		275	+	+	+	+	+	251(100)		281(25)	326(49)		ckrm
D	511	349	–	+	+	–	–	247(100)		283(29)sh	311(51)		cpurm
E	627	333	–	–	–	–	–	246(100)		277(31)	313(58)		cpurm
F	629	335	+	+	+	+	–	247(100)	261(77)sh		325(73)		cparm
G	643	349	+	+	–	–	–	249(100)	263(86)sh		321(73)	365(15)sh	cparm
H	nd	275	–	–	–	–	–	239(87)	253(100)		309(41)	353(21)sh	cparm
I	597	303	–	–	–	–	–	247(100)			319(71)		cbrm

in position 3. The only difference between these two isomers is shown by the spectra recorded using the AlCl_3 reagent. In the case of **6**, an important shift was observed which is characteristic of a chelated hydroxyl group in position 1, whereas for **5** no shift was recorded (Fig. 6). The primeverosyl moiety is thus attached in position 1 in **5** and in position 5 in **6** and the structures can be established as 5-hydroxy-3-methoxy-1-O-primeverosylxanthone (**5**) and 1-hydroxy-3-methoxy-5-O-primeverosylxanthone (**6**).

The structures of all the compounds were deduced following the same procedure (Tables II and III). Xanthones **1–18** have all been isolated from *C. krebsii* for further testing on monoaminooxidases A and B [7] and their structures, established by classical spectroscopic methods, were in good agreement with the on-line spectroscopic information obtained by both LC–MS and LC–UV methods (Table II). The structure of compounds **A–E** was established only on the basis of data obtained on-line (Table III). The structure assignment was not only based on UV and MS data but also on chemotaxonomic considerations.

CONCLUSIONS

LC–MS and LC–UV comparisons of the root methanolic extracts of four *Chironia* species permitted a precise assignment of the peaks

encountered in all species (Fig. 7). From a chemotaxonomic viewpoint, this analysis shows that the 1,3,5-, 1,3,7,8- and 1,3,5,6,7,8-substituted xanthones occur in all species and that several compounds with each substitution pattern are present. The 1,3,7- and 1,3,5,6-substituted xanthones appear to be rare and are not detected in all species (Table IV). Whereas the type of aglycone is almost the same in all four species, the type of glycosidation of the xanthones differs widely from one species to another.

According to this example, the combination of LC–TSP-MS, LC–UV and LC–UV with post-column addition of shift reagents is a powerful tool for the analysis of polyphenols in crude plant extracts. These coupled techniques give a very precise idea of the plant constituents. They allow a rapid screening of the extract and reliable identification with a minute amount of material. MS and UV data provide useful structural information. The detection of minor components is possible using single ion monitoring. MS and UV information for each peak permits a reliable comparison of chromatograms of different plant species. Full structural assignment of unknowns is not possible in all instances, but the information obtained gives a good idea of the type of compounds screened and permits a targeted isolation of the metabolites of interest. Other plant extracts containing different types of

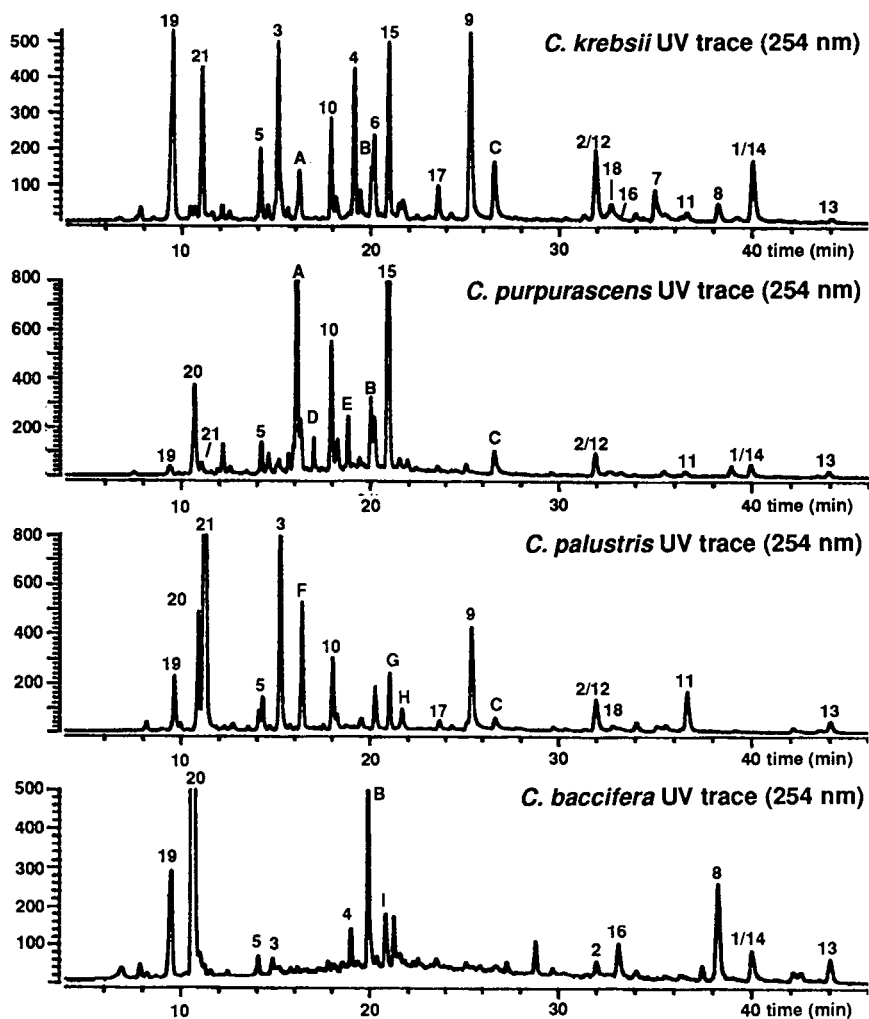


Fig. 7. Comparison of the LC–UV traces (254 nm) of the root methanolic extract of four *Chironia* species. The aglycone peaks are comparable in all chromatograms. Greater variability is observed for the xanthone glycosides between the species.

TABLE IV

OCCURRENCE OF THE IDENTIFIED XANTHONES IN THE FOUR *CHIRONIA* SPECIES

Plus signs in bold type indicate that the corresponding compounds appear as major peak in the LC–UV traces. The ϵ values being of the same order of magnitude for all xanthones [7], their relative abundances can be estimated in a semi-quantitative manner.

Oxidation	1,3,5-			1,3,7-			1,3,5,6- 1,3,7,8-		1,3,5,6,7,8-																	
	Agl	Gly		Agl	Gly		Agl	Agl	Gly	Agl		Gly														
Compounds	1	2	3	4	5	6	16	17	H	18	C	7	8	9	10	B	11	12	13	14	15	A	D	F	G	I
<i>C. krebsii</i>	+	+	+	+	+	+	+	+		+	+	+	+	+	+	+	+	+	+	+	+	+	+	+	+	+
<i>C. purpurascens</i>	+	+			+						+					+	+	+	+	+	+	+	+	+		
<i>C. palustris</i>			+	+					+	+					+	+		+	+	+					+	+
<i>C. baccifera</i>	+	+	+		+		+						+			+				+	+					+

polyphenols are currently being screened by LC using a combination of these on-line detection methods.

ACKNOWLEDGEMENTS

Financial support was provided by the Swiss National Science Foundation.

REFERENCES

- 1 W.G. Van der Sluis and R.P. Labadie, *Pharm. Weekbl.*, 113 (1978) 21.
- 2 K. Hostettmann and H. Wagner, *Phytochemistry*, 16 (1977) 481.
- 3 D. Schaufelberger, *Ph. D. Thesis*, University of Lausanne, Lausanne, 1986.
- 4 O. Suzuki, Y. Katsumata, M. Oya, V.M. Chari, B. Vermes, H. Wagner and K. Hostettmann, *Planta Med.*, 42 (1981) 17.
- 5 D. Schaufelberger and K. Hostettmann, *Planta Med.*, 54 (1988) 219.
- 6 M. Hamburger, M. Hostettmann, H. Stoeckli-Evans, P.N. Solis, M.P. Gupta and K. Hostettmann, *Helv. Chim. Acta*, 73 (1990) 1845.
- 7 J.L. Wolfender, M. Hamburger, J.D. Msonthi and K. Hostettmann, *Phytochemistry*, 30 (1991) 3625.
- 8 R.E.J.R. Weaver and L. Rudenberg, *J. Arnold Arbor. Harv. Univ.*, 56 (1975) 211.
- 9 K. Hostettmann, B. Domon, D. Schaufelberger and M. Hostettmann, *J. Chromatogr.*, 283 (1984) 137.
- 10 I. Mueller-Harvey and P.M.S. Blackwell, *Phytochem. Anal.*, 2 (1991) 38.
- 11 C.R. Blakley and M.L. Vestal, *Anal. Chem.*, 7 (1983) 750.
- 12 K. Hostettmann and M. Hostettmann, in J.B. Harborne (Editor), *Methods in Plant Biochemistry*, Vol. 1, Academic Press, London, 1989, pp. 493–508.
- 13 K. R. Markham, *Techniques of Flavonoids Identification*, Academic Press, London, 1982, p. 36.
- 14 A. A. Lins Mesquita, D. de Barros Correa, O. R. Gottlieb and T. Taveira Magalhaes, *Anal. Chim. Acta*, 42 (1968) 311.
- 15 E. Schroeder and I. Mefort, *Biol. Mass. Spectrom.*, 20 (1991) 11.
- 16 M. Kaldas, *Ph.D. Thesis*, University of Neuchâtel, Neuchâtel, 1977.
- 17 S. Ghosahl, R. Ballava, P.S. Chauhan, K. Biswas and R.K. Chaudhuri, *Phytochemistry*, 15 (1976) 1041.

CHROMSYMP. 2732

Determination of mesocarb metabolites by high-performance liquid chromatography with UV detection and with mass spectrometry using a particle-beam interface

Rosa Ventura*, Teresa Nadal, Pilar Alcalde and Jordi Segura

Departament de Farmacologia i Toxicologia, Institut Municipal d'Investigació Mèdica, Autonomous University of Barcelona, Dr. Aiguader 80, 08003 Barcelona (Spain)

ABSTRACT

A method of screening for mesocarb ingestion in doping control is described. After alkaline extraction with ethyl acetate, samples are analysed by reversed-phase high-performance liquid chromatography (HPLC) with UV detection. A peak with a shorter retention time than and a UV spectrum identical with those of unchanged mesocarb was obtained when positive urine extracts were analysed. The metabolite was identified as the sulphate conjugate of *p*-hydroxymesocarb after HPLC–mass spectrometry with a particle-beam interface and hydrolysis studies. The compound was detected in urine until 48–72 h after administration of single doses of 10 mg. Unchanged mesocarb and free *p*-hydroxymesocarb were not detected in the samples studied.

INTRODUCTION

Mesocarb is a substance with stimulant activity recently added to the list of banned compounds in sport by the Medical Commission of the International Olympic Committee [1]. Hence methods to detect the presence of this compound or its metabolites in human urine are required. Information concerning human and animal metabolism and urinary excretion of mesocarb is limited. Free and conjugated hydroxylated metabolites are the main products described in rat urine [2,3].

In this paper, a method of screening for the presence of mesocarb metabolites in human urine based on high-performance liquid chromatographic (HPLC) separation and UV detection is described. Confirmation analysis is done

by HPLC–mass spectrometry (MS) using a particle-beam interface. The application of the procedure to antidoping control in the 1992 Barcelona Olympic Games allowed the detection and confirmation of a real doping case.

EXPERIMENTAL

Chemical and reagents

7-Propyltheophylline, metandienone and diphenylamine were used as internal standards (ISTD). 7-Propyltheophylline was synthesized from theophylline and propyl iodide in alkaline medium. Metandienone and diphenylamine were purchased from Sigma (St. Louis, MO, USA).

Solutions of β -glucuronidase from *Escherichia coli* (Boehringer-Mannheim, Mannheim, Germany) and β -glucuronidase–arylsulphatase from *Helix pomatia* (Sigma) were used for enzymatic hydrolysis.

Water used in the HPLC eluent was of Milli-Q

* Corresponding author.

purity (Millipore Ibérica, Barcelona, Spain). Methanol, acetonitrile and ethyl acetate were of HPLC grade. Diethyl ether was of analytical-reagent grade and distilled before use. Other reagents were of analytical-reagent grade quality.

High-performance liquid chromatography with ultraviolet detection

HPLC–UV analyses were performed in a Series II 1090 liquid chromatograph equipped with a diode-array detector (Hewlett-Packard, Palo Alto, CA, USA) under the conditions described previously [4]. The column was Ultrasphere ODS (7.5 × 0.46 cm I.D.) with particle size 3 μm (Beckman, Fullerton, CA, USA).

The mobile phase was a mixture of 0.1 M ammonium acetate solution (adjusted to pH 3 with phosphoric acid) and acetonitrile with gradient elution. The acetonitrile content (initially 10%) was increased to 15% in 2 min, to 45% in 3 min, to 60% in 3 min, maintained for 1 min, decreased to the initial conditions in 1 min and stabilized for 2 min before the next injection. The flow-rate was 1 ml/min.

The detector was set to monitor the signals at 240, 270, 290, 300, 318 and 350 nm. In addition, the full spectrum between 200 and 400 nm for each detected peak was stored in the data system and plotted at the end of each run.

High-performance liquid chromatography–mass spectrometry

HPLC–MS analyses were performed in a Model 5989 mass spectrometer coupled to a Model 59980B particle-beam interface and a Series II 1090L liquid chromatograph, all from Hewlett-Packard. The operating parameters of the interface were desolvation chamber temperature 70°C, helium pressure 50 p.s.i. (1 p.s.i. = 6894.76 Pa) and nebulizer position –1.

The liquid chromatographic column was Ultrasphere ODS (25 × 0.2 cm I.D.) with particle size 5 μm (Beckman). The mobile phase was a mixture of 0.1 M ammonium acetate solution (containing 0.5% of formic acid) and acetonitrile, with gradient elution. The acetonitrile content (initially 38% for 3.5 min) was increased to 60% in 3 min, maintained for 1 min, de-

creased to the initial conditions in 1 min and stabilized for 2.5 min before the next injection. The flow-rate was 0.4 ml/min.

Electron impact (EI) ionization (70 eV) and scan acquisition (m/z 65–550) were used. The source temperature was kept at 250°C.

Gas chromatography

Gas chromatographic analyses were performed in a Series II 5890 gas chromatograph with a nitrogen–phosphorus-selective detection (GC–NPD) (Hewlett-Packard). The injection port and detector temperatures were 280°C. The column was 5% phenyl–methyl silicone (12.5 m × 0.2 mm I.D.) with film thickness 0.33 μm (Hewlett-Packard) and the temperature was programmed from 90 to 280°C at 20°C/min. Helium was used as the carrier gas at 0.6 ml/min.

Sample extraction

The samples were extracted using the procedure described previously [4] with some modifications. To 2.5 ml of urine sample, 25 μl of the ISTD solution (100 μg/ml methanolic solution of 7-propyltheophylline for HPLC–UV screening analysis and 100 μg/ml methanolic solution of metandienone for HPLC–MS confirmation analysis) were added. The sample was made alkaline (pH 9.5) with 100 μl of ammonium chloride buffer, salted with 1 g of sodium chloride and extracted with 8 ml of ethyl acetate. After agitation (tilt shaker, 40 movements/min for 20 min) and centrifugation (1100 g for 5 min), the organic layer was separated and evaporated to dryness under a stream of nitrogen. The extract was reconstituted with 100 μl of water–acetonitrile (85:15, v/v) and analysed by HPLC–UV detection (20 μl) or HPLC–MS (10 μl).

For the determination of amphetamine (a potential metabolite of mesocarb), 25 μl of the ISTD solution (1 mg/ml methanolic solution of diphenylamine) were added to urine samples (5 ml). The samples were made alkaline with 0.5 ml of 5 M potassium hydroxide solution and 3 g of anhydrous sodium sulphate and 2 ml of distilled diethyl ether were added. After agitation (tilt shaker, 40 movements/min for 20 min) and centrifugation (800 g for 5 min), 700 μl of the

organic layer were mixed with 300 μl of methanol and 3 μl of the mixture were analysed by GC-NPD.

Acidic hydrolysis

To 2.5 ml of the sample, 0.5 ml of 6 M hydrochloric acid and 50 mg of cysteine were added. The sample was heated for 1 h at 80°C. After incubation, the sample was cooled to room temperature and 400 μl of 5 M potassium hydroxide solution were added before the application of the extraction procedure described above.

Enzymatic hydrolysis

Two enzymatic hydrolyses were used: (i) to 2.5 ml of the sample, 1 ml of 0.2 M sodium phosphate buffer (pH 7) and 50 μl of *E. coli* solution were added and the mixture was usually incubated at 55°C for 1 h; (ii) to 2.5 ml of the sample, 1 ml of sodium acetate buffer (pH 5.2) and 50 μl of *H. pomatia* solution were added and the mixture was usually incubated at 55°C for 3 h. Longer incubation times were used in special studies.

Excretion studies

Two excretion studies were performed with one healthy male (A) and one healthy female (B) volunteer. Mesocarb was administered as Sydnocarb® tablets (10 mg) in single doses. Urine samples were collected for a period of 72 h.

The metabolite detected in the non-hydrolysed urines was determined by HPLC-UV detection using the calibration graph for unchanged mesocarb (0, 1.24, 3.10, 6.20 and 12.40 nmol/ml; molecular mass of mesocarb = 322.37). The extraction recovery and the molar absorptivity of the metabolite were assumed to be the same as those of unchanged mesocarb.

RESULTS AND DISCUSSION

Methodological aspects

The development of a procedure to detect mesocarb ingestion is difficult because only information on rat metabolism has been described previously [2,3] and no pure samples of the metabolites are available.

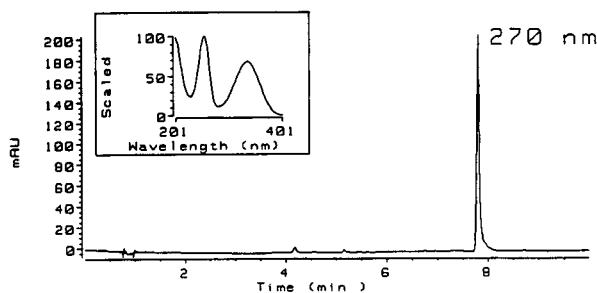


Fig. 1. Analysis of a methanolic solution of mesocarb by HPLC-UV detection and characteristic UV spectrum of mesocarb.

Normally, new compounds included in the list of banned substances in sport are tested by existing analytical procedures to avoid an increase in the complexity of doping control analysis. Most analytical methods used in doping control are based on gas chromatographic separations. The detection of mesocarb and its metabolic products is not directly amenable to gas chromatography because of their thermal lability [5,6]. Pyrolysis of mesocarb and its *p*-hydroxy metabolite to give N-nitroso-N-cyanomethylamphetamine takes place in the injection port.

Using the HPLC conditions of our routine screening method for diuretics and masking

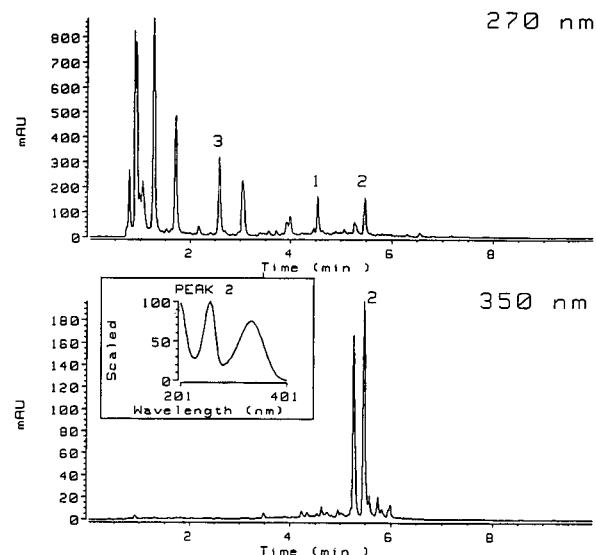


Fig. 2. HPLC-UV analysis of a urine sample obtained after mesocarb intake (real doping case). Peaks: 1 = ISTD; 2 = suspected mesocarb metabolite; 3 = caffeine.

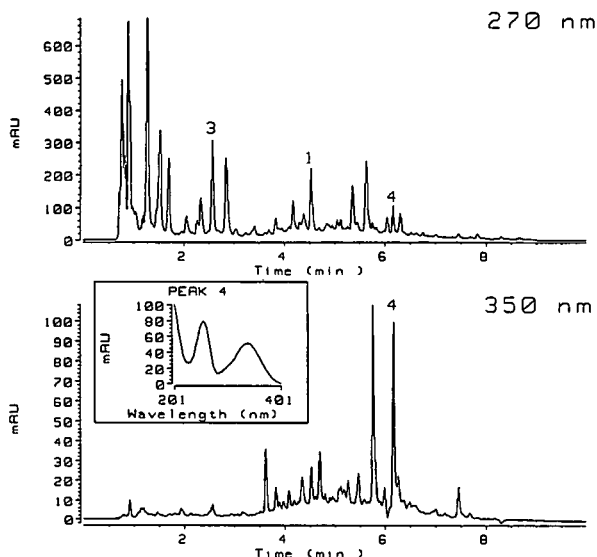


Fig. 3. HPLC-UV analysis of a hydrolysed urine sample obtained after mesocarb intake (real doping case). Peaks: 1 = ISTD; 3 = caffeine; 4 = suspected mesocarb metabolite.

agents [4], mesocarb gave a narrow peak at 7.8 min with a characteristic UV spectrum (Fig. 1). Therefore, this method was used to test urines obtained after mesocarb administration. A peak with the same UV spectrum as unchanged

mesocarb was detected at 5.4 min after the analysis of urine extracts (Fig. 2). No unchanged mesocarb was present. After acidic hydrolysis and the same extraction procedure, this peak disappeared and another peak with the same UV spectrum appeared at 6.1 min (Fig. 3). Again, unchanged mesocarb was not detected.

On HPLC-EI-MS with a particle-beam interface and a source temperature of 250°C (Fig. 4), mesocarb showed a mass spectrum identical with that described by other workers using direct introduction of the compound into the mass spectrometer [2,3]. At lower source temperatures broader peaks appeared, indicating poor vaporization of the compound in the ion source.

Analysis by HPLC-MS of extracts from non-hydrolysed urines (Fig. 5) gave a peak with a mass spectrum related to that of the *p*-hydroxy-mesocarb previously reported in rat urine [2,3]. The mass spectrum showed a characteristic peak at m/z 135, indicating *p*-hydroxylation of the phenylisocyanate moiety, but the relative abundance between the ions of m/z 91 and 135 did not fit with that of *p*-hydroxymesocarb [2,3].

When extracts from urines subjected to acidic hydrolysis were analysed by HPLC-MS, a peak showing a mass spectrum corresponding to *p*-

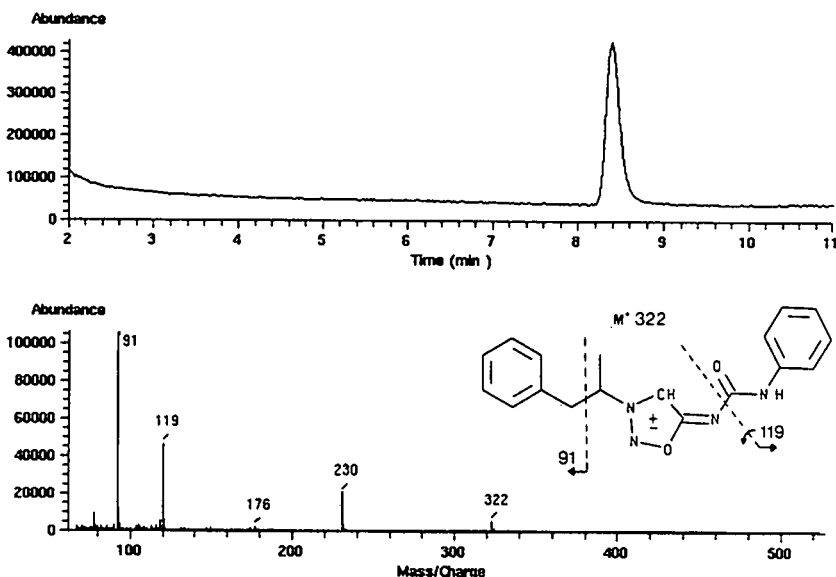


Fig. 4. Analysis by HPLC-MS of a methanolic solution of mesocarb and mass spectrum of the peak obtained.

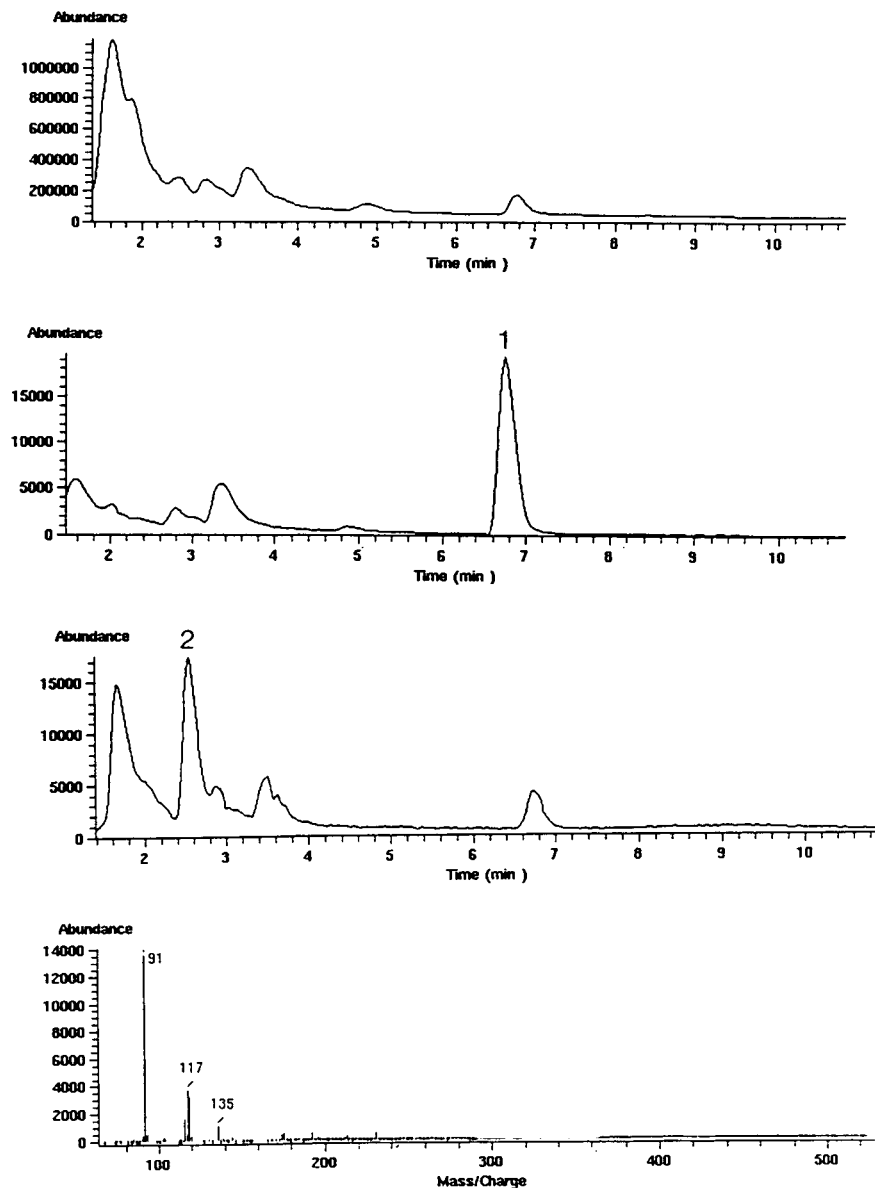


Fig. 5. Analysis by HPLC–MS of a positive urine sample. From top to bottom: total ion chromatogram; chromatogram of m/z 122 (characteristic ion of the ISTD); chromatogram of m/z 91; and mass spectrum of the peak detected at 2.5 min. Peaks: 1 = ISTD; 2 = mesocarb metabolite.

hydroxymesocarb was detected (Fig. 6). In addition to the ions described [2,3], a low-molecular-mass ion (m/z 338) was also observed.

Hence the compound detected in the HPLC–UV screening of non-hydrolysed urines appears to be a conjugate of *p*-hydroxymesocarb. Concentrations of this compound in urines from

excretion studies were calculated using the calibration graph for mesocarb ($y = 342.35x + 0.006$, $r = 0.999$, where y is the peak-area ratio between mesocarb and the ISTD and x is the concentration). Results are presented in Table I. The compound can be detected in urine until 48–72 h after intake and accounts for 26.5–

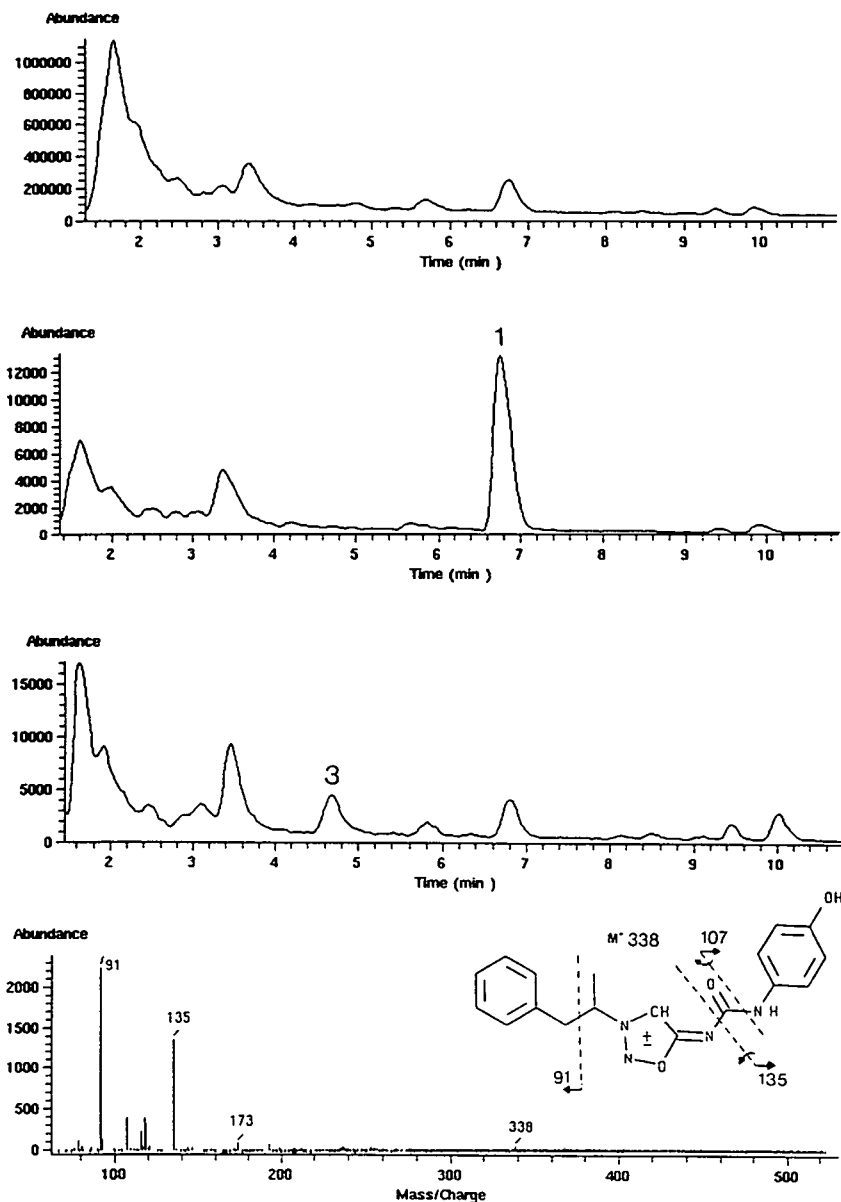


Fig. 6. Analysis by HPLC–MS of an extract from a hydrolysed urine sample. From top to bottom: total ion chromatogram; chromatogram of m/z 122 (characteristic ion of the ISTD); chromatogram of m/z 91; and mass spectrum of the peak detected at 4.6 min corresponding to *p*-hydroxymesocarb. Peaks: 1 = ISTD; 3 = *p*-hydroxymesocarb.

29.4% of the administered dose. Other metabolites found in rat urine, such as free *p*-hydroxymesocarb, unchanged mesocarb and amphetamine [3], were not detected in the samples studied here.

Additional studies

In order to identify the conjugated metabolite, different HPLC–MS assays were performed. EI ionization at low electron energy (12 eV) and chemical ionization (CI) with methane, ammonia

TABLE I

CONCENTRATIONS OF CONJUGATED *p*-HYDROXYMESOCARB DETECTED IN HUMAN URINE AFTER ADMINISTRATION OF 10 mg (31.02 μ mol) OF MESOCARB TO HEALTHY VOLUNTEERS

Volunteer	Time (h)	Volume (ml)	Concentration (nmol/ml)	Total excreted (nmol)	% of dose excreted	Cumulative %
A	0–6	400	4.93	1972	6.36	6.36
	6–12	880	1.98	1742	5.62	11.98
	12–24	625	3.69	2306	7.43	19.41
	24–48	1450	2.14	3103	10.00	29.41
	48–72	1180	ND ^a	–	–	29.41
B	0–6	1300	0.99	1287	4.14	4.14
	6–12	1000	1.86	1860	5.99	10.13
	12–24	900	2.17	1953	6.29	16.42
	24–48	1800	1.08	1944	6.26	22.68
	48–72	1300	0.93	1209	3.89	26.57

^a Not detected.

or isobutane were tested in order to obtain a mass spectrum with the molecular ion of the compound or a characteristic fragment of the conjugated moiety (e.g., *m/z* 194 characteristic fragment of glucuronides described using ammonia CI [7]). No relevant results were obtained.

The hydrolysis of the conjugate was also studied (Fig. 7). Enzymatic hydrolyses under conditions used routinely in our laboratory gave lower yields than acidic hydrolysis (Fig. 7A). After acidic hydrolysis, only *p*-hydroxymesocarb was detected with a recovery of 38.9% and no conjugated *p*-hydroxymesocarb was left in the sample (Fig. 7A). When unchanged mesocarb was subjected to the same conditions of acidic hydrolysis, only 49.9% of the compound was recovered. Mesocarb, and probably *p*-hydroxymesocarb formed after acidic hydrolysis, are thus unstable under these conditions, which explains the low recovery of the acidic hydrolysis.

After enzymatic hydrolysis under our routine conditions, both free and conjugated *p*-hydroxymesocarb were detected; *p*-hydroxymesocarb accounted only for 11.4 and 14.2%, depending on the enzyme used (Fig. 7A). When the sample was incubated in the same conditions without

enzyme, no free *p*-hydroxymesocarb was detected, indicating that this compound is formed due to the enzymatic activity.

After longer incubation times (up to 144 h) with β -glucuronidase from *E. coli*, no increase in the amount of free *p*-hydroxymesocarb was observed. However, similar incubation of the urines with β -glucuronidase-arylsulphatase from *H. pomatia* led to complete hydrolysis of the conjugate to *p*-hydroxymesocarb.

When the samples were hydrolysed after extraction of conjugated *p*-hydroxymesocarb from the urines (Fig. 7B), only traces of *p*-hydroxymesocarb were detected when conventional incubation (55°C, 1 h) with *E. coli* was used. On the other hand, conventional incubation (55°C, 3 h) with *H. pomatia* led to nearly complete hydrolysis of the conjugate to *p*-hydroxymesocarb. Further studies are needed to determine the reason (*i.e.*, the absence of interfering salts) for the higher rate obtained when the hydrolysis takes place after extraction of the conjugate compared with that obtained when the hydrolysis is performed directly in the urine.

Based on these results, conjugation of *p*-hydroxymesocarb with glucuronic acid appears to be a minor metabolic route and the conjugate of *p*-hydroxymesocarb extracted from the urines

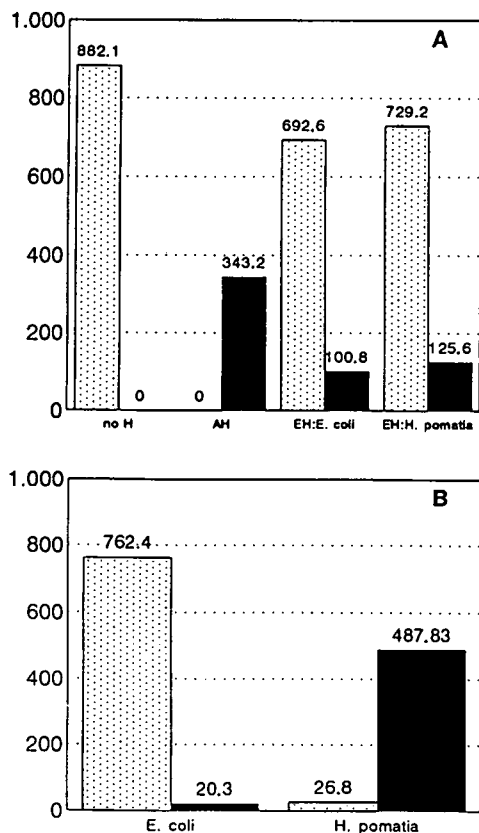


Fig. 7. Mean ($n = 3$) of the areas of the peaks of conjugated (dotted area) and free (solid area) *p*-hydroxymesocarb obtained after hydrolysis studies. (A) Comparison of different hydrolyses of the urines (no H = no hydrolysis; AH = acidic hydrolysis; EH = enzymatic hydrolysis); (B) enzymatic hydrolysis with *E. coli* or *H. pomatia* of the conjugate of *p*-hydroxymesocarb previously extracted from the urine.

and detected in the HPLC–UV screening appears to be a sulphate.

CONCLUSIONS

A HPLC–UV screening method is used routinely in our laboratory to screen for the presence of mesocarb, diuretics and other banned compounds in urine [4]. Its application

during the 1992 Barcelona Olympic Games allowed the detection of a real positive case. The confirmation was performed HPLC–MS of the non-hydrolysed and hydrolysed urines, and also by GC–MS with identification of the pyrolysis product. Figs. 2, 3, 5 and 6 correspond to this positive urine. Similar results to those presented in these figures were obtained with control urines from the above-cited excretion studies carried out in the same analytical batch. These results illustrate the utility of the described method to detect the ingestion of mesocarb during routine doping control analyses.

ACKNOWLEDGEMENTS

The collaboration of M.J. Pretel, A. Solans, M. Salmerón and M. Carnicero and helpful discussions with Dr. J.A. Pascual and Dr. R. de la Torre are gratefully appreciated. The technical assistance of R. Masagué is acknowledged. The authors thank Professor M. Donike for the supply of Sydnocarb tablets.

REFERENCES

- 1 Medical Commission, International Olympic Committee, *International Olympic Charter Against Doping in Sport*, IOC, Lausanne, 1990, updated December 1991.
- 2 J. Tamás, M. Polgár, G. Czira and L. Vereczkey, in *Proceedings of the 5th International Symposium on Mass Spectrometry in Biochemistry and Medicine, Rimini (Italy), 1978*, p. 43.
- 3 M. Polgár, L. Vereczkey, L. Szporny, G. Czira, J. Tamás, E. Gács-Baitz and S. Holly, *Xenobiotica*, 9 (1979) 511.
- 4 R. Ventura, T. Nadal, P. Alcalde, J.A. Pascual and J. Segura, *J. Chromatogr.*, in press.
- 5 M. Donike, personal communication.
- 6 R. Ventura, T. Nadal, M.J. Pretel, A. Solans, J.A. Pascual and J. Segura, in M. Donike, H. Geyer, A. Gotzmann, U. Mareck-Engelke and S. Rauth (Editors), *Proceedings of the 10th Cologne Workshop on Doping Analysis, Cologne (Germany), 1992*, Sport und Buch Strauss, Edition Sport, Cologne, 1993, pp. 231–248.
- 7 T. Cairns and E.G. Siegmund, *Anal. Chem.*, 54 (1982) 2456.

CHROMSYMP. 2771

Evaluation of liquid chromatography–thermospray mass spectrometry in the determination of some phenylglycidyl ether–2'-deoxynucleoside adducts

F. Lemière

Department of Chemistry, University of Antwerp (RUCA), Groenenborgerlaan 171, B-2020 Antwerp (Belgium)

E.L. Esmans*

Department of Chemistry, University of Antwerp (RUCA), Groenenborgerlaan 171, B-2020 Antwerp (Belgium) and Departments of Biology and Chemistry, University of Antwerp (UIA), Universiteitsplein 1, B-2610 Wilrijk (Belgium)

W. Van Dongen

Department of Chemistry, University of Antwerp (RUCA), Groenenborgerlaan 171, B-2020 Antwerp (Belgium)

E. Van den Eeckhout

College of Pharmacy, University of Ghent, Harelbekestraat 72, B-9000 Ghent (Belgium)

H. Van Onckelen

Department of Biology, University of Antwerp (UIA), Universiteitsplein 1, B-2610 Wilrijk (Belgium)

ABSTRACT

The adducts formed between 2'-deoxyadenosine (dAdo), 2'-deoxycytidine (dCyd) and 2'-deoxyuridine (dUrd) and phenyl glycidyl ether (PGE) were analysed by HPLC and LC–thermospray (TSP)–MS. Good results were obtained on a 10 RP Select B column (12.5 cm × 4 mm I.D.) using 0.1 M NH₄OAc–CH₃OH at a flow-rate of 0.8 ml/min. The mass spectra of the 2'-deoxynucleoside–PGE adducts, obtained under LC–TSP–MS conditions were all characterized by the presence of the protonated molecule [MH]⁺ and [BH + H]⁺ ions. The PGE–dCyd adduct underwent hydrolytic deamination to the corresponding PGE–dUrd adduct. There was an indication that this process of hydrolytic deamination also took place in the TSP interface. Localization of the alkylation site was possible in the PGE–dUrd adduct by the presence of an RDA rearrangement leading to a fragment ion at *m/z* 194. Preliminary sensitivity studies on PGE–dUrd showed a detection limit of 500 pg (signal-to-noise ratio = 2) in multiple ion monitoring at *m/z* 263 and 379.

* Corresponding author. Address for correspondence:
Department of Chemistry, University of Antwerp
(RUCA), Groenenborgerlaan 171, B-2020 Antwerp, Belgium.

INTRODUCTION

Epoxides are important chemicals which are frequently used in numerous industrial chemical

processes. From a number of investigations it is clear that some of these epoxides, depending on the structure, are mutagenic. Therefore, the study of the interaction of these epoxides with DNA is warranted.

In the past, the interaction between these epoxides and DNA or nucleosides has been investigated mainly with the aid of HPLC and UV-Vis data. In a few instances chemical ionization mass spectrometry has been reported for the identification of adducts formed with small aliphatic epoxides [1,2], but the full potential of mass spectrometric techniques has certainly not been elaborated to its full extent.

EXPERIMENTAL

Instrumentation and materials

Off-line HPLC experiments were carried out on a Hewlett-Packard (Brussels, Belgium) Model 1090 liquid chromatograph equipped with an automatic injection system, a diode-array detector and a Hewlett-Packard Model 9000/300 data system. Separations were performed on a 5- μ m particle size RP-18 column (15 cm \times 4.6 mm I.D.) [Bio-Rad, Ghent (Eke), Belgium] and a 5- μ m particle size LiChrospher 60 RP-Select B column (12.5 cm \times 4 mm I.D.) (Merck, Darmstadt, Germany). HPLC spectro-grade methanol was purchased from Alltech (Applied Science Labs., Deerfield, IL, USA). Methylene dichloride, tetrahydrofuran (THF) and CCl₄ (Caldic, Hemiksem, Belgium) were distilled three times prior to use. 2'-Deoxyuridine (dUrd), 2'-deoxycytidine (dCyd) and 2'-deoxyadenosine (dAdo) were obtained from Janssen Chimica (Beerse, Belgium). Phenyl glycidyl ether was supplied by Fluka (Bornem, Belgium) and distilled prior to use. Ammonium acetate (analytical-reagent grade) was purchased from Janssen Chimica and a 0.1 M solution was prepared using Millipore Milli-Q purity water.

Thermospray (TSP) mass spectra were recorded on a VG-2000 quadrupole mass spectrometer equipped with a Waters HPLC system consisting of a Waters 600-MS pump, a Waters 700 satellite W 158 autosampler and a Waters 486 UV-Vis detector set at 260 nm. The source temperature was 250°C unless stated otherwise.

The temperature of the thermospray capillary was ca. 200°C and was optimized on the solvent clusters. The repeller was operated between 175 and 180 V unless stated otherwise. The scan time was 1.0 s for a scan range from 100 to 550 u. In the multiple ion detection (MID) mode the dwell time was 100 ms. It should be noted that in the LC-TSP-MS set-up, the UV detector is installed between the HPLC column and the TSP interface. Therefore, the retention times found in the UV trace and the ion chromatograms are slightly different.

Synthesis of PGE-2'-deoxynucleoside compounds

A solution of 2 mg of a 2'-deoxynucleoside in 2 ml of methanol and 1 ml of a 1 M methanolic solution of phenyl glycidyl ether was stirred at 37°C in a Pierce Reacti-vial. After 24 h the solution was evaporated and the residue dissolved in 1 ml of water. The mixture was extracted twice with 4 ml of CCl₄ to remove the excess of PGE. The aqueous layer was evaporated under reduced pressure on a rotary evaporator. The residue was dissolved in 1 ml of water and used for HPLC and LC-MS analyses.

Semi-preparative synthesis of the adduct of PGE-dUrd

In order to investigate the detection limit, the PGE-dUrd-adduct was prepared and isolated by circular centrifugal thin-layer chromatography (TLC) as outlined below. The yield of the reaction between dUrd and PGE is low. Therefore, PGE was reacted with dCyd and the corresponding PGE-dCyd adduct was converted into the PGE-dUrd adduct by hydrolytic deamination.

A solution of 50 mg of dCyd in 50 ml of CH₃OH and 25 ml of a 1 M methanolic solution of PGE was stirred at 37°C. After 4 days, 10 ml of water were added and the mixture was heated under reflux for 24 h. The reaction mixture was evaporated, the residue dissolved in 25 ml of water and the solution extracted twice with 50 ml of CCl₄. The aqueous layer was lyophilized and the residue was dissolved in 1 ml of THF containing 3 drops of CH₃OH. This solution was purified by semi-preparative centrifugal TLC on

a Chromatotron (Harrison Research, Palo Alto, CA, USA) [Kieselgel 60 F₂₅₄, CaSO₄, 2-mm layer thickness, mobile phase THF–CH₂Cl₂ (40:60), flow-rate 7 ml/min). Three bands were collected: $R_F = 0.77$, 1-methoxy-2-hydroxy-3-phenoxypropane (methoxy-PGE); $R_F = 0.64$, PGE-diol; and $R_F = 0.38$, PGE-dUrd. Under these conditions, unreacted dCyd and PGE-dCyd have R_F values of almost zero and can be eluted by switching to 100% CH₃OH. Each PGE-dUrd fraction collected was evaporated to dryness and the residue dissolved in 0.5 ml of CH₂Cl₂ and purified a second time on the Chromatotron but using THF–CH₂Cl₂ (50:50). Two bands were collected: $R_F = 0.64$, PGE-diol; and $R_F = 0.14$, PGE-dUrd. The purity of the PGE-dUrd fraction was checked by TLC; a small amount of PGE-diol (<2%) was still present. At present a semi-preparative HPLC method using a poly(styrene–divinylbenzene) copolymer column (PRP1) in order to remove the last traces of PGE-diol is being investigated.

RESULTS AND DISCUSSION

If DNA is allowed to react with epoxides, covalent adducts are formed because the epoxides react with different nucleophilic sites on the purine and pyrimidine moieties. The assignment of the point of attachment on the heterocyclic moiety is certainly an important aspect of these studies and it has been shown that UV data on the isolated adducts can give an idea of the alkylation site [3]. However, it is our belief that assignment of the alkylation site based solely on the UV data can be risky and that other independent methodologies should be developed in order to obtain additional information.

In the past, the adducts formed between a series of 2'-deoxynucleosides and PGE have been analysed by HPLC and identified by fast atom bombardment (FAB) MS [4–8]. In view of experiments planned with calf thymus DNA, we started to investigate the possibilities of using LC–TSP–MS in this particular application.

As shown previously [5,6], the PGE–2'-deoxynucleoside adducts (see Fig. 1) can be analysed by reversed-phase chromatography on a standard 25 cm × 4.6 mm I.D. RP-18 column using differ-

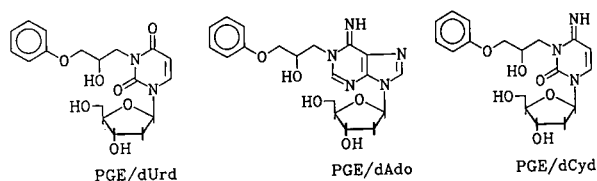


Fig. 1. Structures of PGE–2'-deoxynucleoside adducts.

ent ratios of methanol and water (0.1 M HCOONH₄, pH 5.1) at a flow-rate of 1.8 ml/min. However, especially with the purine series, better results could be obtained on a poly(styrene–divinylbenzene) copolymer column. In most instances the total analysis time was *ca.* 40 min. Because LC–TSP–MS experiments require a flow-rate of 0.8–1 ml/min, we realized that under these conditions the analysis of a PGE–2'-deoxynucleoside mixture on a 25-cm RP column would be impractical. Therefore, we decided to evaluate two short RP columns, *i.e.*, a 15 cm × 4.6 mm I.D. 5RP-18 and a 12.5 cm × 4 mm I.D. 5RP-8 Select B column. Both columns were mounted on an HP 1090 HPLC system equipped with a diode-array detector.

5RP-18 column

In order to evaluate this column, the reaction mixture obtained from the interaction between dAdo and PGE was analysed using different ratios of CH₃OH and 0.1 M NH₄OAc (pH 5.1). Provided the excess of PGE present in the reaction mixture was removed by extraction with CCl₄, good results were obtained with CH₃OH–0.1 M NH₄OAc (45:55) (see Fig. 2).

Five compounds were detected with k' values

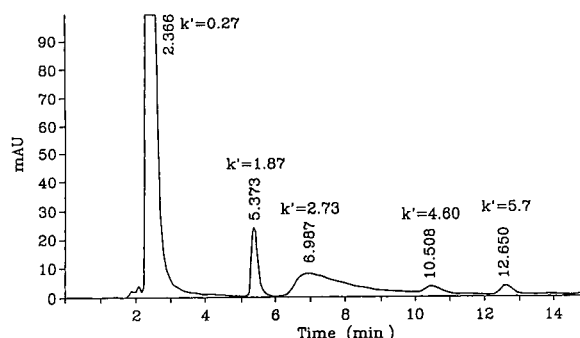


Fig. 2. HPLC of a PGE–dAdo mixture on a 5RP-18 column (detection at 260 nm) using CH₃OH–0.1 M NH₄OAc (45:55). Flow-rate, 0.8 ml/min.

of 0.27, 1.87, 2.73, 4.60 and 5.7. The last compound was identified as unreacted PGE, still present in small amounts after extraction. The compound with $k' = 0.27$ was unreacted dAdo. Identification was achieved with the aid of reference compounds and by examining the UV data. The UV spectra of the compounds with $k' = 1.87$ and 4.60 were very similar to that of PGE, suggesting a structural relationship. The compound with $k' = 2.73$, characterized by an asymmetric peak shape, was tentatively assigned to the PGE–dAdo adduct until further LC–TSP–MS data became available.

Analogous conditions were applied to the analysis of the PGE–dUrd and PGE–dCyd reaction mixtures. In all these instances CH_3OH – $0.1\text{ M NH}_4\text{OAc}$ (55:45) gave a baseline separation of all compounds together with a short analysis time. With the PGE–dUrd reaction mixture again five compounds were detected with k' values of 0.16, 1.81, 2.19, 5.28 and 7.30. The compound with $k' = 0.16$ was identified as dUrd. For the k' value of 2.19 (retention time 5.79 min), the PGE–dUrd adduct was assigned from the UV data. Almost the same features were observed with the PGE–dCyd reaction mixtures: five compounds with k' values of 0.12, 1.82, 2.93 (broad) 5.27 and 7.16 were found. However, an extra component eluted after 6.02 min ($k' = 2.21$). From preliminary inspection of the UV data for the different compounds present in the mixture, the products with k' values of 2.21 and 2.93 could be PGE–2'-deoxynucleoside adducts.

5RP-8 Select B column

Asymmetric peaks on an RP column are often the result of interactions of basic components with residual silanol groups or can be due to pH-dependent equilibrium phenomena. These asymmetric broadened peaks were observed in the chromatograms of PGE–dAdo and PGE–dCyd reaction mixtures when analysed on a 5RP-18 column. Therefore, all the analyses described above were repeated on a 5RP-8 Select B column using CH_3OH – $0.1\text{ M NH}_4\text{OAc}$ (45:55). As shown in Fig. 3, all asymmetric peaks were absent under these chromatographic conditions.

More detailed examination of the results ob-

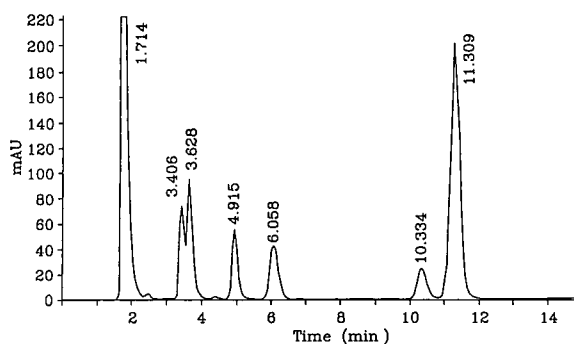


Fig. 3. HPLC of a PGE–dCyd mixture on a 5RP-8 Select B column (detection at 260 nm) using CH_3OH – $0.1\text{ M NH}_4\text{OAc}$ (45:55). Flow-rate, 0.8 ml/min.

tained for the PGE–dCyd reaction mixture showed partial resolution of the compounds eluting around 3.5 min. As the corresponding UV data were identical, we assumed that under these conditions both epimers were separated. This assumption was confirmed later by the LC–TSP–MS data.

LC–TSP–MS

The mixtures described above were analysed by LC–TSP–MS using CH_3OH – NH_4OAc (40:60) (pH 5.1) on a 5RP-8 Select B column at a flow-rate of 0.8 ml/min. The instrument was tuned as such that the intensity of the solvent clusters was optimized. The optimum temperature of the thermospray capillary was usually around 200°C . The source temperature was 250°C unless stated otherwise.

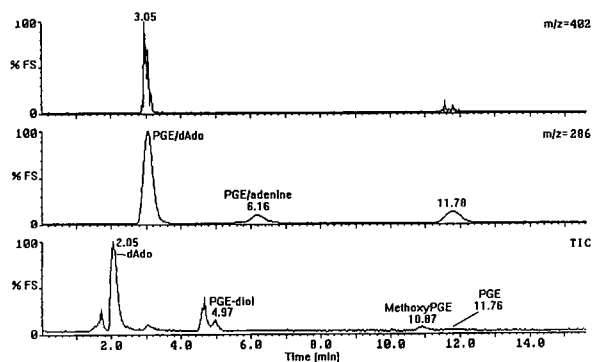


Fig. 4. LC–TSP–MS of a PGE–dAdo on a 5RP-8 Select B column using CH_3OH – $0.1\text{ M NH}_4\text{OAc}$ (40:60). Flow-rate, 0.8 ml/min. $[\text{MH}]^+ = m/z\ 402$; $[\text{BH} + \text{H}]^+ = m/z\ 286$.

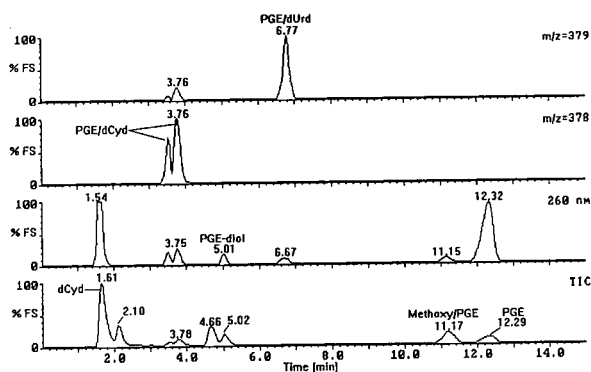


Fig. 5. LC-TSP-MS of a PGE-dCyd mixture on a 5RP-8 Select B column using CH_3OH -0.1 M NH_4OAc (45:55). Flow-rate, 0.8 ml/min.

Analyses of the PGE-dAdo reaction mixture (see Fig. 4) confirmed the presence of unreacted dAdo ($t_r = 2.05$ min) and a PGE-dAdo adduct ($t_r = 3.05$ min). Unreacted dAdo was characterized by the presence of a protonated molecule $[\text{MH}]^+$ at m/z 252 (23%) and an $[\text{M} + \text{Na}]^+$ adduct at m/z 274 (9%). Other ions present were $[\text{BH} + \text{H}]^+$ (m/z 136; 100%), $[\text{BH} + \text{Na}]^+$ (m/z 158; 7%) and m/z 117 ($[\text{S}]^+$; 8%). The PGE-dAdo adduct was localized with the aid of the reconstructed ion chromatogram for m/z 402 ($[\text{MH}]^+$) and its mass spectrum was characterized by m/z 402 (7%), 286 ($[\text{BH} + \text{H}]$; 100%), 268 ($[\text{BH} + \text{H}]^+ - \text{H}_2\text{O}$; 92%), 366 ($[\text{MH}]^+ - 2\text{H}_2\text{O}$; 8%) and 348 ($[\text{MH}]^+ - 3\text{H}_2\text{O}$; 3%). If the reconstructed ion chromatogram for m/z 286 was selected, another compound with $t_r = 6.16$

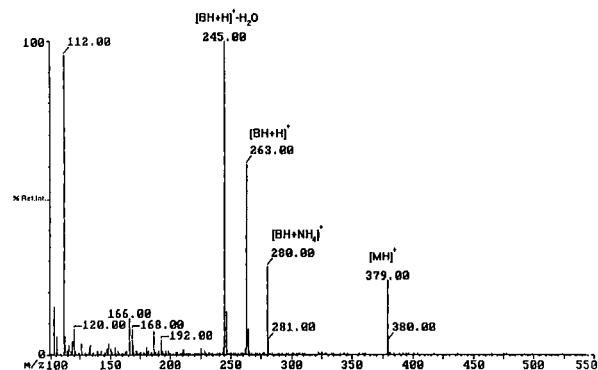


Fig. 6. Mass spectrum of the PGE-dUrd adduct in the PGE-dCyd mixture ($t_R = 6.77$ min).

min responded. Its mass spectrum was characterized by ions at m/z 286 ($[\text{MH}]^+$; 100%), 268 ($[\text{MH} - \text{H}_2\text{O}]^+$; 12%) and 136 ($[\text{MH} - \text{PGE}]^+$) and therefore identified as a PGE-adenine adduct. Whether this compound was formed by a depurination reaction or by reaction of PGE with a minor amount of adenine present in dAdo has not been clarified. All other compounds were PGE or PGE-derived: $t_r = 4.97$ (PGE-diol), 10.87 (monomethoxy-PGE derivative) and 11.76 (PGE). However, as can be seen in Fig. 4, a second compound characterized by m/z 402 and 286 is present. This compound co-elutes with PGE. This means there are two PGE-dAdo adducts present in the reaction mixture. They are monoalkylated at different positions on the heterocyclic moiety.

The total ion chromatogram obtained for the PGE-dCyd reaction mixture is shown in Fig. 5. PGE-dCyd eluted after 3.75 min and its mass spectrum was characterized by ions at m/z 378 ($[\text{MH}]^+$; 2%), 262 ($[\text{BH} + \text{H}]^+$; 23%) and 244 ($[\text{BH} + \text{H}]^+ - \text{H}_2\text{O}$; 23%) (see Fig. 7). When the chromatogram depicted in Fig. 5 was examined more closely, it was observed that two unresolved compounds were eluting around 3.75 min. The spectra of both compounds were identical. This led us to the conclusion that the two epimers of the PGE-dCyd adduct were partially resolved. Other known components, PGE-diol ($t_r = 5.01$ min), methoxy-PGE ($t_r = 11.15$ min) and PGE ($t_r = 12.32$ min), could easily be assigned from the mass spectral data. Unreacted dCyd had a retention time of 1.54 min.

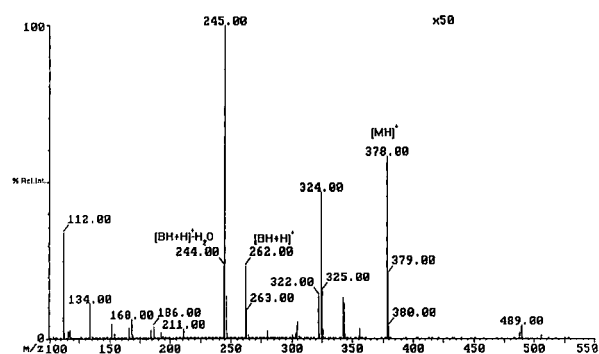


Fig. 7. Mass spectrum of the PGE-dCyd adduct in the PGE-dCyd mixture ($t_R = 3.75$ min).

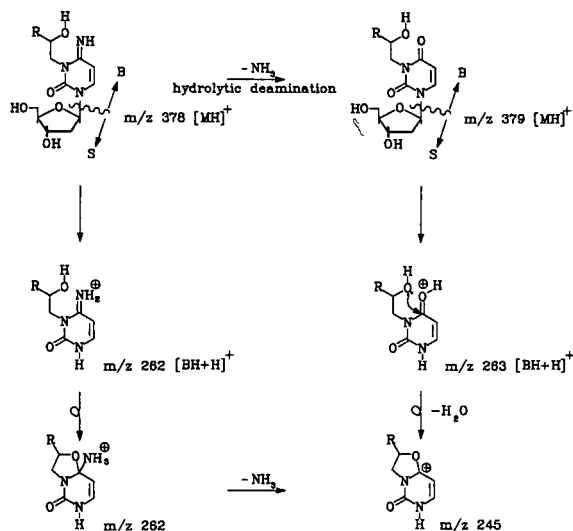


Fig. 8. Possible pathways for the formation of m/z 245 in the TSP-MS of PGE-dCyd.

Conversion of PGE-dCyd into PGE-dUrd

In a study published by Solomon and co-workers [1,2], it was found that the adduct formed between propylene oxide and dCyd had a limited lifetime in aqueous solution and was converted into the corresponding dUrd adduct by hydrolytic deamination. Such observations were also made here with the PGE-dCyd adduct. Indeed,

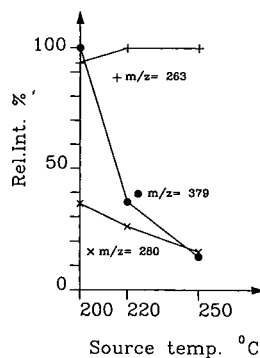


Fig. 10. Influence of the source temperature on the intensity of some diagnostic ions in the mass spectrum of PGE-dUrd. [MH]⁺ = m/z 379; [BH + H]⁺ = m/z 263; [BH + NH₄]⁺ = m/z 280.

when the LC-TSP-MS analysis of the PGE-dCyd reaction mixture was investigated further for the presence of ions typical of a PGE-dUrd adduct, a signal was observed in the reconstructed ion chromatograms not only at 6.77 min but also at 3.76 min, the retention time of the PGE-dCyd adduct (Fig. 5). The mass spectrum of the compound eluting at 6.77 min, depicted in Fig. 6, is characterized by ions at m/z 379 ([MH]⁺), 263 ([BH + H]⁺), 280 ([BH + NH₄]⁺) and 245 ([BH + H]⁺ - H₂O), which unequivocally

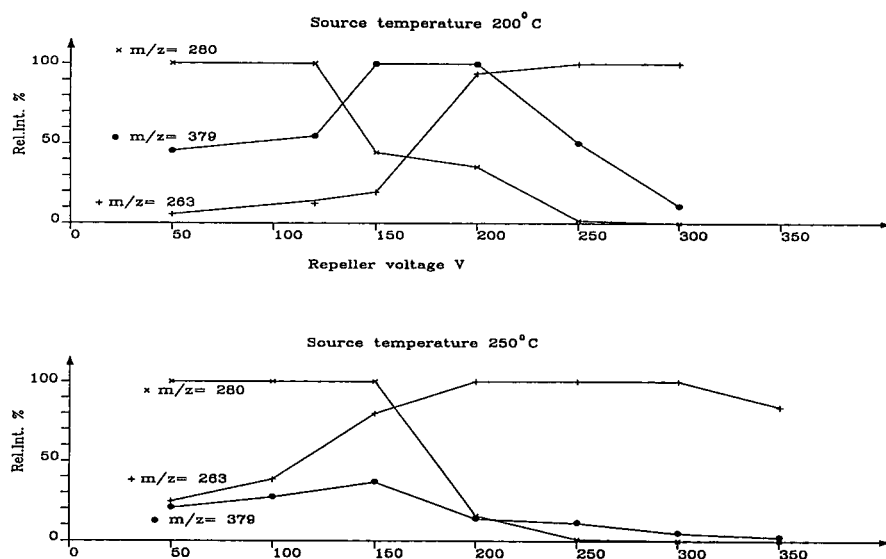


Fig. 9. Influence of the repeller voltage on the intensity of some diagnostic ions in the mass spectrum of PGE-dUrd. [MH]⁺ = m/z 379; [BH + H]⁺ = m/z 263; [BH + NH₄]⁺ = m/z 280.

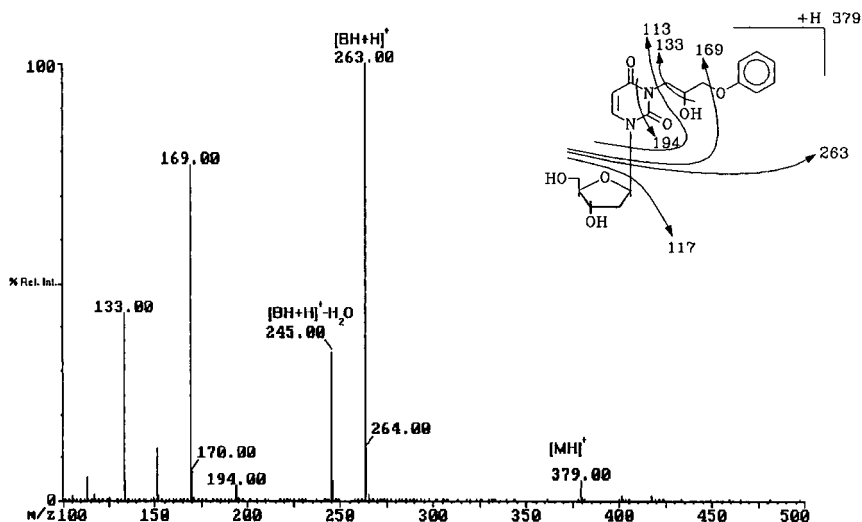


Fig. 11. Mass spectrum of the PGE–dUrd adduct. Repeller voltage, 300 V; source temperature, 250°C.

ally confirm the presence of PGE–dUrd in the reaction mixture.

When the mass spectrum of the PGE–dCyd adduct (see Fig. 7) was examined more closely, an intense ion at m/z 245 was observed and the relative abundance of the m/z 379 and 263 ions was higher than could be explained in terms of natural isotope abundance. Therefore, this phenomenon must be the result of a hydrolytic deamination of the PGE–dCyd adduct in the TSP interface.

Some diagnostic ions observed in the TSP mass spectrum of the PGE–dCyd adduct can be rationalized by Fig. 8. The fragment ion at m/z 244 can only be the result of the elimination of a molecule of H_2O from the $[BH + H]^+$ ion of the PGE–dCyd adduct. Whether the ion at m/z 245 is formed by elimination of NH_3 from the m/z 262 ion and/or by loss of H_2O from the m/z 263 ion is not known and should be resolved with the aid of isotopically labelled compounds.

Influence of repeller voltage

As it has been shown that the voltage applied on the repeller electrode can influence the TSP mass spectra, the mass spectrum of the PGE–dUrd adduct was recorded at fixed source temperatures (200 and 250°C) (see Fig. 9) but at different repeller voltages. The intensities of $[MH]^+$ (m/z 379), $[BH + H]^+$ (m/z 263) and

$[BH + NH_4]^+$ (m/z 280) are shown in Fig. 9. At low voltage (<150 V) $[BH + NH_4]^+$ predominates. Repeller voltages between 150 and 200 V gave optimum intensities for the molecular ion at m/z 379 $[MH]^+$ and the protonated base moiety at m/z 263 $[BH + H]^+$. Higher voltages (>200 V) resulted in increased fragmentation.

Influence of source temperature

The effect of the source temperature was evaluated at a constant repeller voltage of 200 V at 200, 220 and 250°C (see Fig. 10). As expected, the intensity of $[MH]^+$ rapidly diminished in favour of the $[BH + H]^+$ ion at m/z 263.

Alkylation site

In order to investigate whether LC–TSP–MS could give information about the alkylation site, the PGE–dUrd adduct was analyzed at a high repeller voltage and high source temperature (see Fig. 11). As already shown by Claereboudt [8], some daughter ions in the FAB tandem mass spectra of PGE–pyrimidine nucleoside adducts can be used for localization of the PGE moiety on the pyrimidine nucleus. Fig. 11 shows the LC–TSP–MS of PGE–dUrd (300 V; 250°C). An important ion that is diagnostic for the alkylation site was found at m/z 194, which can be explained by a retro Diels–Alder (RDA) rearrangement of the m/z 263 ion. Although these results

are very preliminary, the present data justify a deeper study.

Sensitivity

The purified PGE–dUrd adduct was used for sensitivity studies. Full-scan spectra (positive-ion mode, capillary temperature 205°C, source temperature 200°C) were obtained for 20 ng injected on-column. Using multiple-ion detection (m/z 263 and 379) 500 pg were detected at a signal-to-noise ratio of 2. In the near future, sensitivity will be evaluated in the negative-ion mode.

ACKNOWLEDGEMENTS

We thank the National Fund for Scientific Research for financial support and Merck-Belgolabo (Belgium) for the RP Select B column. F. Lemière thanks the IWONL for a grant.

REFERENCES

- 1 J.J. Solomon, K. Decker, F. Mukai and A. Segal, *36th ASMS Conference on Mass Spectrometry and Allied Topics, San Francisco, CA, 1988*, Abstracts, p. 929.
- 2 J.J. Solomon, K. Decker-Samuelian, F.-J. Li, F. Mukai and A. Segal, *38th ASMS Conference on Mass Spectrometry and Allied Topics, Tucson, AZ, 1990*, Abstracts, p. 1413.
- 3 E.L. Liebes, N. Guzman and L. Alterman, in A.M. Krstulovic, G. Zweig and J. Sherma (Editors), *CRC Handbook of Chromatography, Nucleic Acids and Related Compounds*, CRC Press, Boca Raton, FL, 1987, pp. 133–139.
- 4 J. Claereboudt, E.L. Esmans, E.G. Van den Eeckhout, W. Baeten and M. Claeys, *37th ASMS Conference on Mass Spectrometry and Allied Topics, Miami Beach, FL, 1989*, Abstracts, p. 923.
- 5 E. Van den Eeckhout, J. Coene, J. Claereboudt, F. Borremans, M. Claeys, E. Esmans and J. Sinsheimer, *J. Chromatogr.*, 541 (1991) 317.
- 6 E. Van den Eeckhout, A. De Bruyn, H. Pepermans, E. Esmans, I. Vrijens, J. Claereboudt and M. Claeys, *J. Chromatogr.*, 504 (1990) 113.
- 7 M.S. Bryant, J.O. Lay, Jr., and M.P. Chiarelli, *J. Am. Soc. Mass Spectrom.*, 3 (1992) 360.
- 8 J. Claereboudt, *Ph.D. Thesis*, University of Antwerp (UIA), Wilrijk, 1992.

CHROMSYMP. 2787

Surfactants: non-biodegradable, significant pollutants in sewage treatment plant effluents

Separation, identification and quantification by liquid chromatography, flow-injection analysis–mass spectrometry and tandem mass spectrometry

H.Fr. Schröder

Institut für Siedlungswasserwirtschaft, Technical University of Aachen, Templergraben 55, D-52056 Aachen (Germany)

ABSTRACT

Effluents from biological waste water treatment plants contain mainly non-biodegradable polar compounds. Methods for the detection, identification and determination of these hardly or non-eliminatable polar organic compounds are described. Flow-injection analysis (FIA) and liquid chromatographic (LC) separation on an analytical column by mass spectrometric (MS) and tandem mass spectrometric (MS–MS) detection coupled by a thermospray (TSP) interface were performed. The results showed that non-ionic surfactants and their metabolites (primary degradation products) besides linear alkyl benzene sulphonates (LABS) may dominate the range of pollutants. LC–MS confirmed that retention time shifts may occur if waste water extracts are separated on analytical columns. This cannot be recognized by UV detection. The identification of a biochemical degradation product of a non-ionic surfactant was carried out by both FIA–MS–MS and LC–MS–MS. Quantification of this compound was performed by standard addition analysis using FIA–MS or LC–MS in the selected-ion monitoring (SIM) mode. The time required for quantification is 25–30 times higher using LC–MS instead of FIA–MS.

INTRODUCTION

Normally, surfactants are discharged with waste water after application. In addition to their surface activity, these compounds should have a certain stability towards heat, hydrolysis and/or biochemical degradation according to the different application purposes. Although they are not classed with dangerous compounds within the meaning of Section 7a of the German Federal Water Act, their ecotoxicological potential must not be neglected because of the large amounts produced and applied. Depending on their structure, they have a more or less toxic effect on aquatic life forms such as fish, daphnia and algae [1]. Not only the chronic but also the acute

toxicity can be far below 1 mg/l. Some of these compounds are relevant in drinking water because of their high polarity. They have been detected in drinking water produced from river Rhine water [2]. The accumulation of these surfactants in biological sewage sludge is also worth mentioning. Surfactants are partially released from sludge used as fertilizer in agriculture or deposited on a landfill and are able to desorb and to dissolve highly toxic compounds adsorbed in the soil [3]. Together with toxic compounds, the surfactants will then appear in the groundwater [4].

Knowledge about the presence and concentration of such compounds in the environmental compartments water and soil is therefore of great

importance. For a long time, however, scientists have contented themselves with sum-parameter examination of these surfactants, which were distinguished only between three main types, anionic [5,6], cationic [7] and non-ionic [8,9]. However, interferences between the analytes and the matrix may arise, leading to high or low results. Biochemical degradation products of surfactants, so-called "primary degradation products", with only very small changes in the molecular structure with respect to the precursor compound, cannot be determined by these substance class-specific methods [10,11].

Substance-specific determination of these compounds is, in general, possible only after separation of the matrix compounds. As these compounds are only slightly or non-volatile, either large-scale derivatization reactions are necessary [12] to make gas chromatographic (GC) separation possible, or LC separation methods have to be employed for the non-volatile compounds. As, however, waste water extracts of municipal sewage treatment plants normally contain large numbers of surface-active compounds in each fraction even after preliminary separation, poor chromatographic separations and/or considerable retention-time shifts still result from such separations on analytical columns. If unspecific detectors such as UV, fluorescence, conductivity and refraction index types are employed, the results cannot be interpreted [13]. The application of the mass spectrometer as a specific detector, where separation can be achieved off-line [14] or by selective ionization methods [15], improved the analytical possibilities and led to high sensitivity in such examinations. The ionization methods fast atomic bombardment (FAB), field desorption (FD) and negative field desorption (NFD) did not produce fragments so that structure information could only be obtained after collisionally induced dissociation (CID) by tandem mass spectrometry (MS–MS) [14,16]. The use of MS–MS equipment allowed direct mixture analysis for the examination of complex mixtures [17,18] without chromatographic separation. However, great difficulties still remain during the detection and quantification of surfactants and their primary degradation products in environmental samples, even if these analytical techniques were applied.

In this paper, methods for the qualitative and quantitative determination of polar pollutants having been recognized as relevant (surfactants and their biochemical primary degradation products) in sewage treatment plant influents and effluents are presented. Analytical techniques using the MS–MS function of a tandem mass spectrometer for mixture analysis or performing CID after chromatographic separation on an analytical column should help to solve some of these problems.

EXPERIMENTAL

Materials

Waste water samples were taken from two different waste water treatment plants in the city of Aachen or from municipal treatment plants in northwest Germany located near the river Rhine. Waste water and sludge for the generation of metabolites were taken from a treatment plant in Aachen (Aachen-Süd).

The primary degradation product (metabolite) of alkanol polyglycol ether surfactants was generated by aeration of the sewage treatment plant influent and of bacterial sludge from this plant. During aeration the mixture was stirred and the degradation process was monitored by flow-injection analysis (FIA)–MS. The separation of this metabolite from the waste water matrix was carried out after C_{18} solid-phase enrichment and elution with hexane, hexane–diethyl ether (1:1, v/v), methanol–water (2:8, v/v) and methanol, the methanol eluate being collected. This procedure yields a mixture of more than 95% purity for the metabolite.

Water pollutants were extracted either using continuous liquid–liquid extraction or solid-phase extraction cartridges from Baker (Deventer, Netherlands). Solid-phase extraction materials were conditioned as prescribed by the manufacturer. Glass-fibre and membrane filters used for the pretreatment of the water samples were obtained from Schleicher & Schüll (Dassel, Germany). Before use, the glass-fibre and membrane filters were heated to 400°C or were treated with ultra-pure water obtained with a Milli-Q system (Millipore, Milford, MA, USA) for 24 h and then washed with 100 ml of the same water. Diethyl ether and methanol used for

the liquid–liquid extraction or desorption of water pollutants from the solid-phase material were Nanograde solvents from Promochem (Wesel, Germany). Acetonitrile, chloroform, dimethyl sulphoxide and methanol used for column-cleaning purposes were of analytical-reagent grade from Merck (Darmstadt, Germany). Nitrogen for drying of solid-phase cartridges was of 99.999% purity (Linde, Germany). All surfactant standards for identification via daughter ion spectral library and for waste water spiking purposes were gifts from the producers (Hüls, Marl; Hoechst, Frankfurt and BASF, Ludwigshafen, Germany) and were of technical grade. Polyethylene glycol (PEG 400) was of technical grade.

GC analyses were done on a DB-17 fused-silica column (J&W Scientific, Folsom, CA, USA) and helium of 99.999% purity (Linde) was used as the carrier gas. LC separations were done on a Nucleosil C₁₈ (5 μm, spherical) column (25 cm × 4.6 mm I.D.) (Chromatography Service Römer). The mobile phase was methanol and acetonitrile (HPLC grade) from Promochem and Milli-Q-purified water. Ammonium acetate for thermospray (TSP) ionization was of analytical-reagent grade from Merck.

Sampling, sample preparation and handling

All samples from the waste water treatment plants were taken as grab samples in glass bottles. The bottles were rinsed carefully with several portions of the same water that was subsequently stored in them. The storage temperature was 4°C.

For continuous liquid–liquid extraction, 2 l of waste water were extracted with 300 ml of diethyl ether over a period of 5 h. Liquid–liquid extracts were dried by anhydrous sodium sulphate, filtered and concentrated to 2 ml (influent) or 0.1 ml (effluent) under nitrogen, resulting in a concentration factor of 1000 or 20 000 respectively.

Depending on the degree of pollution, different amounts of water were used for solid-phase extraction. Water samples for FIA and LC–MS analysis were forced through the solid-phase extraction cartridges after passage through a glass-fibre filter. The adsorbed pollutants were desorbed separately. Solvents of different

polarities (hexane, hexane–diethyl ether, diethyl ether, water–methanol and methanol) were used for this purpose. All eluates except those with methanol and methanol–water were evaporated to dryness with a stream of nitrogen, and the residue was dissolved in 1 ml of methanol. The samples were rinsed into glass bottles after solid-phase extraction and freeze-drying was applied to enrich non-C₁₈-adsorbable compounds. After freeze-drying the samples were dissolved in 1 ml of methanol and used for FIA or LC–MS investigations.

Volumes of 1 or 2 μl of waste water extracts of influent and effluent, respectively, were injected for GC–MS analysis, and 20 or 100 μl of solid-phase eluates were injected for qualitative FIA–MS and LC–MS analysis, respectively.

A stock solution containing 12 μg/μl was prepared in order to determine the primary degradation product of the non-ionic surfactants. After evaporation of the solvents to dryness, three aliquots (2 ml) of the methanolic eluate of the waste water extract containing the unknown concentration of the metabolite were spiked with 50, 100 or 200 μl of the stock solution. The samples were diluted to 2 ml. This series of solutions were used to examine the relationship between the peak area and the concentration of the metabolites in both FIA–MS and LC–MS. For quantification by FIA–MS a minimum of five injections was made. The injection volumes for FIA–MS and LC–MS were 20 and 100 μl per injection, respectively.

Gas chromatographic system

A Varian (Darmstadt, Germany) Model 3400 GC system with a fused-silica capillary column was used. The conditions were as follows: carrier gas, helium; linear gas velocity, 15 cm/s; injector temperature, 250°C; transfer line temperature, 250°C; column, DB-17, film thickness 0.25 μm (30 m × 0.32 mm I.D.).

Combined with GC, electron impact (EI) ionization was applied with an ionization energy of 70 eV. Under these conditions the pressure in the ion source was $8 \cdot 10^{-6}$ Torr (1 Torr = 133.322 Pa) and in the vacuum system of the mass spectrometer $3 \cdot 10^{-2}$ Torr. The electron multiplier was operated at 1200 V with a conver-

sion dynode voltage at 5 kV. The temperature in the ion source was 150°C.

Liquid chromatographic system

LC separations coupled with MS, MS–MS and UV detection were achieved with a Waters (Milford, MA, USA) Model 600 MS system. A Waters Model 510 pump was used for post-column addition of 0.1 M ammonium acetate solution in the TSP mode. A Waters Model 490 MS UV detector was connected in-line with the TSP interface. The conditions in FIA bypassing the analytical column were as follows: mobile phase I, methanol–water (60:40); mobile phase II, 0.1 M ammonium acetate in water. The overall flow-rate was 1.5 ml/min with a ratio of 0.8 ml/min of mobile phase I and 0.7 ml/min of mobile phase II.

The chromatographic separations on the analytical column were carried out after optimization of the conditions by a standardized method, shown in Table I.

The flow-rate for column separation was 1.0 ml/min of mobile phase I. After passing the UV detector, 0.5 ml/min of mobile phase II was added, which resulted in an overall flow-rate of 1.5 ml/min.

The reversed-phase column was cleaned with a mixture of acetonitrile, chloroform, methanol and dimethyl sulphoxide (3:3:3:1, v/v) after finishing analysis and before equilibration for a new separation.

TABLE I
GRADIENT ELUTION SCHEME AND COMPOSITION OF MOBILE PHASE I

Solvent A = acetonitrile; solvent B = water–methanol (80:20, v/v).

Time (min)	Solvent A (%)	Solvent B (%)
0	10	90
10	30	70
25	60	40
35	90	10

MS and MS–MS systems

The mass spectrometer was a TSQ 70 combined with a PDP 11/73 data station. The TSP interface was obtained from Finnigan MAT. For coupling the LC system with the mass spectrometer, the conditions for TSP ionization using ammonium acetate were chosen as vaporizer temperature, 90°C and jet block temperature, 250°C. The conditions varied during the analytical separations. Under the above conditions the ion source pressure was 0.5 Torr and the pressure in the vacuum system of the mass spectrometer was $2 \cdot 10^{-5}$ Torr.

The electron multiplier was operated at 1200 V and the conversion dynode at 5 kV. In the MS–MS mode the ion source pressure was also 0.5 Torr. Under CID conditions the pressure in quadrupole 2 (collision cell) normally was 1.3 mTorr or is specified in the captions of the figures. The collision energy was adjusted from –10 to –50 eV. The electron multiplier voltage in quadrupole 3 was 1500 V with a conversion dynode voltage at 5 kV.

GC–MS analysis was performed by scanning at 1 s from 45 to 500 u.

FIA and LC analyses were applied, recording TSP mass spectra scanning from 150 to 1200 u at 1 or 3 s, respectively. FIA bypassing the analytical column with MS detection was performed accumulating 50 scans after injection. The mass spectrum averaging the total ion current from the beginning of the signal up to the end is called the “overview spectrum”.

TSP ionization was normally carried out in the positive mode, unless specified otherwise.

For quantification the mass spectrometer was operated in the selected ion monitoring (SIM) mode using a dwell time of 200 ms for each mass.

RESULTS AND DISCUSSION

The elimination of non-polar volatile compounds from municipal waste water in the biological waste water treatment process is successful with an efficiency of more than 95%, as the GC–MS total ion current (TIC) chromatograms (Fig. 1a and b) of a representative treatment plant influent and effluent demonstrate. Regard-

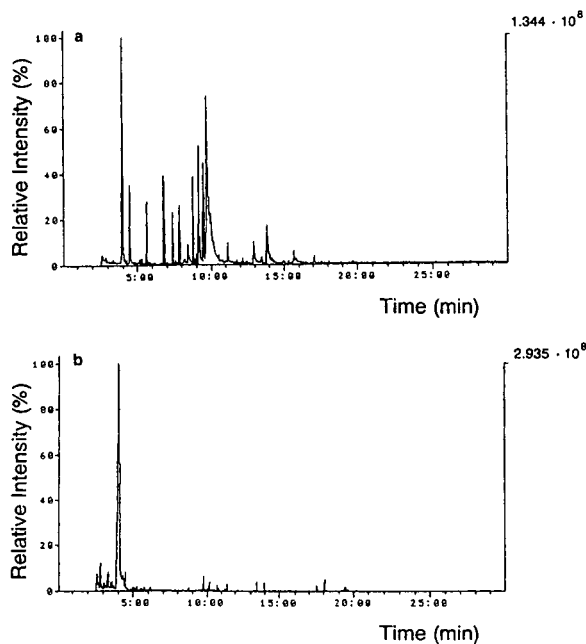


Fig. 1. (a) GC-MS total ion current trace for municipal waste water treatment plant influent. Liquid-liquid extract; solvent, diethyl ether. (b) GC-MS total ion current trace for the effluent of waste water treatment plant as in (a). For concentration factor, see Experimental.

ing the chromatograms the effluent seems to be relatively pure, although a concentration factor of 20 related to the influent extract was chosen. The examination of the influent and effluent by the sum parameter total organic carbon (TOC), however, showed an organic carbon load of 420 and 53 mg/l respectively. The examination of the same waste waters concerning polar organic compounds by means of liquid chromatography coupled with a TSP interface doing flow-injection analysis bypassing the analytical column (FIA-MS) gave mass spectra averaged from a maximum of 50 scans, as shown in Fig. 2a and b. This type of spectrum will be called here and later an "overview spectrum". Recording these spectra, the polar organic compounds existing in the extracts are registered in the form of their molecular and cluster ions, respectively, consisting of molecule and ammonium ion. Normally no fragments are produced in this way (compare the TSP ionization of alkyl ether sulphates [11]) and, consequently, no structure information, but

molecular mass information will be obtained. Thus, comparing the spectra shown in Fig. 2a and b and the intensities of the ion currents, it can be recognized that the number of signals, *i.e.*, of the different molecular ions has not decreased. The concentration of compounds in the water, however, has slightly decreased. This means that the elimination mechanisms of the biological treatment process are well able to eliminate non-polar compounds from the liquid phase; however, the efficiency of the waste water treatment process diminishes if polar anthropogenic compounds or those being formed chemically or biochemically during the sewage treatment process dominate the range of pollutants. This is caused by the physical properties of polar waste water compounds: on the one hand they cannot be stripped with air because of their polarity, but on the other hand they cannot be adsorbed at the lipophilic activated sludge. If they are then hardly biodegradable, or degradation is not possible because the compounds first have to be adsorbed on the activated sludge and then absorbed by the cell, they can be detected unchanged and only slightly decreased in the treatment plant effluent. This is especially true for surfactants as they are polar and, as described above, successfully resist any biochemical degradation because of their tasks and the properties connected with them.

Non-ionic surfactants of the polyethylene or polypropylene glycol ether type (Fig. 3a and b) can be clarified at once by their distinct pattern arising in the overview spectra in Fig. 2a and b generated by FIA-MS. Non-ionic surfactants of this type show equidistant signals at $\Delta m/z$ 44 and 58 when polyethylene or polypropylene glycol ether chains, respectively, are present. This finding, however, has to be checked by further examination, via the generation of characteristic daughter ions. In contrast to EI ionization after GC separation, where the ionized compounds are identified by their fragment spectra, unfortunately only molecular ions are typically generated during the TSP ionization process. This means that certain ions have to be selected by mass filtration before decomposing them by CID into fragment ions to permit a positive identification. For this procedure a spectrometer with an

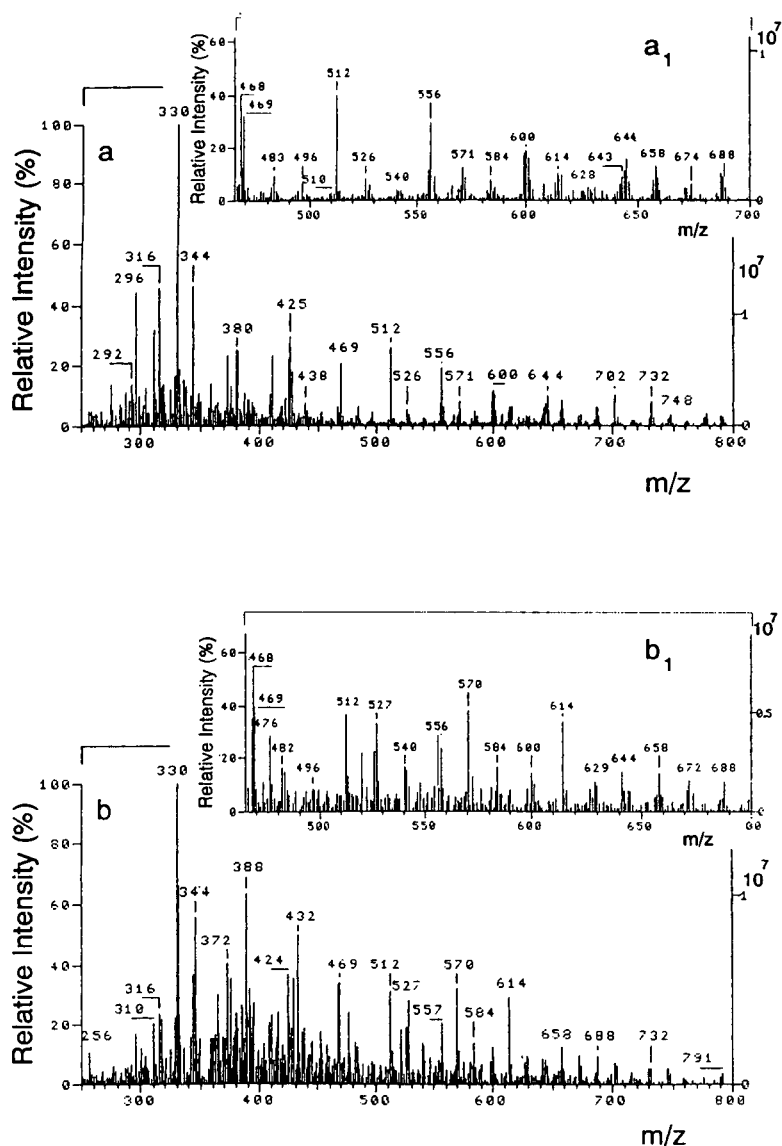


Fig. 2. (a) TSP-MS loop injection trace obtained by bypassing the analytical column (FIA-MS), subsequently called "overview spectrum", for waste water treatment plant influent as in Fig. 1a. (a₁) Detail of mass spectrum in (a). (b) FIA-MS overview spectrum of waste water treatment plant effluent as in Fig. 1b. (b₁) Detail of mass spectrum in (b). Positive TSP ionization. For FIA conditions, see Experimental. C₁₈ solid-phase extract; eluent, methanol.

MS-MS option is necessary. A laboratory-made, computer-aided daughter ion library may be very helpful in this instance [2] if a similar or the same compound is present.

The ions generated by positive ionization at m/z 316, 330 and 344 in Fig. 2a and b can be classed at once with an anionic surfactant — linear alkylbenzene sulphonic acid (LABS; see

Fig. 3c). This is demonstrated by generating negative daughter ions by CID, resulting in only the fragment at m/z 183. This fragment is characteristic of an unbranched alkylbenzene sulphonic acid (ABS) [19]. Negative TSP ionization, shown in Fig. 4, which is the typical ionization method for these waste water compounds, yields only compounds that can be

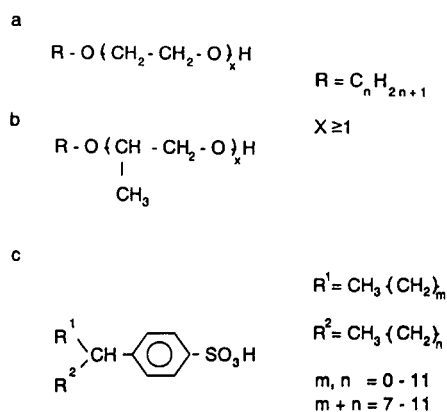


Fig. 3. Formulae of (a, b) non-ionic surfactants and (c) anionic surfactant. (a) Alkanol polyethylene glycol ether; (b) alkanol polypropylene glycol ether; (c) linear alkylbenzene sulphonic acid (LABS).

ionized negatively. In addition to the fragment ion at m/z 183 it confirms again this type of anionic surfactant. In the overview spectrum the signals of the negative LABS ions are at m/z 297, 311 and 325, generating the $[\text{M}-1]^-$ ions instead of the ammonium cluster ions $[\text{M}+\text{NH}_4]^+$ at m/z 316, 330 and 344 in the positive TSP mode.

The striking signals of the ions at m/z 468, 512, 556, etc., up to 732 appearing at $\Delta m/z$ 44 during positive TSP ionization (see Fig. 2a and b) can be classed with non-ionic surfactants of the polyethylene glycol ether type. Here negative ionization is not successful, and therefore they cannot be recognized in Fig. 4. The repre-

sentative daughter ion spectrum of the ion at m/z 468 chosen by mass filtration is shown in Fig. 5. It contains both the alkyl fragments at m/z 57, 71, 85, 99 and 113 which are characteristic of an alkanol polyglycol ether, and the polyglycol ether fragments at m/z 45, 89, 133 and 177 consisting of 1–4 ethylene glycol units. The fundamental structure of the surfactant, characterized by its daughter ion spectrum, is shown in Fig. 5. This or similar surfactants that differ in a characteristic way in their chromatographic behaviour from alkanol polyethers previously recorded [19,20] were not present in our daughter ion library.

Detailed reports are available that include excellent results concerning the examination of waters and waste waters for polar compounds by means of mixture analysis by MS–MS [2,13,16,18,21–24]. In this mode of operation, however, it is not always possible to obtain all the information necessary for identification and quantification. A chromatographic separation of the same extract that had previously been examined in the FIA–MS mode was carried out to obtain further information serving to confirm the structure proposed in Fig. 5. In parallel, UV traces at different wavelengths were recorded. A C_{18} analytical column and gradient elution according to Table I were chosen. The UV trace at 210 nm and the reconstructed ion current (RIC) of this separation are shown in Fig. 6a and b. Although this waste water extract was highly matrix charged, the chromatographic separation

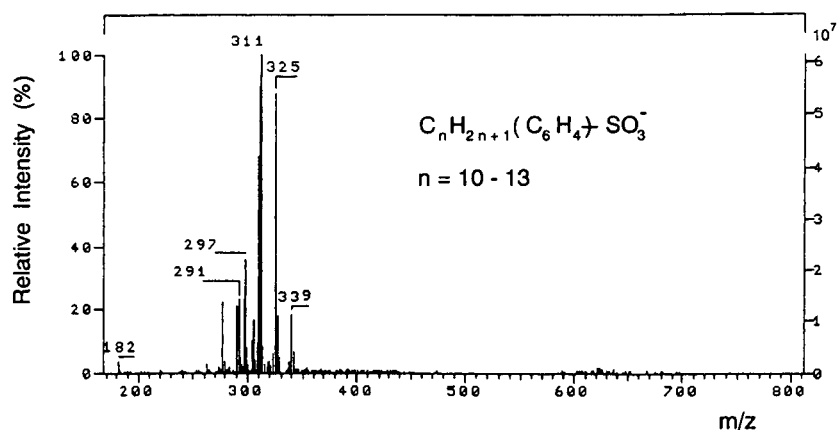


Fig. 4. FIA–overview mass spectrum as in Fig. 2b for extract of waste water treatment plant effluent. Negative TSP ionization.

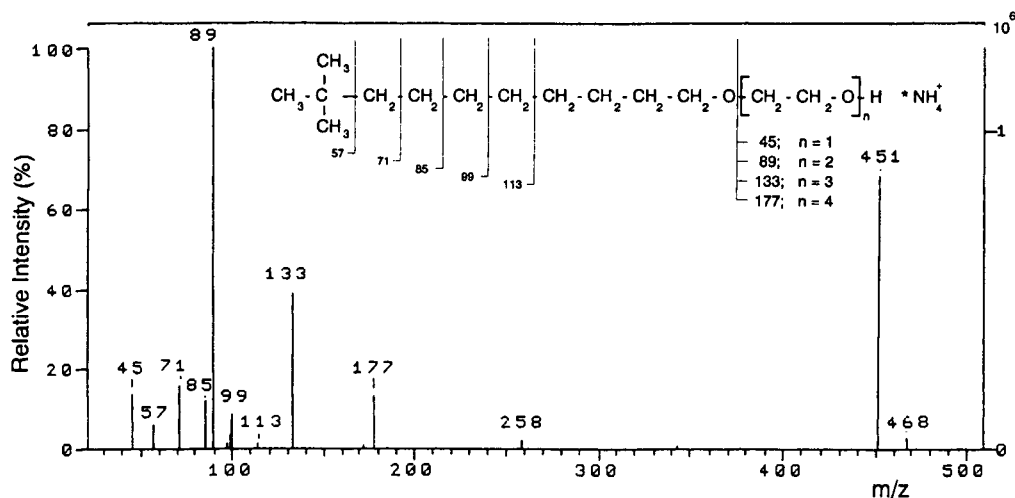


Fig. 5. Daughter ion mass spectrum (FIA-MS-MS) and fragmentation scheme of non-ionic surfactant cluster ion [m/z 468; $C_{12}H_{25}O(CH_2CH_2O)_nH \cdot NH_4^+$] from waste water extract (influent) as in Fig. 2a. Collision energy, -25 eV.

was very successful. As the mass spectra in Fig. 7 show, non-ionic surfactants are hidden under the three peaks marked 1, 2 and 3 in the UV spectrum and in the ion current trace. These surfactants are identical in their fundamental structure, as shown in Fig. 5; only the chain lengths of their polyether residue vary (compare peak 3 with peaks 1 and 2). The reason for the different retention times of the signals was first the number of polyether units in the ether chain. Second, as the daughter ion spectra recorded during chromatographic separation demonstrate, different isomeric surfactant structures are due to this effect. A UV spectrum recorded from 200 to 400 nm shows that these surfactants have an absorption at λ_{max} 203 nm, *i.e.*, they differ in their characteristic properties from alkanol propylene glycol ethers, which have an absorption below 190 nm [23].

Additional information about the presence of polyethylene glycols (PEGs) of different chain lengths was obtained during chromatographic separation. Usually these compounds are metabolites of biochemically well degradable non-ionic surfactants and represent the polar primary degradation products of these compounds in the biological waste water treatment process. If non-ionic surfactants are present in the influent of the sewage treatment plant, these metabolites appear in the waste water treatment process in

increasing concentration. Owing to the absence of a chromophore in the molecule they cannot be detected by UV spectrophotometry although these polar compounds may have a share of up to 15% of the organic carbon compounds in sewage treatment plant effluents.

Although the chance of a successful analytical separation can be increased during the elution step after enrichment on the solid-phase extraction cartridge by quasi-“selective” elution, new problems may arise. To effect selective elution, the polarity of the solvents and their mixtures used for desorption was increased. The overview spectra (Fig. 8) of the diethyl ether, methanol-water (2:8, v/v) and methanol eluates of the waste water extract, obtained using FIA, show a distinct pre-separation depending on the eluent chosen. Further examination of the extract obtained by methanol-water (2:8, v/v) elution, which should consist mainly of polyethylene glycols with 5–16 chain links (see Fig. 8b), leads to the UV trace at 210 nm and the ion current shown in Fig. 9a and b, respectively. Comparing the analytical separation of the eluate produced by “selective” elution (Fig. 9b) with the chromatogram of the total extract of the same waste water (Fig. 6b), it can be seen that an obvious retention time shift of the polyethylene glycols from one sample to another has taken place in spite of identical chromatographic conditions.

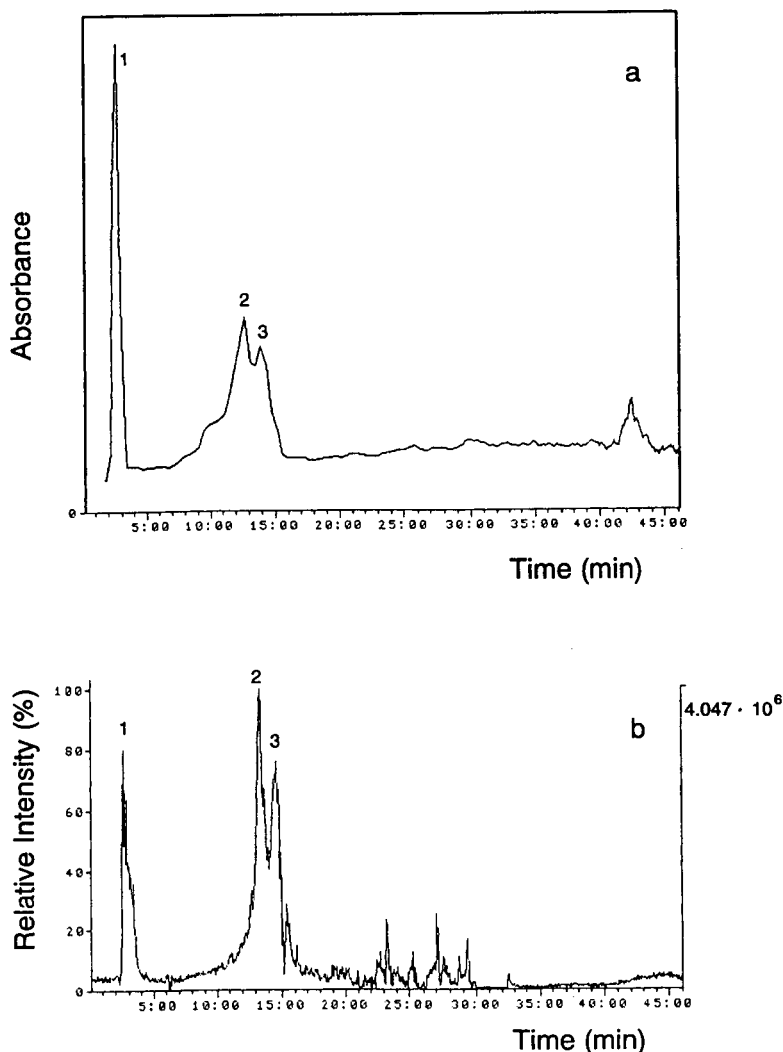


Fig. 6. (a) LC-UV (210 nm) trace for waste water extract as in Fig. 2a (influent). Enrichment and elution as in Fig. 2a; C_{18} column; for chromatographic conditions, see Experimental and Table I. (b) LC-MS total ion current trace of waste water extract in (a). LC conditions as in (a).

This phenomenon of uncontrollable retention time modification of identical samples under the same chromatographic conditions seems to be typical of waste water extracts, especially if they contain surface-active compounds [13]. Constancy of retention times in chromatographic separations of waste water extracts can only be achieved by time-consuming cleaning procedures, as described under Experimental, which have to be carried out between two analyses. These cleaning and equilibration phases are very

time and manpower consuming and restrict the sample throughput considerably. Fig. 10 shows a separation, which is reproducible, of a methanolic PEG standard solution without additional matrix compounds under the same chromatographic conditions as before and without intermediate cleaning steps. Possible problems of retention time shifts induced by matrix compounds can be recognized by means of specific detection with a mass spectrometer using mass chromatograms, as demonstrated in Fig. 11. This

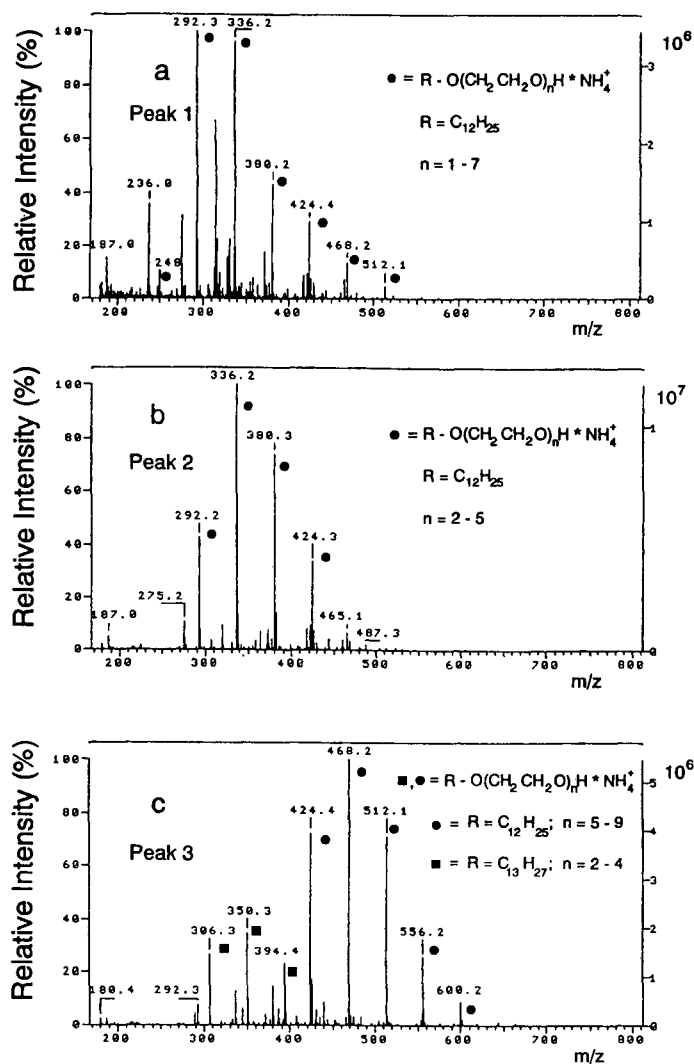


Fig. 7. LC-mass spectra of (a) peak 1, (b) peak 2 and (c) peak 3 in Fig. 6b.

method demonstrates whether a separation such as that shown in Fig. 8b for the matrix-charged waste water extract has been successful or not.

The difficulties during the examination of waste waters for unknown compounds, both by FIA-MS and after LC separation on analytical columns with subsequent MS detection and generation of daughter ions, have been considered earlier. Much greater problems arise, however, if for the anthropogenic compounds to be identified no standard compounds are available for comparison purposes or if corresponding spectra are absent from the daughter ion library. In spite

of the fact that these substances are components of common commercially available products, produced in large amounts and inevitably reaching waste waters, so far producers and distributors have made little or no effort to overcome this lack of information. Identification has to be achieved instead by interpreting CID spectra. This very time-consuming procedure becomes especially necessary if hardly degradable polar waste water compounds, in particular surfactants, are submitted to conventional biological treatment processing. Because of their polarity and persistence, the usual elimination

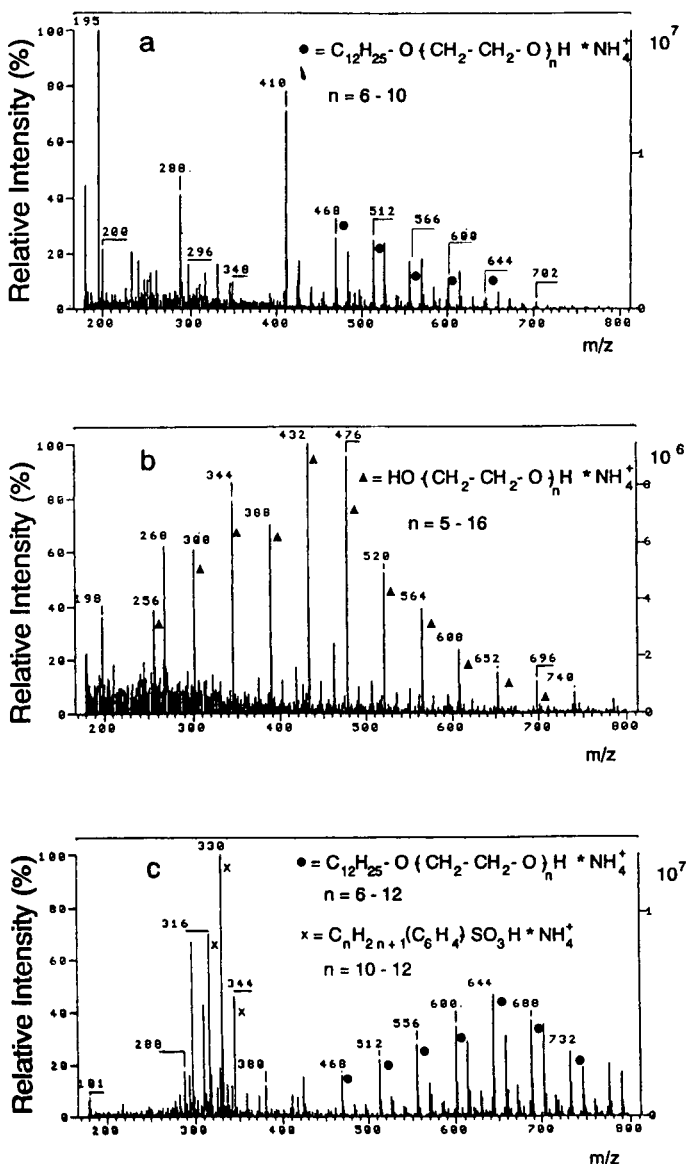


Fig. 8. FIA-overview mass spectra of (a) diethyl ether, (b) methanol-water (2:8, v/v) and (c) methanol eluates. C_{18} solid-phase extract of waste water as in Fig. 6b.

mechanisms of biochemical waste water treatment have no effect. Either the hardly degradable surfactants appear unchanged in the treatment plant effluent or the metabolites of these compounds are present in the water running off. These metabolites cannot be eliminated by stripping or adsorption because biochemical primary degradation has increased the polarity of the molecules. These compounds cannot be detected

by substance class-specific determination [5–9,11], but it is possible to determine them by MS [11] coupled with LC. This procedure requires a certain knowledge of the biochemical degradation pathways of the different types of surfactant in order to make a target analysis for the sought compounds in this matrix. Biochemical primary degradation of surfactants during waste water treatment may lead both to non-polar and polar

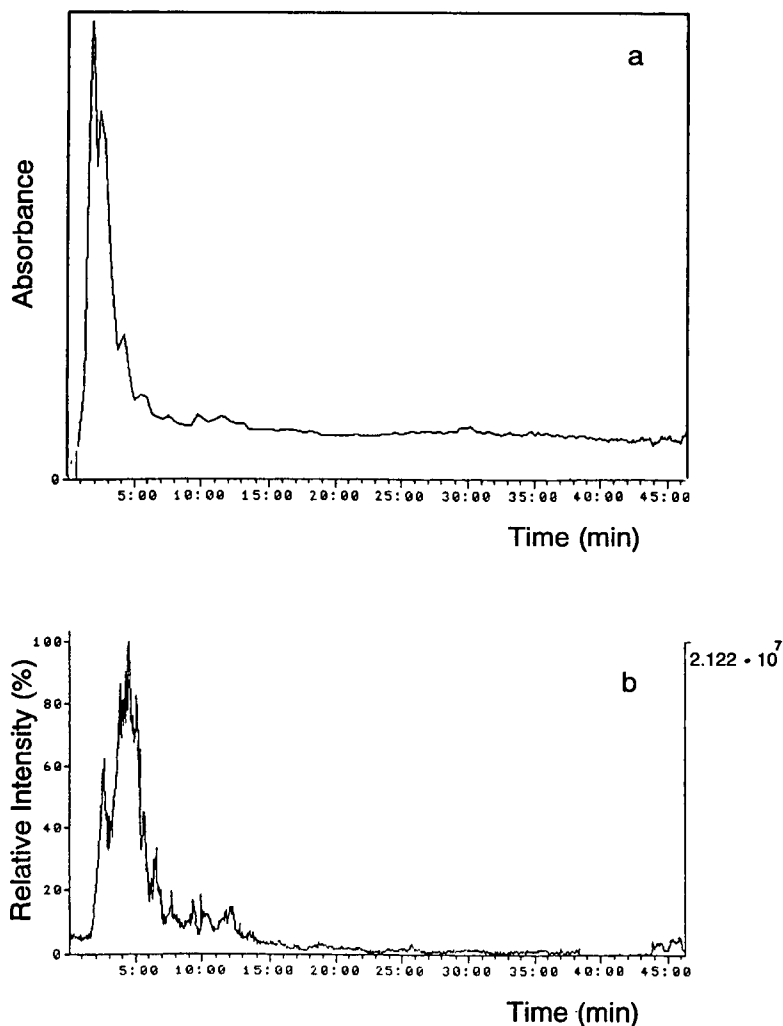


Fig. 9. (a) LC-UV (210 nm) trace for waste water extract. (b) LC-MS total ion current trace for the same extract. Enrichment and elution as in Fig. 8b. C_{18} column; for chromatographic conditions, see Experimental and Table I.

metabolites; the polar degradation products then dissolve in the waste water, whereas the non-polar products are adsorbed at the sludge. One of the best known examples is the degradation of nonyl- and octylphenol ethoxylates because in this instance the biogenic degradation product is more toxic than the original compound [25]. During primary degradation of these compounds the polyethylene glycol chain is cleaved, generating the polar metabolite PEG. Because of the loss of its hydrophilic polyether chain, the aromatic cyclic system with the coupled alkyl residue will then be found as a lipophilic alkylphenol in the activated sludge. Equally spaced

signals at m/z 44 or 58 help to identify the metabolites of non-ionic surfactant precursor compounds if the ether chain with polyethylene or polypropylene glycol units remains in the degradation product.

Additional problems arise during the quantification of primary degradation products both after chromatographic separation on an analytical column and by mixture analysis using MS-MS. The compound to be determined has to be available as a standard that has to be added to the samples in order to obtain reliable concentration data by the standard addition method. Any other procedure, *e.g.*, using compounds

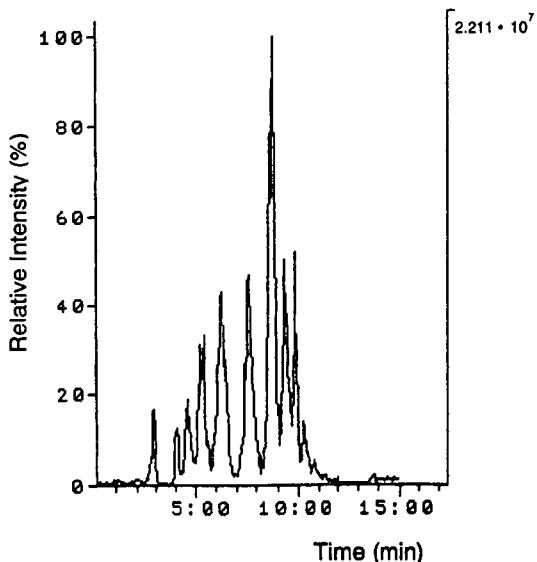


Fig. 10. LC-MS total ion current trace for standard solution of PEG 400. C₁₈ column; for chromatographic conditions, see Experimental and Table I.

resembling each other in structure, will provide an estimate. The ion current of the compound to be determined is dependent on its proton affinity. Interferences with matrix compounds will be larger in the FIA-MS mode, but cannot be excluded and even non-ionization can result. To

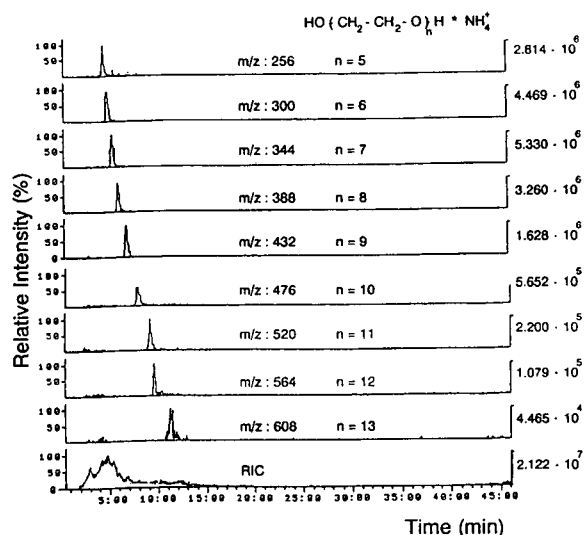


Fig. 11. LC-MS of PEG from total ion current trace for waste water extract in Fig. 8b. Chromatographic conditions as in Fig. 9.

exclude this source of error in our examinations, *i.e.*, for the determination of the primary degradation product of a non-ionic surfactant in the effluent of a sewage treatment plant in Aachen, we first generated in a batch experiment by biochemical degradation the metabolites in as pure a form as possible. These compounds dominate the effluent of the large-scale treatment plant (Fig. 12b) whereas the original compound, an alkanol polyethylene glycol ether, can be detected in the FIA-MS overview spectrum shown in Fig. 12a. By biochemical oxidation of the terminal hydroxyl function of the polyglycol ether, a carboxyl function has been formed that resists further biochemical degradation. Compounds of this type are able to pass through charcoal filters and could be detected in drinking water [26]. Precursor and metabolite compounds were identified by means of their CID spectra

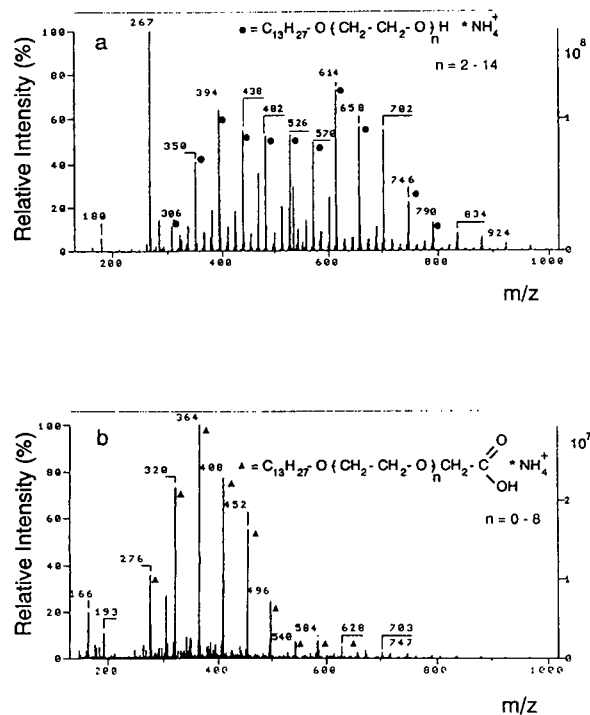


Fig. 12. (a) FIA-overview mass spectrum of waste water treatment plant influent containing surfactant molecules (●). C₁₈ solid-phase extract; eluent, diethyl ether; (b) FIA-overview mass spectrum of waste water treatment plant effluent containing metabolite molecules (▲). C₁₈ solid-phase extract of effluent; eluent, methanol. Positive TSP ionization; for FIA conditions, see Experimental.

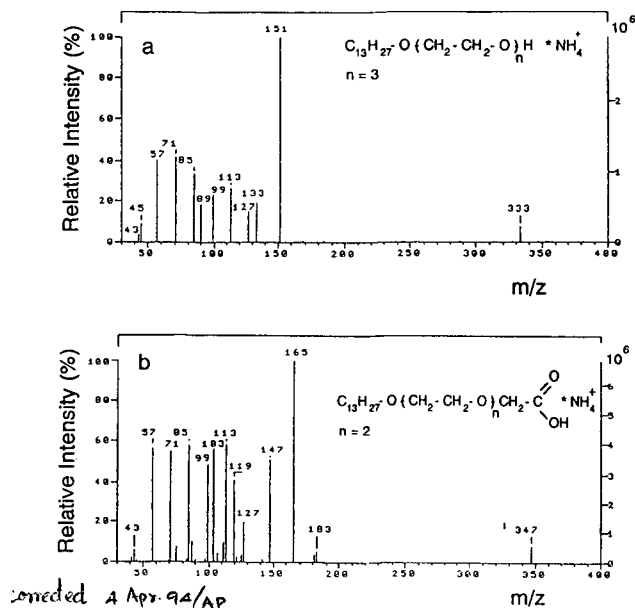


Fig. 13. (a) Daughter ion mass spectrum (FIA–MS–MS) of selected ion (m/z 350) from waste water extract as in Fig. 12a. (b) Daughter ion mass spectrum as in (a) of selected ion (m/z 364) from waste water extract as in Fig. 12b. For FIA conditions, see Experimental; collision energy, -15 eV.

shown in Fig. 13a and b, respectively. In Fig. 14a and b the structures of the compounds and their fragmentation behaviour under CID conditions are shown.

For the generation of the metabolite standard from the batch experiment it was helpful that a preliminary separation of the original compound present in the treatment plant effluent from the

primary degradation product was successfully achieved by selective elution. The original compound was eluted with diethyl ether and the metabolite with methanol from the C_{18} material. The purity of this metabolite mixture was confirmed by FIA–MS and MS–MS.

The chromatographic separation of the metabolite from the total waste water matrix on an analytical column is shown in Fig. 15, which contains the RIC of the separation together with the mass spectrum of peak 1.

After successful chromatographic separation, quantification by the standard addition method with four different concentrations of the metabolite was carried out. The original samples and the three samples spiked with a standard solution of the standards were analysed both in the FIA and after chromatographic separation by SIM recording the ion current of the cluster ions at m/z 320, 364 and 408. These ions are the main components of peak 1 in Fig. 15, representing more than 90% of the area under the TIC. The results of the standard addition analysis showed that the peak area obtained in FIA–MS and LC–MS was linearly related to the metabolite concentration in the chosen range and under the selected conditions. Concentration of 880 and 960 $\mu\text{g/l}$ of metabolite in the treatment plant effluent were determined by FIA–MS and LC–MS, respectively.

The results agree well; the time required for determination after LC separation, however, was much higher than that in the FIA mode. This

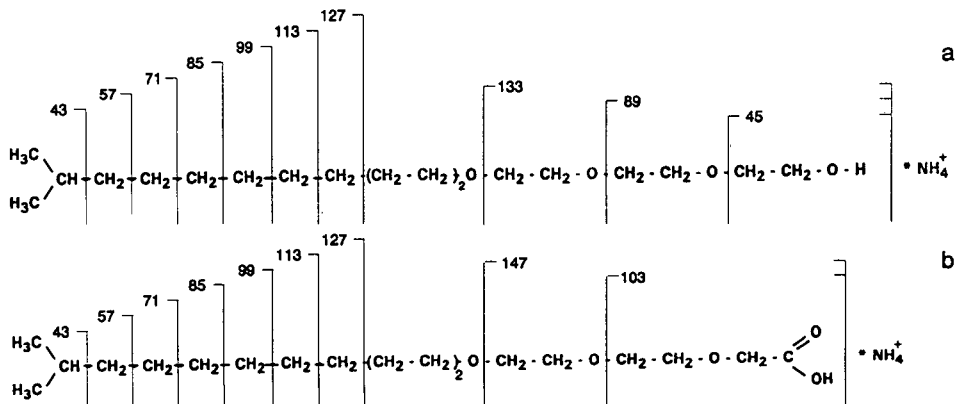


Fig. 14. (a) Structural formula and fragmentation scheme under CID conditions of non-ionic surfactant of alkanol polyethylene glycol ether type. (b) Metabolite (primary degradation product) of non-ionic surfactant in (a).

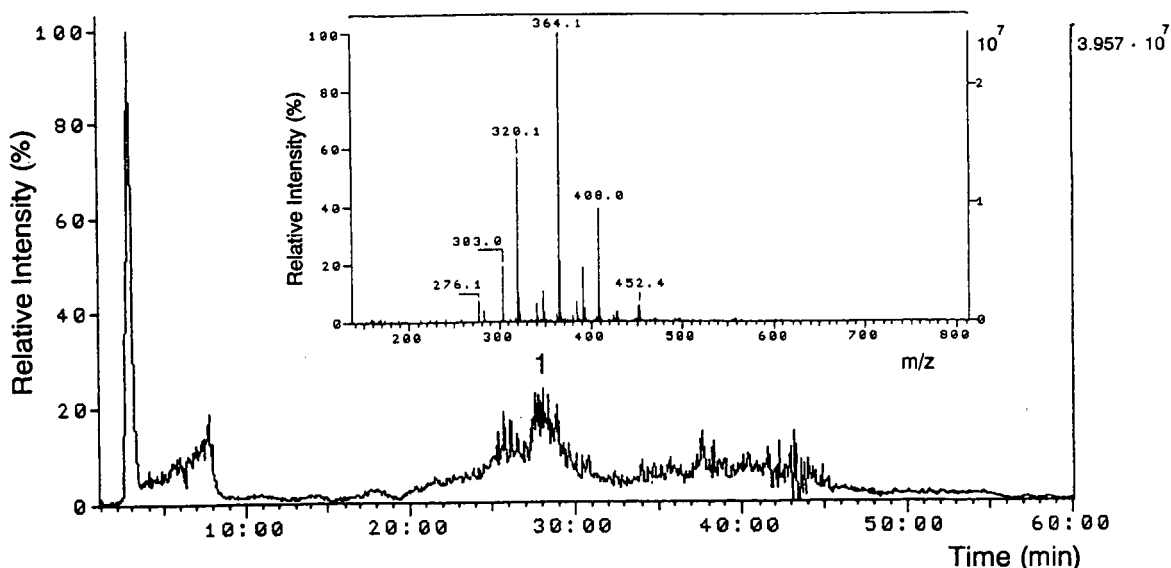


Fig. 15. LC-MS total ion current trace for waste water extract containing the metabolite in Fig. 14b. Inset: LC-mass spectrum of peak 1.

was caused by the prolonged analytical separations (45 min and more) and by the time-consuming cleaning and equilibration procedures (60 min) before each analytical separation. As this cycle of analysis, column cleaning and equilibration could not be done automatically, it was possible to make only three runs at different concentrations on an analytical column per day (8.5 h). In the FIA mode less than 10 min were required to acquire data at one concentration with a minimum of five injections per concentration. As the quantification of one compound by the standard addition method requires a minimum of four different concentrations, about 30 min are necessary for this examination. For quantification in the LC-MS mode 1.5 days are required for the whole procedure, assuming that the mass spectrometer is working well within the whole cycle of quantification. Taking these times into account, LC-MS takes 25–30 times longer than by FIA-MS.

CONCLUSIONS

The examination of some representative municipal sewage treatment plants, which apply biological treatment processes, showed that in spite of considerable pollutant concentrations in

the influents, only small amounts of non-polar organic compounds can be detected in the effluents. While these compounds could be eliminated up to 99%, considerable amounts of both anthropogenic and biogenic polar organic compounds, mainly anionic and non-ionic surfactants, could be detected.

Detection and identification of these surfactants and their biogenic metabolites can be carried out in the FIA-MS or FIA-MS-MS mode and also after chromatographic separation (LC-MS or LC-MS-MS). UV detection is possible only if there is a chromophore in the surfactant molecule. Standard retention time shifts induced by surface-active compounds can be recognized at once by using a mass spectrometer as detector. An exact quantitative determination of each pollutant by FIA-MS or LC-MS, however, requires in both instances that it exists as a standard and makes standard addition necessary. The results of the two methods correspond well. Determination by LC-MS took 25–30 times longer than FIA-MS.

The presence of some of these pollutants in drinking water produced from surface waters [2,26] has to make us think, for the toxicity of the precursor compound or the primary degradation product, respectively, is not always cleared

up. In the future, efforts to avoid or to replace some of these persistent substances will have to be considered. The surface activity of these compounds in combination with their non-biodegradability in water and soil enables them to introduce compounds into the groundwater which are more toxic than themselves.

The analytical possibilities have proven their suitability, now the legislator is challenged.

ACKNOWLEDGEMENTS

The author acknowledges financial support by the German Minister for Research and Technology in project 02 WT-87332. Mr. Scheduling, Mr. Lohoff, Mr. Gschwendtner and Mr. Meesters are thanked for their support in recording the spectra and preparing numerous samples.

REFERENCES

- 1 P. Rudolph, *Aquatic Toxicity Data Base*, Federal Environmental Agency, Berlin, 1989.
- 2 H.Fr. Schröder, *J. Chromatogr.*, 554 (1991) 251.
- 3 Z. Liu, S. Laha and R.G. Luthy, *Water Sci. Technol.*, 23 (1991) 475.
- 4 J.A. Field, L.B. Barber, II, E.M. Thurman, B.L. Moore, D.L. Lawrence and D.A. Peake, *Environ. Sci. Technol.*, 26 (1992) 1140.
- 5 *Standard Methods for the Examination of Water and Wastewater*, American Public Health Association, Washington, DC, 17th ed., 1989, 5540 C.
- 6 *German Standard Methods for the Examination of Water, Waste Water and Sludge; General Measures of Effects and Substances (Group H). Determination of Methylene Blue Active Substances (H 23-1)*, VCH, Weinheim, 1992.
- 7 *German Standard Methods for the Examination of Water, Waste Water and Sludge; General Measures of Effects and Substances (Group H). Determination of the Disulfine Blue Active Substances (H 20)*, VCH, Weinheim, 1992.
- 8 *Standard Methods for the Examination of Water and Wastewater*, American Public Health Association, Washington, DC, 17th ed., 1989, 5540 D.
- 9 *German Standard Methods for the Examination of Water, Waste Water and Sludge; General Measures of Effects and Substances (Group H). Determination of Bismuth Active Substances (H 23-2)*, VCH, Weinheim, 1992.
- 10 H.Fr. Schröder, *Vom Wasser*, 78 (1992) 211.
- 11 H.Fr. Schröder, *Vom Wasser*, 79 (1992) 193.
- 12 J. Pollerberg, *Fette Seifen Anstrichm.*, 69 (1967) 179.
- 13 H.Fr. Schröder, *J. Chromatogr.*, 643 (1993) 145.
- 14 E. Schneider, K. Levsen, P. Dähling and F.W. Röllgen, *Fresenius' Z. Anal. Chem.*, 316 (1983) 277.
- 15 P. Dähling, F.W. Röllgen, J.J. Zwinselman, R.H. Fokkens and N.M.M. Nibbering, *Fresenius' Z. Anal. Chem.*, 312 (1982) 335.
- 16 P.A. Lyon, W.L. Stebbings, F.W. Crow, K.B. Tomer, D.L. Lippstreu and M.L. Gross, *Anal. Chem.*, 56 (1984) 8.
- 17 H. Schwarz, *Nachr. Chem. Tech. Lab.*, 29 (1981) 687.
- 18 R. Weber, K. Levsen, G.J. Louter, A.J. Henk Boerboom and J. Haverkamp, *Anal. Chem.*, 54 (1982) 1458.
- 19 A.J. Borgerding and R.A. Hites, *Anal. Chem.*, 64 (1992) 1449.
- 20 H.Fr. Schröder, *Vom Wasser*, 73 (1989) 111.
- 21 H.Fr. Schröder, *Water Sci. Technol.*, 25 (1992) 241.
- 22 H.Fr. Schröder, *Korr. Abwasser*, 39 (1992) 387.
- 23 H.Fr. Schröder, in *DVGW Deutscher Verein des Gas- und Wasserfachs, DVGW-Schriftenreihe Wasser, No. 108, Wirtschafts- und Verlagsgesellschaft Gas und Wasser mbH, Bonn, 1990, pp. 121–144.*
- 24 H.Fr. Schröder, *Vom Wasser*, 77 (1991) 277.
- 25 M. Ahel and W. Giger, *Anal. Chem.*, 57 (1985) 1577.
- 26 F. Ventura, D. Fraisse, J. Caixach and J. Rivera, *Anal. Chem.*, 63 (1991) 2095.

Thermospray mass spectral studies of pesticides

Temperature and salt concentration effects on the ion abundances in thermospray mass spectra

D. Volmer*, A. Preiss and K. Levsen

Department of Analytical Chemistry, Fraunhofer Institute of Toxicology and Aerosol Research, Nikolai-Fuchs-Strasse 1, W-3000 Hannover 61 (Germany)

G. Wünsch

Institute of Inorganic Chemistry and Analytical Chemistry, University of Hannover, Callinstrasse 3, W-3000 Hannover 1 (Germany)

ABSTRACT

The dependence of the ion abundances in the thermospray (TSP) mass spectra of several pesticides, including anilides, carbamates, N-heterocyclic and organophosphorus compounds and phenylureas on the vaporizer and the gas-phase temperatures and under collision-activated dissociation conditions was investigated. The results clearly demonstrate that fragmentation in the TSP mass spectra of the investigated pesticides was mainly caused by gas- or liquid-phase “chemical dissociation” reactions of neutral analyte molecules or, in some instances, of the quasi-molecular ions in the ion source or the vaporizer probe, probably induced by solvent or buffer ions which can be described by well defined mechanisms. A linear relationship was observed for most of those pesticides which showed combinations of the two quasi-molecular ions $[M + H]^+$ and $[M + NH_4]^+$, when the logarithm of the ion abundance ratio for the $[M + H]^+$ ion relative to the $[M + NH_4]^+$ ion was plotted against the reciprocal of the absolute temperature of the gas phase. It is shown that this dependence can be used to generate TSP mass spectra with mainly one quasi-molecular ion. This may be of value for selected-ion monitoring experiments, because the total ion current (*i.e.*, the sum of the $[M + H]^+$ and $[M + NH_4]^+$ ions) is less dependent on the gas-phase temperature than the ion currents of the individual quasi-molecular ions. It was found that additional adduct ions beside these quasi-molecular ions could be observed in the spectra of several pesticides for which the formation was limited to low gas-phase temperatures. In addition, the results for the investigated quaternary ammonium compounds clearly show that the addition of a volatile buffer salt to the mobile phase induces chemical reactions in the gas phase which have a strong influence on the ion abundances. However, addition of buffer salt was necessary to obtain intense signals although the compounds are already completely dissociated in the aqueous solvent and fragmentation was enhanced as the buffer concentration was raised.

INTRODUCTION

The increasing use of pesticides in agriculture and thus the resulting concern about residues from these compounds in food and drinking water demands the development of highly sensitive and selective methods for their determina-

tion at trace levels. Unfortunately, universal methods are not available. As a result of their thermal instability and polarity, many of these compounds are not amenable to analysis by GC or GC-MS. In many instances they can, however, be analysed by liquid chromatographic (LC) methods. The former lack of a sensitive and selective LC detector has been overcome by combining LC with mass spectrometry (LC-MS). LC-MS offers major advantages over GC-

* Corresponding author.

MS for analysing thermally labile and polar compounds [1,2]. Different types of LC–MS interfaces have been applied to the analysis of these compounds in the last decade, such as a moving belt [3,4], direct liquid introduction (DLI) [5,6], fast atom bombardment (FAB) [7], thermospray (TSP) [8–10] and, more recently, particle beam [11]. Among these different interfaces, the TSP technique is the one most widely used. Some major classes of pesticides including carbamates [12,13], organophosphorus [14–16] and quaternary ammonium compounds [17], phenylureas [18,19], phenoxy acids [18,20], triazines [13,21] and some other classes have been analysed by LC–TSP–MS.

We have developed an LC–TSP–MS method for the extraction, separation and determination of approximately 130 pesticides, including anilides, carbamates, phenylureas, phenoxy acids, oximes, organophosphorus and quaternary ammonium compounds, triazines and other N-heterocyclic compounds and some other classes in aqueous environmental samples. Special attention was paid to pesticides produced in the former German Democratic Republic (GDR): the application of most of these compounds has been prohibited in Germany since the beginning of 1993, but they may still be found in aqueous samples. For many of these compounds no methods for their determination at trace levels are available. Examples for GDR-specific pesticides are presented in this paper. A more detailed description of the extraction, chromatographic separation and determination of all investigated compounds will be presented in a following paper.

Apart from demonstrating the applicability of TSP for the identification of a wide variety of pesticides, another aim of this work was to investigate the dependence of the ion abundances in the TSP mass spectra of several pesticides on the gas-phase and vaporizer temperatures. An increase in these temperatures may lead to enhanced fragmentation, whereas a decrease often results in additional cluster ions with several pesticides, which is useful for confirming a tentative identification based on the quasi-molecular ion alone as TSP ionization often results in spectra with insufficient structural information (*i.e.*,

one or two ions). Many attempts have been made to overcome this problem by using, *e.g.*, filaments, discharge ionization or MS–MS techniques [22] and by using additives to the mobile phase [23]. Moreover, the complementary information gained from positive- and negative-ion TSP mass spectra may be used to obtain additional structural information. The work described here will demonstrate the usefulness of varying the gas-phase and the vaporizer temperatures for inducing controlled chemical reactions during TSP vaporization and ionization. Fragmentation pathways for several pesticides will be discussed. The effect of temperature on the formation of additional cluster ions will also be demonstrated. In addition, methods for enhancing the sensitivity of the TSP detection are presented for several pesticides, including the variation of interface temperatures and the variation of the concentration of the volatile buffer salt.

EXPERIMENTAL

Materials

Organic-free water (Millipore, Bedford, MA, USA) and HPLC-grade methanol (Riedel-de Haën, Hannover, Germany) were passed through a 0.45- μm filter (Satorius, Göttingen, Germany) before use. Analytical-reagent grade ammonium acetate and ammonium formate were obtained from Aldrich (Steinheim, Germany) and Riedel-de Haën, respectively. Standards of the pesticides were purchased from Riedel-de Haën and Promochem (Wesel, Germany). They were of purity >98% and were used as received. Buminafos and butonate were a gift from Dr. J. Efer (University of Leipzig, Leipzig, Germany). Stock standard solutions of the chemicals were made up individually in methanol. From these stock standard solutions, serial dilutions with methanol or the mobile phase were made to obtain working standard solutions. PEG-300 and PEG-400 were purchased from Fluka (Buchs, Switzerland).

Liquid chromatography

The LC system consisted of a Varian (Palo Alto, CA, USA) Model 5000 gradient liquid chromatograph and a Shimadzu (Duisburg, Ger-

many) Model LC-9A pump for the postcolumn addition of buffer solution. The connection between the column and the TSP interface consisted of a low-dead-volume tee (Valco, Houston, TX, USA), a Rheodyne (Cotati, CA, USA) Model 7125 injector with a 50- μ l sample loop for flow injections and a 2- μ m screen filter (Valco). The buffer solution and the mass calibration mixture were added postcolumn through the tee. For chromatographic separations the samples were injected with a second Rheodyne injector equipped with a 20- μ l loop and separated with methanol–water gradient mixtures using a narrow-bore Nucleosil C₁₈ (5 μ m) column (125 \times 3 mm I.D.) (Machery–Nagel, Düren, Germany). A final flow-rate of 1.2 ml min⁻¹ in the TSP vaporizer was used in all experiments. A flow-rate of 0.6 ml min⁻¹ was maintained through the column, while 0.6 ml min⁻¹ of 150 mM aqueous buffer solution was added postcolumn. As the percentage of organic modifier in aqueous solvent mixtures strongly affects the sensitivity of the thermospray ionization, the post-column technique ensures that the final composition of the vaporized liquid varies only slightly (with a constant value of added salt), thus resulting in limits of detection that are virtually independent of the composition of the gradient mixture. The use of a high water content in the final solvent leads to a significant increase in TSP sensitivity. This increase can be attributed to the increase in the dielectric constant of the solvent as the water fraction is raised [24]. There is a second advantage of postcolumn buffer addition: the liquid chromatographic separation and TSP ionization analysis can be optimized separately, thus avoiding the possible negative influence of the precolumn addition of buffer on the chromatographic separation [25,26].

Mass spectrometry

The TSP interface (Vestec, Houston, TX, USA) was installed on a Finnigan MAT (San José, CA, USA) Model 4500 mass spectrometer. All experiments were performed with a 125- μ m tip-diameter vaporizer. Both the vaporizer and the source jet temperature were monitored. It is not clear which of the measured temperatures reflects the “gas-phase” temperature T_g and the

“reaction” temperature, *i.e.*, the temperature at which the gas-phase ion–molecule reactions occur. With the Vestec source, a thermocouple at the position of the repeller electrode would allow the closest measurement of this temperature. For calculations reported below, T_g can be approximated by the source jet (= vapour) temperature which is measured beyond the ion exit orifice because the difference between the source (“block”) temperature and the source jet temperature is small in most instances, typically between 10 and 20°C. In future experiments, a further thermocouple that will replace the repeller electrode will be used. The term T_g used below refers to the source jet temperature.

Typical operating conditions of the thermospray interface were as follows: vaporizer control temperature T_1 , *ca.* 135–150°C; vaporizer temperature T_v , *ca.* 190–210°C; vaporizer tip temperature T_3 , 270°C; source temperature T_s , 250°C; source jet temperature T_g , *ca.* 230–240°C; and exit line pressure p_g , *ca.* 2–4 Torr (1 Torr = 133.322 Pa) (the pressure is strongly dependent on the composition of the mobile phase and the flow-rate). For all variations of T_g , T_3 was set to the actual value of T_s , while T_v was kept constant. The mass spectrometer was operated in the positive-ion (PI) and negative-ion (NI) modes. The vaporizer temperature was optimized before each analysis to obtain a stable maximum ion intensity of the solvent cluster ions in the range m/z 18–139 for the positive ions and m/z 59–183 for the negative ions. The presence of these cluster ions limited the lower mass range available in TSP analysis. In this work, scanning was in general restricted to m/z values ≥ 140 (PI) and ≥ 185 (NI). The mass spectrometer was scanned at a rate of 1 s per scan over the mass range m/z 140–450 (PI) and 185–450 (NI).

The mass scale was calibrated with an aqueous solution of PEG-300 and PEG-400 containing 100 mM ammonium acetate, where the solution was continuously pumped into the TSP ion source. The polyethylene glycol–ammonium adduct ions were also used to tune the instrument.

LC–TSP–MS–MS experiments were performed on a Finnigan MAT TSQ 70 triple-stage quadrupole mass spectrometer (Q_1 , Q_2 , Q_3). In these MS–MS experiments, the $[M + H]^+$ or

$[M + NH_4]^+$ quasi-molecular ions were chosen as precursor ions and selectively transmitted by Q_1 for further collisional dissociation to Q_2 . Argon was used as the collision gas with a collision chamber pressure of $1.3 \cdot 10^{-3}$ Torr. A collision offset (COFF) of 10 V was applied to Q_2 . The collision-activated dissociation (CAD) daughter ions thus obtained were then analysed by scanning with the third quadrupole (Q_3) over the mass range m/z 10–300. For the LC–MS–MS studies, direct flow injection was used to introduce the samples into the mass spectrometer. The TSP vaporizer control temperature was set to 90°C and the aerosol temperature was kept at 240°C.

RESULTS AND DISCUSSION

Dependence of ion abundances in thermospray mass spectra on the vaporizer and gas-phase temperatures

TSP ionization of pesticides often results in mass spectra with insufficient structural information, *i.e.*, only the $[M + H]^+$ ion or the $[M + NH_4]^+$ ion or combinations of both ions appear in the spectra. However, in many instances it is possible to induce fragmentation by raising the vaporizer or the gas-phase temperature T_g . The examples in the following subsections will demonstrate that thermal decomposition is rare in TSP mass spectra of pesticides in the investigated temperature ranges of $T_g = 150$ – 320°C and $T_v = 140$ – 240°C . The degradation can be described by well defined reaction mechanisms. In addition, the dependence of the relative intensities of the quasi-molecular and cluster ion species on T_g was investigated. Relative abundances of the ions observed in the TSP mass spectra of the investigated compounds are summarized in Table I. Fig. 1 shows a full-scan TSP PI chromatogram of 26 pesticides under typical operating conditions.

Degradation reactions of organophosphorus pesticides. The TSP mass spectra of the investigated organophosphorus pesticides show a significantly increased fragmentation compared with other pesticides such as phenylureas and triazines. Special attention was paid to GDR-specific pesticides, *e.g.*, the phosphonic diesters

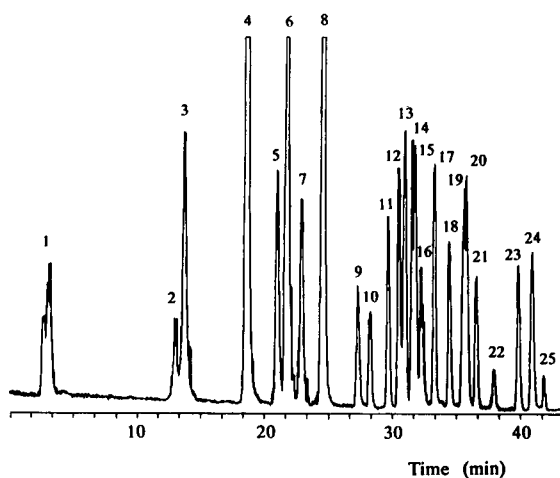


Fig. 1. Full-scan TSP PI chromatogram of several pesticides (180 ng each). Experimental conditions: filament-off, $T_s = 250^\circ\text{C}$, $T_g \approx 235^\circ\text{C}$ and $T_v = 205 \rightarrow 193^\circ\text{C}$ [gradient mixture: methanol–water, 10:90–90:10 (v/v), linear in 45 min; for details see Experimental]. Peak assignment: 1 = asulam; 2 = aldicarb sulphone; 3 = oxamyl; 4 = desisopropyl-atrazine; 5 = fenuron; 6 = dimethoate/metamitron; 7 = chloridazon; 8 = desethyl-atrazine; 9 = aldicarb; 10 = metoxuron; 11 = cyanazine; 12 = terbacil; 13 = monuron; 14 = carbofuran; 15 = simazine; 16 = hexazinon; 17 = carbaryl; 18 = monolinuron; 19 = chlorotoluron; 20 = atrazine; 21 = isoproturon; 22 = diuron; 23 = terbutylazine; 24 = propazine; 25 = chlorobromuron.

buminafos and butonate (the structures of which are shown in Figs. 2 and 5) and their degradation products. The investigated temperature range was $T_g = 150$ – 320°C .

Fig. 2 shows the TSP mass spectra of butonate at three different gas-phase temperatures (180, 235 and 300°C , $T_v = \text{constant}$). The quasi-molecular ion, $[M + NH_4]^+$, is the base peak in all instances, but a strong increase in the fragment ion abundance is observed as T_g is raised.

The fragmentation pathways suggested for butonate, the tentative structures of the fragments and the m/z values of the ions formed therefrom are shown in Fig. 3. The reaction starts with the hydrolysis of the phosphonic ester 1 to form trichlorfon (2), which after protonation or ammonium addition leads to the ions at m/z 257 and 274. In a second step, the elimination of HCl leads to the formation of dichlorvos (4) with the corresponding ions at m/z 221 and 238. This step probably involves an ylide-type electrophilic phosphor-to-oxygen 1,2-rearrangement of 3. Al-

TABLE I

DIRECT FLOW-INJECTION TSP POSITIVE-ION MASS SPECTRA OF THE INVESTIGATED PESTICIDES

Experimental parameters: $T_s = 250^\circ\text{C}$; $T_g = 235^\circ\text{C}$; $T_v = 202^\circ\text{C}$; mobile phase, MeOH–100 mM NH_4OAc (20:80); flow-rate, 1.2 ml min^{-1} ; the filament and the discharge electrode were not used in all experiments.

Compound	M_r	m/z (relative abundance, %)	Tentative identification
<i>Anilides</i>			
Alachlor	269	226 (62)	$[\text{M} + \text{H}_2\text{O} - \text{CH}_3\text{OCH}_2\text{OH} + \text{H}]^+$
		238 (36)	$[\text{M} - \text{CH}_3\text{OH} + \text{H}]^+$
		243 (70)	$[\text{M} + \text{H}_2\text{O} - \text{CH}_3\text{OCH}_3 + \text{NH}_4]^+$
		270 (100)	$[\text{M} + \text{H}]^+$
		287 (30)	$[\text{M} + \text{NH}_4]^+$
		305 ^a	$[\text{M} + \text{H}_2\text{O} + \text{NH}_4]^+$
		319 ^a	$[\text{M} + \text{MeOH} + \text{NH}_4]^+$
		329 ^a	$[\text{M} + \text{NH}_4\text{OAc} - \text{H}_2\text{O} + \text{H}]^+$
<i>Carbamates</i>			
Asulam	230	156 (4)	$[\text{M} - \text{CH}_3\text{OC}(\text{O})\text{NH}_2 + \text{H}]^+$
		173 (5)	$[\text{M} + \text{H}_2\text{O} - \text{CH}_3\text{OC}(\text{O})\text{OH} + \text{H}]^+$
		190 (100)	$[\text{M} + \text{H}_2\text{O} - \text{CH}_3\text{OC}(\text{O})\text{OH} + \text{NH}_4]^+$
		231 (5)	$[\text{M} + \text{H}]^+$
		248 (68)	$[\text{M} + \text{NH}_4]^+$
Carbaryl	201	145 (3)	$[\text{M} - \text{CH}_3\text{NCO} + \text{H}]^+$
		202 (18)	$[\text{M} + \text{H}]^+$
		219 (100)	$[\text{M} + \text{NH}_4]^+$
Carbofuran	221	165 (5)	$[\text{M} - \text{CH}_3\text{NCO} + \text{H}]^+$
		182 (3)	$[\text{M} - \text{CH}_3\text{NCO} + \text{NH}_4]^+$
		222 (100)	$[\text{M} + \text{H}]^+$
		239 (35)	$[\text{M} + \text{NH}_4]^+$
Chlorpropham	213	214 (20)	$[\text{M} + \text{H}]^+$
		231 (100)	$[\text{M} + \text{NH}_4]^+$
		249 ^a	$[\text{M} + 46]^+$
		263 ^a	$[\text{M} + \text{NH}_4\text{OAc} - 2\text{H}_2\text{O} + \text{NH}_4]^+$
Desmedipham	300	120 ^b	$[\text{M} - \text{C}_2\text{H}_5\text{OCONHC}_6\text{H}_4\text{OH} + \text{H}]^+$
		137 (20)	$[\text{M} - \text{C}_2\text{H}_5\text{OCONHC}_6\text{H}_4\text{OH} + \text{NH}_4]^+$
		182 (50)	$[\text{M} - \text{C}_6\text{H}_5\text{NCO} + \text{H}]^+$
		199 (100)	$[\text{M} - \text{C}_6\text{H}_5\text{NCO} + \text{NH}_4]^+$
		213 (7)	$[\text{M} - \text{C}_2\text{H}_5\text{OC}(\text{O})\text{NH} + \text{H}]^+$
		301 (<1)	$[\text{M} + \text{H}]^+$
		318 (3)	$[\text{M} + \text{NH}_4]^+$
Oxamyl	219	163 (33)	$[\text{M} - \text{CH}_3\text{NCO} + \text{H}]^+$
		180 (13)	$[\text{M} - \text{CH}_3\text{NCO} + \text{NH}_4]^+$
		220 (3)	$[\text{M} + \text{H}]^+$
		237 (100)	$[\text{M} + \text{NH}_4]^+$
Phenmedipham	300	134 ^b	$[\text{M} - \text{CH}_3\text{OC}(\text{O})\text{NHC}_6\text{H}_4\text{OH} + \text{H}]^+$
		151 (40)	$[\text{M} - \text{CH}_3\text{OC}(\text{O})\text{NHC}_6\text{H}_4\text{OH} + \text{NH}_4]^+$
		168 (45)	$[\text{M} - \text{C}_6\text{H}_5(\text{CH}_3)\text{NCO} + \text{H}]^+$

(Continued on p. 240)

TABLE I (continued)

Compound	M_r	m/z (relative abundance, %)	Tentative identification
		185 (100)	$[M - C_6H_5(CH_3)NCO + NH_4]^+$
		210 (17)	$[M - C_6H_5CH_3 + H]^+$
		301 (<1)	$[M + H]^+$
		318 (3)	$[M + NH_4]^+$
<i>Triazines and other N-heterocyclic compounds</i>			
Atrazine	215	216 (100)	$[M + H]^+$
		248 ^a	$[M + MeOH + H]^+$
		275 ^a	$[M + NH_4OAc - H_2O + H]^+$
Cyanazine	240	241 (100)	$[M + H]^+$
		273 ^a	$[M + MeOH + H]^+$
		300 ^a	$[M + NH_4OAc - H_2O + H]^+$
Terbacil	216	161 (23) ^c	$[M - CH_2=C(CH_3)_2 + H]^+$
		178 (100) ^c	$[M - CH_2=C(CH_3)_2 + NH_4]^+$
		217 (<1)	$[M + H]^+$
		234 (<1)	$[M + NH_4]^+$
<i>Organophosphorus compounds</i>			
Azinphos-ethyl	345	160 (100)	$[M - (C_2H_5)_2PS_2 + H]^+$
		346 (65)	$[M + H]^+$
		363 (33)	$[M + NH_4]^+$
Buminafos	347	154 (10)	$[M - HOP(OC_4H_9)_2 + H]^+$
		195 (30)	$[M - C_6H_5NHC_4H_9 + H]^+$
		212 (100)	$[M - C_6H_5NHC_4H_9 + NH_4]^+$
		293 (1)	$[M + H_2O - C_4H_9NH_2 + H]^+$
		348 (2)	$[M + H]^+$
Butonate	326	221 (1)	$[M + H_2O - C_3H_7CO_2H - HCl + H]^+$
		238 (2)	$[M + H_2O - C_3H_7CO_2H - HCl + NH_4]^+$
		257 (2)	$[M + H_2O - C_3H_7CO_2H + H]^+$
		274 (5)	$[M + H_2O - C_3H_7CO_2H + NH_4]^+$
		291 (15)	$[M - HCl + H]^+$
		308 (70)	$[M - HCl + NH_4]^+$
		327 (30)	$[M + H]^+$
		344 (100)	$[M + NH_4]^+$
Dichlorvos	220	221 (12)	$[M + H]^+$
		238 (100)	$[M + NH_4]^+$
		281 (5)	$[M + NH_4OAc - H_2O + H]^+$
Dimethoate	229	230 (100)	$[M + H]^+$
		247 (38)	$[M + NH_4]^+$
Disulfoton	274	275 (100)	$[M + H]^+$
		292 (10)	$[M + NH_4]^+$
Naled	380	221 (<1)	$[M - Br_2 + H]^+$
		238 (2)	$[M - Br_2 + NH_4]^+$
		381 (7)	$[M + H]^+$
		398 (100)	$[M + NH_4]^+$

TABLE I (continued)

Compound	M_r	m/z (relative abundance, %)	Tentative identification
Phorate	260	261 (100)	$[M + H]^+$
		278 (1)	$[M + NH_4]^+$
Phosmete	317	318 (35)	$[M + H]^+$
		335 (100)	$[M + NH_4]^+$
Trichlorfon	256	221 (1)	$[M - HCl + H]^+$
		238 (12)	$[M - HCl + NH_4]^+$
		257 (18)	$[M + H]^+$
		274 (100)	$[M + NH_4]^+$
<i>Phenylureas</i>			
Chlorotoluron	212	213 (100)	$[M + H]^+$
		230 (5)	$[M + NH_4]^+$
		245 ^a	$[M + MeOH + H]^+$
		258 ^a	$[M + 46]^+$
		271 ^a	$[M + NH_4OAc - 2H_2O + NH_4]^+$
		272 ^a	$[M + NH_4OAc - H_2O + H]^+$
Fenuron	164	165 (100)	$[M + H]^+$
		182 (40)	$[M + NH_4]^+$
		197 ^a	$[M + MeOH + H]^+$
		210 ^a	$[M + 46]^+$
Isoproturon	206	207 (100)	$[M + H]^+$
		224 (23)	$[M + NH_4]^+$
		239 ^a	$[M + MeOH + H]^+$
		252 ^a	$[M + 46]^+$
		265 ^a	$[M + NH_4OAc - 2H_2O + NH_4]^+$
<i>Quaternary ammonium compounds^d</i>			
Diquat	184 ^e	92 ^f (5)	$[Cat]^{2+}$
		157 (29)	$[Cat - CH_2CH_2 + H]^+$
		183 (6)	$[Cat - H]^+$
		184 (100)	$[Cat]^+$
		185 (23)	$[Cat + H]^+$
Paraquat	186 ^e	93 ^f (7)	$[Cat]^{2+}$
		157 (20)	$[Cat - 2CH_3 + H]^+$
		171 (5)	$[Cat - CH_3]^+$
		172 (100)	$[Cat - CH_3 + H]^+$
		186 (27)	$[Cat]^+$
		187 (84)	$[Cat + H]^+$
		221 (1)	$[Cat + Cl]^+$

^a These adduct ions were observed only at low gas-phase temperatures (see text).

^b CAD daughter ion spectrum.

^c The hydrolysis reaction in the vaporizer should also be considered (see text).

^d Cat = cation.

^e Nominal mass of the divalent cation (Cat^{2+}).

^f The intact dication is only observed in the TSP spectra with pure water as the solvent.

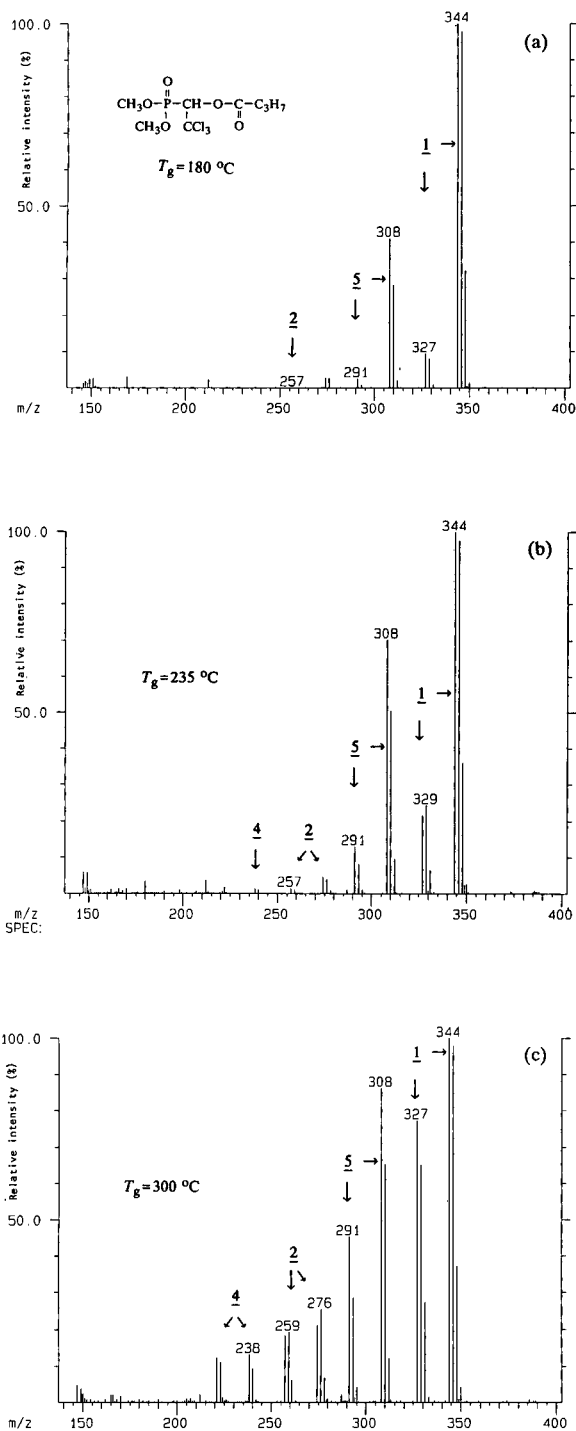


Fig. 2. Direct flow-injection TSP PI mass spectra of butonate for different gas-phase temperatures: T_g = (a) 180; (b) 235; (c) 300°C. Amount injected, 600 ng. The assignments of the tentative structures are shown in Fig. 3.

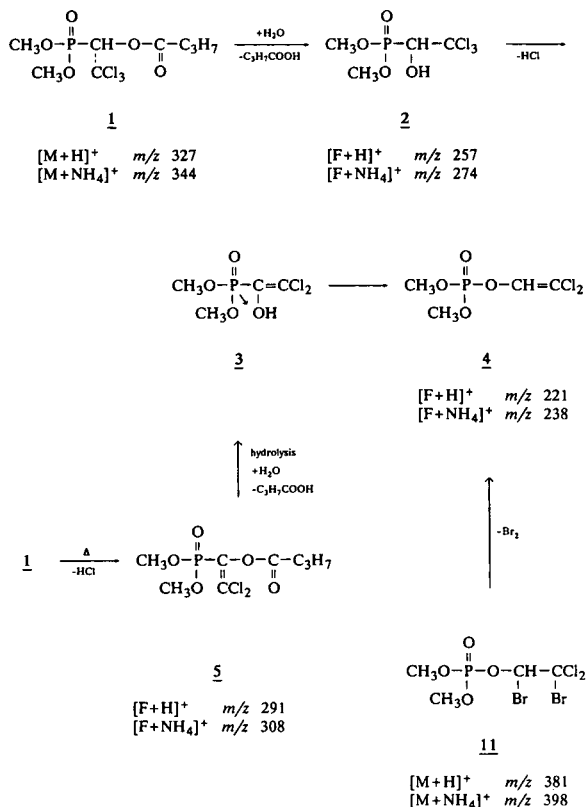


Fig. 3. Proposed fragmentation pathways for butonate and naled and observed ions in the TSP PI mass spectra.

ternatively, the fragmentation of 1 can also start with the direct elimination of HCl, which leads to the ions $[\text{F} + \text{H}]^+$ (m/z 291) and $[\text{F} + \text{NH}_4]^+$ (m/z 308), where F is a neutral fragment molecule. The corresponding ions from both reaction pathways are observed in the spectra in Fig. 1 (the HCl elimination in steps 2→3 and 1→5 was confirmed by the observed isotropic abundances of the chlorine atoms). The amount of fragmentation depends strongly on the gas-phase temperature, T_g (see Fig. 2a–c), while variation of the vaporizer temperature has only a slight influence. The conclusion that degradation of neutral butonate leads to the formation of trichlorophon and dichlorvos is corroborated on the one hand by a comparison with the TSP PI mass spectra of these two compounds which are shown in Fig. 4a and b for $T_g = 235^\circ\text{C}$. One observes that trichlorophon is degraded in the same manner as butonate to give dichlorvos. On the other

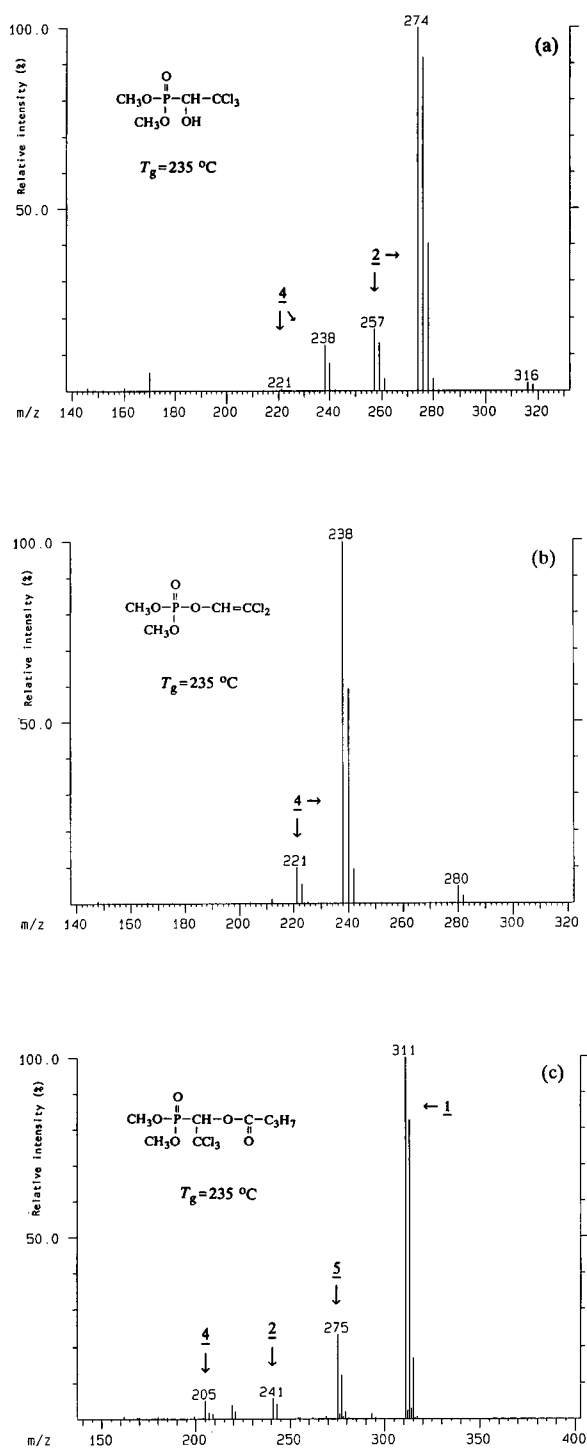


Fig. 4. TSP mass spectra of (a) trichlorfon (PI), (b) dichlorvos (PI) (amount injected, 600 ng) and (c) butonate (NI, filament-on, 2 μg) for $T_g = 235^\circ\text{C}$.

hand, further evidence for gas-phase and/or liquid-phase degradation processes is gleaned from the TSP NI spectra of butonate (Fig. 4c). In this mode, intense ions corresponding to $[\text{M} - \text{R}]^-$ or $[\text{F} - \text{R}]^-$ ions ($\text{R} = \text{CH}_3$) of 1, 2, 4 and 5 are observed which complement the $[\text{M} + \text{H}]^+$ and $[\text{M} + \text{NH}_4]^+$ or $[\text{F} + \text{H}]^+$ and $[\text{F} + \text{NH}_4]^+$ ions observed in the TSP PI mode. These ions are due to dissociative electron-capture reactions of neutral precursors [27]. This further demonstrates that when degradation products are formed from the neutral molecule, they readily produce quasi-molecular ions in both the PI and NI modes. If degradation products 2, 4 and 5 were produced by means of fragmentation of the quasi-molecular ions, it is unlikely that complementary fragment ions would appear in both the PI and NI spectra.

Dichlorvos is also formed by debromination of the pesticide naled, a phosphorus naled, a phosphorus diester (11, see Fig. 3 and Table I). Again, both $[\text{M} + \text{H}]^+$ and $[\text{M} + \text{NH}_4]^+$ ions are formed, where the latter leads to the base peak. The fragment ion abundances are lower than for the other organophosphorus pesticides. Thus the reaction yield is low in the temperature range $T_g = 150\text{--}320^\circ\text{C}$ ($< 5\%$ relative abundance). At $T_g > 340^\circ\text{C}$ thermal decomposition occurs and leads to undefined products.

The PI mass spectra of the herbicide buminafos show a protonated molecular ion of very low abundance (m/z 348) and a significantly higher fragmentation level (see Fig. 5). The tentative ion structures can be explained as follows (Fig. 6). The phosphonic diester 6 is readily cleaved at the P–C bond to give the phosphoric diester 7 and the carbenium-iminium ion 8 after proton addition. The mass spectra are dominated by the ions corresponding to the phosphoric diester 7, viz., $[\text{F} + \text{H}]^+$ (m/z 195) and $[\text{F} + \text{NH}_4]^+$ (m/z 212). The intermediate 8 undergoes direct elimination to the enamine 10, followed by gas-phase ionization (m/z 154).

The relative abundance of the $[\text{F} + \text{H}]^+$ ion with respect to the $[\text{F} + \text{NH}_4]^+$ ion depends strongly on the interface temperatures (both T_g and T_v), as can be seen from Fig. 5. However, the intensity of the quasi-molecular ion at m/z 348 is very low at each temperature, indicating

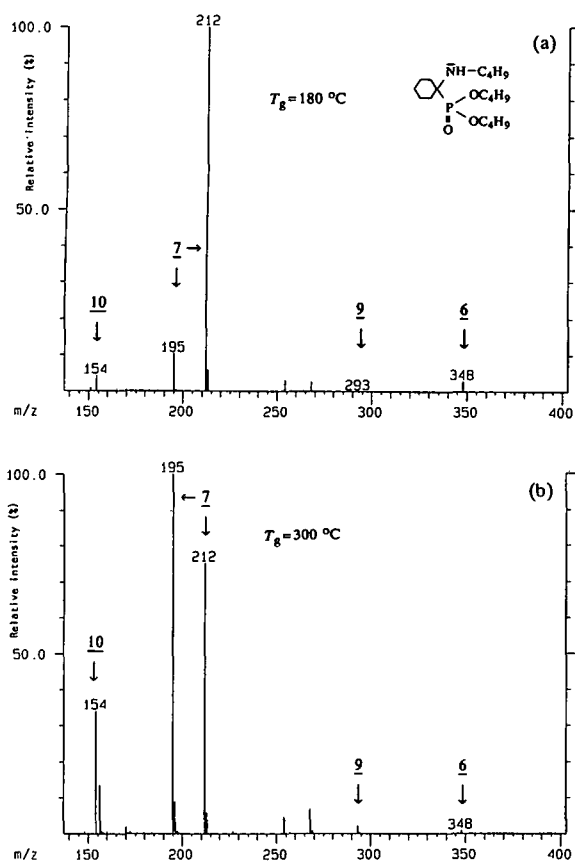


Fig. 5. TSP PI mass spectra of buminafos for different gas-phase temperatures: $T_g =$ (a) 180 and (b) 300°C. Amount injected, 600 ng. See Fig. 6 for tentative identification.

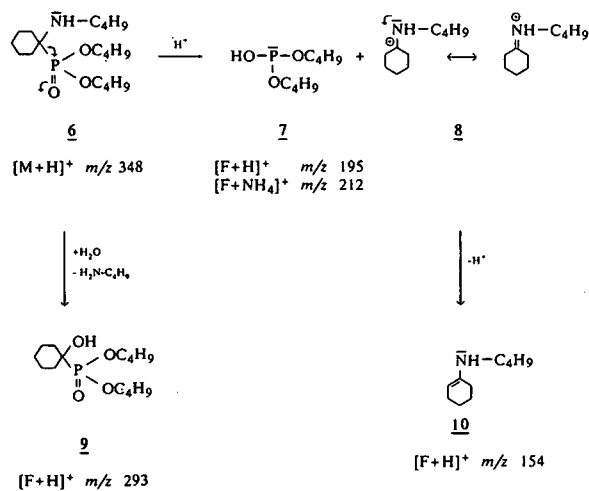


Fig. 6. Proposed fragmentation scheme for the GDR-specific herbicide buminafos and observed ions in the TSP PI mass spectra.

that dissociation occurs in the liquid phase during vaporization (in principle this dissociation could already occur during the chromatography, but the observation of only one sharp peak in the chromatogram rules this possibility out; another possibility, the decomposition of the quasi-molecular ion, is not probable in this instance because buminafos is known to dissociate readily in aqueous solution at low or high pH to give the phosphoric diester). The small signal at m/z 293 can be attributed to a hydrolysis of the N–C bond of the neutral molecule to give 9 (Fig. 6), although this reaction is not a major channel for the production of fragments even at higher temperatures.

In contrast, the PI mass spectrum of azinphos-ethyl exhibits a fragment ion (m/z 160) particularly at higher gas-phase temperatures (see Fig. 7

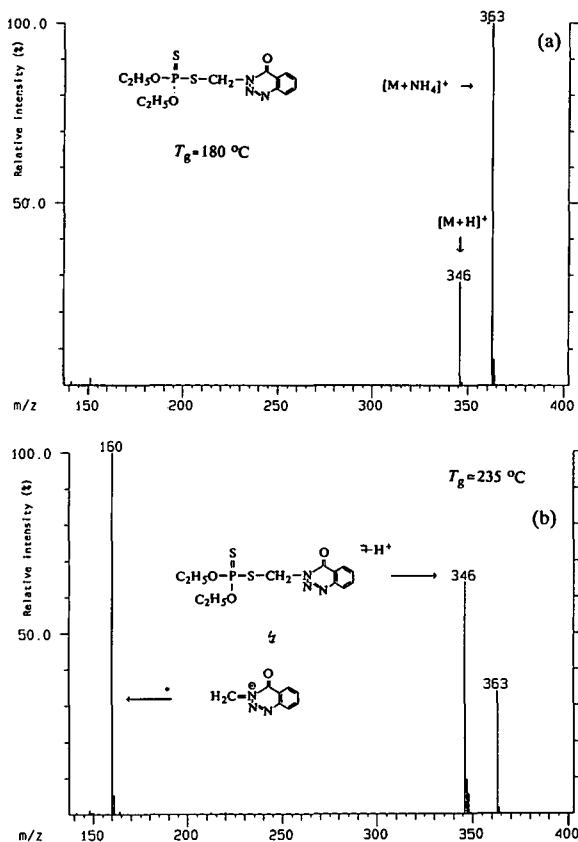


Fig. 7. TSP PI mass spectra of azinphos-ethyl for different gas-phase temperatures and proposed structure of the fragment ion. $T_g =$ (a) 180 and (b) 235°C. Amount injected, 300 ng.

for 180°C versus 235°C), which can be attributed to the decomposition of the quasi-molecular ions (m/z 346 and 363). Roach and Andrzejewski [28] have shown that azinphos analogues generally show a daughter ion of 160 u in the CAD spectra of the $[M + H]^+$ parent ions. Surprisingly, this ion is formed from the $[M + H]^+$ and/or the $[M + NH_4]^+$ ion under regular TSP conditions, whereas in the spectra of similar compounds, e.g., phosmete and phorate, no such ions are observed (Table I).

The TSP mass spectra of most of the investigated organophosphorus compounds exhibit the $[M + NH_4]^+$ and $[F + NH_4]^+$ ions as the base peak even at higher values of T_g . This is due to the proton affinity (PA) of these compounds, which is lower than that of ammonia. As an exception, the phosphorodithioates dimethoate, disulfoton and phorate show $[M + H]^+$ ions as the base peaks at each investigated temperature (see Table I for mass assignment and relative abundances). This can be attributed to the higher gas-phase basicity and PA of these compounds in comparison with phosphorothioates and phosphates, owing to the lower electronegativity of the sulphur atom instead of the oxygen atom.

Summarizing the results, one can state that many of the fragment ions in the TSP mass spectra of organophosphorus compounds are due to proton or ammonium adduct ions of thermally induced degradation products generated in the vaporizer probe or in the ion source. Lowering the gas-phase temperature leads to an increase in the quasi-molecular ion intensities for several organophosphorus pesticides as fragmentation is reduced. However, lowering T_g to <200°C leads to an increase in noise. Therefore, one has to find a temperature where the signal-to-noise ratio reaches an optimum. This increase in noise is probably caused by the more difficult formation of primary ions owing to a more difficult and interfered desolvation of the droplets when the spray was expanded in a “cold” ion source, i.e., for $T_g < T_v$ ($T_v \approx 200^\circ\text{C}$). Generally, we observed a decreasing noise for $T_g > T_v$ with a minimum value at $T_g \approx 235^\circ\text{C}$ and $T_s \approx 250^\circ\text{C}$ for most of the investigated pesticide compound classes. However, for azinphos-ethyl, butonate and trichlorfon one has to take the above-

mentioned fragmentations into account when performing selected-ion monitoring (SIM) experiments. Thus for these compounds we found optimum temperatures of $T_g \approx 220^\circ\text{C}$ and $T_s \approx 235^\circ\text{C}$.

Thermally induced chemical reactions during thermospray vaporization and ionization. TSP is often described as a “soft” ionization method that leads to little fragmentation. Although this may be true as far as a fragmentation of quasi-molecular ion is concerned, the examples shown above demonstrate that TSP mass spectra may contain abundant fragments where, however, dissociation is predominantly induced by chemical reactions of the neutral species which may be assisted by heat, solvent or buffer ions in the liquid phase of the vaporizer probe or in the gas phase of the ion source. In the following these fragmentations are termed “chemical dissociations”. Examples for “chemical dissociations” of neutral molecules during TSP ionization including hydrolysis, acetolysis and eliminations have also been reported by other workers [29–31]. Further examples will demonstrate that fragmentation must be considered in TSP mass spectra even at low interface temperatures.

As an example, the TSP PI mass spectra of the N-heterocyclic compound terbacil is dominated by fragment ions at m/z 161 and 178 while the quasi-molecular ion abundances at m/z 217 ($[M + H]^+$) and 234 ($[M + NH_4]^+$) are low (<10%). This behaviour can be explained by the fact that the C–N bond is readily hydrolysed and/or isobutene is eliminated in the vaporizer probe or gas phase. Decreasing the vaporizer temperature T_v increases the quasi-molecular ion intensities whereas raising the gas-phase temperature probably promotes the loss of isobutene in the gas phase and hence a decrease in the quasi-molecular ion intensities is observed (see Table I and Fig. 8 for $T_g = 200^\circ\text{C}$ versus 300°C).

The dominant ion in the TSP mass spectra of the carbamate asulam (Fig. 9a) appears at m/z 190 and corresponds to an ammonium cationized fragment molecule ($[F + NH_4]^+$) with a corresponding proton adduct ion (m/z 173 = $[F + H]^+$) over the entire temperature range investigated (variation of both T_g and T_v). Asulam is probably hydrolysed during the vaporization

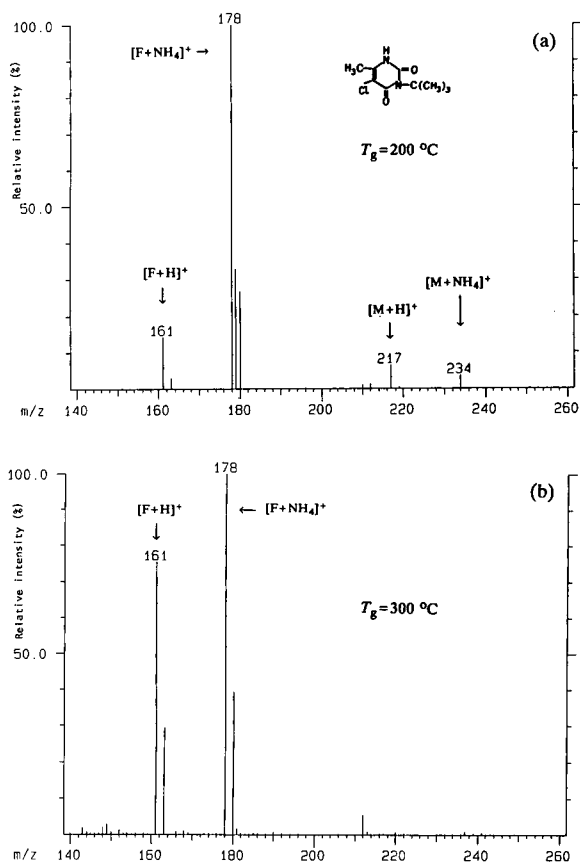


Fig. 8. TSP PI mass spectra of terbacil for $T_g =$ (a) 200 and (b) 300°C. Amount injected, 600 ng.

leading to the sulphonamide and the carbonic ester (Fig. 9a). The hydrolysis reaction was confirmed by LC-TSP-MS-MS experiments using the quasi-molecular ion $[M + NH_4]^+$ (m/z 248) as the parent ion and a low collision offset of 10 V. The daughter ions obtained are summarized in Table II (the tentative structures of the ions are presented in Fig. 9b). The ions corresponding to the degradation product are observed only in the TSP spectra and not in the CAD spectra. The ion at m/z 156 in the CAD daughter ion spectrum is probably the resonance stabilized species shown in Fig. 9b which is formed by cleavage of the S–N single bond of ionized asulam. The CAD analysis suggests that asulam, once ionized, exclusively gives the ion at m/z 156 and does not undergo a dissociation of the C–N single bond, whereas this reaction is preferred by

TABLE II

TSP POSITIVE-ION CAD DAUGHTER ION SPECTRA OBTAINED FROM THE INVESTIGATED PESTICIDES

CAD conditions: COFF, 10 V; collision cell pressure (argon), $1.3 \cdot 10^{-3}$ Torr.

Compound	Parent ion	m/z	Daughter ion spectrum: m/z (relative abundance, %)
Alachlor	$[M + H]^+$	270	270 (40)
			238 (100)
	$[M + NH_4]^+$	287	162 (42)
			270 (100)
			238 (98)
			162 (5)
			238 (100)
			224 (5)
			220 (5)
			208 (5)
Asulam	$[M + NH_4]^+$	248	162 (80)
			90 (20)
			231 (95)
			214 (5)
Desmedipham	$[M + NH_4]^+$	318	156 (100)
			182 (5)
			137 (100)
			94 (3)
			318 ^a
Oxamyl	$[M + NH_4]^+$	237	137 (55)
			120 (15)
			94 (100)
			163 (2)
			90 (58)
			72 (100)

^a COFF 30 V.

the neutral molecule probably by means of a hydrolysis in the liquid phase of the vaporizer probe.

A further example will demonstrate that raising T_g promotes “chemical dissociations”. The TSP mass spectrum of the anilide alachlor **12** exhibits the quasi-molecular ions $[M + H]^+$ (m/z 270) and $[M + NH_4]^+$ (m/z 287) almost exclusively at gas-phase temperatures lower than 200°C (Fig. 10a). However, at higher values of T_g the fragmentation increases significantly (Fig. 10b and c). The TSP mass spectra are dominated by the loss of 32 and 44 u, which can be attributed to the degradation reactions presented in

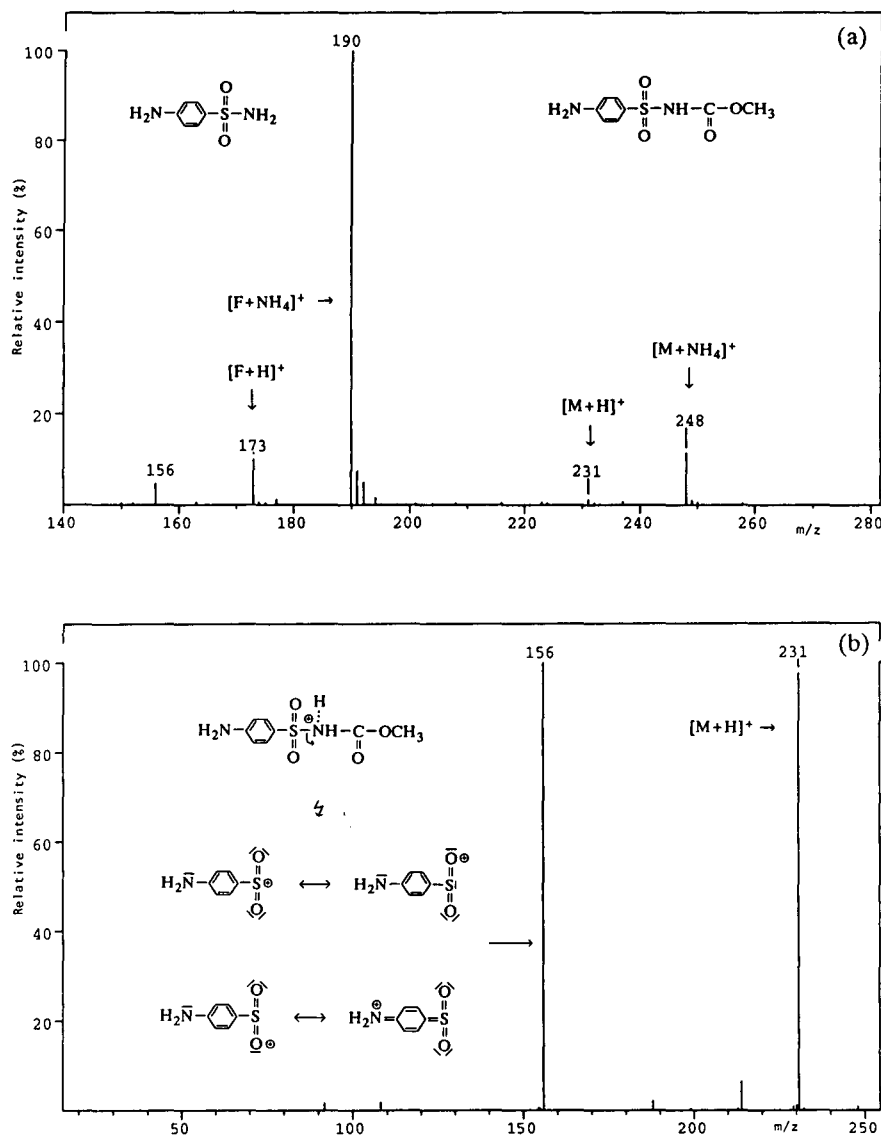


Fig. 9. CAD TSP mass spectra of asulam. (a) TSP PI spectrum and (b) daughter ion spectrum (parent ion at m/z 248). Amount injected, 100 ng.

Fig. 11. These reactions show a strong dependence on T_g as can be seen from Fig. 10a–c. Two different reaction mechanisms are probable: on the one hand a decomposition of the quasi-molecular ion $[M+H]^+$ of **12**, which gives the resonance-stabilized carbenium-imminium ion **14** at m/z 238, and on the other a simple hydrolysis reaction of the neutral tertiary amine, which leads to the secondary amine **13** with the corresponding $[F+H]^+$ and $[F+NH_4]^+$ ions in the PI

spectra, *viz.*, m/z 226 and 243. The latter was confirmed by the fact that during the low-energy CAD experiments (COFF 10 V) of the parent ions $[M+H]^+$, $[M+NH_4]^+$ and **14**, no ions are formed that can be attributed to the loss of 44 u (Fig. 12 and Table II). These results are consistent with hydrolysis of alachlor prior to ionization.

The TSP mass spectra of several N-substituted carbamates show abundant fragments even at

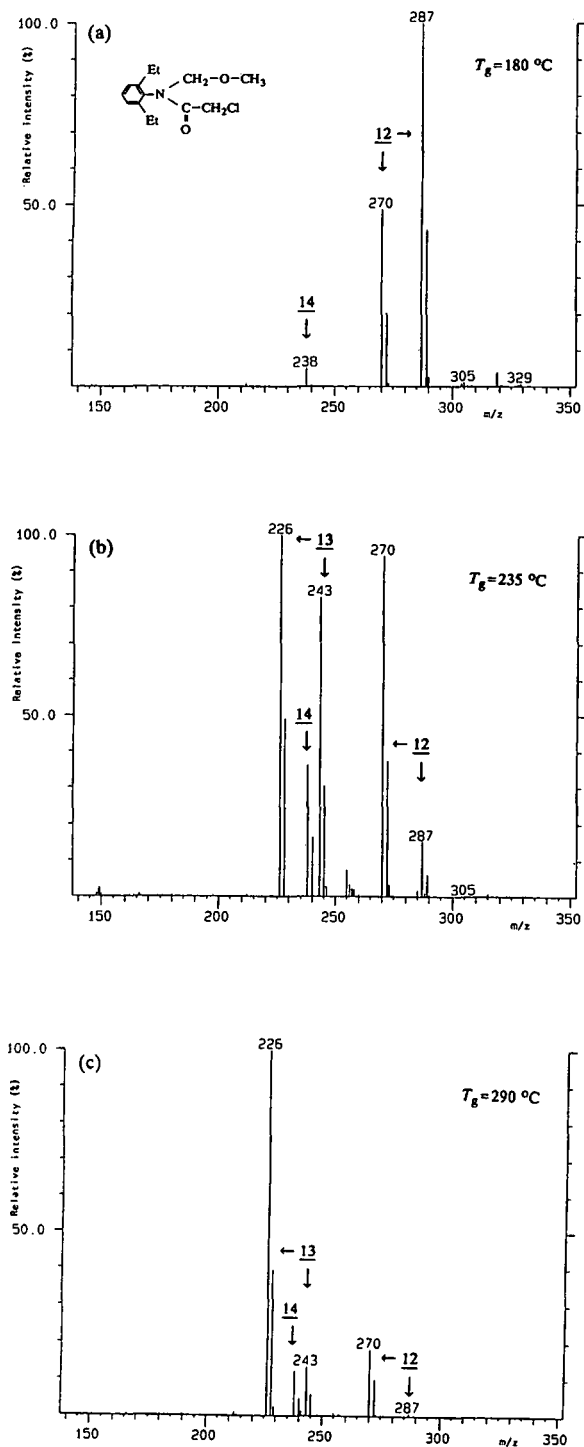


Fig. 10. TSP PI mass spectra of alachlor for different gas-phase temperatures: T_g = (a) 180; (b) 235; (c) 290°C (see Fig. 11). Amount injected, 600 ng.

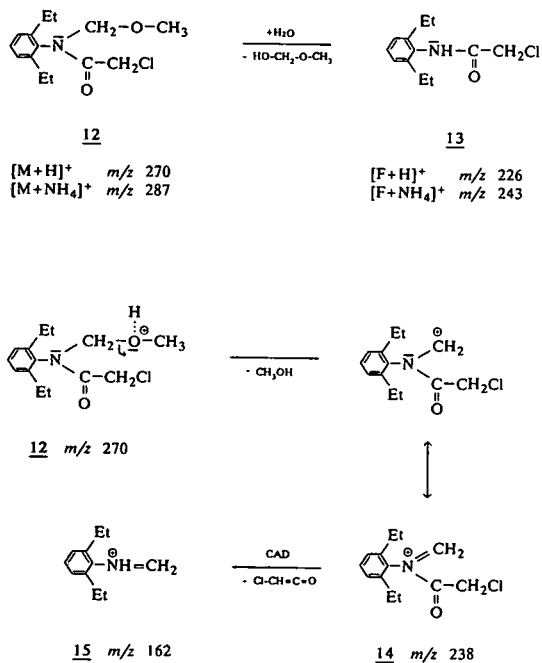


Fig. 11. Dissociation pathways for the anilide alachlor.

low vaporizer and gas-phase temperatures. These fragment ions are mainly due to the loss of the isocyanate group from the quasi-molecular ion, although fragmentation can also be explained by means of a reaction of the neutral carbamates in the liquid or gas phase. Stamp *et al.* [32] proposed a major fragmentation pathway for carbamates from CI mass spectral data which involves a proton-bound bimolecular complex (Fig. 13). This mechanism yields structurally related protonated product ions **17** and **18** which are due to the isocyanate and the alcohol formed (Table III). The weak signals at m/z 145 and 165 in the TSP PI mass spectra of carbaryl and carbofuran can probably be explained by means of this mechanism. They can be attributed to the loss of neutral methyl isocyanate from the protonated molecular ion **16**. However, in the TSP PI mass spectra of desmedipham, phenmedipham and oxamyl, abundant ammonium adduct ions of the alcohol and the isocyanate are observed in addition to the protonated product ions. As an example, the TSP mass spectra of oxamyl exhibit the $[M+NH_4]^+$ ion as the base peak (m/z 237) for low values of T_g . However,

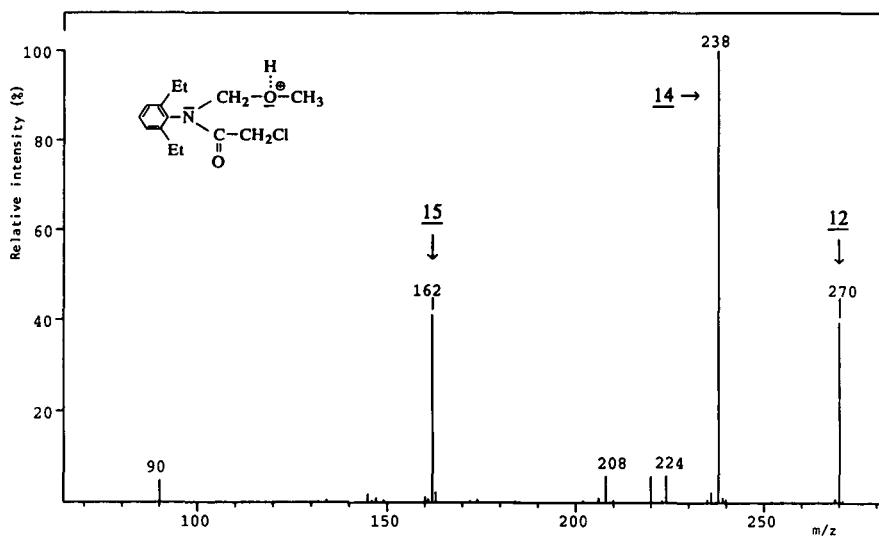
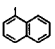
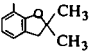
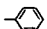
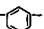
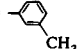
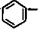

Fig. 12. CAD daughter ion spectrum of alachlor (parent ion at m/z 287).

TABLE III

DEGRADATION PRODUCTS OF N-SUBSTITUTED CARBAMATE PESTICIDES OBTAINED FROM THE TSP AND CAD SPECTRA

Carbamate	$R^1-NH-C(O)O-R^2$	Observed product ions (m/z) ^a	
		$[R^1-NCO + X]^+$	$[R^2-OH + X]^+$
Carbaryl	$R^1 = CH_3$ $R^2 =$ 	— ^b	145
Carbofuran	$R^1 = CH_3$ $R^2 =$ 	— ^b	165, 182
Desmedipham	$R^1 =$  $R^2 = C_2H_5O-C(=O)-NH-$ 	120, 137	182, 199
Phenmedipham	$R^1 =$  $R^2 = CH_3O-C(=O)-NH-$ 	134, 151	168, 185
Oxamyl	$R^1 = CH_3$ $R^2 = (CH_3)_2N-CO-C(=N)-$ 		163, 180

^a X = H⁺ or NH₄⁺.^b Note: detection of ammonia and/or proton cationized methyl isocyanate was not possible under regular TSP recording conditions.

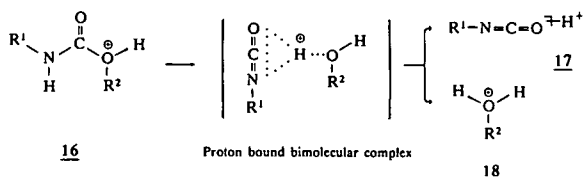


Fig. 13. Dissociation pathway for N-substituted carbamate pesticides (from Stamp *et al.* [32]).

with increasing temperature the fragment ions at m/z 163 and 180 become more abundant (Fig. 14). These ions can be attributed to the proton and ammonium adduct ion of the alcohol formed. It is probable that these ions correspond to the loss of isocyanate from the $[M + H]^+$ and $[M + NH_4]^+$ quasi-molecular ions, but the mechanism is not yet clear. Further, the spectra of the dicarbamates desmedipham and phenmedipham contain less abundant quasi-molecular ions and significantly more ammonium and proton cationized fragment ions (Table III). The intensity of the quasi-molecular ion $[M + NH_4]^+$ is low in each instance (<5% relative abundance). The base peak is due to the fragment ion at either m/z 182 or 199 for desmedipham (m/z 168 and 185 for phenmedipham), the abundance of which depends on T_g and which can be attributed to the formed alcohol. The ions at m/z 137 and 151 are probably due to the ammonium adducts of the isocyanates. These results were confirmed by performing additional CAD experiments (Table II). As an example, the CAD daughter ion spectrum of oxamyl (parent ion at m/z 237) and the structures of the ions formed are shown in Fig. 14c. The results are in agreement with those of other workers [22]. The ions at m/z 72 and 90 can be attributed to fragments formed from the protonated alcohol after the loss of methyl isocyanate. In the CAD spectra of desmedipham the ions formed compare well with those obtained from the normal TSP spectra (Table II), although no ammonium adduct ions of the alcohol fragments are observed in the CAD spectra even with the low COFF of 10 V.

The examples discussed in this and the preceding section clearly confirm the conclusion that "chemical dissociations" in the vaporizer probe or the ion source are predominantly responsible for the fragments observed in the TSP mass

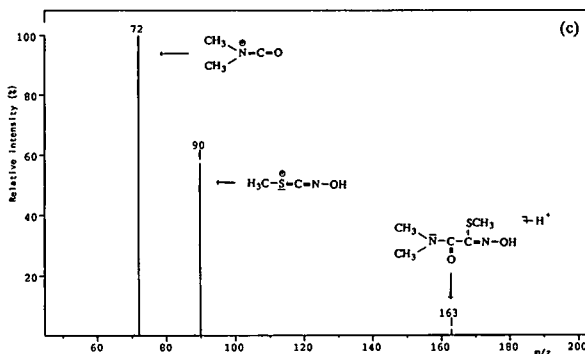
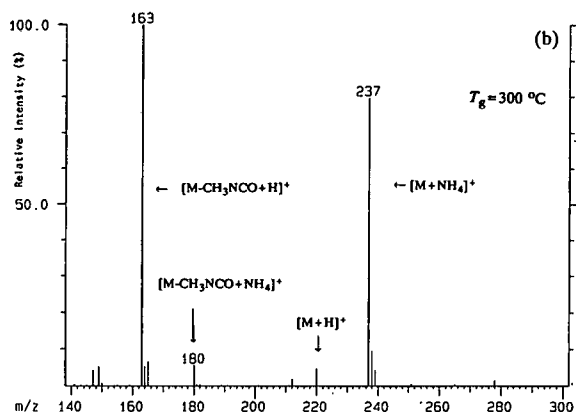
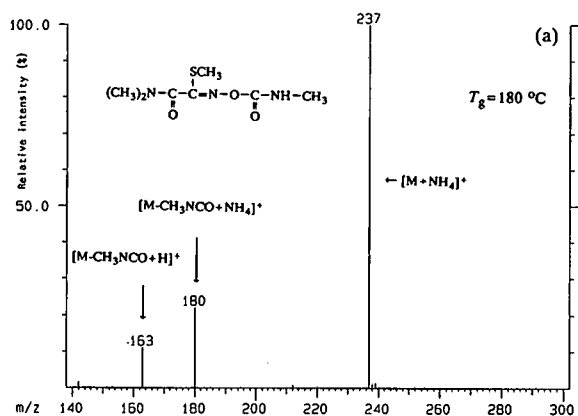
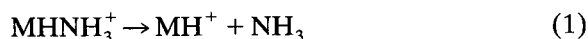


Fig. 14. TSP PI mass spectra of oxamyl for $T_g =$ (a) 200 and (b) 300°C and (c) CAD daughter ion spectrum (parent ion at m/z 237). Amount injected, 200 ng.

spectra of the investigated pesticides, particularly at lower temperatures. In many instances fragment ions formed by such “chemical dissociations” dominate the TSP mass spectra. In these instances the intensities of the quasi-molecular ions can often be increased by lowering T_g , whereas lowering T_v is not recommended in most instances because the sensitivity decreases drastically at temperatures lower than the take-off temperature (*i.e.*, at the point of complete vaporization). However, in some instances fragmentation is unavoidable (*e.g.*, asulam, desmedipham and terbacil). Hence for quantification in the SIM mode these fragment ions have to be used.

Ion abundance ratio of the quasi-molecular ions $[M + H]^+$ and $[M + NH_4]^+$. As mentioned in the previous sections, the relative intensity of the quasi-molecular ions $[M + H]^+$ and $[M + NH_4]^+$ is strongly dependent on the gas-phase temperature T_g for several carbamates, phenylureas and organophosphorus compounds (see Figs. 2, 5, 7–10, 14 and 17) where with increasing temperature $[M + H]^+$ becomes more abundant, *i.e.*, a dissociation of $[M + NH_4]^+$ leads to $[M + H]^+$:



It was observed that as T_g is raised the ion abundance ratio of the $[M + H]^+$ relative to the $[M + NH_4]^+$ ions, $r(M)$, increases exponentially whereas the sum of the ion currents of both quasi-molecular ions remains almost constant, as can be seen from Fig. 15, in which the absolute ion intensities of the different quasi-molecular ion species of chlorpropham and buminafos are plotted against T_g . For most investigated compounds the dependence of $r(M)$ on T_g can be described by the equations

$$r(M) = \frac{I[M + H]^+}{I[M + NH_4]^+} = A e^{-C/T_g} \quad (2)$$

$$\ln r(M) = \ln A - C/T_g \quad (3)$$

Thus a plot of $\ln r(M)$ against $1/T_g$ leads to a straight line in the investigated temperature range $T_g = 150\text{--}320^\circ\text{C}$. Examples of this behaviour are summarized in Fig. 16a–c for several

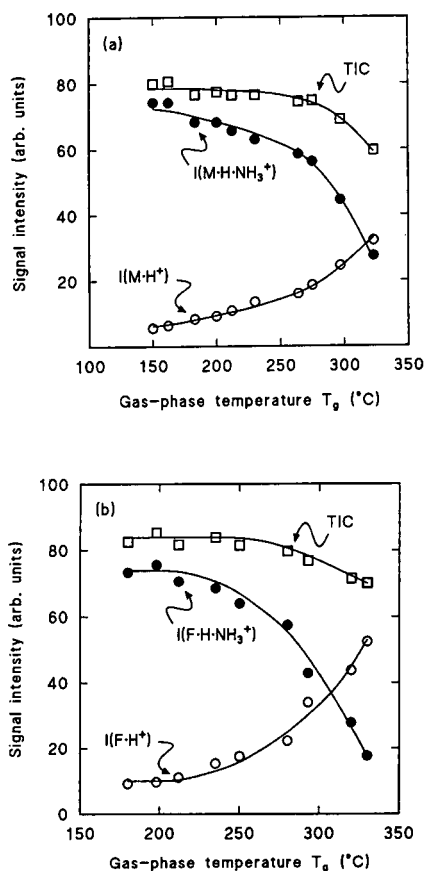
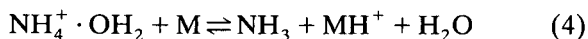


Fig. 15. Absolute quasi-molecular ion intensities and total ion current as a function of the gas-phase temperature T_g for (a) the MH^+ (m/z 214) and $(MHNH_3)^+$ (m/z 231) ions of chlorpropham (see Fig. 17) and (b) the FH^+ (m/z 195) and $(FHNH_3)^+$ (m/z 212) ions of the phosphoric diester 7 formed from buminafos (see Fig. 5).

pesticides which show combinations of both quasi-molecular ions in the TSP mass spectra.

Alexander and Kebarle [33] used the $NH_4^+ \cdot OH_2$ ion as a representative primary cluster ion for gas-phase protonation, although other cluster ions with different cluster dissociation energies, D_c , and proton affinities, PA , may be involved. Using this primary ion the processes leading to protonation and ammonium addition are described by the equations



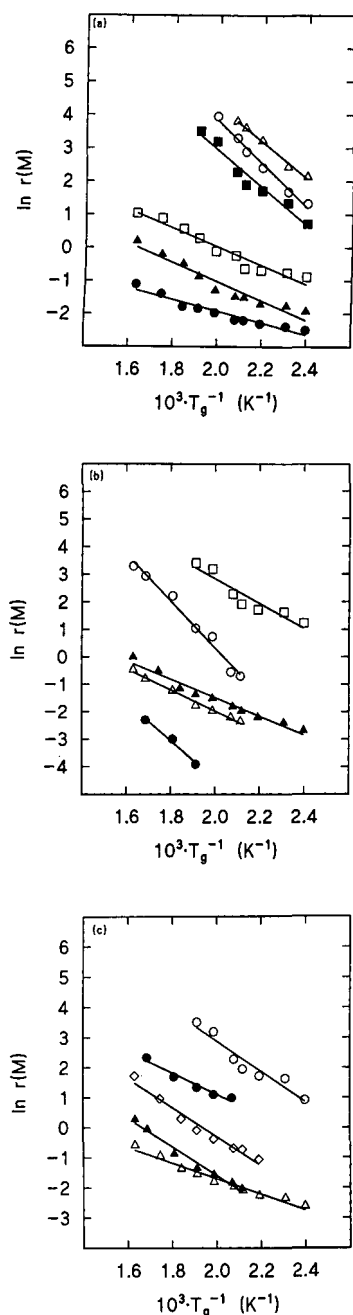
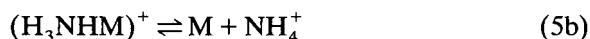


Fig. 16. In $I(\text{MH}^+)/I(\text{MHNH}_3^+) [= \ln r(\text{M})]$ as a function of the reciprocal of the absolute temperature of the gas phase for several pesticides. (a) ● = Carbaryl; ■ = fenuron; □ = desmedipham; ○ = methabenzthiazuron; ▲ = phenmedipham; △ = difenoxuron. (b) ● = Azinphos-ethyl; △ = tri-chlorphon; □ = oxamyl; ● = naled; ▲ = chloroprotham. (c) ○ = Chlorotoluron; ▲ = buminafos; ● = terbacil; ◇ =alachlor; △ = butonate.



Protonation of M according to eqn. 4 is only possible if $PA(\text{M})$ is $\geq 224 \text{ kcal mol}^{-1}$ $\{\Delta H_4 = D_c + PA(\text{NH}_3) - PA(\text{M})$, where $PA(\text{NH}_3) = 204 \text{ kcal mol}^{-1}$ and $D_c \approx 20 \text{ kcal mol}^{-1}$ [33] $\}$ (1 kcal = 4.184 kJ). In this case no $[\text{M} + \text{NH}_4]^+$ signal is observed as found for N-heterocyclic pesticides, morpholines, many anilides and carbamates and some other pesticide classes. Compounds with a PA in the range 204–224 kcal mol⁻¹ will undergo reactions 5 and 5a. The TSP mass spectra show both $[\text{M} + \text{H}]^+$ and $[\text{M} + \text{NH}_4]^+$ ions if their PA is equal to or slightly higher than $PA(\text{NH}_3)$ as found for phenylureas and some organophosphorus compounds (e.g., the dithiophosphorus esters dimethoate, disulfoton and phorate). The equilibrium described by reaction 5a and thus the ratio $r(\text{M})$ depends sensitively on T_g , where $r(\text{M})$ can be described by eqns. 2 and 3. Compounds having PA slightly less than ammonia ($PA < 204 \text{ kcal mol}^{-1}$) can give reactions 5a and 5b. Thus, the $[\text{M} + \text{NH}_4]^+$ ion dominates the spectra, as is found for most phosphorus and phosphonic esters where eqns. 1–3 are still valid. However, if $PA(\text{M})$ is 20–30 kcal mol⁻¹ lower than $PA(\text{NH}_3)$, no analyte ions are formed [34].

The parameters A and C in eqns. 2 and 3 as determined from the temperature dependence of the investigated pesticides are summarized in Table IV. The correlation coefficient demonstrates that the ion intensity ratio $r(\text{M})$ can be well described by eqn. 3 for almost all compounds. However, at gas-phase temperatures $> 320^\circ\text{C}$ deviations from eqn. 3 are observed which can be attributed to undefined thermal decompositions. Even a variation of the vaporizer temperature influences $r(\text{M})$ because T_g is directly influenced by T_v . Eqn. 3 is also valid for other solvent compositions, although the values of the parameters A and C change slightly.

In general, at higher gas-phase temperatures ($T_g = 250\text{--}300^\circ\text{C}$) the TSP mass spectra of most investigated pesticides exhibit $[\text{M} + \text{H}]^+$ ions and $[\text{F} + \text{H}]^+$ ions as base peaks (with the exception of several organophosphorus pesticides), whereas at lower temperatures the $[\text{M} + \text{NH}_4]^+$ ion often dominates. These effects have to be taken

TABLE IV
EXPERIMENTAL FIT PARAMETERS A AND C (EQN. 3)

Compound	M_r [M(F)] ^a	–C	ln A	–r ^b
Alachlor	269	2.5761	3.4509	0.9838
Azinphos-ethyl	345	4.4557	11.7455	0.9945
Buminafos	195	4.7221	7.8154	0.9895
Carbaryl	201	1.7488	1.5734	0.9967
Chloroprotham	213	3.3679	5.2527	0.9425
Chlorotoluron	212	5.0495	12.9934	0.9602
Desmedipham	181	2.8015	5.6146	0.9709
Difenoxyuron	286	5.3706	14.9647	0.9947
Fenuron	164	5.5814	14.0559	0.9778
Methabenzthiazuron	206	6.4229	16.6071	0.9930
Naled	380	7.0916	9.7122	0.9922
Phenmedipham	150	2.8680	4.6961	0.9662
Oxamyl	162	8.4902	17.3094	0.9909
Terbacil	160	3.5217	8.1583	0.9785
Trichlorphon	256	3.8667	5.7569	0.9944

^a Molecular mass of the molecule (M) or fragment (F).

^b Correlation coefficient.

into account when pesticides are determined in the SIM mode because the total ion current (*i.e.*, the sum of both quasi-molecular ions) is less dependent on T_g than the ion current of the individual quasi-molecular ions (see Fig. 15a and b).

Additional adduct ions. According to Maeder [35], TSP PI quasi-molecular ions $[M_{qm}]^+$ have the general formula

$$[M_{qm}]^+ = [M + A + xB - yC]^+ \quad (6)$$

where M is the nominal mass of the analyte molecule, A is the attached ion (*e.g.*, H^+ , NH_4^+), B is the attached solvent molecule (H_2O , $MeOH$) and/or additive molecule (NH_4OAc , $HCOONH_4$), C is the eliminated molecule (H_2O , $MeOH$) and x and y are integers beginning with zero.

We investigated the ion abundance of several pesticides in the temperature range $T_g = 150$ – $320^\circ C$. As an example, the TSP PI mass spectra of four phenylurea and carbamate pesticides are shown in Fig. 17a–d for $T_g = 150^\circ C$. All compounds give adduct ions which can in part be explained by applying eqn. 6. The base peak was the $[M + H]^+$ ion and the second most abundant ion was the $[M + NH_4]^+$ ion for the phenylureas.

This is also the case for some other investigated phenylureas, the spectra of which are not shown here. This is in contrast to reports by other workers [18,36], who found that $[M + NH_4]^+$ is always the base peak for phenylurea herbicides. This difference is probably due to the different designs of the ion sources, whereas the use of different ionization media (filament-off, filament, discharge) has only a slight influence on the abundance ratios of the quasi-molecular ions. Chloroprotham exhibits $[M + NH_4]^+$ as the base peak. At lower gas-phase temperatures additional adduct ions besides the “normal” quasi-molecular ions such as $[M + MeOH + H]^+$ and $[M + NH_4OAc - 2H_2O + H]^+$ appear in the spectra with relative abundances of *ca.* 2–15% (see Table I for mass assignment). These ions follow eqn. 6. In addition, we found an $[M + 46]^+$ ion which is not described by eqn. 6 and the origin of which at present is not clear. In the spectra of the anilide alachlor different adduct ions can be observed which, however, are still in agreement with eqn. 6 (Table I and Fig. 10).

For all phenylureas the $[M + H]^+$ ion remains the base peak when T_g is raised while the $[M + NH_4]^+$ is still present. However, the other adduct ions completely disappear at $T_g > 200^\circ C$,

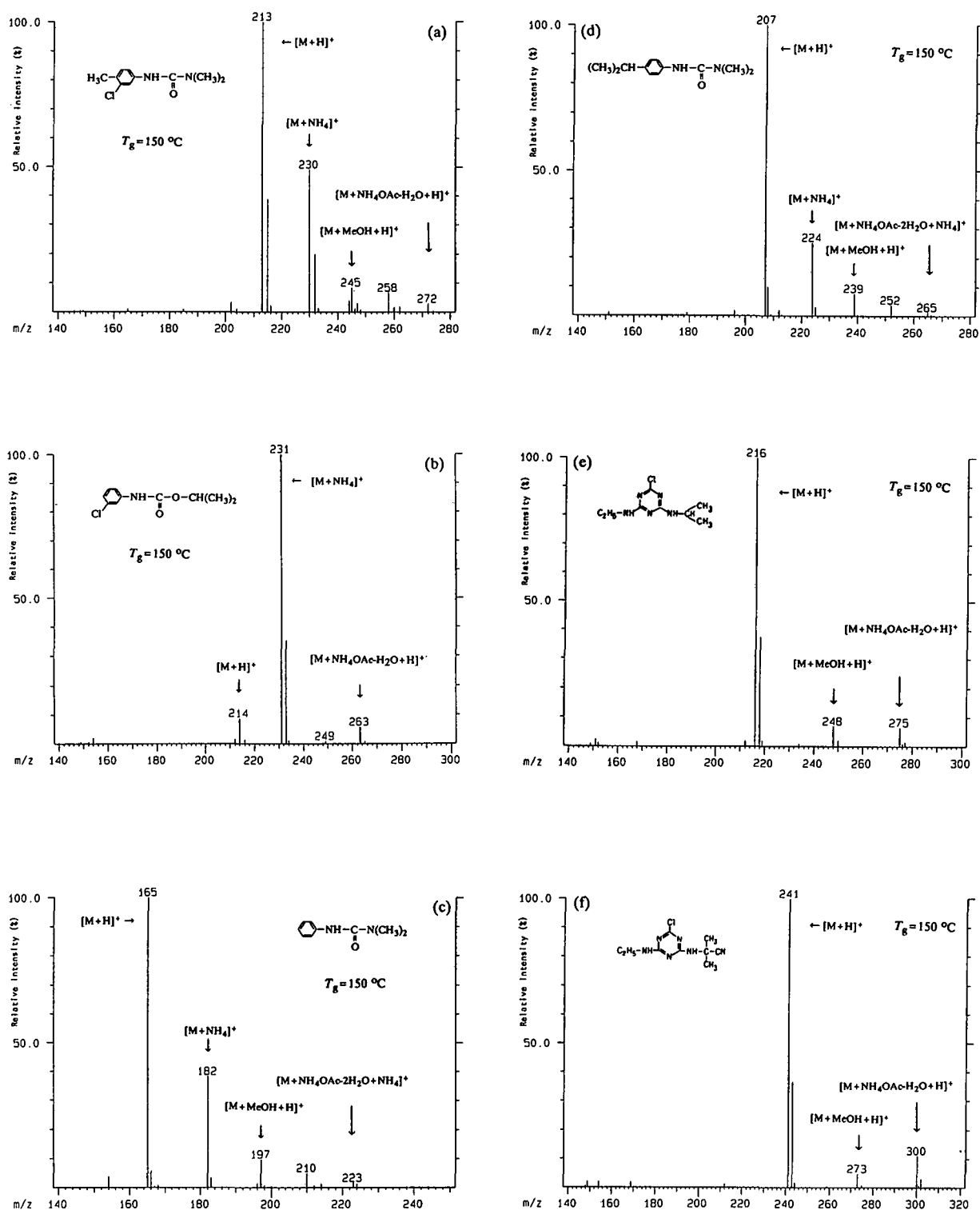


Fig. 17. TSP PI mass spectra of (a) chlorotoluron, (b) chlorpropham, (c) fenuron, (d) isoproturon, (e) atrazine and (f) cyanazine for $T_g = 150\text{ }^\circ\text{C}$ (600 ng each).

indicating that these adduct ions undergo thermal decomposition.

Adduct ion formation and its temperature dependence were also studied for several triazine herbicides using ammonium acetate as the volatile buffer salt. The adduct ion formation can be rationalized as described above. The TSP spectra of atrazine and cyanazine are shown as examples in Fig. 17e and f for $T_g = 150^\circ\text{C}$. The $[\text{M} + \text{H}]^+$ ion is always the base peak and no $[\text{M} + \text{NH}_4]^+$ signal is obtained, as triazine compounds have proton affinity values that are higher than that of ammonia. At lower temperatures we observed two additional adduct ions in the spectra that can be attributed to the $[\text{M} + \text{MeOH} + \text{H}]^+$ and $[\text{M} + \text{NH}_4\text{OAc} - \text{H}_2\text{O} + \text{H}]^+$ ions (see Table I) with relative abundances of ca. 10–15%. At $T_g > 200^\circ\text{C}$ these ions disappear. In contrast, Barceló *et al.* [23,36,37] observed the $[\text{M} + \text{NH}_4\text{OAc} - \text{H}_2\text{O} + \text{H}]^+$ ion as the base peak for

low gas-phase temperatures (200°C) and the $[\text{M} + \text{H}]^+$ ion at higher temperatures (270°C). As mentioned above, this difference is probably due to the different designs of the TSP sources, some of which favour high clustering with the solvent [27,36].

Under typical operating conditions ($T_s = 220\text{--}300^\circ\text{C}$ and $T_g \approx 210\text{--}290^\circ\text{C}$; see Experimental) no additional adduct ions were observed. Adduct ion formation can be used to gain additional structural information, as shown by Barceló *et al.* [23].

Dependence of the ion abundance in thermospray mass spectra on the buffer concentration. Application to quaternary ammonium herbicides

The direct flow-injection TSP mass spectra of the diquaternary ammonium herbicides diquat and paraquat using pure water and 50 mM am-

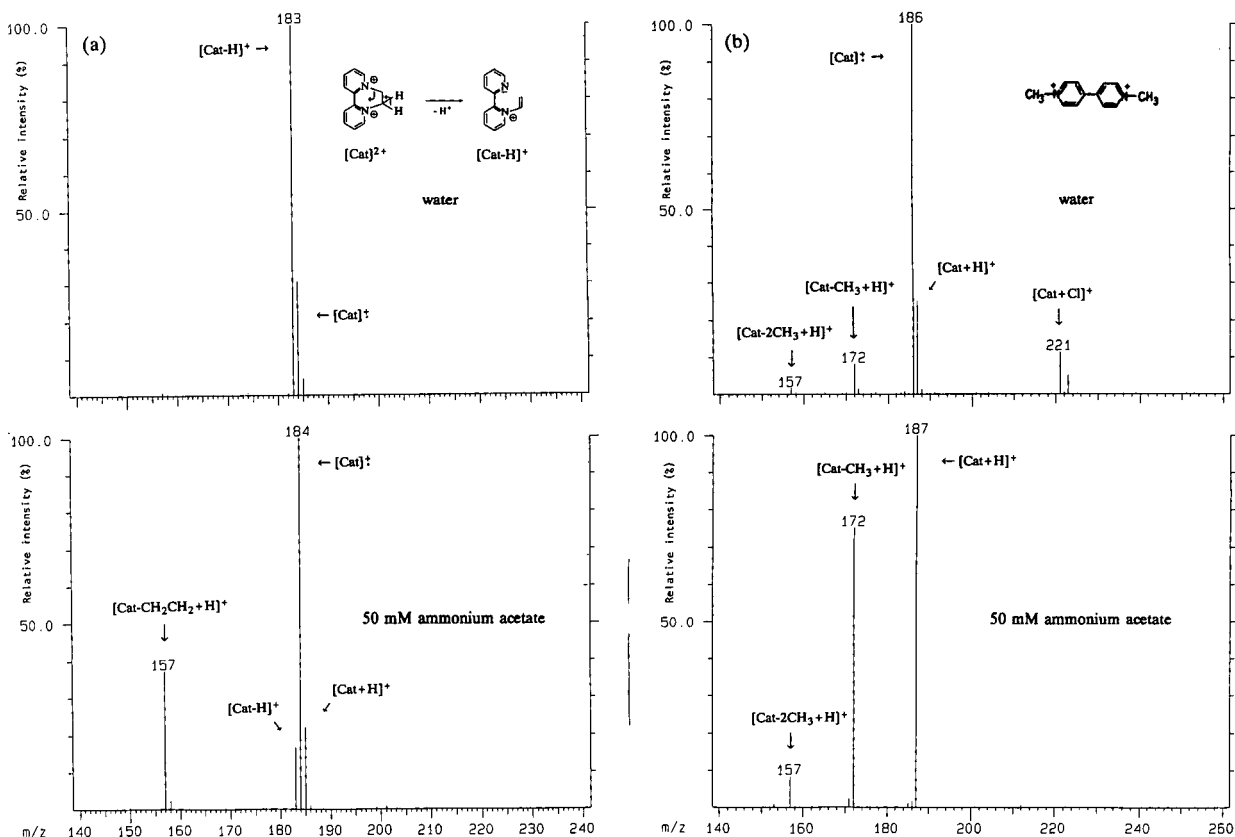


Fig. 18. Direct flow-injection TSP mass spectra of 300 ng of (a) diquat and (b) paraquat. Mobile phase: (top) water and (bottom) 50 mM ammonium acetate.

monium acetate as the mobile phase are shown in Fig. 18.

The signal at m/z 183 dominates the TSP spectra of diquat in pure water (without salt). The peak can be attributed to the unusual deprotonated dication $[\text{Cat} - \text{H}]^+$ which is probably formed by "fragmentation" of the intact dication (Fig. 18). No other ions except the intact dication (m/z 92) could be observed (Table I). This leads to the conclusion that only thermal dissociations are possible without the buffer salt.

With ammonium acetate in the mobile phase, the TSP mass spectra exhibit more ions which are due to additional chemical reactions in the gas phase induced by buffer ions. The major difference between the spectra with aqueous ammonium acetate and pure water as solvent is on the one hand the increased production of ions by reduction of the dication (formation of $[\text{Cat}]^+$) and on the other the enhanced formation of fragment ions formed by cleaving off the C_2H_4 chain (doubly positively charged!) from the dication followed by protonation of the formed neutral amine rather than loss of H^+ as shown in Fig. 18. This results in enhanced relative abundances of $[\text{Cat}]^+$, $[\text{Cat} + \text{H}]^+$ and $[\text{Cat} - \text{C}_2\text{H}_4 + \text{H}]^+$ versus $[\text{Cat} - \text{H}]^+$ and $[\text{Cat}]^{2+}$ (Fig. 18a). This behaviour can be explained by the fact that bipyridinium compounds are easily reduced to the free radicals by reducing agents [38].

In contrast to other investigations [39,40], we found an increase in the intensity of the intact dication at m/z 92 as the salt concentration c_s is raised. However, this increase is not as strong as for the monovalent reaction products.

Under TSP conditions paraquat behaves similarly to diquat, although the $[\text{Cat} - \text{H}]^+$ ion is absent (Fig. 18b). Paraquat exhibits a loss of 15 and 30 u from the intact dication owing to the loss of one or two methyl groups, simultaneously taking away one positive charge (of course, in the event of the cleavage of both methyl groups, the formed neutral molecule is protonated to give $[\text{Cat} - 2\text{CH}_3 + \text{H}]^+$). However, the signal at m/z 172 leads to the conclusion that the reduced dication is also fragmented ($[\text{Cat} - \text{CH}_3 + \text{H}]^+$). The peak at m/z 221 can be attributed to the addition of the anion (Cl^-) to the dication with the corresponding ^{37}Cl isotopic peak (m/z 223).

The dication (m/z 93) appears in the spectra only in solutions without salt addition, but the intensity is low (<5% relative abundance). The base peak can be attributed to the $[\text{Cat} + \text{H}]^+$ ion (m/z 187), while the $[\text{Cat}]^+$ ion (m/z 186) dominates in pure water.

Divalent quaternary ammonium salts can be separated on highly deactivated reversed-phase materials using methanol–water or acetonitrile–water gradient mixtures as the mobile phase. For this reason, it was of interest to investigate the behaviour of these compounds in such mixed solvents, particularly the dependence of the abundances and the intensities of the different ion species on c_s .

Results for the repetitive injection of 300 ng of paraquat using methanol–water (50:50, v/v) at

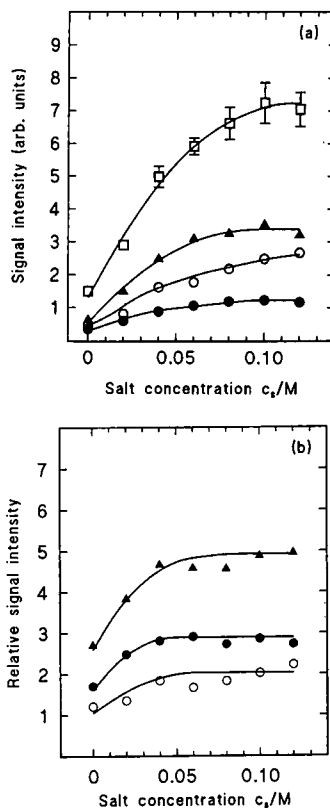


Fig. 19. (a) Absolute and (b) relative ion intensities as a function of the concentration of ammonium acetate in methanol–water (50:50, v/v) for injections of 300 ng of paraquat. (a) \square = TIC; \blacktriangle = $[\text{M} - \text{R} + \text{H}]^+$; \circ = $[\text{M} - 2\text{R} + \text{H}]^+$; \bullet = $[\text{M}]^+ + [\text{M} + \text{H}]^+$. (b) \blacktriangle = $I(\text{fragment ions})/I(\text{M})$; \bullet = $I([\text{M} - \text{R} + \text{H}]^+)/I(\text{M})$; \circ = $I([\text{M} - 2\text{R} + \text{H}]^+)/I(\text{M})$.

different salt concentrations are summarized in Fig. 19a and b. In Fig. 19b the ratio of the fragment ion intensity relative to the sum of the molecular ion intensity is plotted against the salt concentration. One observes that fragmentation is enhanced as c_s is raised. This phenomenon can probably be explained by considering the possibility of solid particle formation in the ion source at higher c_s and the subsequent thermal decomposition of these solid particles, thus releasing the analyte ions [40,41]. The thermal stress of the analyte molecule is apparently much higher in the solid particles and thus thermal fragmentation is enhanced. In comparison with the aqueous solution (Fig. 18), fragmentation is much higher in the case of the mixed solvent whereas the intact dication (m/z 93) is absent even without added salt. This observation leads to the conclusion that the dication is mainly degraded to the monovalent fragment ions or reduced to the monovalent cation. However, the intensity of the monovalent cation is nevertheless strongly enhanced as c_s is increased (Fig. 19a).

The use of the filament or the discharge electrode leads to unsatisfactory results in both solvents (methanol–water and pure water) because the increase in the signal intensity of all ions cannot compensate for the strong increase in the noise.

In conclusion, we do not recommend the determination of quaternary ammonium herbicides without the use of a buffer salt. The decrease in sensitivity due to fragmentations on raising the salt concentration is readily compensated for by a much higher gain in sensitivity for each ion. The curves obtained (Fig. 19a) are very similar to those reported for neutral analytes, *i.e.*, the optimum concentration of ammonium acetate is in the range 50–100 mM. When chromatographic conditions restrict high concentrations of salt, *e.g.*, for ion-exchange separations [17], one has to add the salt postcolumn.

CONCLUSIONS

The principal conclusions derived from these investigations for the determination of pesticides by means of LC–TSP–MS are the following. Organophosphorus pesticides are thermally

labile. The compounds show gas-phase thermal degradation reactions that are strongly dependent on the gas-phase temperature. These reactions are mainly due to “chemical dissociations” of the neutral precursors, followed by gas-phase protonation or ammonium addition. However, decreasing the gas-phase temperature and the ion source temperature to optimum values leads to an increase in the quasi-molecular ion abundances. Under these conditions, the compounds investigated are stable under TSP conditions, *i.e.*, the fragmentation is minimized.

The examples presented demonstrate that for some pesticide compound classes fragmentation reactions occur during TSP vaporization and ionization. However, thermal decompositions are less important in TSP mass spectra. Most bond cleavages can be explained by hydrolysis reactions and/or rearrangements and eliminations of the neutral molecules, and only in some instances of the quasi-molecular ions, induced by buffer or solvent ions which depend strongly on the gas-phase temperature, indicating the domination of gas-phase processes. In some instances these fragmentation reactions are unavoidable. However, if the reactions involved have high yields and the fragments formed reflect the structure of the original pesticide, this is not necessarily a disadvantage, especially for quantification purposes. Further, LC–TSP–MS can be used as an ideal confirmatory method in some instances.

For most of the investigated compounds a linear relationship is observed when the logarithm of the ion abundance ratio for the $[M + H]^+$ ion relative to the $[M + NH_4]^+$ ion is plotted against the reciprocal of the absolute temperature of the gas phase in the range $T_g = 150$ – 320°C . As several pesticide compound classes show both $[M + H]^+$ and $[M + NH_4]^+$ ions, this temperature dependence can be used to generate TSP spectra with mainly one quasi-molecular ion, thus concentrating the main ion current into one instead of two ions. This may be of value in trace analyses for pesticides if the mass spectrometer is operated in the SIM mode, because the total ion current (*i.e.*, the sum of both quasi-molecular ions) is less dependent on T_g than the ion current of the individual quasi-

molecular ions.

It was found that additional adduct ions beside the quasi-molecular ions may be observed in TSP PI mass spectra of several pesticides (*e.g.*, carbamates, organophosphorus pesticides, phenylureas and triazines). These additional ions are expected to be useful for an unambiguous identification of pesticides in real environmental samples. However, the intensity of these ions is low in each instance and the formation is limited to low gas-phase and ion source temperatures.

The results reported for the divalent quaternary ammonium herbicides demonstrate that the addition of a volatile buffer salt to the mobile phase is necessary although the compounds are already completely dissociated in the aqueous solvent. The observed relationships for the ion intensity *versus* salt concentration are similar to those reported for neutral molecules. Although fragmentation is enhanced as the salt concentration is raised, this disadvantage can readily be compensated for by the strong increase in sensitivity.

ACKNOWLEDGEMENTS

We thank Dr. J. Schmidt (Solvay Deutschland, Hannover, Germany) for facilitating the CAD experiments. We acknowledge financial support from the Bundesministerium für Forschung und Technologie.

REFERENCES

- 1 T.R. Covey, E.D. Lee, A.P. Bruins and J.D. Henion, *Anal. Chem.*, 58 (1986) 1451A.
- 2 K. Levsen, *Org. Mass Spectrom.*, 23 (1988) 406.
- 3 L.H. Wright, *J. Chromatogr. Sci.*, 20 (1982) 1.
- 4 T. Cairns, E.G. Siegmund and G.M. Dose, *Biomed. Mass Spectrom.*, 10 (1983) 24.
- 5 R.D. Voyksner and J.T. Bursey, *Anal. Chem.*, 56 (1984) 1582.
- 6 T.R. Covey and J.D. Henion, *Anal. Chem.*, 55 (1983) 2275.
- 7 M. Barber, R.S. Bordoli, G.J. Elliot, R.D. Sledgewick and A.N. Tyler, *Anal. Chem.*, 54 (1982) 645A.
- 8 C.R. Blakely and M.L. Vestal, *Anal. Chem.*, 55 (1983) 750.
- 9 M.L. Vestal, *Anal. Chem.*, 56 (1984) 2590.
- 10 P. Arpino, *Mass Spectrom. Rev.*, 9 (1990) 631.
- 11 T.D. Behymer, T.A. Bellar and W.L. Budde, *Anal. Chem.*, 62 (1990) 1686.
- 12 S. Pleasance, J.F. Anacleto, M.R. Baily and D.H. North, *J. Am. Soc. Mass Spectrom.*, 3 (1992) 378.
- 13 T.A. Bellar and W.L. Budde, *Anal. Chem.*, 60 (1988) 2076.
- 14 E.R.J. Wils and A.G. Hulst, *Fresenius' J. Anal. Chem.*, 342 (1992) 749.
- 15 D. Barceló, *Biomed. Environ. Mass Spectrom.*, 17 (1988) 2076.
- 16 A. Farran, J. De Pablo and D. Barceló, *J. Chromatogr.*, 455 (1988) 163.
- 17 C.H. Vestal, *Vestec Thermospray Newsl.*, 3 (1987) 2.
- 18 D. Barceló, *Org. Mass Spectrom.*, 24 (1989) 219.
- 19 R.D. Voyksner, in J.D. Rosen (Editor), *Applications of New Mass Spectrometry Techniques in Pesticide Chemistry*, Wiley, New York, 1987, p. 146.
- 20 T.L. Jones, L.D. Betowsky and J. Yinon, in M.A. Brown (Editor), *Liquid Chromatography/Mass Spectrometry. Applications in Agricultural, Pharmaceutical, and Environmental Chemistry (ACS Symposium Series, No. 420)*, American Chemical Society, Washington, DC, 1990, p. 62.
- 21 R.D. Voyksner, in J.D. Rosen (Editor), *Applications of New Mass Spectrometry Techniques in Pesticide Chemistry*, Wiley, New York, 1987, p. 247.
- 22 K.S. Chiu, A. Van Langenhove and C. Tanaka, *Biomed. Environ. Mass Spectrom.*, 18 (1989) 200.
- 23 D. Barceló, G. Durand, R.J. Vreeken, G.J. De Jong, H. Lingeman and U.A.Th. Brinkman, *J. Chromatogr.*, 553 (1991) 311.
- 24 D.J. Liberato and P. Kebarle, *Anal. Chem.*, 58 (1986) 6.
- 25 R.D. Voyksner, J.T. Bursey and E.D. Pellizari, *Anal. Chem.*, 56 (1984) 1507.
- 26 T.M. Chen, J.E. Coutant, A.D. Sill and R.R. Fike, *J. Chromatogr.*, 396 (1987) 382.
- 27 D. Barceló and J. Albaiges, *J. Chromatogr.*, 474 (1989) 163.
- 28 J.A.G. Roach and D. Andrzejewski, in J.D. Rosen (Editor), *Application of New Mass Spectrometry Techniques in Pesticide Chemistry*, Wiley, New York, 1987, p. 187.
- 29 M.M. Siegel, R.K. Isensee and D.J. Beck, *Anal. Chem.*, 59 (1987) 989.
- 30 M.F. Bean, S.L. Pallante-Morell and C. Fenselau, *Biomed. Environ. Mass Spectrom.*, 18 (1989) 219.
- 31 W.M. Lagna and P.S. Callery, *Biomed. Mass Spectrom.*, 12 (1985) 699.
- 32 J.J. Stamp, E.G. Siegmund, T. Cairns and K.K. Chan, *Anal. Chem.*, 58 (1986) 873.
- 33 A.J. Alexander and P. Kebarle, *Anal. Chem.*, 58 (1986) 471.
- 34 A. Harrison, *Chemical Ionization Mass Spectrometry*, CRC Press, Boca Raton, FL, 1983, p. 33.
- 35 H. Maeder, *Rapid Commun. Mass Spectrom.*, 4 (1990) 52.
- 36 D. Barceló, *Chromatographia*, 25 (1988) 295.
- 37 D. Barceló, in M.A. Brown (Editor), *Liquid Chromatography/Mass Spectrometry. Applications in Agricultural, Pharmaceutical, and Environmental Chemistry (ACS*

- Symposium Series*, No. 420), American Chemical Society, Washington, DC, 1990, p. 48.
- 38 H.P. Thier and H. Zeumer (Editors), *Manual of Pesticide Residue Analysis*, Vol. 1, Deutsche Forschungsgemeinschaft, Pesticides Comm., VCH, Weinheim, 1987, p. 177.
- 39 T.R. Covey, A.P. Bruins and J.D. Henion, *Org. Mass Spectrom.*, 20 (1988) 178.
- 40 G. Schmelzeisen-Redeker, F.W. Röllgen, H. Wirtz and F. Voegtle, *Org. Mass Spectrom.*, 20 (1985) 752.
- 41 G. Schmelzeisen-Redeker, M.A. McDowall, U. Giessmann, K. Levsen and F.W. Röllgen, *J. Chromatogr.*, 323 (1985) 127.

CHROMSYMP. 2862

Development of a high-performance liquid chromatographic–mass spectrometric technique, with an ionspray interface, for the determination of platelet-activating factor (PAF) and lyso-PAF in biological samples

L. Silvestro* and R. Da Col

Res Pharma Pharmacological Research Srl, Via Belfiore 57, 10125 Turin (Italy)

E. Scappaticci and D. Libertucci

Servizio di Fisiopatologia Respiratoria e Broncologia, Ospedale San Giovanni, Turin (Italy)

L. Biancone and G. Camussi

Laboratorio di Immunopatologia, Cattedra di Nefrologia, Università di Torino e Cattedra di Nefrologia Sperimentale, Dipartimento di Biochimica e Biofisica, I Facoltà di Medicina e Chirurgia, Naples (Italy)

ABSTRACT

An HPLC–mass spectrometric technique with an ionspray interface was developed for the determination of platelet-activating factor (PAF) and PAF-related compounds in biological samples. HPLC separations were performed using a reversed-phase column. The mass spectra showed intense $[M + H]^+$ ions. Collision-induced dissociation of protonated molecular ions gave characteristic daughter ions corresponding to the phosphorylcholine group. By selective-ion monitoring, a detection limit of 0.3 ng was obtained for all molecules; by multiple reaction monitoring, the same sensitivity was achieved for PAF whereas for lyso-PAF the limit was 3 ng. Finally, PAF was comparatively determined by bioassay and HPLC–MS after extraction from the cell pellets and the supernatants of human polymorphonuclear neutrophils unstimulated or stimulated with opsonized zymosan. The good correlation observed between these techniques indicated the reliability of HPLC–MS for biochemical studies on PAF and PAF-related molecules.

INTRODUCTION

Platelet-activating factor (PAF) is a lipid chemical mediator of inflammation with a broad spectrum of diverse and potent biological activities [1–3]. In addition to its activity on platelets [4], PAF promotes the aggregation,

chemotaxis and granule secretion of polymorphonuclear neutrophils (PMN), eosinophils and monocytes [5]. Moreover, PAF enhances vascular permeability and adhesion of PMN to endothelial cells, leading oedema formation and leukocyte accumulation [1–3,5].

On the basis of its multiple biological activities, of its synthesis by a number of cell types involved in the development of inflammatory reaction and of the effect of PAF receptor

* Corresponding author.

antagonists, it was postulated that PAF plays a critical role in the physiopathology of inflammation [5] and of endotoxic/septic shock [6,7].

PAF was characterized as an 1-O-alkyl-2-acetyl-*sn*-glyceryl-3-phosphorylcholine (AGEPC) [8], synthesized either via a “remodelling pathway” of membrane phospholipids through acetylation of 2-lyso-PAF generated from 1-O-alkyl-2-acyl-*sn*-glyceryl-3-phosphorylcholine by phospholipase A2 activity or via the “*de novo*” biosynthetic pathway that involves the synthesis of 1-O-alkyl-2-acetyl-*sn*-glycerol which is then converted into PAF by a unique cytidine diphospho (CDP)-choline:1-alkyl-2-acetyl-*sn*-glycerol choline phosphotransferase [9]. The inflammatory cells synthesize PAF mainly via the remodeling pathway [9–11]. The assay of PAF bioactivity performed after TLC and HPLC purification has been extensively used for the quantitative assay of PAF production because of its high sensitivity (10^{-11} M) [10–13]. Normal-phase [14] and reversed-phase [15] HPLC have been demonstrated to be valuable techniques for the separation of different molecular species of PAF derived from biological samples. Indeed, it was recently found that PAF belongs to a class of structurally related mediators and that a number of different molecules, some with structures different from AGEPC, share PAF-like bioactivity [16]. Mass spectrometric methods such as GC-MS [17], fast atom bombardment (FAB) MS [18] and FAB-MS-MS [19] were instrumental for the definition of the chemical heterogeneity of PAF molecules. However, the application of these techniques for quantitative studies of PAF extracted from cells or biological fluids was limited by the complexity of these methods. An interesting HPLC-MS technique with thermospray ionization was also developed [20] but the sensitivity was inadequate for biological studies.

Recently, an HPLC system interfaced to a tandem triple-quadrupole mass spectrometer by an electrospray pneumatically assisted ionization source was successfully used for structural analysis and chemical characterization of PAF extracted from clinical samples [21,22]. The aim of this study was to optimize this HPLC-MS technique for the quantitative evaluation of PAF and related compounds in biological samples. For

this purpose, cell-associated PAF and PAF released in the supernatant were extracted from human PMN unstimulated or stimulated with opsonized zymosan.

EXPERIMENTAL

Chemicals

1-O-Hexadecyl-*sn*-glyceryl-3-phosphorylcholine (lyso-PAF), 1-O-hexadecyl-2-acetyl-*sn*-glyceryl-3-phosphorylcholine (C_{16} -PAF) and 1-O-octadecyl-2-acetyl-*sn*-glyceryl-3-phosphorylcholine (C_{18} -PAF) were purchased from Bachem, Feinchemikalien (Bubendorf, Switzerland).

Deuterium-labelled (2H_3) PAF (d_3 - C_{16} -PAF) was prepared by acetylation of lyso-PAF in the presence of 1 ml of deuterated acetic-anhydride (Aldrich Chemie, Steinheim, Germany) and 1 ml of pyridine for 20 h at room temperature [23]. After lipid extraction by the method of Bligh and Dyer [14], d_3 - C_{16} -PAF was purified by TLC and HPLC as described previously [21]. Acetonitrile and all other chemicals, of the purest grade available, were purchased from Fluka (Buchs, Switzerland); ultrapure water was obtained with a Milli-Q system (Millipore, Bedford, MA, USA).

Standard solutions

Stock solutions of 2.5 mg/ml of C_{16} -PAF, C_{18} -PAF and lyso-PAF were prepared in water-methanol (20:80, v/v). The internal standard, d_3 - C_{16} -PAF, was dissolved at 2.5 mg/ml in deuterated chloroform. These solutions were prepared freshly each month and stored at $-20^\circ C$.

PAF extraction from human PMN

Human PMN were prepared as described previously [10,11] and resuspended at $2.5 \cdot 10^6$ /ml in Tris-buffered Tyrode's solution containing 0.25% of delipidated bovine serum albumin (BSA). Cells were stimulated at $37^\circ C$ for 20 min with 0.2 mg/ml complement-activated zymosan. Lipids were extracted from the supernatant and cells according to Bligh and Dyer's technique [14]. After extraction, chloroform-methanol-water (1:1:0.9, v/v/v) was used for phase separation and the chloroform-rich phase was retained

[13]. The extracted lipids were divided into two samples to compare the PAF determined, after TLC and HPLC purification, by the bioassay and that determined by HPLC–MS. The first sample was submitted to TLC on silica gel plates 60 F₂₅₄ (Merck, Darmstadt, Germany) developed with chloroform–methanol–water (65:35:6, v/v/v) [13] and to HPLC on a μ Porasil column (Millipore Chromatographic Division, Waters, Milford, MA, USA) eluted with chloroform–methanol–water (60:55:5, v/v/v) at a flow-rate of 1 ml/min as described previously [21]. The overall recovery of PAF, evaluated in parallel experiments by addition of 10 nCi of [³H]C₁₆-PAF (New England Nuclear, NET 910; 30 Ci/mM) to the cells or supernatants followed by extraction as described above, was 90–95% [10,21]. After extraction and purification, the PAF bioactivity was determined by aggregometry using washed rabbit platelets in the presence of 10 μ M indomethacin, which inhibits cyclooxygenase, and of a creatinine phosphate (312.5 μ g/ml)–creatinine phosphokinase (152.5 μ g/ml) enzymatic system which converts ADP to ATP [10,11,21]. The specificity of PAF-induced aggregation was evaluated by inhibition with the PAF-receptor antagonists WEB 2170 and CV 3128 [21]. The amount of PAF was expressed in ng/ml and calculated from a calibration graph for synthetic PAF constructed for each test. PAF extracted from biological samples shared with synthetic C₁₆-PAF the same TLC and HPLC chromatographic patterns and physico-chemical characteristics such as inactivation by strong bases, resistance to acidic and weakly basic conditions [13,24] and inactivation by phospholipase A2 but not phospholipase A1 [25].

The second sample (0.5 ml of the chloroformic phase) was applied to a disposable silica column (Alltech, Milan, Italy; extra-clean silica column, 200 mg) as described [13], eluted sequentially with chloroform, acetone–methanol (1:1, v/v) and finally with chloroform–methanol (1:4, v/v) which retained PAF activity [13], and then submitted to HPLC–MS analysis.

In selected experiments, d₃-C₁₆-PAF was added to cells and supernatants (10 ng per sample) as an internal standard and then extracted as above.

Chromatographic separations

All the HPLC separations were performed with Applied Biosystems Model 140A HPLC syringe pumps and a Perkin-Elmer ISS-101 auto-sampler. In the first experiments we used reversed-phase chromatography [21,22], with a water–acetonitrile gradient containing trifluoroacetic acid (TFA), but we subsequently found that better results could be achieved with isocratic conditions, following the methods described by Kim and Salem [20]. Separations were obtained with a reversed-phase column (Phase Separations, Spherisorb C₁₈, 5 μ m, 100 \times 1 mm I.D.). The mobile phase was methanol–2-propanol–hexane–0.1 M aqueous ammonium acetate (100:10:2:5, v/v); the flow-rate was 50 ml/min.

Mass spectrometry

The effluent from the HPLC micropore column was connected to a PE-Sciex API III triple quadrupole mass spectrometer (Sciex, Thornhill, Canada) equipped with an atmospheric pressure articulated ionspray source. To set up the technique, analyses were previously performed scanning in the range m/z 100–600 in the positive-ion mode. Then, under MS–MS conditions, daughter ions, obtained by collision-induced dissociation (CID) of parent ions with m/z values corresponding to $[M + H]^+$ of PAF and PAF-related molecules, were acquired in the positive-ion mode; CID was optimized by collision with argon at a collision gas thickness of $2.7 \cdot 10^{12}$ atoms/cm² and at an impact energy of 70 eV. Finally, quantitative analyses were performed both by selective-ion monitoring (SIM), with m/z corresponding to protonated molecular ions, and by multiple reaction monitoring (MRM), following the reactions m/z 524 \rightarrow 184, 552 \rightarrow 184, 482 \rightarrow 184 and 527 \rightarrow 185, characteristic of C₁₆-PAF, C₁₈-PAF, lyso-PAF and d₃-C₁₆-PAF, respectively; the conditions of collision were the same as given previously.

Calibration and quantification procedures

Samples of unstimulated PMN, cellular or supernatant fractions, were spiked with C₁₆-PAF, C₁₈-PAF and lyso-PAF, using stock solutions containing 0.3, 1, 3, 30 and 100 ng of each

per sample; appropriate volumes of solvent [methanol–water (80:20, v/v)] were also added to ensure an equivalent total volume (0.5 ml) in each instance. In another series of spiked samples, to be analysed only by HPLC–MS, an internal standard was also added. Both series of standard additions were treated in the same way as the unknown samples. Calibration graphs, separately for C₁₆-PAF, C₁₈-PAF and lyso-PAF, were constructed as concentration *versus* peak area for these molecules. In the samples spiked with the internal standard the results were corrected by an extraction factor calculated from the internal standard areas. Calibration graphs for bioassay could measure only the PAF-like bioactivity without separating C₁₆-PAF from C₁₈-PAF and without evaluating lyso-PAF.

RESULTS

Fig. 1A shows the mass spectra obtained from 100 ng each of C₁₆-PAF, lyso-PAF, d₃-C₁₆-PAF

and C₁₈-PAF analysed, as described above, during an HPLC separation; with all molecules the most intense ion had the *m/z* corresponding to the protonated molecular ion [M + H]⁺. Fig. 1B shows the mass spectra of daughter ions obtained by CID of protonated ions from the same molecules as in Fig. 1A using identical HPLC conditions. In these spectra the most intense daughter ion, with the exception of d₃-C₁₆-PAF, had *m/z* 184 corresponding to the mass of phosphorylcholine; for d₃-C₁₆-PAF the most intense ion was shifted by 1 u, corresponding to the phosphorylcholine fragment with an increase in mass due to the redistribution of a deuterium atom within the molecule during the fragmentation process, as described previously [19].

Fig. 2A shows chromatograms obtained in the SIM mode for *m/z* values corresponding to the [M + H]⁺ of lyso-PAF, C₁₆-PAF, d₃-C₁₆-PAF and C₁₈-PAF; a mixture containing 10 ng of each molecule was injected. Under these mass spectrometric conditions the same sensitivity was

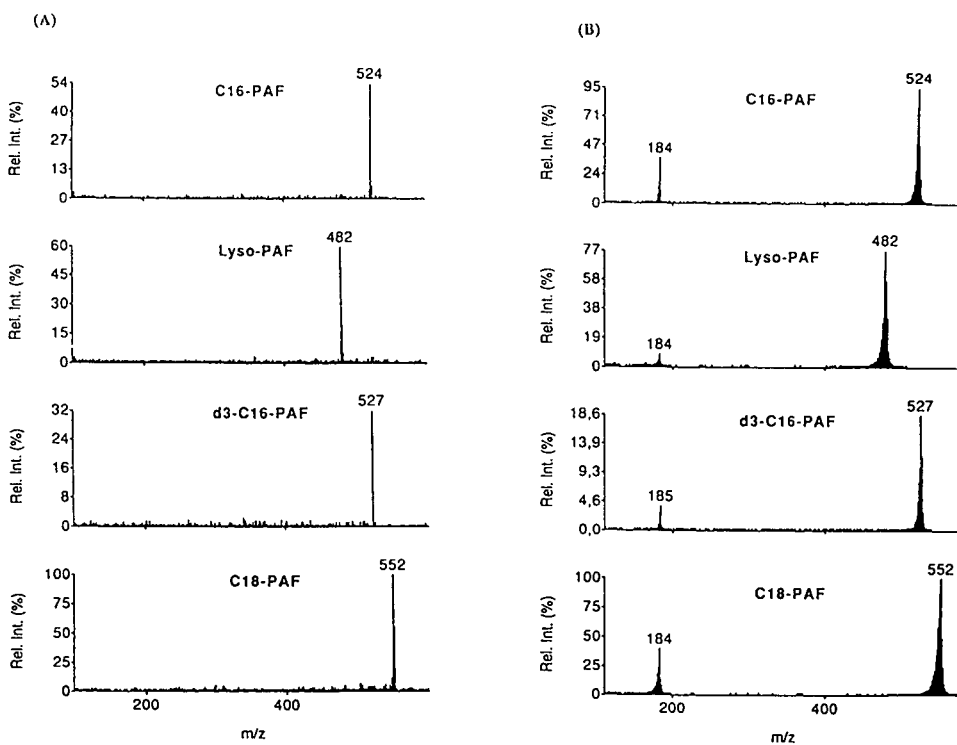


Fig. 1. (A) Mass spectra, positive-ion mode, obtained during an HPLC separation of a standard mixture containing C₁₆-PAF, lyso-PAF, d₃-C₁₆-PAF and C₁₈-PAF, 100 ng each. (B) Tandem mass spectra, daughter-ion mode, from CID of the protonated molecular ions of C₁₆-PAF, lyso-PAF, d₃-C₁₆-PAF and C₁₈-PAF.

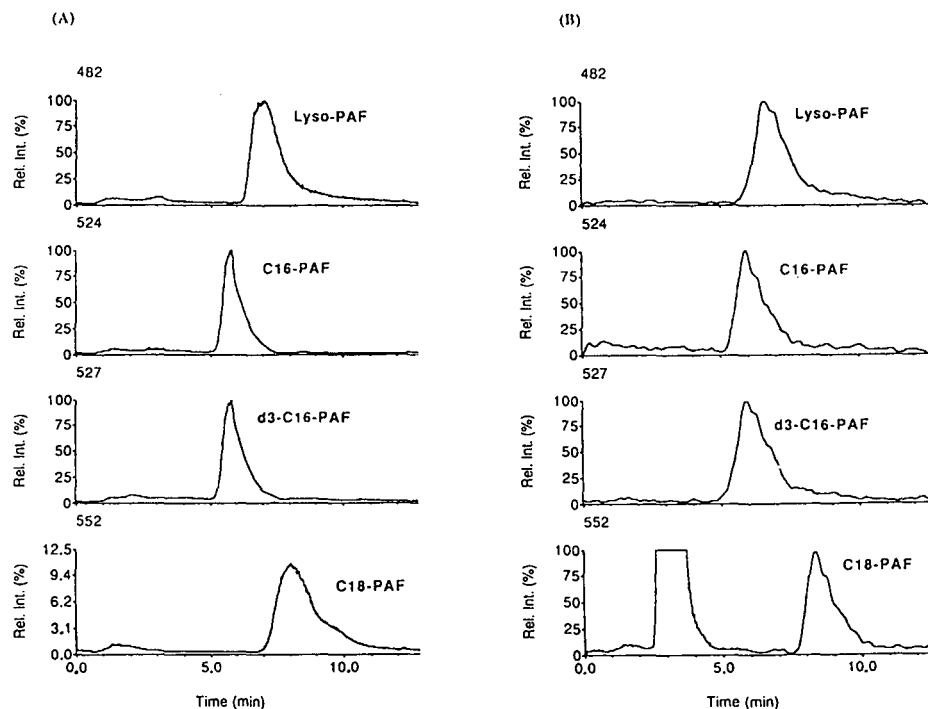


Fig. 2. Chromatographic traces, SIM at m/z 482, 524, 527 and 552 (corresponding to lyso-PAF, C_{16} -PAF, d_3 - C_{16} -PAF and C_{18} -PAF, respectively), obtained by injection of (A) a pure standard containing C_{16} -PAF, lyso-PAF, d_3 - C_{16} -PAF and C_{18} -PAF (10 ng each) in comparison with (B) an analysis performed, with the same conditions, on a cellular PMN pellet spiked with 3 ng of each analyte and then extracted.

observed for each molecule. The separation obtained was sufficient to identify our analytes; if necessary, modifications of the mobile phase, as described by Kim and Salem [20], permitted (data not shown) the chromatographic resolution to be improved. By analysing samples of decreasing concentrations (data not shown), a detection limit of 0.3 ng, with a signal-to-noise ratio of 3:1, was obtained for all molecules.

Fig. 2B shows the chromatograms obtained with a sample of cellular pellet spiked with 3 ng each of lyso-PAF, C_{16} -PAF, d_3 - C_{16} -PAF or C_{18} -PAF and extracted as described above. The retention times of PAF and PAF-related compounds were reproducible in both sample in Fig. 2A and B, showing that in spiked samples no relevant effects arose from compounds present in the biological samples. Only at m/z 552, corresponding to C_{18} -PAF, was a peak from an interfering compound observed, but it was eluted early in the chromatogram. This peak was also detected in the blank cellular pellets, indicating

that it is not derived from C_{18} -PAF added but rather from a component of the cellular extract.

Fig. 3 shows the regression lines of the peak areas, obtained with standard mixtures of different concentrations, to evaluate the analytical linearity for quantitative analysis by SIM (A) on pure standards or (B) on PMN pellets spiked with the same concentrations of C_{16} -PAF, d_3 - C_{16} -PAF, C_{18} -PAF and lyso-PAF and then analysed after extraction and, finally, (C) by MRM on pure standards. Good linearity was observed with the different analytical conditions tested in a range of concentrations far below the amounts detectable in biological samples. A comparison of the areas in Fig. 3A and B confirmed the high efficiency of the extraction procedure; in fact, considering that only part of the extracted samples was injected, a mean recovery of 85–90% was calculated. The results obtained in MRM showed that the detection limits were different depending on the molecule; for C_{16} -PAF and the internal standard the detection limit was the

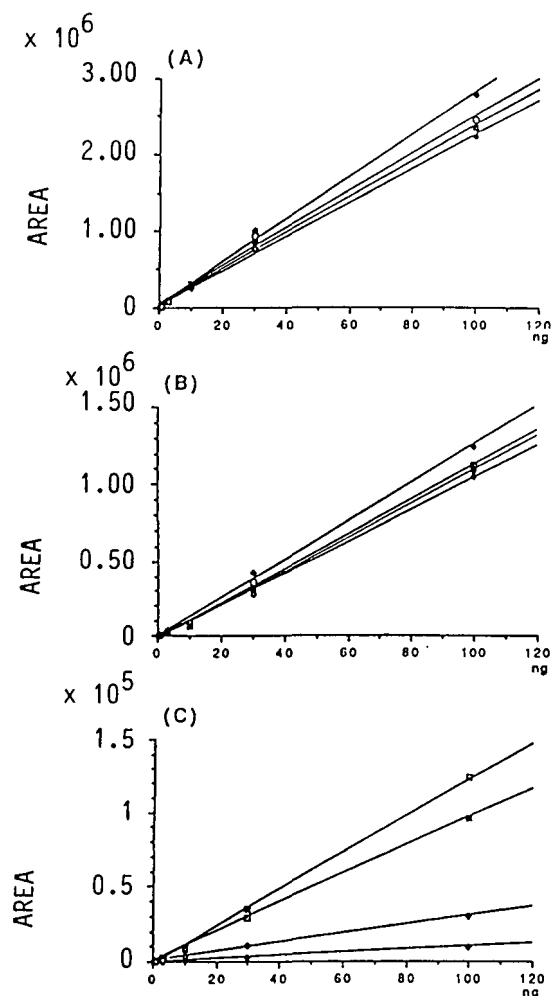


Fig. 3. Linear regressions, peak area versus amount of PAF and PAF-related compounds, estimated from SIM analysis of (A) pure standards $\square = C_{16}$ -PAF ($R^2 = 0.994$); $\blacklozenge =$ lyso-PAF ($R^2 = 0.996$); $\blacksquare = d_3$ - C_{16} -PAF ($R^2 = 0.995$); $\diamond = C_{18}$ -PAF ($R^2 = 0.998$); or (B) spiked samples: $\square = C_{16}$ -PAF ($R^2 = 0.997$); $\blacklozenge =$ lyso-PAF ($R^2 = 0.996$); $\blacksquare = d_3$ - C_{16} -PAF ($R^2 = 0.997$); $\diamond = C_{18}$ -PAF ($R^2 = 0.998$); and (C) MRM analysis of pure standards.

same as observed with SIM whereas with C_{18} -PAF and lyso-PAF the sensitivities were substantially lower (1.5 and 3 ng, respectively). Modifications of the CID conditions did not improve the fragmentation of these compounds, in accordance with MS-MS data reported elsewhere for lyso-PAF [26].

Fig. 4 shows the chromatograms obtained with SIM at m/z corresponding to C_{16} -PAF and lyso-PAF from a sample of (A) stimulated or (B)

unstimulated PMN pellet extracts. A peak corresponding to C_{16} -PAF was observed only in the sample of stimulated PMN whereas a small amount of lyso-PAF was present in both samples; C_{18} -PAF (data not reported) was undetectable in both samples. The results obtained by the analysis of the supernatants of the stimulated PMN are presented in Fig. 4C in comparison with the unstimulated sample Fig. 4D. Again, a significant peak of C_{16} -PAF but not of C_{18} -PAF was observed in the stimulated PMN sample.

Table I shows the net amounts of C_{16} -PAF and lyso-PAF detected by SIM, as cell-associated or as released in the supernatants, in unstimulated and stimulated PMN samples. These amounts are comparable to those observed by bioassay [11] or other MS techniques [19].

Fig. 5 presents the results obtained from the stimulated PMN samples, (A) cellular pellets and (B) supernatants, by MRM. Using this technique the presence of C_{16} -PAF was confirmed in both samples without any interfering peak from the background. In contrast, lyso-PAF, despite its presence as shown by SIM (Fig. 4), could not be quantified by MRM because of the lower sensitivity of this technique compared with SIM.

The linear regression analysis of the same samples determined by bioassay or by HPLC-MS using SIM, reported in Fig. 5C, gave a good correlation ($r = 0.979$) between the techniques, confirming the reliability of HPLC-MS for quantitative analysis of biological samples.

The mean recovery, evaluated by standard addition to the biological samples ($n = 15$) of d_3 - C_{16} -PAF as internal standard, was $84 \pm 5.1\%$. These results confirmed the recovery evaluated by bioassay or [3 H] C_{16} -PAF as described under Experimental.

DISCUSSION

The mass spectra in Fig. 1 show that good ionization can be obtained for PAF-related phospholipids; these findings are not unexpected considering the high polarity of the phosphorylcholine group. A molecular ion is always observed without relevant fragmentations in the source.

The CID spectra show a characteristic frag-

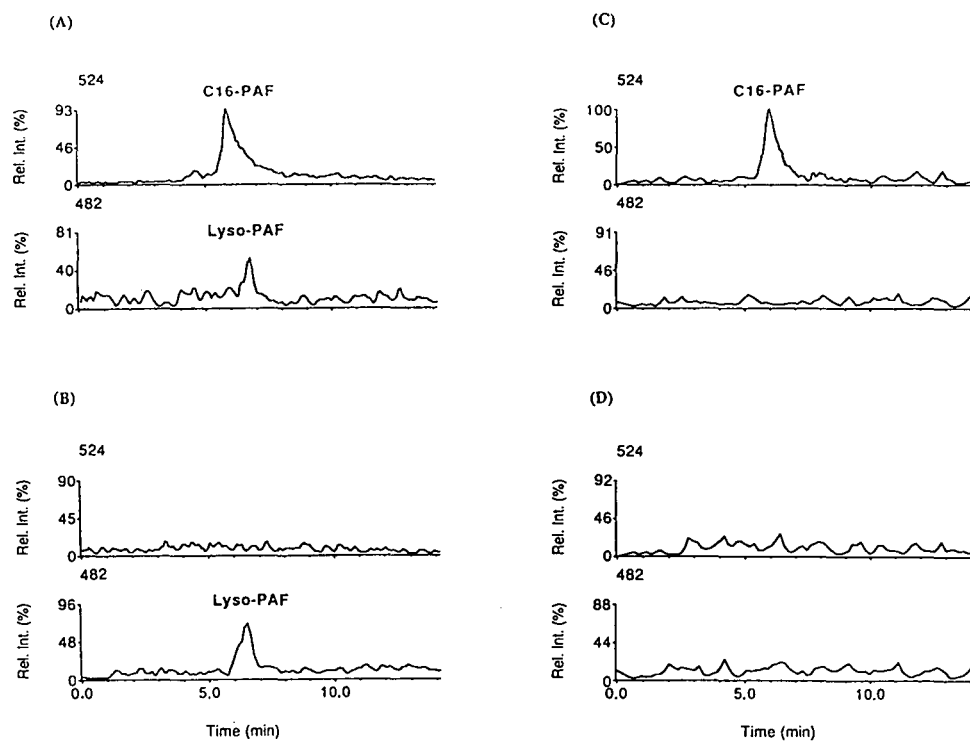


Fig. 4. Chromatographic traces obtained by SIM at m/z values corresponding to C_{16} -PAF (524) or lyso-PAF (482) on cellular pellets of (A) stimulated or (B) unstimulated PMN and supernatants of (C) stimulated or (D) unstimulated PMN.

mentation giving an intense daughter ion corresponding to the phosphorylcholine group; the presence of such a typical product ion can be useful in detecting other uncommon PAF-related phospholipids, such as unsaturated or 1-acyl derivatives, performing acquisition under MS-

MS conditions and monitoring the parent ions undergoing fragmentation with daughter ions of m/z 184.

In previous experiments [21,27] we used a reversed-phase column eluted with a mobile phase gradient (water–acetonitrile containing

TABLE I

NET AMOUNTS OF C_{16} -PAF AND LYSO-PAF IN UNSTIMULATED ($n = 5$) AND STIMULATED ($n = 5$) PMN SAMPLES AS DETERMINED BY HPLC-MS AND SELECTIVE-ION MONITORING

Sample	C_{16} -PAF		Lyso-PAF	
	Cell-associated (ng) ^a	Released in the supernatant (ng) ^b	Cell-associated (ng) ^a	Released in the supernatant (ng) ^b
Unstimulated PMN	NE ^c	NE ^c	1.1 ± 0.2	NE ^c
Stimulated PMN	6.1 ± 0.9	4.3 ± 0.7	0.6 ± 0.2	NE ^c

^a C_{16} -PAF and lyso-PAF in PMN pellets (10^6 cells); mean ± standard deviation.

^b C_{16} -PAF and lyso-PAF in PMN supernatants (10^6 cells); mean ± standard deviation.

^c NE = Non-evaluable concentrations.

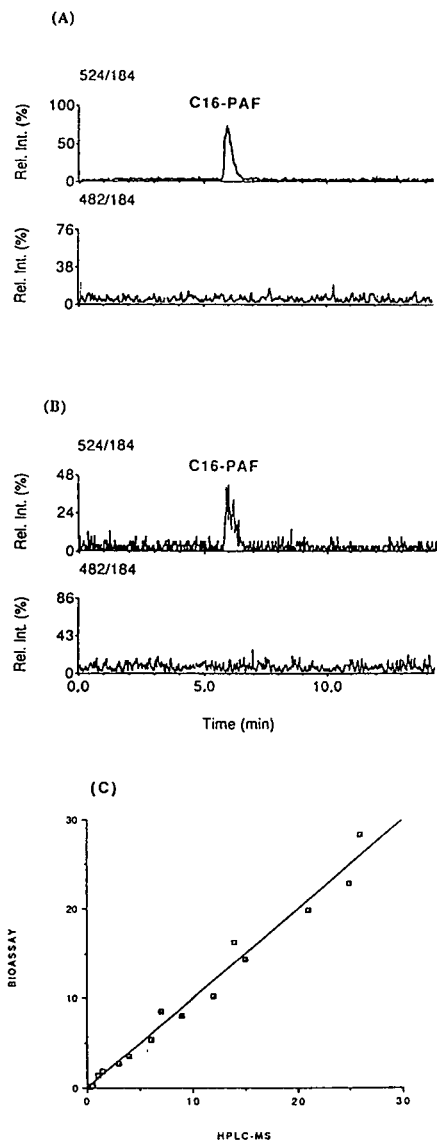


Fig. 5. Chromatographic traces obtained by MRM, following the fragmentations characteristic of C_{16} -PAF m/z (524 \rightarrow 184) and lyso-PAF (m/z 482 \rightarrow 184) on samples of (A) cellular pellets or (B) supernatants of stimulated PMN. (C) Regression line analysis comparing the results obtained by HPLC-MS or bioassay on the same samples: $y = -0.10277 + 0.99891x$; $R^2 = 0.979$.

TFA). Chromatographic runs of 30 min were necessary to obtain a reasonable separation; moreover, the acidic environment could degrade some PAF-related molecules. Normal-phase chromatography, tested in preliminary studies (unpublished data), was shown to enhance the separation but only provided that biological

samples were submitted to an additional purification step by TLC to avoid rapid deterioration of the column. The reversed-phase method, described in this paper, gave good separations without the need for a gradient or pH conditions detrimental to the samples.

The use of an effective separative technique, according to Haroldsen and Gaskell [19], is particularly important for obtaining a correct determination of different PAF-related compounds having the same molecular mass.

Both the SIM and MRM modes showed good linearity of plots of peak area *versus* concentration within the range tested. The amount of PAF detected by bioassay in the biological samples was within 1–10 ng per sample. Despite the femtomole sensitivity of the bioassay, a widely accepted technique for PAF determination, the range of linearity was significantly lower than that obtained by mass spectrometry. Moreover, compounds without a PAF-like activity such as lyso-PAF could not be directly determined by bioassay but an additional step to generate active PAF was required [21]. Comparison of the results obtained from extraction of biological samples and those from pure standards clearly showed the absence of matrix interference in the ionization. Evaluations of the recovery of the extraction technique used confirmed the reliability of this method for both PAF-related molecules and the internal standard as previously reported [10,21]. The sensitivity observed with MRM on C_{16} -PAF suggests a possible application of this technique also for determinations in biological samples. In contrast, the low sensitivity observed for other PAF-related molecules, notably lyso-PAF, is a restriction for studies of low concentrations.

The peak of C_{16} -PAF produced by stimulated PMN was clearly detected using the SIM and MRM modes, both in the cellular fractions and in the supernatants; interferences from other molecules were never found. The HPLC-MS technique described here was applied in preliminary experiments to the characterization of PAF in broncoalveolar lavage [21] and cultured mesangial cells [27] with good results. To attain the optimization of HPLC-MS for a quantitative evaluation of PAF in biological samples, this technique was compared with the bioassay. The

results illustrated in Fig. 5C show a good correlation between C_{16} -PAF values determined by HPLC–MS and those obtained by a bioassay on the same samples.

Several studies were previously performed using MS techniques. GC/MS gave reliable results and the technique was very sensitive; however, an enzymatic degradation step and a subsequent derivatization were required in order to obtain volatile products amenable to GC separation. These steps, which require a skilled operator, are time consuming and complicate the method. The already proposed HPLC–MS, with a thermospray interface, and FAB-MS techniques do not require enzymatic or derivatization steps and therefore minimize the problems related to these procedures. However, thermospray ionization exhibits a low sensitivity [20]; concerning FAB-MS the detection limits are good but HPLC interfacing is complex and TLC separation is generally used to discriminate isobaric compounds.

In conclusion, the results of this study indicate that the proposed HPLC–MS technique, based on a pneumatically assisted electrospray interface, may be useful for further research on PAF and PAF-related molecules in biological samples. The sensitivity and the reliability when compared with the bioassay and the relative simple methodology are the relevant features of this method. The wide possibilities offered by this ionization technique for the selection of mobile phases is a further advantage on the assumption that with certain samples different reversed-phase or normal phase separations may be required to overcome problems of interference by other molecules.

ACKNOWLEDGEMENT

This work was supported by the National Research Council (CNR), Targeted Project “Prevention and Control of Disease Factors”, Subproject “Causes of Infective Disease” (CT 920037.PF4 1).

REFERENCES

1 R.N. Pinckard, L.M. McManus and D.J. Hanahan, *Adv. Inflammation Res.* 4 (1982) 147.

- 2 S.M. Prescott, G.A. Zimmerman and T.M. McIntyre, *J. Biol. Chem.*, 265 (1990) 7381.
- 3 P. Braquet, L. Touquoi, T.S. Shell and B.B. Vargaftig, *Pharmacol. Rev.*, 39 (1987) 97.
- 4 J. Benveniste, P.M. Henson and C.G. Cochrane, *J. Exp. Med.*, 136 (1972) 1356.
- 5 G. Camussi, C. Tetta and C. Baglioni, *Clin. Immunol. Immunopathol.*, 57 (1990) 331.
- 6 Z. Terashita, Y. Imura, K. Nishikawa and S. Sumida, *Eur. J. Pharmacol.*, 109 (1985) 257.
- 7 T.W. Doebber, M.S. Wu, J.C. Robbins, B.M. Choy, M.N. Chang and T.Y. Shen, *Biochem. Biophys. Res. Commun.*, 127 (1985) 799.
- 8 C.A. Demopoulos, R.N. Pinckard and D.J. Hanahan, *J. Biol. Chem.*, 254 (1979) 9355.
- 9 F. Snyder, *Med. Res. Rev.*, 5 (1985) 107.
- 10 G. Camussi, F. Bussolino, G. Salvidio and C. Baglioni, *J. Exp. Med.*, 166 (1987) 1390.
- 11 G. Camussi, F. Bussolino, C. Tetta and C. Baglioni, *Eur. J. Biochem.*, 182 (1989) 661.
- 12 P. Inarrea, J. Gomez-Cambronero, J. Pascual, M.D. Ponte, L. Hernando and M. Sanchez-Crespo, *Immunopharmacology*, 9 (1985) 45.
- 13 R.N. Pinckard, R.S. Farr and D.J. Hanahan, *J. Immunol.*, 123 (1979) 1847.
- 14 E.G. Blish and W.J. Dyer, *Can. J. Biochem. Physiol.*, 37 (1959) 911.
- 15 H. Salari, *J. Chromatogr.*, 382 (1986) 89.
- 16 R.N. Pinckard, E.M. Jackson, C. Hoppens, S.T. Weintraub, J.C. Ludwig, L.M. McManus and G.E. Mott, *Biochem. Biophys. Res. Commun.*, 122 (1984) 325.
- 17 C.S. Ramesha and W.C. Pickett, *Biomed. Environ. Mass Spectrom.*, 13 (1986) 107.
- 18 S.T. Weintraub, J.C. Ludwig, G.E. Mott, L.M. McManus, C. Lear and R.N. Pinckard, *Biochem. Biophys. Res. Commun.*, 129 (1985) 868.
- 19 P.E. Haroldsen and S.J. Gaskell, *Biomed. Environ. Mass Spectrom.*, 18 (1989) 439.
- 20 H.Y. Kim and N. Salem, *Anal. Chem.*, 59 (1987) 722.
- 21 E. Scappaticci, D. Libertucci, F. Bottomicca, L. Silvestro, R. Da Col, C. Tetta and G. Camussi, *Am. Rev. Respir. Dis.*, 146 (1992) 433.
- 22 P. Borgeat, P. Braquet and B. Shushan, *Fourth International Congress on PAF and Related Lipid Mediators*, 1992, abstract C7.3.
- 23 J. Polonsky, M. Tencé, P. Varenne, B.C. Das, J. Lunel and J. Benveniste, *Proc. Natl. Acad. Sci. U.S.A.*, 77 (1980) 7019.
- 24 P.O. Clark, D.J. Hanahan and R.N. Pinckard, *Biochim. Biophys. Acta*, 628 (1980) 69.
- 25 J. Benveniste, J.P. Le Couedic, J. Polonsky and M. Tencé, *Nature*, 269 (1977) 170.
- 26 R.D. Plattner, R.J. Stack, J.M. Al-Hassan, B. Summers and R.S. Criddle, *Organic Mass Spectrom.*, 23 (1988) 834.
- 27 G. Camussi, L. Biancone, E. Iorio, L. Silvestro, R. Da Col, C. Capasso, F. Rossano, L. Servillo, C. Balestrieri and M. Tufano, *Kidney Int.*, 42 (1992) 1309.

CHROMSYMP. 2814

Determination of quaternary amine pesticides by thermospray mass spectrometry

D. Barceló* and G. Durand

Department of Environmental Chemistry, CID-CSIC, c/Jordi Girona 18–26, 08034 Barcelona (Spain)

R.J. Vreeken

Laboratoire de Technologie des Poudres, EPFL, Ecublens, CH-1015 Lausanne (Switzerland)

ABSTRACT

Positive-ion (PI) thermospray mass spectrometry (TSP-MS) with methanol–water (50:50) + 0.05 M ammonium formate as eluent was used for the characterization of the quaternary amine pesticides paraquat, difenzoquat, diquat, mepiquat and chlormequat and gave as base peaks $[\text{Cat} + \text{H}]^{+\bullet}$, $[\text{Cat} - \text{CH}_3 + \text{H}]^{+\bullet}$, $[\text{Cat}]^{+\bullet}$, $[\text{Cat}]^{+\bullet}$ and $[\text{Cat}]^{+\bullet}$, respectively. A postcolumn ion-pair extraction system was developed for the determination of difenzoquat from water samples whereas the other quaternary amine pesticides were not extracted. An aqueous mobile phase with various sulphonate counter ions such as dodecanesulphonic acid, methyl orange, Blue Acid 113, Mordant Red 9 and sodium picrate was tested in combination with an extraction solvent containing cyclohexane–dichloromethane–*n*-butanol (45:45:10) with UV diode-array spectra and PI TSP-MS detection. Applications are reported for the TSP-MS determination of 500 $\mu\text{g/l}$ of difenzoquat in spiked water samples using the postcolumn extraction system. Diquat and paraquat were determined at levels of 0.10–0.17 $\mu\text{g/g}$ in soil samples from the Ebro delta (Tarragona, Spain) using a reversed-phase eluent containing 0.05 M ammonium formate.

INTRODUCTION

The determination of quaternary ammonium compounds is tedious and involves either multi-step extraction and derivatization processes prior to GC determination [1,2] or cation-exchange LC and UV detection [1,3,4]. Of the different quaternary amine pesticides, mainly paraquat and diquat have been determined. The EPA method 549 was developed for the isolation of diquat and paraquat from water samples and involves solid-phase ion-pair extraction with further analysis using LC–diode-array detection at 308 and 257 nm [5]. Ion-pair formation in LC with UV detection is a common method for the determination of quaternary ammonium com-

pounds, *e.g.*, by using as counter ions either sodium 1-heptanesulphonate or sodium *p*-xylenesulphonate and it has been applied to the determination of diquat and paraquat residues in potatoes [3] and to industrial cationic surfactant homologues [6], respectively.

Ion pairs can be extracted from a reversed-phase eluent by using appropriate extraction solvents. The extraction ability of quaternary ammonium compounds, which form an extractable ion pair with anionic dyes, has been reported [7]. In the last few years, ion-pairing systems have been coupled on-line to LC. In such systems, by using continuous-flow post-column extraction and detection, the LC eluent is segmented by an immiscible solvent, containing a UV–Vis-absorbing or fluorescent counter ion. Ion-pair formation takes place in an extraction coil. Before detection is possible, the two phases

* Corresponding author.

are separated by means of a phase separator, which is the most critical part of the postcolumn extraction system. The use of a sandwich phase separator permitted the determination of cationic surfactants in environmental samples with UV or fluorescence detection [8]. Vouros *et al.* [9] were the first to incorporate an ion-pair extraction as an on-line chemical step before MS using a moving-belt interface. Recently, we have also reported preliminary results on the postcolumn ion-pair extraction of difenzoquat using thermospray (TSP) MS detection [10]. On-line postcolumn extraction systems can significantly enhance the power of LC–MS, as they allow the chromatographic part to be operated separately from the MS detection and therefore permitting to use non-volatile salts, *e.g.*, phosphate buffers, which cannot be used in conventional LC–MS work [11].

Diquat and paraquat have also been determined using reversed-phase systems in LC–TSP–MS, although chromatographic tailing is evident owing to the restrictive chromatographic conditions [12–15]. Fast atom bombardment (FAB) tandem mass spectrometry (MS–MS) [16] has also been used for the characterization of such group of pesticides.

The purposes of this work were to use TSP–MS for the characterization of a variety of quaternary amine pesticides which are of importance within the monitoring programmes of pesticides in environmental matrices [1], such as chlormequat, difenzoquat and mepiquat, in addition to the more often studied diquat and paraquat, to test the postcolumn ion-pair extraction system for these compounds and to evaluate its extraction efficiency with different counter ions prior to MS detection, achieving an independent chromatography from the MS detection, and to apply LC–TSP–MS to the determination of diquat and paraquat residues in real soil samples.

EXPERIMENTAL

Chemicals

HPLC-grade water, methanol and acetonitrile from Merck (Darmstadt, Germany) were passed through a 0.45- μm filter (Waters Chromatog-

raphy Division, Millipore, Bedford, MA, USA) before use. Cyclohexane and dichloromethane were of pesticide grade obtained from SDS (Peypin, France). Ammonium formate was supplied by Fluka (Buchs, Switzerland). Hydrochloric acid was of analytical-reagent grade from Merck. The sulphonate counter ions used were dodecanesulphonic acid, methyl orange, Blue Acid 113, Mordant Red and sodium picrate and were gifts from F. Ventura (Barcelona Water Supply, Barcelona, Spain). Analytical-reagent grade paraquat, diquat, difenzoquat, mepiquat and chlormequat were purchased from Promochem (Wesel, Germany).

Sample preparation

Sample pretreatment for the determination of paraquat and diquat in soil samples was carried out using a slight modification of the procedure reported by Needham *et al.* [17]. The procedure includes freeze-drying of soil samples and sieving (120 μm). A 10-g amount of soil was wetted with 10 ml of water and 10 ml of 6 M HCl were added. The samples were allowed to soak for 30 min, then sonicated for 20 min. Subsequently they were filtered through a Whatman glass-fibre filter-paper and the acidic solutions were extracted with 2 \times 20 ml of dichloromethane. The aqueous layer was then evaporated to dryness under nitrogen. Finally, methanol was added to yield a final volume of 50 μl and 20 μl were injected into the LC–MS system.

Chromatographic and postcolumn extraction conditions

Eluent delivery was provided by a high-pressure pump (Waters Model 510). Injection was carried out with a Model 7125 injection valve with a 20- μl loop (Rheodyne, Cotati, CA, USA). A LiChroCART cartridge column (12.4 cm \times 4.0 mm I.D.) packed with 5- μm LiChrospher 100 RP-18 (Merck) was used. In reversed-phase experiments, an eluent mixture of methanol–water (50:50) + 0.05 M ammonium formate was used at a flow-rate of 1 ml/min.

The postcolumn extraction system has been described elsewhere [8,11] and consisted of a laboratory-made sandwich phase separator equipped with two stainless-steel blocks with and

without a PTFE disc with a groove. The extraction solvent was delivered by a second high-pressure pump (Waters Model 510). A schematic diagram of the experimental set-up is given in ref. 11. The aqueous phase contained acetonitrile–water (60:40) + $1 \cdot 10^{-4}$ M of sulphonate counter ion and the organic phase was cyclohexane–dichloromethane–*n*-butanol (45:45:10) at a flow-rate of 1 ml/min. The organic phase was added to the aqueous phase via a Valco (Houston, TX, USA) T-piece with a 0.25-mm bore. The extraction took place in a 1.5 m \times 0.8 mm I.D. stainless-steel capillary (helix diameter 40 mm). After separation of the phases, the analytes together with the organic normal phase were introduced either into the UV or the TSP-MS detection system. A rapid-scanning UV-Vis detector was obtained from Barspec (Rehovot, Israel). With this phase separator, a purely organic normal phase can be obtained. The organic flow through the detector was regulated by means of a PTFE capillary equipped with a restrictor.

Mass spectrometric analysis

A Hewlett-Packard (Palo Alto, CA, USA) Model 5988A thermospray quadrupole mass spectrometer and a Hewlett-Packard Model 59970C instrument for data acquisition and processing were employed. The temperatures of the TSP were 100, 188 and 270°C for the stem, vapour and ion source, respectively. In all experiments the filament was on. Full-scan conditions were used in most of the experiments, with scanning from m/z 90 to 500. In the analysis of spiked water and soil samples, the selected-ion monitoring (SIM) mode was used. Ions used for monitoring were m/z 235 and 249 (difenzoquat), 172 and 187 (paraquat) and 157 and 184 (diquat).

RESULTS AND DISCUSSION

TSP-MS characterization

The flow-injection analysis and the TSP spectra of the quaternary amine pesticides obtained in the positive-ion (PI) mode of operation and using methanol–water (50:50) + 0.05 M ammonium formate as eluent are shown in Figs. 1

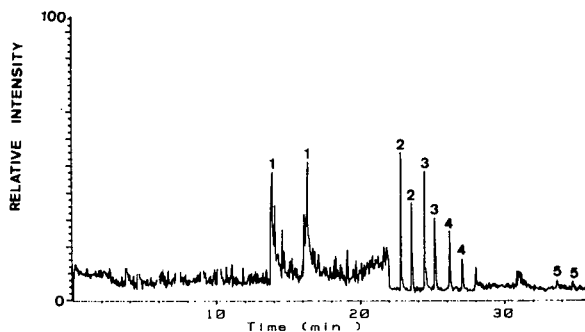


Fig. 1. Total ion current chromatogram obtained under flow-injection analysis of (1) mepiquat, (2) paraquat, (3) diquat, (4) difenzoquat and (5) chlormequat. Carrier stream, methanol–water (50:50) + 0.05 M ammonium formate; flow-rate, 1 ml/min; TSP temperatures, 100, 188 and 270°C for the stem, vapour and ion source, respectively.

and 2. The base peaks for paraquat, diquat, difenzoquat, mepiquat and chlormequat were at m/z 187, 184, 235, 114 and 122, corresponding to $[\text{Cat} + \text{H}]^{+\bullet}$, $[\text{Cat}]^{+\bullet}$, $[\text{Cat} - \text{CH}_3 + \text{H}]^{+\bullet}$, $[\text{Cat}]^{+\bullet}$ and $[\text{Cat}]^{+\bullet}$, respectively. The formation of the different ions under TSP conditions for difenzoquat [10] and paraquat [12] is usually dependent on the TSP temperature. In addition, the composition of the mobile phase has been reported to be a key factor in the ion formation of various pesticides under TSP conditions [13,18]. In this work, and comparing our results with literature data obtained using a TSP interface [12], it was noted that the base peak for paraquat was previously obtained at m/z 186. We attribute this discrepancy to the mobile phase composition, since in ref. 12 a mobile phase of methanol–water (80:20) + 0.1 M ammonium acetate (adjusted with trifluoroacetic acid to pH 5 as buffer) was used. Jones *et al.* [13] also reported relevant information; the base peak for paraquat was obtained at m/z 186 and 187 when water and ammonium acetate, respectively, were used as post-column solvents. It was proposed by Vestal [14] that the attachment of a hydride ion forms the m/z 187 ion. By MS-MS it was demonstrated that losses of CH_4 and a methyl radical occurred for m/z 186 and 187 after a prior loss of 15 u [13].

The results obtained in this work follow similar fragmentation patterns as previously published by Schmelzeisen-Redeker *et al.* [15], who

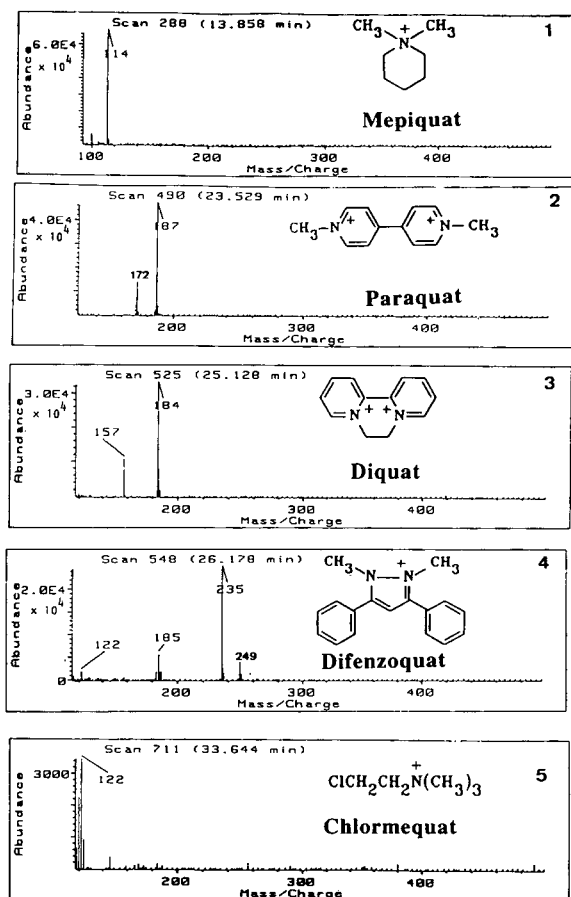


Fig. 2. TSP mass spectra of the compounds in Fig. 1. Conditions as in Fig. 1.

carried out the TSP-MS characterization of diquaternary salts using pure water as eluent in the TSP jet. Singly charged ions were formed, $[\text{Cat} - \text{CH}_3]^+$ ions resulting from dealkylation reactions being the most frequently found ions in the spectra [15].

The formation of an m/z 186 ion has also been observed in particle beam LC-MS using electron impact ionization, although in this instance the base peak corresponded to m/z 171 (due to a loss of CH_3) [19], and indicates that the absence of ammonium acetate gives as base peak the m/z 186 ion. The discrepancy between our results and the values reported in ref. 12, also obtained using a TSP interface, can be attributed to the use of a different mobile phase, thus giving the possibility of the formation of more hydride ions

in our case as ammonium formate is used and consequently m/z 187 is favoured over m/z 186. Yoshida *et al.* [12] also observed the ion at m/z 187, although always with a lower abundance than that at m/z 186, thus indicating the presence of both ions (probably due to the presence of ammonium acetate).

On comparing our results with the use of FAB-MS [16,20], it can be seen that some of the ions formed match, *e.g.*, those at m/z 171, 184 and 249 for paraquat, diquat and difenzoquat, respectively, although their relative abundances in the spectra differ. These similarities in fragmentation between the two techniques indicate that TSP-MS should be considered not only as a gas-phase chemical ionization-dependent technique but also as a solution chemistry method, in a similar manner to FAB-MS [20].

Mepiquat and chlormequat were characterized for the first time by TSP-MS in this work. Owing to the low molecular masses of these two compounds, it is important to start scanning at m/z of 100, so both compounds can be identified. This may be a problem when analysing real samples owing to matrix interferences.

Postcolumn extraction

As mentioned in the Introduction, it was the purpose of this work to achieve an independent

TABLE I

AVERAGE RECOVERIES AND RELATIVE STANDARD DEVIATIONS (R.S.D.s) FOR THE DETERMINATION OF QUATERNARY AMINE PESTICIDES FROM WATER AND SOIL SAMPLES

Compound	Water samples (postcolumn extraction)		Soil samples	
	Average recovery (%) ^a	R.S.D. (%)	Average recovery (%) ^a	R.S.D. (%)
Difenzoquat	81	7	n.r. ^b	
Diquat	17	21	85	7
Paraquat	n.e. ^c		91	4

^a $n = 5$.

^b Not reported.

^c Not extractable.

chromatography from the TSP-MS detection, so a postcolumn extraction system for difenzoquat with appropriate sulphonate counter ions was developed. This is an extension to the method developed by De Ruiter *et al.* [8] for the analysis of cationic detergents with sulphonate counter ions via postcolumn ion-pair formation and subsequent extraction. Various sulphonated counter ions (methyl orange, dodecanesulphonate, Acid Blue 113 and Mordant Red 9) [21] were tested. All these sulphonates showed good extraction efficiencies of 80% for difenzoquat (see Table I) when it was extracted from an aqueous phase [acetonitrile–water (60:40) containing $1 \cdot 10^{-4}$ M of the sulphonate] into an organic phase [cyclohexane–dichloromethane–*n*-butanol (45:45:10)].

Fig. 3 shows the different postcolumn extraction UV spectra obtained by direct flow injection

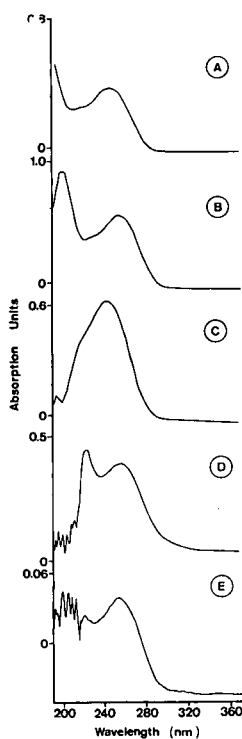


Fig. 3. UV mass spectra of difenzoquat obtained using (A) a reversed-phase eluent of acetonitrile–water (60:40), and after the postcolumn extraction system using cyclohexane–dichloromethane–*n*-butanol (45:45:10) at 1 ml/min of an aqueous ion pair containing $1 \cdot 10^{-4}$ M of (B) dodecanesulphonic acid, (C) methyl orange, (D) Blue Acid 113 and (E) Mordant Red.

tions of difenzoquat using a carrier stream of acetonitrile–water (A) and via the postcolumn extraction system, where difenzoquat was extracted as an ion pair with dodecanesulphonic acid (B), methyl orange (C), Blue Acid 113 (D) and Mordant Red 9 (E). The limit of detection after the postcolumn extraction under full-scan conditions was 100 ng, which is comparable to that obtained with postcolumn reduction using alkaline sodium dithionite and UV detection [1,4]. The UV spectra of difenzoquat in the carrier stream and in the extraction solvent exhibited maxima at 254 nm, being slightly different on the blue side of the spectrum, thus indicating that the UV spectra are dependent on the eluent composition and that the ion pair was extracted. Although the observed changes in both UV spectra could prove the formation of the ion pair (difenzoquat–sulphonate complex) and its extraction into the organic phase, it could not be proved by TSP-MS and always gave the two ions at m/z 235 and 249. When using Acid Blue 113 the background TSP spectra contained a peak at m/z 344, probably corresponding to a cleavage near the azo group. This fragment was also observed in FAB-MS experiments [21].

Although the extraction efficiency for difenzoquat was 81%, for diquat it was only *ca.* 17% and paraquat was not extracted at all (see Table I). Other problems encountered were the absence of a chromophore for mepiquat and chlormequat. As other alternatives for ion-pair extraction, picrate counter ion is known to offer relatively high extraction constants [22,23] and so it was also tested. A mobile phase containing sodium picrate at $1 \cdot 10^{-4}$ M (at pH 8) was used in combination with the common extraction solvent. Also in this instance none of the quaternary amine pesticides was extracted, with the exception of difenzoquat, which showed a similar extraction efficiency as previously. A drawback in these experiments was the relatively high noise level, due to the partial extraction of picrate into the organic phase.

As the use of picrate did not represent an improvement for the determination of quaternary amine pesticides, it was decided to use one of the previous sulphonate ion pairs, such as Acid Blue 113, in combination with the post-

column extraction solvent described earlier. The analysis of a spiked water sample using TSP-MS detection is shown in Fig. 4. The SIM mode was used for the ions corresponding to m/z 235 and 249. The method permitted the determination of 500 $\mu\text{g/l}$ of difenzoquat in spiked river water samples, thus representing an absolute amount of 10 ng of difenzoquat detected.

Environmental analysis

The use of the different quaternary ammonium pesticides within European countries has recently been reported [24]. They are currently applied as herbicides (*e.g.*, paraquat) and as growth regulators (*e.g.*, chlormequat). After application to the soil, paraquat and diquat are good examples of compounds with a cationic structure that can be sorbed into clay minerals in a process that is dependent on the cation-exchange capacity of the clay. They can be rapidly sorbed between the layers of the clay platelets and as a consequence they exhibit low mobility [25].

Paraquat and diquat are being currently applied in fields located at the Ebro delta (Tarragona, Spain). Two environmental soils from this area containing paraquat and diquat were analysed following the analytical protocol de-

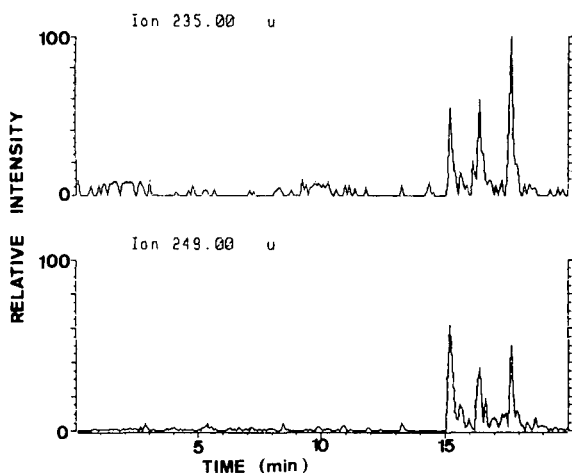


Fig. 4. TSP-MS under SIM conditions for three repetitive injections of a river water solution spiked with 500 $\mu\text{g/l}$ of difenzoquat after postcolumn extraction with cyclohexane-dichloromethane-*n*-butanol (45:45:10) at 1 ml/min of an aqueous phase of acetonitrile-water (60:40) and $1 \cdot 10^{-4}$ M of Blue Acid 113. TSP temperatures as in Fig. 1.

scribed here and good recoveries were obtained (Table I). Fig. 5 shows the SIM traces obtained using LC-TSP-MS for these two soil samples corresponding to (A) paraquat with ions at m/z 172 and 187 and (B) diquat with the ions at m/z 157 and 184. The samples analysed contained 0.10 and 0.17 $\mu\text{g/g}$ of paraquat and diquat, respectively. This corresponded to an injection of 400–600 ng of each compound into the analytical column.

Calibration graphs for paraquat and diquat were constructed by using the SIM mode. They were linear between 100 and 1200 ng. Volumes of 20 μl of each of five standard solutions of paraquat and diquat concentrations from 5 to 60 ng/ μl were injected ($n = 3$) into the system.

The chromatographic traces in Fig. 5 exhibit tailing, similarly as reported by Yoshida *et al.* [12]. In contrast, the postcolumn extraction chromatogram in Fig. 4 for difenzoquat is much better. Two comments can be made: first, the tailing observed under reversed-phase conditions is a common behaviour for these compounds when using either with UV [6] or TSP-MS detection [12]. This could be avoided by using another type of column, *e.g.*, a cyano- or amino-

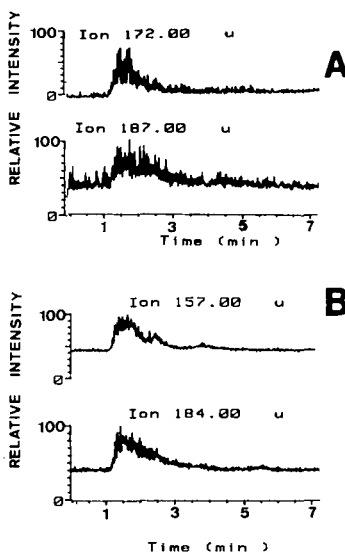


Fig. 5. LC-TSP-MS under SIM conditions for a soil sample from the Ebro delta containing 0.10 and 0.17 $\mu\text{g/g}$ of paraquat and diquat, respectively. Ions monitored were at m/z values of (A) 172 and 187 (paraquat) and (B) 157 and 184 (diquat). LC column, 5- μm LiChrospher 100 RP-18; LC mobile phase, methanol-water (50:50) + 0.05 M ammonium formate; flow-rate: 1 ml/min; TSP temperatures as in Fig. 1.

bonded phase with a chloroform–methanol–acetonitrile mixture in combination with a post-column extraction system, as described previously for cationic surfactants [8]. However, this approach could not be used for paraquat and diquat owing to the non-extraction of these two compounds under the above-described analytical conditions. The use of an ion-pair system without postcolumn extraction will evidently damage the MS source owing to the introduction of non-volatile salts. The use of an ion-exchange column with an ionic strength gradient mixture has also been described by Vestal [14].

CONCLUSIONS

LC–TSP–MS was used for the characterization of a variety of quaternary ammonium pesticides. Under reversed-phase conditions and using ammonium formate as an ionizing additive, 1–2 µg of each compound could be positively identified when injected under full-scan conditions. A postcolumn ion-pair system using different types of counter ions was developed for the characterization of difenzoquat, thus permitting the extraction and determination of this pesticide in water samples. This system could not be used with the other quaternary amine pesticides. The determination of paraquat and diquat in soil samples was feasible by using LC–TSP–MS with SIM and with the two main ions of each compound.

ACKNOWLEDGEMENT

This work was supported by the Environment R & D Programme 1991–94 (Commission of the European Communities Contract No. EV5V-CT-92-0061).

REFERENCES

- 1 A. Wagott, in B. Crathorne and G. Angeletti (Editors), *Pesticides: Analytical Requirements for Compliance with EC Directives*, Commission of the European Communities, Brussels, 1989, pp. 58–87.
- 2 J. Hajslová, P. Cuhra, T. Davídek and J. Davídek, *J. Chromatogr.*, 479 (1989) 243.
- 3 B.L. Worobey, *Pestic. Sci.*, 18 (1987) 245.
- 4 V.A. Simon and A. Taylor, *J. Chromatogr.*, 479 (1989) 153.
- 5 *Methods for Determination of Organic Compounds in Drinking Water, PB91-146027*, US Environmental Protection Agency, National Technical Information Service, Springfield, VA, 1990, method 549.
- 6 Ch.J. Dowle, W.C. Campbell and B.G. Cooksey, *Analyst*, 114 (1989) 883.
- 7 H.Y. Mohammed and F.F. Cantwell, *Anal. Chem.*, 52 (1980) 553.
- 8 C. De Ruiter, J.C.H.F. Hefkens, U.A.Th. Brinkman, R.W. Frei, M. Evers, E. Matthijs and J.A. Meijer, *Int. J. Environ. Anal. Chem.*, 31 (1987) 325.
- 9 P. Vouros, E.P. Lankmayr, M.J. Hayes, B.L. Karger and J.M. McGuire, *J. Chromatogr.*, 251 (1982) 175.
- 10 D. Barceló, G. Durand, R.J. Vreeken, G.J. De Jong, H. Lingeman and U.A.Th. Brinkman, *J. Chromatogr.*, 553 (1991) 311.
- 11 D. Barceló, G. Durand, R.J. Vreeken, G.J. De Jong and U.A.Th. Brinkman, *Anal. Chem.*, 62 (1990) 1696.
- 12 M. Yoshida, T. Watabiki, T. Tokiyasu and N. Ishida, *J. Chromatogr.*, 628 (1993) 235.
- 13 T.L. Jones, L.D. Betowski and J.M. Van Emmon, presented at the 36th ASMS Conference on Mass Spectrometry and Applied Topics, San Francisco, CA, June 5–10, 1988.
- 14 C.H. Vestal, *Vestec Termspray Newsl.*, 3 (1987) 2.
- 15 G. Schmelzeisen-Redeker, F.W. Röllgen, H. Wirtz and F. Voegtle, *Org. Mass Spectrom.*, 20 (1985) 752.
- 16 Y. Tondeur, C.W. Sovocool, R.K. Mitchum, W.J. Niederhut and J.R. Donnely, *Biomed. Environ. Mass Spectrom.*, 14 (1987) 733.
- 17 L. Needham, D. Paschal, Z.J. Rollen, J. Liddle and D. Bayse, *J. Chromatogr. Sci.*, 17 (1979) 87.
- 18 G. Durand, N. de Bertrand and D. Barceló, *J. Chromatogr.*, 562 (1991) 507.
- 19 M.A. Brown, I.S. Kim, F.I. Sasinos and R.D. Stephens, in M.A. Brown (Editor), *Liquid Chromatography/Mass Spectrometry. Applications in Agricultural, Pharmaceutical and Environmental Chemistry (ACS Symposium Series, No. 420)*, American Chemical Society, Washington, DC, 1990, pp. 198–214.
- 20 D. Barceló, *Anal. Chim. Acta*, 263 (1992) 1.
- 21 F. Ventura, A. Figueras, J. Caixach, D. Fraisse and J. Rivera, *Fresenius' Z. Anal. Chem.*, 335 (1989) 272.
- 22 G. Schill, R. Modin, K.O. Borg and B.A. Persson, in K. Blau and G.S. King (Editors), *Handbook of Derivatives for Chromatography*, Heyden, London, 1977, pp. 500–529.
- 23 J.F. Lawrence, U.A.Th. Brinkman and R.W. Frei, in I.S. Krull (Editor), *Reaction Detection in Liquid Chromatography*, Marcel Dekker, New York, 1987 pp. 259–302.
- 24 M. Fielding, D. Barceló, A. Helweg, S. Galassi, L. Torstensson, P. Van Zoonen, R. Wolter and G. Angeletti, in *Pesticides in Ground and Drinking Water (Water Pollution Research Reports, No. 27)*, Commission of the European Communities, Brussels, 1992, pp. 1–136.
- 25 C.J. Smith, in D.H. Huston and T.R. Roberts (Editors), *Environmental Fate of Pesticides (Progress in Pesticide Biochemistry and Toxicology, Vol. 7)*, Wiley, Chichester, 1990, pp. 47–99.

Electrospray mass spectrometry of neutral and acidic oligosaccharides: methylated cyclodextrins and identification of unknowns derived from fruit material

A.P. Tinke, R.A.M. van der Hoeven, W.M.A. Niessen* and J. van der Greef

Division of Analytical Chemistry, Leiden/Amsterdam Center for Drug Research, P.O. Box 9502, 2300 RA Leiden (Netherlands)

J.-P. Vincken and H.A. Schols

Wageningen Agricultural University, Department of Food Chemistry, Bomenweg 2, 6703 HD Wageningen (Netherlands)

ABSTRACT

A qualitative study of the characteristics in the mass spectrometric analysis of various neutral and acidic oligosaccharides using electrospray ionization is reported. Experiments were performed in both positive- and negative-ion modes. In the positive-ion mode molecular mass information for neutral non-derivatized oligosaccharides could be obtained up to M_r 4000. The method was applied to the determination of the degree of methylation of methylated β -cyclodextrins and the identification of unknown oligosaccharides enzymatically derived from pear and apple fruit material.

INTRODUCTION

Oligosaccharides are compounds of major biological importance, either as free carbohydrates or as constituents of glycoconjugates. There is special interest in the characterization of oligosaccharides in a variety of fields such as biochemistry, medicine, plant physiology and pathology and human and animal nutrition. As mass spectrometry is able to offer structural and/or molecular mass information considerable efforts have been made to characterize oligosaccharides by mass spectrometry. The analysis of both derivatized and non-derivatized oligosaccharides by fast atom bombardment mass spectrometry has been reported [1–3]. Addition of small amounts of alkali metal salts to the sample matrix appeared to improve the signal [4,5].

More recently, ^{252}Cf plasma desorption [6], direct chemical ionization [7] and matrix-assisted laser desorption [8] mass spectrometry have been reported to be suitable for the analysis of neutral non-derivatized oligosaccharides of M_r ca. 4000, 7000 and 10 000, respectively.

The application of on-line liquid chromatography–mass spectrometry (LC–MS) to the analysis of oligosaccharides has not been extensively described in the literature [9–12]. Until 1991, the use of fast atom bombardment (FAB) directly from a moving belt [11] or the use of an atmospheric-pressure spray system [12] appeared most suitable.

More recently, the use of thermospray [13–16], electrospray [13] and ionspray [17,18] techniques in oligosaccharide analysis has been reported and appear to be serious alternatives in the on-line LC–MS analysis of oligosaccharides. For thermospray, addition of sodium acetate appears to enhance the ion intensity significantly

* Corresponding author.

[13,14], whereas for electrospray, signal enhancement can be achieved by the addition of sodium acetate or ammonium acetate [13,17,18]. In thermospray, sodium acetate rather than ammonium acetate must be used in order to avoid ammoniolysis of the oligosaccharides to their constituent monomers [14]. The coupling of high-performance anion-exchange chromatography (HPAEC) via either a thermospray [15,16] or an ionspray [18] interface appears to be a very powerful tool in the analysis of complex oligosaccharide mixtures.

In this paper, the characteristics of neutral and acidic oligosaccharides in both positive- and negative-ion electrospray ionization are described. It concerns a qualitative rather than a quantitative study. Initially, various model compounds were studied. The information obtained from this study was used in the qualitative analysis of unknown oligosaccharide samples. In that respect, the characterization of dimethyl- β -cyclodextrin and the analysis of some unknown oligosaccharides isolated from water-unextractable solids from apple and pear fruit material are described.

EXPERIMENTAL

Apparatus

All experiments were performed with a Finnigan MAT (San José, CA, USA) TSQ-70 mass spectrometer, equipped with a 20-kV conversion dynode and a Finnigan MAT electrospray interface.

Sample introduction was performed either by constant infusion or by on-line liquid chromatography. A Model 2400 syringe pump (Harvard Apparatus, Edinbridge, UK) was used for sheath liquid delivery and in all constant infusion experiments. In the latter type of experiments methanol–water (90:10, v/v) or 2-propanol–water (90:10, v/v) was used as a sheath liquid at a flow-rate of 1–2 μ l/min.

For solvent delivery in liquid chromatography, a Model 2150 LC pump (LKB, Bromma, Sweden) was used. Sample injection was done with a Rheodyne (Cotati, CA, USA) injection valve, equipped with a 20- μ l sample loop.

Chromatography

For the LC separation, a laboratory-packed 150 mm \times 2 mm I.D. C₁₈ column (5- μ m particle size) was used. The mobile phase was 0.1 mM aqueous sodium acetate at a flow-rate of 1 ml/min, which was split 1:500 postcolumn to 2 μ l/min for electrospray nebulization. In these experiments, methanol–water (80:20, v/v) was used as a sheath liquid at a flow-rate of 2 μ l/min.

Mass spectrometry

The experiments in the positive-ion mode were performed at a nebulization potential of –3.5 to –4 kV, whereas in the negative-ion mode a nebulization potential of +2.8 to +3.3 kV was used. In the Finnigan MAT electrospray interface used, the counter electrode is at high potential relative to the spray needle, which is grounded. Nitrogen was used as a drying gas at a gas pressure setting of 5; no drying gas heating was applied. The tube lens potential and the nozzle–skimmer potential were optimized before each experiment.

Chemicals

Throughout these experiments, demineralized water was used. Methanol and 2-propanol were purchased from Baker (Deventer, Netherlands). Sodium chloride, sodium acetate, sodium hydroxide, ammonium chloride and ammonium acetate were obtained from Merck (Darmstadt, Germany).

The maltodextrin MD-25 sample was supplied by Roquette (Lille, France). Dimethyl- β -cyclodextrin samples were obtained from Janssen (Tilburg, Netherlands), Wacker (Munich, Germany), Rameb (Budapest, Hungary) and Avebe (Veendam, Netherlands). The monomeric sugars, sucrose and the maltose oligomers were commercially available.

Unsaturated oligomers of galacturonic acid were isolated from an enzyme digest of polygalacturonic acid (Fluka, Buchs, Switzerland) according to the procedure described by Voragen *et al.* [19].

Water-unextractable solids from apple and pear fruit material were subjected to sequential extractions with increasing strength of alkali.

The 1 M KOH-extracted pear material and the 4 M KOH-extracted apple material were degraded with endo-glucanase IV [20] and subsequently fractionated on a Bio-Gel P2 column by preparative HPAEC with pulsed electrochemical detection.

RESULTS AND DISCUSSION

Initial characterization of the electrospray ionization of oligosaccharides was performed with both neutral and acidic oligosaccharides as model compounds in both positive- and negative-ion modes. The group of neutral oligosaccharides consisted of sucrose ($M_r = 342$), maltotetraose ($M_r = 666$), maltoheptaose ($M_r = 1152$) and a maltodextrin MD-25 mixture. The group of acidic oligosaccharides consisted of glucuronic acid ($M_r = 194$), galacturonic acid ($M_r = 194$), unsaturated digalacturonic acid ($M_r = 352$) and unsaturated trigalacturonic acid ($M_r = 528$). The experiments were performed in the constant infusion mode, unless stated otherwise.

Positive-ion mode

A small amount of alkali metal contamination was present in the liquid phases that were used in these experiments. Further, samples prepared by enzymic degradation of plant cell wall polysaccharides followed by preparative HPAEC are also contaminated with sodium ions. Considering the high sodium affinity of oligosaccharides, the positive-ion mass spectra in most constant infusion experiments are dominated by sodium adduct ions. Obviously, most of the sample contamination can be eliminated by performing on-column reversed-phase LC experiments. However, because the sodium adduct ions of oligosaccharides are so readily formed, it is recommended to work with sodium-containing buffers in order to avoid the generation of mixed spectra. For on-column LC experiments, the addition of 0.1–1 mM sodium acetate to the mobile phase was applied to ensure a well defined sodium concentration.

For constant infusion of a 30 $\mu\text{g/ml}$ solution of sucrose or maltotetraose in methanol–water (90:10, v/v), only $[\text{M} + \text{Na}]^+$ and $[2\text{M} + \text{Na}]^+$

ions are observed. At higher analyte concentrations the intensity of the $[2\text{M} + \text{Na}]^+$ peak increases and even other sodiated clusters such as $[3\text{M} + \text{Na}]^+$ appear in the spectrum. Similar signal intensities are observed for sucrose and maltotetraose.

The mass spectra of acidic oligosaccharides show a high degree of sodium exchange, *i.e.*, in addition to $[\text{M} + \text{Na}]^+$ also $[\text{M} - \text{H} + 2\text{Na}]^+$ and eventually $[\text{M} - (n - 1)\text{H} + n\text{Na}]^+$ are observed (Fig. 1). The sodium exchange is more extensive at a lower analyte concentration, which can be explained by a more favourable sodium-to-analyte concentration ratio at lower analyte concentrations. Further, the total ion intensities for glucuronic acid and galacturonic acid are similar for 10 and 100 $\mu\text{g/ml}$ solutions. Remarkably, for 10 $\mu\text{g/ml}$ glucuronic acid solution the intensity of the sodiated dimer $[2\text{GlcA} + \text{Na}]^+$ was found to be higher than for a 100 $\mu\text{g/ml}$ solution. One would expect a more abundant clustering at higher analyte concentrations, as is observed for sucrose.

The mass chromatograms for the analysis of a maltodextrin MD-25 sample using a reversed-phase C_{18} column and a 10^{-4} M aqueous sodium acetate mobile phase are shown in Fig. 2. Methanol–water (80:20, v/v) was used as the sheath liquid for electrospray nebulization. The relative response (area/ μmol) in electrospray ionization is plotted as a function of the degree of polymerization (DP) in Fig. 3 and compared with earlier data on the response in thermospray ionization [14]. The degree of polymerization indicates the

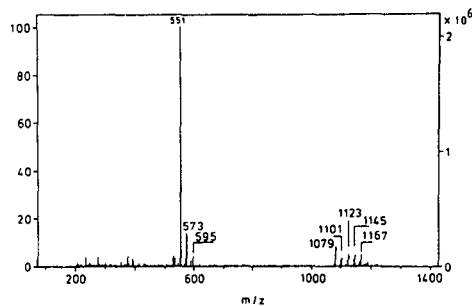


Fig. 1. Positive-ion electrospray mass spectrum of unsaturated trigalacturonic acid ($M_r = 528$), obtained by constant infusion of a 10 $\mu\text{g/ml}$ solution in 2-propanol–water (90:10, v/v) at a flow-rate of 1 $\mu\text{l/min}$.

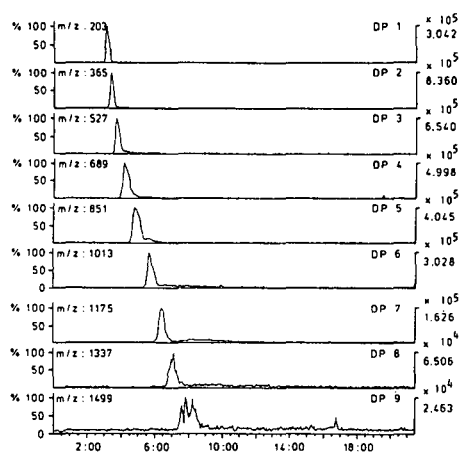


Fig. 2. Mass chromatograms for the LC-electrospray MS analysis of a maltodextrin MD-25 mixture. Multiple-ion detection in the positive-ion mode. Conditions: 150 mm \times 2 mm I.D. C_{18} column, 10^{-4} M aqueous sodium acetate as a mobile phase at 1 ml/min, postcolumn splitting to 2 μ l/min into the mass spectrometer, injection volume 20 μ l, sheath liquid methanol-water (80:20, v/v) at 2 μ l/min. After splitting, 0.5 μ g of sample is consumed in the mass spectrometer.

number of sugar monomers present in the oligosaccharide. As higher responses are observed in electrospray ionization than in thermospray for the higher DP oligomers, it can be concluded that the former is the more appropriate for the analysis of the larger oligosaccharides.

The positive-ion mass spectrum of a maltodex-

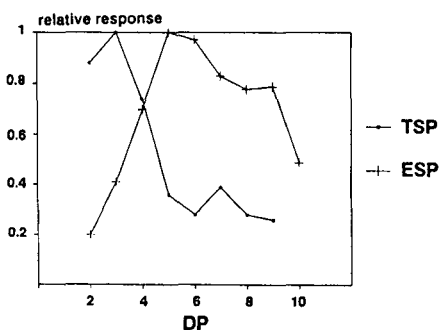


Fig. 3. Relative response measured as peak area per amount injected (mol) in LC-thermospray MS and LC-electrospray MS as a function of the degree of polymerization (DP). The injected amount of each oligomer was calculated from the mass percentages of each oligomer, obtained from the separation of MD-25 on an Aminex HPX-22H stationary phase with a refractive index detector [14].

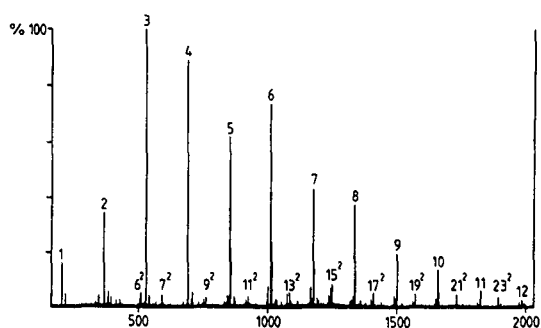


Fig. 4. Positive-ion electrospray mass spectrum of a 1 mg/ml maltodextrin MD-25 sample obtained by constant infusion at 1 μ l/min in $3 \cdot 10^{-4}$ M sodium acetate in methanol-water (40:60, v/v) for 5 min. DP values are given on the peaks; DP^2 values indicate doubly charged ions.

trin MD-25 sample (1 mg/ml) obtained via constant infusion for 5 min at 1 μ l/min is shown in Fig. 4. Singly charged sodiated species $[M + Na]^+$ are observed for the oligomers with $DP = 1-11$ and doubly charged disodiated species $[M + 2Na]^{2+}$ for the $DP 6-23$ oligomers. The molecular mass of the $DP 23$ oligomer (3744) further emphasizes the advantage of electrospray over thermospray ionization in the LC-MS analysis of oligosaccharides. An additional advantage of electrospray is the low flow-rate, which permits constant infusion of sample for several minutes with the consumption of only a small amount of sample. This is especially important in the characterization of unknowns in samples obtained from enzymic degradation of polysaccharides where the sample amounts are limited.

Negative-ion mode

Constant infusion in the negative-ion mode of a solution of 30 μ g/ml sucrose in methanol-water (90:10, v/v) results in $[M - H]^-$ and $[2M - H]^-$ ions, as illustrated in Fig. 5a. Addition of 10^{-4} M sodium chloride results in the formation of both deprotonated $[M - H]^-$ and chloridated $[M + Cl]^-$ molecules and clusters. By further increasing the chloride concentration to 10^{-3} M, the negative-ion spectrum almost entirely consists of chloridated molecules (Fig. 5b). The total ion intensity of sucrose with or without sodium chloride addition does not differ significantly. Additionally, the use of either ammonium or sodium chloride does not have much

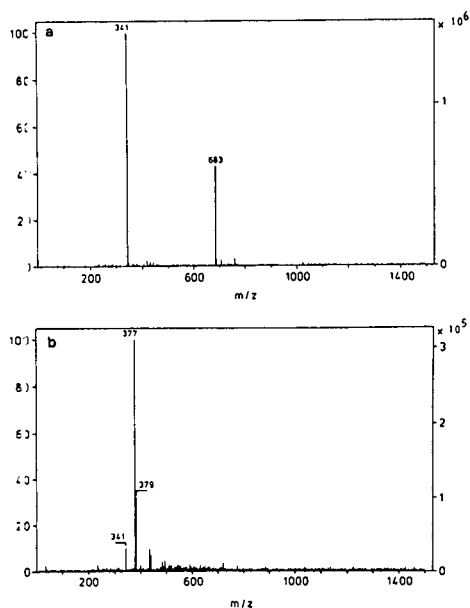


Fig. 5. Negative-ion electrospray mass spectra of sucrose ($M_r = 342$) obtained by constant infusion of a $30 \mu\text{g/ml}$ solution in (a) methanol–water (90:10, v/v) and (b) methanol–water (90:10, v/v) containing $10^{-3} M \text{NH}_4\text{Cl}$. Flow-rate, $1 \mu\text{l/min}$. For further explanation, see text.

influence on the total ion intensity. However, sodium acetate results in a more pronounced deprotonation than ammonium acetate. The latter can be explained by the acidity of the NH_4^+ ions, which prevents deprotonation. In addition, the acidic pH of the ammonium acetate solution might also play a role.

Maltotetraose and maltoheptaose show similar behaviour. However, the total ion intensity in the negative-ion mode for these compounds is about ten times lower than in the positive-ion mode.

For the acidic oligosaccharides the experiments were performed in 2-propanol–water (90:10, v/v) because with methanol stable ionization conditions appeared difficult to achieve. Again, glucuronic acid and galacturonic acid show a ten times better total ion current in the positive- than in the negative-ion mode. The addition of acetate or hydroxide results in a fourfold signal improvement but, in contrast to the neutral oligosaccharides, the addition of chloride hardly affects the spectrum. The addition of sodium hydroxide or sodium acetate induces the formation of the various cluster ions

of the uronic acid: $[2M - H]^-$, $[2M + \text{Na} - 2H]^-$ and $[3M + 2\text{Na} - 3H]^-$.

Similarly to the positive-ion mode, the total ion intensity of $10 \mu\text{g/ml}$ glucuronic acid solution is comparable to that of a $100 \mu\text{g/ml}$ solution, while more extensive sodium exchange and stronger ion cluster formation occur at the lower analyte concentration also.

In contrast to glucuronic acid, but as normally expected, a $100 \mu\text{g/ml}$ unsaturated digalacturonic acid solution shows stronger cluster formation than $10 \mu\text{g/ml}$ solution. Again, the spectrum of the $10 \mu\text{g/ml}$ unsaturated digalacturonic acid solution shows a strong sodium exchange, which in principle gives information about the number of acidic groups in the molecule. On the other hand, from signal-to-noise point of view, the sodium exchange and cluster formation are undesirable. In order to avoid sodium exchange for acidic oligosaccharides the sodium concentration in solution has to be considerably lower than the analyte concentration, which is obviously difficult to achieve, especially at low analyte concentrations. For a $10 \mu\text{g/ml}$ unsaturated trigalacturonic acid solution the ion intensity in the negative-ion mode is comparable to that in the positive-ion mode.

Dimethyl- β -cyclodextrin

Cyclodextrins are an interesting class of compounds that are used in analytical chemistry, e.g., as mobile-phase additives and for fluorescence enhancement. Further, they are under investigation in pharmaceutical technology as metabolically inert drug carriers and also in food technology. Within the class of cyclodextrins, methylated cyclodextrins form a special group of interest because of their high solubility in both water and oil. Their inclusion behaviour is significantly different from that of the parent cyclodextrins. Dimethyl- β -cyclodextrin [heptakis-(2,6-di-O-methyl)- β -cyclodextrin, $(\text{Me})_{14}\beta\text{-CD}$] is expected to be the most useful host molecule for inclusion complexes in pharmaceutical applications. However, considerable difficulties arise with the selective methylation of the hydroxyl groups of β -cyclodextrins and for pharmaceutical applications the purity of

(Me)₁₄β-CD is of extreme importance. Koizumi *et al.* [21] described a laborious procedure for the analysis of (Me)₁₄β-CD samples. In our laboratory, it was observed that (Me)₁₄β-CD samples obtained from various commercial sources show different elution profiles in size-exclusion LC [22]. Therefore, mass spectrometric characterization of the methylated cyclodextrins by means of constant infusion to the electrospray system was attempted. The singly charged sodiated molecule of (Me)₁₄β-CD is expected at m/z 1354 and the doubly charged disodiated molecule at m/z 688.5.

Constant infusion in the positive-ion mode of a 14 μg/ml (Me)₁₄β-CD sample in methanol–water (80:20, v/v) at 1 μl/min resulted in strong [M + Na]⁺ and [M + 2Na]²⁺ peaks, as illustrated in Fig. 6a. The spectrum was acquired at a tube lens potential of 200 V. Significantly different

optima were found for the nozzle–skimmer potential for the singly charged ion (200 V) and the doubly charged ion (10 V). The difference cannot be readily explained. From the mass spectrum in Fig. 6a, it can be concluded that the methylation of the (Me)₁₄β-CD sample is inhomogeneous: (Me)_nβ-CD with $n = 13–17$ at m/z 1340, 1354, 1368, 1382 and 1396, respectively, are found to be present in this particular sample. The mass spectrum of (Me)₁₄β-CD from another commercial source (see Fig. 6b) shows even more inhomogeneity, which in this instance is primarily due to insufficient methylation, *i.e.*, (Me)_nβ-CD with $n = 9–15$, *e.g.*, m/z 1284 corresponds to $n = 9$ and m/z 1326 to $n = 12$. From these results it may be concluded that electrospray ionization can be used as a rapid method for characterizing different (Me)₁₄β-CD batches in terms of methylation non-uniformity.

As expected, no spectrum of (Me)₁₄β-CD could be obtained in the negative-ion mode, because no free hydroxyl groups are available for deprotonation at the outside of the molecule.

Analysis of unknown oligosaccharides

There is considerable interest in the rapid characterization of oligosaccharides obtained by the chemical and/or enzymic degradation of glycoproteins and plant cell wall polysaccharides. Many of these oligosaccharides can be satisfactorily separated by HPAEC but their elution behaviour is unpredictable. For example, fucose-containing oligosaccharides have a tendency to elute faster than oligomers of similar *DP* lacking fucose [23], whereas arabinose and uronic acid show an opposite effect. For mass spectrometric analysis, in most instances FAB-MS and FAB-MS-MS are used. However, as electrospray was found to be a good alternative to FAB, various unknown oligosaccharide samples from enzymatic degradation of plant cell wall polysaccharides were analysed by constant infusion electrospray mass spectrometry in the positive-ion mode. Although the spectra obtained lack structural information, rapid molecular mass determination proved to be extremely useful, as is illustrated by the following examples.

Fractionation of the 1 M KOH-extracted pear

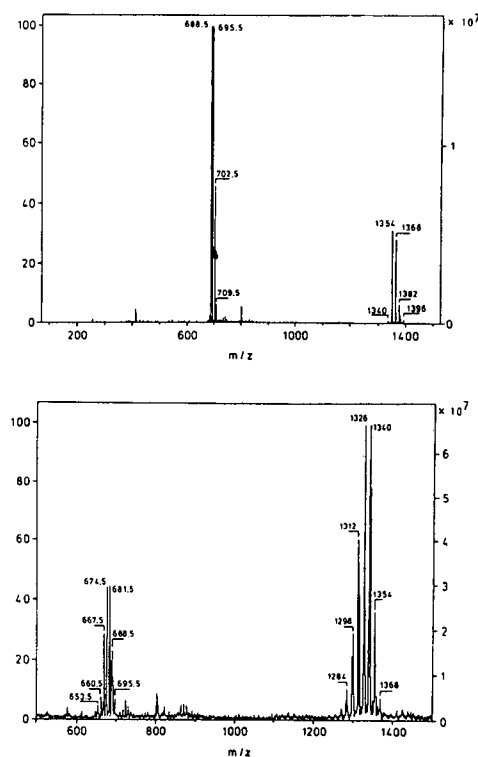


Fig. 6. Positive-ion electrospray mass spectra of 14 μg/ml solutions of dimethyl-β-cyclodextrin ($M_r = 1331$) samples obtained from two different commercial sources. Solvent: methanol–water (80:20, v/v) at 1 μl/min. For further explanation, see text.

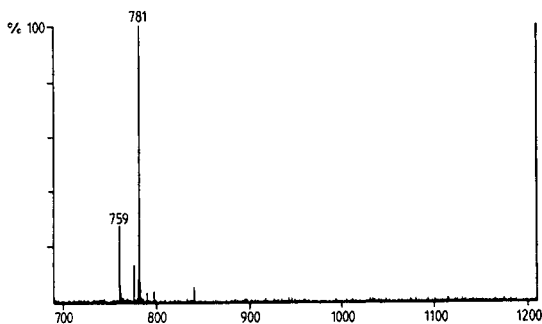


Fig. 7. Positive-ion electrospray mass spectrum of an unknown oligosaccharide after enzymatic digestion of a pear 1 M KOH extract. For further explanation, see text.

digest on Bio-Gel P2 showed some oligomeric products around $K_{av} = 0.15$ with a xylose-to-uronic acid ratio of *ca.* 5:1. In the colorimetric assay used, distinction between GalA, GluA and 4-O-methyl-GlcA was not possible. One oligomer was purified from this pool using preparative HPAEC. Sugar analysis of this fraction revealed the presence of some 4-O-methyl-GluA [24]. However, quantification was not possible as no proper standards were available.

The electrospray positive-ion mass spectrum of this unknown oligosaccharide derived from pear fruit tissue is shown in Fig. 7. Two major peaks are observed at m/z 759 and 781. The mass difference of 22 indicates the presence of one acidic sugar unit in the molecule. Therefore, the peak at m/z 759 is assigned to be the sodiated molecule $[M + Na]^+$, resulting in a molecular mass of 736. Plant cell wall polysaccharides are expected to contain hexoses, particularly glucose, mannose and galactose ($M_r = 180$), pentoses, particularly xylose and arabinose ($M_r =$

150), deoxyhexoses, particularly fucose and rhamnose ($M_r = 164$), hexuronic acids, *e.g.*, glucuronic or galacturonic acid ($M_r = 194$) and/or O-methylhexuronic acids ($M_r = 208$). A short algorithm, developed in our laboratory, was used to calculate all possible combinations of these monomeric units, leading to a molecular mass of 736. The five possible compositions that were found for this sugar oligomer are summarized in Table I. Additional information from sugar analysis rules out all possibilities except one: $(\text{pent})_4(4\text{-O-methyl-GluA})_1$. Hence this method not only easily distinguishes between hexuronic acids and 4-O-methylhexuronic acids, but also permits the determination of the pentose-to-4-O-methyluronic acid ratio. In order to determine the precise configuration of the unknown oligosaccharide, it is necessary to perform additional experiments, *e.g.*, with tandem mass spectrometry [25]. Based on the work of Chanda *et al.* [26], Labavitch and Greve [27] suggested the presence of glucuronoxylan oligomers in a similar Bio-Gel P2 pool. However, no attempts were made to characterize this fraction further. Debeire *et al.* [28] also reported similar fragments derived from larchwood on enzymic treatment.

The DP of an unknown oligomer fractionated from the 4 M KOH-extracted apple digest was estimated to be larger than 10 (based on the Bio-Gel P2 elution pattern). The electrospray mass spectrum of this oligosaccharide is shown in Fig. 8. The base peak in the spectrum is at m/z 958. Because of its even mass, the peak cannot be attributed to a singly charged monosodiated oligosaccharide. Assuming that it is due to a doubly charged disodiated molecule leads to a molecular mass of 1870. The absence of a peak

TABLE I
POSSIBLE SUGAR COMPOSITIONS FOR $M_r = 736$ (CF., FIG. 7)

Hexose	Pentose	Deoxyhexose	Hexuronic acid	4-O-Methylhexuronic acid
1	2	2	0	0
0	3	1	1	0
0	4	0	0	1
0	0	0	3	1
1	0	0	1	2

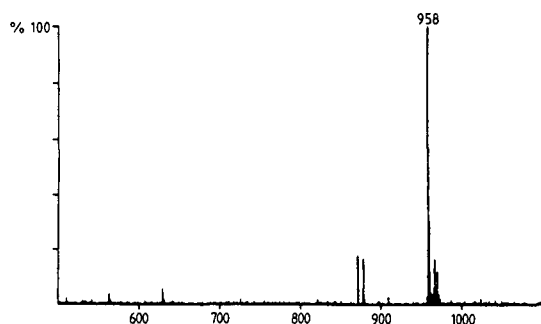


Fig. 8. Positive-ion electropray mass spectrum of an unknown oligosaccharide obtained after enzymatic digestion of an apple 4 M KOH extract. For further explanation, see text.

at m/z 969 (or 947) excludes the presence of an acidic group in the molecule. Using the computer algorithm it was found that there is only one possible composition without acidic sugars, as is illustrated in Table II. Sugar composition analysis confirmed the absence of uronic acids. Actually, the oligomer was found to contain glucose, xylose, galactose and fucose in a ratio of 3:1:1:1. Therefore, from the possible compositions in Table II, $(\text{hex})_8(\text{pent})_2(\text{deoxy})_2$ ($DP = 12$) can be selected as the correct configuration. Other workers have reported xyloglucan oligomers [29,30], but a dodecamer has never been described before. Considering the homology in xyloglucan structure, this oligomer probably has a backbone of six glucose residues and contains two Xyl–Gal–Fuc side-chains. More experiments are needed to determine the exact location of these side-chains.

CONCLUSIONS

Electrospray can be used as an ionization technique for the mass spectrometric analysis of oligosaccharides. The generation of sodiated molecules in the positive-ion mode and either deprotonated or chloridated molecules in the negative-ion mode is to be preferred. Electrospray ionization provides a better response than thermospray ionization for the larger oligosaccharides. Molecular mass information for oligosaccharides up to at least $M_r = 4000$ can be obtained. Spectra of acidic oligosaccharides in both the positive- and negative-ion modes are characterized by sodium exchange, which gives information on the number of acidic groups in the molecule. The better response found for small neutral and acidic oligosaccharides in the positive- than in the negative-ion mode becomes less pronounced for the larger oligosaccharides. Constant infusion of dimethyl- β -cyclodextrins appears to be an accurate and non-laborious method for the determination of the degree of methylation. Further, electrospray appears to be a powerful tool in the characterization of unknown oligosaccharide samples. The molecular mass determined for oligosaccharides allows the calculation of possible sugar compositions in terms of the number of, *e.g.*, pentose, hexose, deoxyhexose and uronic acids. Combination of these data with information concerning the origin of the polysaccharide and the extraction procedure applied generally provides useful information in identifying unknowns, in helping

TABLE II
POSSIBLE SUGAR COMPOSITIONS FOR $M_r = 1870$ (CF., FIG. 8)

Hexose	Pentose	Deoxyhexose	Hexuronic acid	4-O-Methylhexuronic acid
8	2	2	0	0
7	3	1	1	0
6	4	0	2	0
6	0	0	5	0
7	4	0	0	1
7	0	0	3	1
8	0	0	1	2

with the interpretation of NMR data and in the characterization of enzyme activity on certain polysaccharides. Further work along these lines is in progress.

REFERENCES

- 1 A. Dell, H. Egge, H. Von Nicolai and G. Strecker, *Carbohydr. Res.*, 15 (1983) 41.
- 2 J.P. Kamerling, W. Heerma, F.F.G. Vliegthart, B. Green, I.A.S. Lewis, G. Strecker and G. Spik, *Biomed. Mass Spectrom.*, 10 (1983) 420.
- 3 S.A. Carr, V.N. Reinhold, B.N. Green and J.R. Hass, *Biomed. Mass Spectrom.*, 12 (1983) 288.
- 4 A. Dell, J.E. Oates, H.R. Morris and H. Egge, *Int. J. Mass Spectrom. Ion Processes*, 46 (1983) 415.
- 5 T. Keogh, *Anal. Chem.*, 57 (1985) 2027.
- 6 J.O. Metzger, C. Bicke, R. Woisch, F. Hillman and W. Tuszyński, presented at the 12th International Mass Spectrometry Conference, August 26–31, 1991, Amsterdam, abstract S393.
- 7 J.O. Metzger and E. Bruns-Weller, *Rapid Commun. Mass Spectrom.*, 6 (1992) 143.
- 8 B. Stahl, M. Steup, M. Karas and F. Hillenkamp, *Anal. Chem.*, 62 (1990) 1219.
- 9 E. Rajakylä, *J. Chromatogr.*, 353 (1986) 1.
- 10 P.J. Arpino, *Mass Spectrom. Rev.*, 9 (1990) 631.
- 11 S. Santikarn, G.R. Her and V.N. Reinhold, *J. Carbohydr. Chem.*, 6 (1987) 141.
- 12 M. Saikari and H. Kambara, *Anal. Chem.*, 61 (1989) 1159.
- 13 W.M.A. Niessen, R.A.M. van der Hoeven and J. van der Greef, *Org. Mass Spectrom.*, 27 (1992) 341.
- 14 W.M.A. Niessen, R.A.M. van der Hoeven, J. van der Greef, H.A. Schols and A.G.J. Voragen, *Rapid Commun. Mass Spectrom.*, 6 (1992) 197.
- 15 W.M.A. Niessen, R.A.M. van der Hoeven, J. van der Greef, H.A. Schols, G. Lucas-Lokhorst, A.G.J. Voragen and C. Bruggink, *Rapid Commun. Mass Spectrom.*, 6 (1992) 474.
- 16 R.A.M. van der Hoeven, W.M.A. Niessen, H.A. Schols, C. Bruggink, A.G.J. Voragen and J. van der Greef, *J. Chromatogr.*, 627 (1992) 63.
- 17 K.L. Duffin, J. Welply, E. Huang and J.D. Henion, *Anal. Chem.*, 64 (1992) 1440.
- 18 J.J. Conboy and J. Henion, *Biol. Mass Spectrom.*, 21 (1992) 397.
- 19 A.G.J. Voragen, H.A. Schols, J.A. de Vries and W. Pilnik, *J. Chromatogr.*, 244 (1982) 327.
- 20 G. Beldman, M.F. Searle-van Leeuwen and A.G.J. Voragen, *Eur. J. Biochem.*, 146 (1985) 301.
- 21 K. Koizumi, Y. Kubota, T. Utamura and S. Horiyama, *J. Chromatogr.*, 368 (1986) 329.
- 22 H.J.E.M. Reeuwijk, H. Irth, U.R. Tjaden, F.W.H.M. Merkus and J. van der Greef, *J. Chromatogr.*, 614 (1993) 95.
- 23 W.T. Wang and D. Zoph, *Carbohydr. Res.*, 189 (1989) 1.
- 24 G.A. de Ruiter, H.A. Schols, A.G.J. Voragen and F.M. Rombouts, *Anal. Biochem.*, 207 (1992) 176.
- 25 R. Orlando, C.A. Bush and C. Fenselau, *Biomed. Environ. Mass Spectrom.*, 19 (1990) 747.
- 26 S.K. Chanda, E.L. Hirst and E.G.V. Percival, *J. Chem. Soc.*, (1951) 1240.
- 27 J.M. Labavitch and L.C. Greve, *Plant Physiol.*, 72 (1983) 68.
- 28 P. Debeire, B. Priem, G. Strecker and M. Vignon, *Eur. J. Biochem.*, 187 (1990) 573.
- 29 W.S. York, H. van Halbeek, A.G. Darvill and P. Albersheim, *Carbohydr. Res.*, 200 (1990) 9.
- 30 M. Hisamatsu, W.S. York, A.G. Darvill and P. Albersheim, *Carbohydr. Res.*, 227 (1992) 45.

CHROMSYMP. 2809

Characterization of the chemical structure of sulphated glycosaminoglycans after enzymatic digestion

Application of liquid chromatography–mass spectrometry with an atmospheric pressure interface

R. Da Col and L. Silvestro*

Res Pharma Pharmacological Research Srl, Via Belfiore 57, 10125 Turin (Italy)

A. Naggi and G. Torri

Istituto Scientifico di Chimica e Biochimica "G. Ronzoni", Via G. Colombo 81, Milan (Italy)

C. Baiocchi

Dipartimento di Chimica Analitica, Università di Torino, Via P. Giuria 5, 10125 Turin (Italy)

D. Moltrasio and A. Cedro

Crinos SpA, Villaguardia (Italy)

I. Viano

Istituto di Farmacologia e Terapia Sperimentale, Facoltà di Medicina, Università di Torino, Via P. Giuria 13, 10125 Turin (Italy)

ABSTRACT

Pneumatically assisted electrospray was demonstrated to be a powerful ionization source for the analysis of oligosaccharides. A mass spectrometer was interfaced to an HPLC system, using this interface, to determine oligosaccharides from the enzymatic digestion of heparin separated on a reversed-phase column. To set up the technique, and particularly to clarify the ionization process, purified disaccharides, from enzymatic digestion of chondroitin sulphates, were measured. The use of a suitable counter ion in the mobile phase, tetrapropylammonium (TPA), to optimize the HPLC separation, gave, with sulphated di- and oligosaccharides, adducts $[M + n\text{TPA} - (n + m)\text{H}]^{m-}$, which were unexpectedly stable to fragmentation; molecular ions $[M - (n + 1)\text{H}]^{n-}$, in the presence of the counter ion, were observed only with desulphated or monosulphated disaccharides. The stability of the adducts and the use of a deuterated ion-pair reagent permitted an exact evaluation of the molecular masses of disaccharides and oligosaccharides of unknown structure. Spectra obtained in the absence of the counter ion contained singly or multiply charged molecular ions and fragmentation ions mainly from loss of the sulphate groups; under these ionization conditions the exact mass determination and interpretation of the spectra were difficult. After removal of the counter ion, tandem mass spectra could be obtained with some interesting data for the characterization of these molecules. Complete spectral analyses were performed with amounts of samples of 50 μg but, using microbore columns, one twentieth of this amount may give good spectra.

* Corresponding author.

INTRODUCTION

Sulphated glycosaminoglycans (GAGs), such as chondroitin sulphates (CS), dermatan sulphate (DeS), heparan sulphate (HS) and heparin (HEP), are heterogeneous polysaccharides that play important roles in all living organisms and sometimes have notable pharmacological activity [1].

Individual GAGs can be characterized by a variety of electrophoretic, chromatographic and spectroscopic methods, applied either to the intact polysaccharides or to their products of chemical or enzymatic depolymerization [2]. These degradative techniques are very important for obtaining sequence information and have been applied successfully to characterize the antithrombin binding site of heparin [3]. NMR spectrometry is one of the most effective techniques [4] in the analysis of the oligosaccharides from degradation, but it requires relatively large amounts of material and is not suitable for the analysis of very small samples, *e.g.*, most biological samples.

Attempts have been made to use mass spectrometry (MS) [5–7], generally using fast atom bombardment (FAB) [6,7] for ionization, to determine the structures of these oligosaccharides. The reported results were interesting, but some problems were evident: direct connection to high-performance liquid chromatography (HPLC) could not be used and the fractions, after HPLC, must be desalted before FAB analysis. Little information on the carbohydrate sequence could be obtained except with complex derivatization procedures that did not seem practical [6,7]. The extremely high polarity of GAGs is a major problem with other conventional MS techniques.

Recently we used a mass spectrometer equipped with a pneumatically assisted electrospray ionization interface, particularly effective for polar compounds [8], to determine HEP and DeS in human samples, with interesting results in terms of sensitivity and specificity [9]. Another group [10] achieved good results for the analysis of purified oligosaccharides, by enzymatic digestion of GAGs, with the same MS technique.

In this paper, we present the results, obtained with the same MS system, for the on-line charac-

terization of sulphated disaccharides and oligosaccharides from enzymatic depolymerization of HEP, separated, as described previously [9], by ion-pair reversed-phase chromatography (IP-RP-HPLC) and analysed with on-line connection to the mass spectrometer. To set up the technique and elucidate the ionization process in the presence of an ion-pair reagent, purified disaccharides from enzymatic digestion of CS were analysed, dissolved in water or in the buffer used for the HPLC separation; a deuterated derivative of the ion-pair reagent was also used. The possible role of tandem MS (MS–MS) with collisionally induced dissociation (CID) to elucidate the structure and sequence of these molecules was also explored. Similar assays were carried out on real samples by enzymatic digestion.

MATERIALS AND METHODS

Chemicals

The following purified unsaturated disaccharides obtained by enzymatic digestion of CS were purchased from Seikagaku: 2-acetamido-2-deoxy-3-O-(β -D-glucopyranosyluronic acid)-D-galactose (Δ Di-0S), 2-acetamido-2-deoxy-3-O-(β -D-glucopyranosyluronic acid)-4-O-sulpho-D-galactose (Δ Di-4S), 2-acetamido-2-deoxy-3-O-(β -D-glucopyranosyluronic acid)-6-O-sulpho-D-galactose (Δ Di-6S), 2-acetamido-2-deoxy-3-O-(2-O-sulpho- β -D-glucopyranosyluronic acid)-6-O-sulpho-D-galactose (Δ Di-diS_d), 2-O-sulpho- β -D-glucopyranosyluronic acid)-4-O-sulpho-D-galactose (Δ Di-diS_e) and 2-O-sulpho- β -D-glucopyranosyluronic acid)-4,6-bis-O-sulpho-D-galactose (Δ Di-triS). The deuterium-labelled ion-pair reagent tetrapropylammonium bromide (d₂₈TPA), was purchased from MSD Isotopes. Heparinase I (Hepase) (EC 4.2.2.7), HEP from porcine intestinal mucosa sodium salt and all other chemicals of the purest grade available were obtained from Fluka. Research-grade water, produced with a Milli-Q system (Millipore), was used in all experiments.

Enzymatic degradation of HEP

HEP (1 mg), was digested for 24 h at 37°C with 1.5 mU of Hepase in 0.5 ml of 50 mM ammonium acetate buffer (pH 7.0) containing

1.0 mM calcium chloride [11]. At the end of the digestion, to remove the enzyme and the undigested HEP, the reaction mixture was loaded into Ultrafree MC tubes for ultrafiltration (molecular mass cut-off 10 000) and centrifuged at 2000 g for 45 min. Finally, the ultrafiltrates were lyophilized.

Sample introduction and HPLC separation

Purified unsaturated disaccharides were analysed by continuous infusion (Harvard Scientific syringe pump), at 5 $\mu\text{l}/\text{min}$, dissolved in water with 3.3 mM formic acid or in water with 3.3 mM tetrapropylammonium hydroxide (TPA), adjusted to pH 4.0 with formic acid, or with 3.3 mM d_{28}TPA , adjusted to pH 4.0 with formic acid to a concentration of 50 $\mu\text{g}/\text{ml}$.

HPLC separations of oligosaccharides from digestion of HEP were performed on a Spherisorb Hexyl reversed-phase column (250 \times 4.6 mm I.D., 5 μm) from Phase Separations. A Gilson gradient HPLC system (Model 305 + Model 302 Pumps, both with a Model 5.SC head, analytical dynamic mixer and Model 231-401 autosampler with a sample loop of 20 μl) was used. The mobile phase was 3.3 mM TPA adjusted to pH 4.0 with formic acid in water (buffer A) and 3.3 mM TPA adjusted to pH 4.0 with formic acid in acetonitrile–water (90:10) (buffer B), with gradient elution as follows: 3 min isocratic at 100% buffer A then a linear gradient to 50% buffer B in 20 min and a final isocratic step of 7 min at that composition; the flow-rate was 1.00 ml/min. To decrease the mobile phase flow-rate to a level acceptable for the MS system (above 50 $\mu\text{l}/\text{min}$), splitting was performed, connecting to the splitting port of the MS interface a piece of silica capillary of appropriate length. In some experiments buffers A and B were prepared with the same characteristics using d_{28}TPA instead of TPA. All the HPLC–MS experiments were repeated also with a suppressor for cationic counter ions (Dionex MMPC), as described previously [12], with a regenerant composed of 0.1 M sulphuric acid at a flow-rate of 5.0 ml/min.

Mass spectrometric analysis

MS and MS–MS experiments were performed with a Perkin-Elmer–Sciex API III mass spec-

trometer equipped with a pneumatically assisted electrospray source (articulated ionspray source). Mass spectra were acquired in the negative-ion mode and the mass spectrometer was generally operated with scanning from m/z 200 to 2000. When MS–MS experiments were performed the mass spectrometer was operated in the daughter-ion scanning mode and argon was used to obtain CID. In these experiments the collisional energy was optimized at 70 eV and the collision gas had an effective target thickness of *ca.* 2.5×10^{14} atoms/cm².

RESULTS

Figs. 1 and 2 show the mass spectra obtained with the purified disaccharides by enzymatic degradation of CS dissolved in water with 3.3 mM formic acid (top), in water with 3.3 mM TPA adjusted to pH 4.0 with formic acid (middle) or in d_{28}TPA (bottom) in order to examine the ionization processes under different conditions.

The spectra from $\Delta\text{Di-0S}$ are presented in Fig. 1A–C; under the three different MS conditions only a relevant $(\text{M-H})^-$ ion (m/z 377) can be observed and no adduct with TPA or fragments are present. Fig. 1D–F show the mass spectra obtained with $\Delta\text{Di-4S}$.

The most relevant ion in all the spectra has m/z 457, corresponding exactly to the predicted m/z of the $(\text{M-H})^-$ ion of this monosulphated disaccharide. In the spectrum obtained without TPA a second ion shifted of 22 u (m/z 479) can be observed and corresponds to an adduct with sodium, $(\text{M} + \text{Na} - 2\text{H})^-$. Another ion with m/z 299, probably derived from fragmentation, is also present; this m/z value in fact corresponds to the mass of O-sulpho-N-acetylgalactosamine. In presence of TPA an ion of m/z 642 with an intensity similar to that of the deprotonated molecular ion is present; the difference in mass between these two ions is 185 u, corresponding exactly to the calculated mass increase for an adduct with the ion-pair reagent (TPA) used, therefore suggesting that this ion is $(\text{M} + \text{TPA} - 2\text{H})^-$. This hypothesis is confirmed by the mass spectrum obtained with the sample dissolved in a solution of d_{28}TPA . In fact, with this buffer the $(\text{M-H})^-$ ion (m/z 457) is still present, whereas

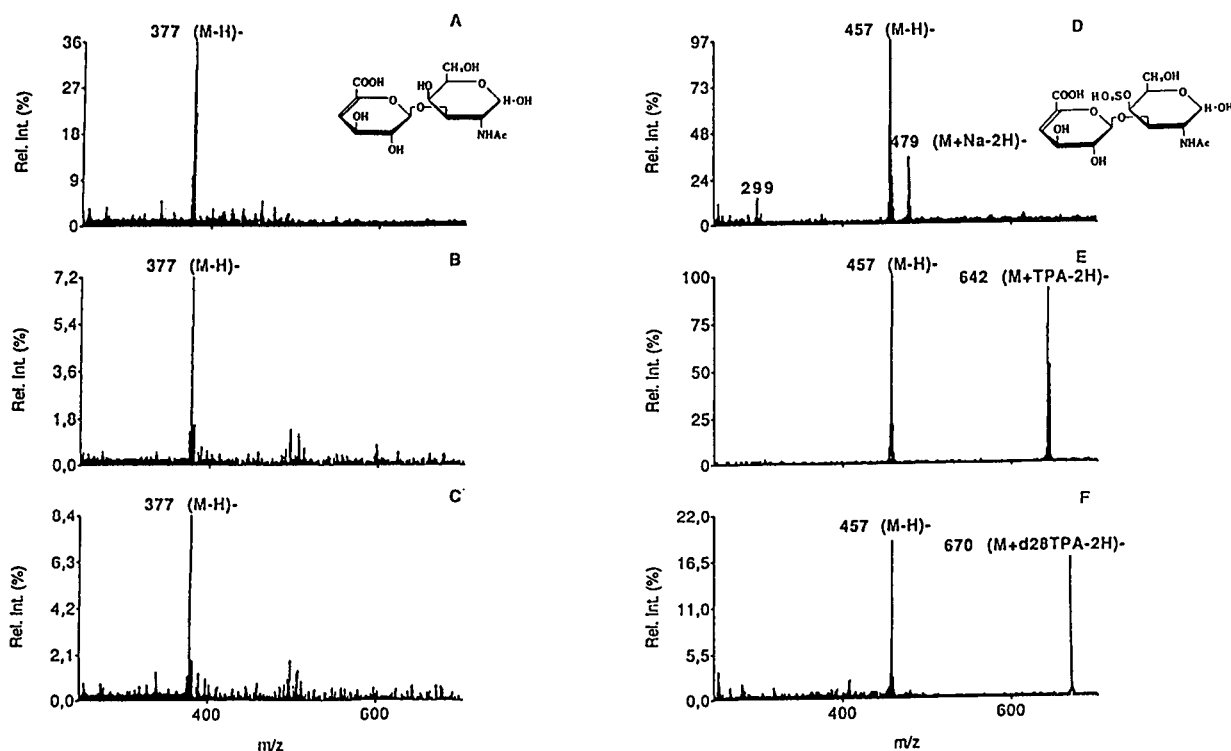


Fig. 1. Mass spectra obtained with the purified desulphated (Δ Di-0S, left) and monosulphated (Δ Di-4S, right) disaccharides by enzymatic digestion of CS. The mass spectra were recorded in the negative-ion mode by injections of the samples dissolved at 50 μ g/ml in 3.3 mM formic acid in water (top), or TPA-formate buffer (pH 4.0, 3.3 mM) (middle) or d_{28} TPA-formate (pH 4.0, 3.3 mM) (bottom).

the ion at m/z 642 has disappeared and a strong ion at m/z 670 is present; the m/z difference between this ion and the adduct with TPA, $(M + \text{TPA} - 2\text{H})^-$, is 28, corresponding to the molecular mass difference between TPA and d_{28} TPA. No ions from fragmentation can be observed. The mass spectra obtained from Δ Di-6S (data not reported) show the same ions as observed with Δ Di-4S and also the absolute intensity of ionization is similar.

The spectra from Δ Di-diS_d are summarized in Fig. 2A–C. In the spectrum without TPA, singly, $(M - \text{H})^-$, and doubly charged, $(M - 2\text{H})^{2-}$, molecular ions can be observed, with m/z 268–537. The adduct with a sodium ion, $(M + \text{Na} - 2\text{H})^-$, is also relevant (m/z 559), followed (m/z 581) by a weak ion with two sodium ions, $(M + 2\text{Na} - 3\text{H})^-$. Ions from fragmentation are also of relevant intensity; the ion with m/z 457 derives from the loss of a sulphate group, $(M - \text{SO}_3\text{H} - 2\text{H})^-$, and others with $m/z < 300$ may be related

to O-sulpho-N-acetylgalactosamine. In the spectrum obtained with TPA only ions formed by adducts with counter ions can be observed: at m/z 722 the adduct with one TPA, $(M + \text{TPA} - 2\text{H})^-$, and at m/z 907 that with two TPA, $(M + 2\text{TPA} - 3\text{H})^-$. Similar results were obtained with d_{28} TPA. The spectra obtained from the other disulphated disaccharide, Δ Di-diS_e, (data not shown) are very similar to those observed with Δ Di-diS_d.

The results from the trisulphated disaccharides, Δ Di-triS, are shown in Fig. 2D–F. In the spectrum without TPA the deprotonated $(M - \text{H})^-$ ion, m/z 617, is present but the adducts with sodium, m/z 639, $(M + \text{Na} - 2\text{H})^-$, and m/z 661, $(M + 2\text{Na} - 3\text{H})^-$, are more important. Ions derived from fragmentation are relevant; the ion of m/z 559 corresponds to the loss of a sulphate group from a sodium adduct, $(M - \text{SO}_3\text{H} + \text{Na} - \text{H})^-$, that with m/z 519 is due to the loss of sulphate from the molecular ion but

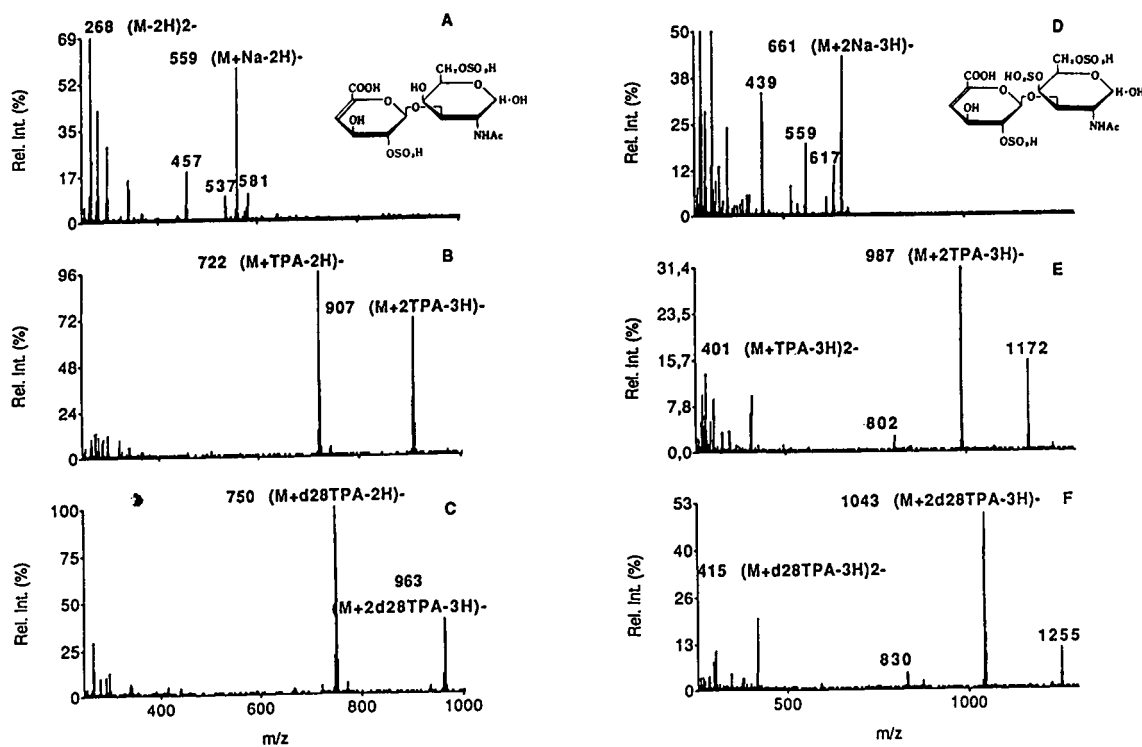


Fig. 2. Mass spectra obtained with the purified disulphated (Δ Di-DiS₂, left) and trisulphated (Δ Di-triS, right) disaccharides by enzymatic digestion of CS. The mass spectra were recorded using the same conditions as in Fig. 1 and are displayed in the same order.

with the oxygen involved in the ester bond, $(M - OSO_3H - 2H)^-$, and finally the loss of these two groups gives the ion of m/z 439, $(M - SO_3H - OSO_3H - 2H)^-$. In the spectrum with TPA the strongest ions correspond to the adduct with 2TPA, $(M + 2TPA - 3H)^-$, m/z 987, and other relevant adducts with TPA are present with m/z 1172 ($(M + 3TPA - 4H)^-$), and m/z 802, $(M + TPA - 2H)^-$. The results obtained with d_{28} TPA confirm the interpretation given to this spectrum.

In Fig. 3 are summarized the tandem mass spectra obtained by CID of the deprotonated molecular ions from each of the previous disaccharides with the aim of understanding the possible role of this technique in characterizing the structure of these molecules. These spectra were acquired from samples dissolved in water with 3.3 mM formic acid because no results could be obtained with the same disaccharides dissolved with ion-pair reagents from both mo-

lecular and adduct ions. With Δ Di-0S (A) only a relevant daughter ion (m/z 174) can be observed; the m/z value corresponds to the hexuronic acid residue with the oxygen of the glycosidic bond. The tandem mass spectrum (B) obtained with Δ Di-6S shows the same fragment (m/z 299), related to the O-sulpho-N-acetylgalactosamine, as observed in the spectrum in Fig. 1D, and two other ions, m/z 281 and 341, derived from the same group; the first corresponds to O-sulpho-N-acetylgalactosamine with a further loss of water, in comparison with m/z 299, and the other (m/z 341) is the hexosamine group linked, by the glycosidic linkage, with a fragment (C_1-C_2) of the hexuronic acid. A daughter ion corresponding to the hexuronic acid, m/z 174, can also be observed in this spectrum as reported for Δ Di-0S. The CID mass spectrum (C) from Δ Di-4S, despite the results obtained with scanning, presents interesting differences compared with Δ Di-6S. All the ions

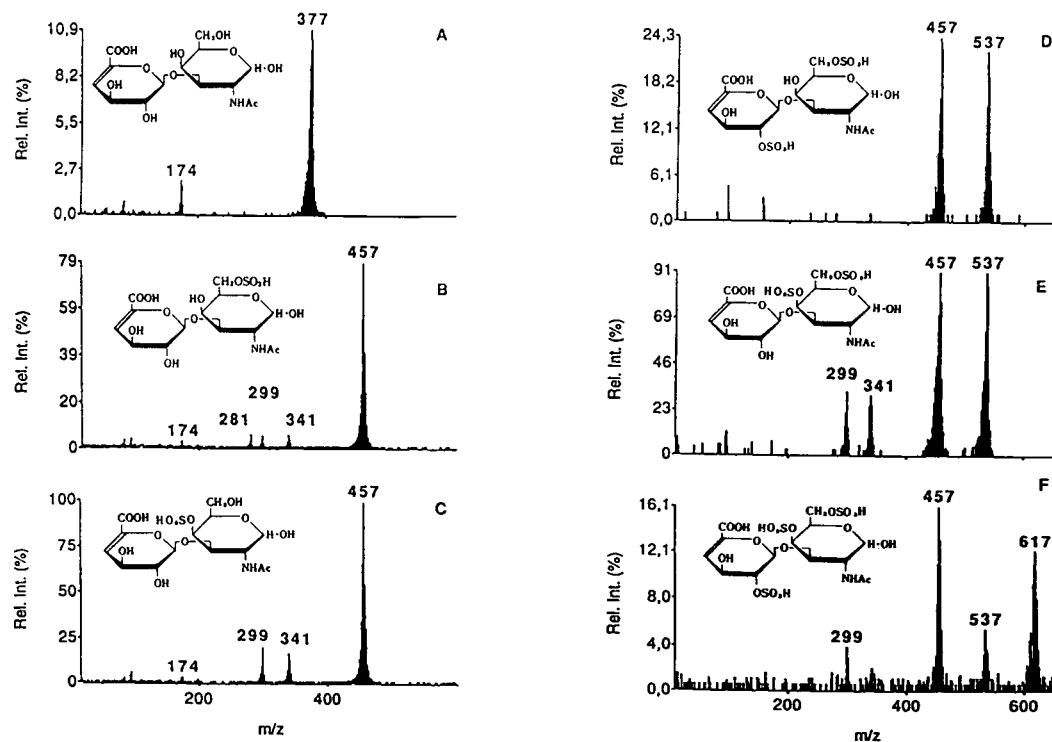


Fig. 3. Tandem mass spectra obtained from the following purified disaccharides by enzymatic digestion of CS : (A) Δ Di-0S; (B) Δ Di-6S; (C) Δ Di-4S; (D) Δ Di-diS _{α} ; (E) Δ Di-diS _{ϵ} ; (F) Δ Di-triS. The spectra were acquired following injection of the samples dissolved in a mobile phase of 3.3 mM formic acid in water.

observed with this last disaccharide are present but the relative intensities of the daughter ions are different. First, the ion of m/z 281 is very weak, the intensity in comparison with the ion of m/z 299 is *ca.* 1/25, whereas with Δ Di-6S the intensities of these two ions are similar. The ions of m/z 299 and 341 have similar intensities and it is *ca.* 25% of that of the parent ion; in the spectrum of Δ Di-6S the relative intensity of these ions was only 5% of that of the parent ion. The fragment corresponding to hexuronic acid (m/z 174) is weak for both disaccharides, above 5% of the parent ion. The tandem mass spectrum (D) of Δ Di-diS _{α} shows only a relevant fragment of m/z 457 derived from the loss of a sulphate group. As observed with the monosulphated disaccharides, differences can be observed between the tandem mass spectrum (E) obtained with the two disulphated disaccharides; in fact, with Δ Di-diS _{ϵ} (E), CID induces not only the formation of a fragment by desulphation but also cleavages such as those observed with Δ Di-4S

giving O-sulpho-N-acetylgalactosamine (m/z 299) and the same group with a fragment of the hexuronic acid (m/z 341). Finally, the tandem mass spectrum (F) from Δ Di-triS is characterized by products of progressive desulphation, m/z 537 and 457, and by the fragment, already observed with the other disaccharides, corresponding to the sulpho-N-acetylgalactosamine.

In Fig. 4 is shown, on the left, the TIC chromatogram obtained for the separation of oligosaccharides from digestion of HEP with Heparase; 50 μ g of depolymerized HEP were injected. Four major peaks can be observed and the mass spectra acquired with suppression of the ion-pair reagent are reported on the right. The spectra are very complex, perhaps owing to the presence of molecular and fragmentation ions with different numbers of charges. The spectra are presented with an m/z range of 200–1000 because no relevant ions was observed at higher m/z , including the expected m/z values of singly charged ions. The spectra are very differ-

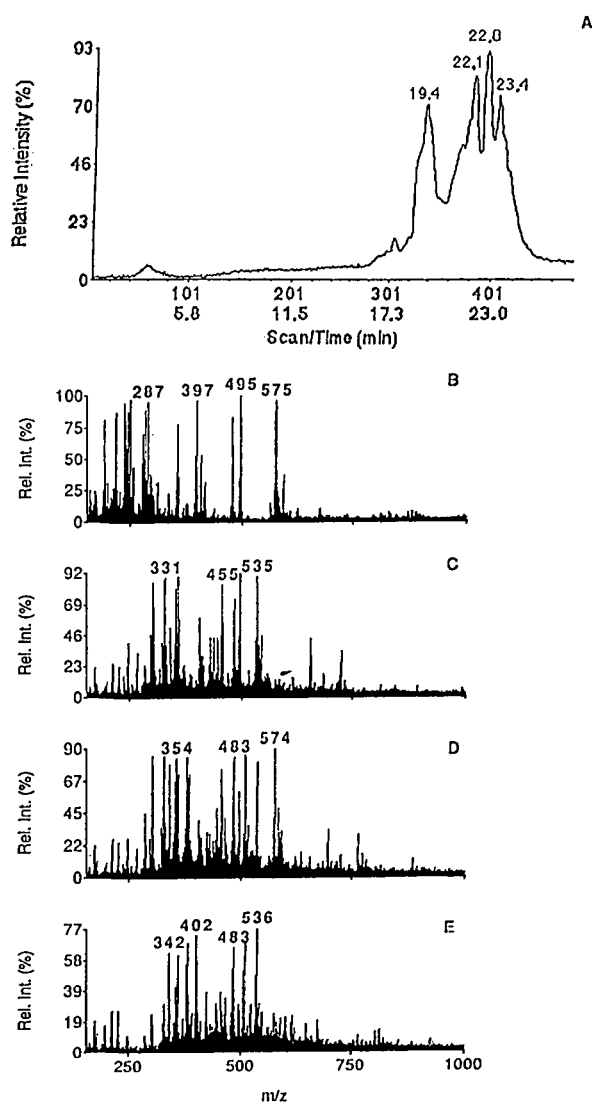


Fig. 4. (A) TIC chromatogram obtained during an RP-HPLC separation, with ion-pair reagent (TPA), of HEP (50 μg) degraded with Hepase. The mass spectra were recorded in the negative-ion mode scanning over the range m/z 100–1500. The mass spectra corresponding to the main peaks from the HPLC run in (A) are reported on the right; the ion-pair reagent was suppressed, from the mobile phase, with a membrane ion suppressor before the MS analysis. The spectra correspond to the peaks at (B) 19.4, (C) 22.1, (D) 22.8 and (E) 23.4 min.

ent in comparison with those obtained in the presence of ion-pair reagents, and the interpretation would be extremely complex and hazardous without the molecular mass assignments obtained from the spectra with TPA and d_{28}TPA .

In Fig. 5 are reported the mass spectra from these more relevant peaks in the presence of TPA (left) or d_{28}TPA (right). The spectral interpretations were obtained by comparing the spectra obtained with the different ion-pair reagents. A quick overview of the corresponding spectra, obtained with the different ion-pair reagents, shows that above all the ions are adducts; in fact, the m/z values of the relevant ions change completely when d_{28}TPA is used instead of TPA.

The spectra in the first row (A and E) were obtained from the peak eluting at 19.4 min. The ions, spectrum with TPA, of m/z 945 and 1130 are singly charged TPA adducts; in fact, the m/z difference between them is 185 (expected mass increase of an adduct with TPA); in the spectrum with d_{28}TPA a group of ions with similar characteristics can be easily identified (m/z 1001 and 1214) and the m/z difference is 213 (calculated mass increase of an adduct with d_{28}TPA). The difference in m/z between the ions of highest intensity in the spectra obtained with TPA or d_{28}TPA (945 – 1001) is 56, corresponding, in the case of singly charged ions, to the m/z difference between two molecules of d_{28}TPA and two molecules of TPA. Therefore, the ions of m/z 945 and 1001 are $(\text{M} + 2\text{TPA} - 3\text{H})^-$ and $(\text{M} + 2\text{d}_{28}\text{TPA} - 3\text{H})^-$, respectively. In these spectra two doubly charged ions of adducts with one or two molecules of ion-pair reagents are also relevant; m/z 380 and 472 with TPA and m/z 394 and 502 with d_{28}TPA . On the basis of the ion interpretations given to these spectra, the molecular mass of the molecule eluting in this peak is 576; this corresponds to the mass of a trisulphated disaccharide that is the main component of the oligosaccharides obtained by Hepase digestion of HEP [13] (see Fig. 6A).

Spectra B and F in Fig. 5 derive from the second relevant peak with a retention time of 22.1 min. In B a group of three intense ions with an m/z difference of 92–93, corresponding to doubly charged TPA adducts, can be observed (m/z 681, 773 and 866). As expected, in F three ions with an m/z difference of 106–107, deriving from doubly charged d_{28}TPA adducts, are present (m/z 710, 816 and 923); also ions with m/z differences corresponding to triply charged adducts with TPA and d_{28}TPA (very weak) can be

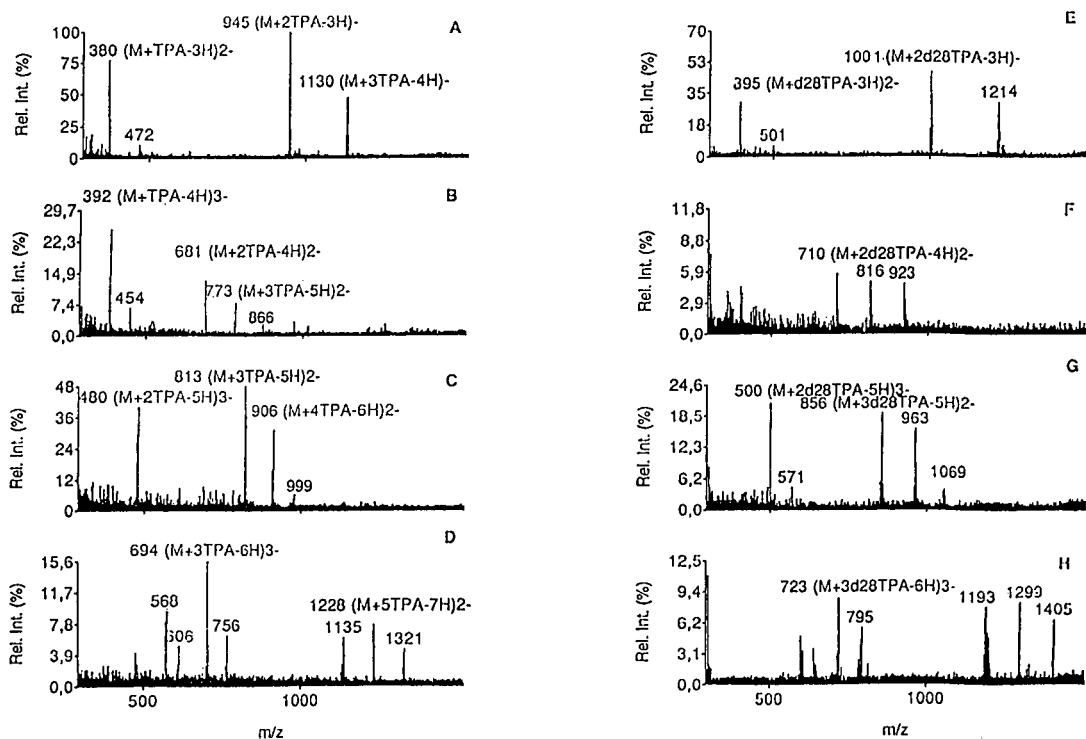


Fig. 5. Mass spectra on the left were recorded during an HPLC separation as in Fig. 4 but without using a membrane ion suppressor for TPA. The spectra on the right were acquired under similar conditions using d_{28} TPA instead of TPA. The spectra in the different rows correspond to those in Fig. 4, in the same order.

observed in both spectra. The m/z difference between the ions of m/z 710 and 681, multiplied according to the number of charges, corresponds to the mass difference between adducts with two TPA or two d_{28} TPA; in the same way it can be calculated that ions with m/z 816 and 773 are adducts with three TPA or three d_{28} TPA. The molecular mass of the oligosaccharide eluting in this peak, in accordance with the above-described spectral interpretation, is 994, corresponding to a tetrasulphated tetrasaccharide (see Fig. 6B) that may derive by enzymatic digestion of HEP [13].

Spectra C and G in Fig. 5 correspond to the peak eluting at 22.8 min. The most relevant ion with TPA, at m/z 813, is followed by an ion of m/z 906, with an m/z difference corresponding to a doubly charged TPA adduct. Two similar ions can be observed with d_{28} TPA (m/z 856 and 963) and the m/z difference corresponds to a doubly charged d_{28} TPA adduct. Considering the

ions of m/z 813 (TPA) and 856 (d_{28} TPA), the m/z difference corresponds to three doubly charged ion-pair molecules, and therefore these ions are $(M + 3\text{TPA} - 5\text{H})^{2-}$ and $(M + 3d_{28}\text{TPA} - 5\text{H})^{2-}$, respectively. With this spectral interpretation the ions derive from an oligosaccharide with M_r 1074; a pentasulphated tetrasaccharide that may be derived from digestion of HEP with Hepase (see Fig. 6C) has exactly this mass [13]. In the same spectra ions corresponding to triply charged adducts are also present and the mass calculations performed from them give the same result.

Spectra D and H in Fig. 5 correspond to the peak at 23.4 min. Groups of ions derived from doubly or triply charged adducts are present in both spectra with the characteristic m/z differences. The m/z difference of the more intense doubly charged ions with TPA, m/z 1228, and with d_{28} TPA, m/z 1299, taking into account the number of charges, correspond to adducts with

five molecules of TPA or d_{28} TPA. The resulting molecular mass of this last-eluting oligosaccharide, calculated from the above interpretation, is 1534; this is characteristic of a hexasulphated hexasaccharide by enzymatic degradation with HEP (see Fig. 6D) [13]. The same result was reached on evaluating the other relevant ions in these spectra.

The proposed structures of the oligosaccharides with molecular masses corresponding to those calculated from the major peaks observed in these samples from enzymatic digestion of HEP are presented in Fig. 6. The positions of sulphation reported in these formulae are only indicative; in fact, from the present MS data, no definitive rule can be obtained.

The CID spectra obtained from some relevant ions during an HPLC separation of the same HEP enzymatic digest, with TPA suppression, are presented in Fig. 7. In spectrum A, acquired during the elution of the peak at 19.4 min corresponding to a trisulphated disaccharide, daughter ions were obtained by fragmentation of a parent of m/z 576 corresponding to the $(M -$

$H)^-$ of this molecule. The spectrum is characterized by three relevant ions, including the parent ion, with m/z differences of 80, corresponding to the loss of sulphate groups.

Spectrum B was obtained under the same chromatographic conditions but from parent ions of m/z 287, therefore corresponding to $(M - 2H)^{2-}$ ions of the disaccharide analysed in the first spectrum. Apart from the parent ion, the most relevant daughter ion has m/z 247, corresponding to a doubly charged ion of the molecule without a sulphate group.

Spectrum C was recorded at the HPLC retention time (22.8 min) corresponding to the penta-sulphated tetrasaccharide from the parent ion of m/z 536, presumably corresponding to the $(M - 2H)^{2-}$ ion of this oligosaccharide. The spectrum is characterized by four relevant ions, including the parent ion, with an m/z difference of 40 between them and therefore corresponding to the sequential loss of sulphate groups from the molecule, which always remains doubly charged. Another weak ion is present in this spectrum with m/z 257; presumably it derives from a

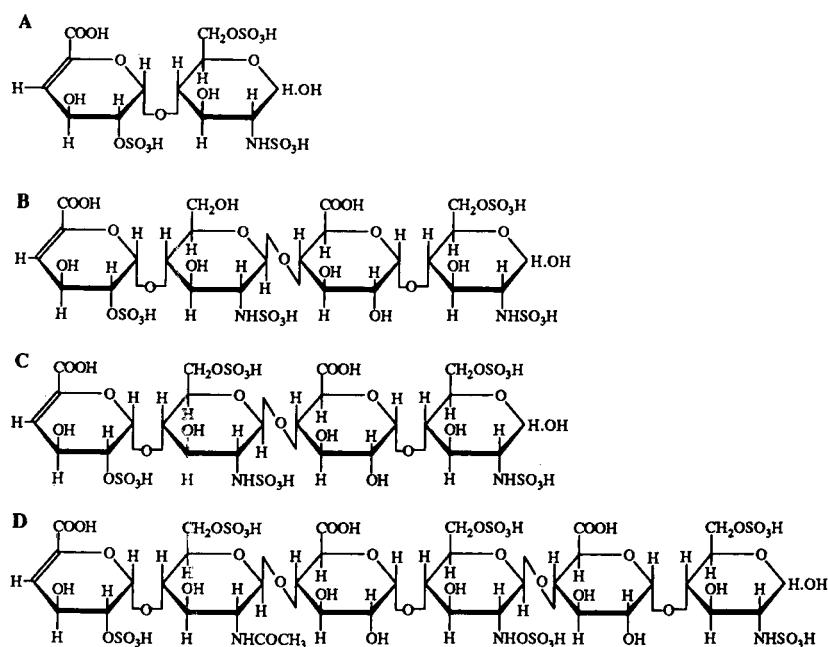


Fig. 6. Formulae of the di- and oligosaccharides that may be derived from HEP degradation with HEPase whose molecular masses correspond to those determined in the more relevant peaks of the separation in Fig. 4. Molecular masses: A = 577; B = 994; C = 1074; D = 1534.

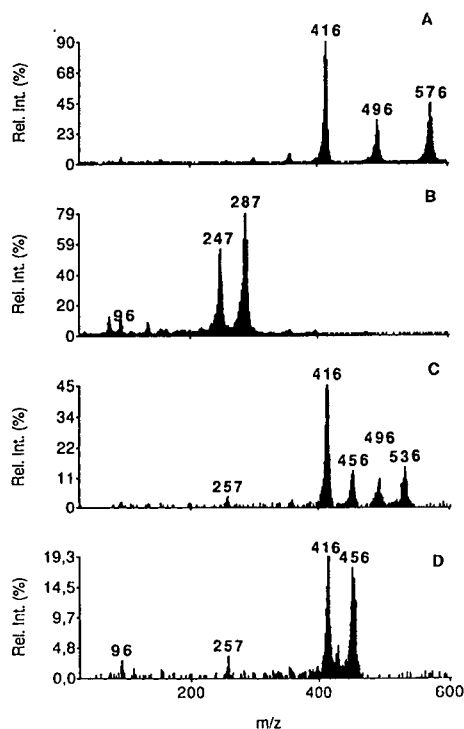


Fig. 7. Tandem mass spectra recorded during an HPLC separation as in Fig. 3 from some relevant ions. Two spectra were obtained from molecular ions of the trisulphated disaccharide (A) singly or (B) doubly charged. (C) Results for the $(M - 2H)^{2-}$ ions of the pentasulphated tetrasaccharide and (D) for an ion of m/z 455 derived by fragmentation of this molecule.

singly charged fragment with the structure of a monosulphated glucosamine.

Spectrum D was acquired during the elution of the pentasulphated tetrasaccharide from a parent ion with m/z , 456, which seems to correspond to a fragment of the oligosaccharide with unknown charge. This spectrum is characterized by an intense parent ion followed by a second peak shifted by m/z 40 and therefore corresponding to the loss of a sulphate group from a doubly charged ion keeping the two charges. Two other weak ions are present with m/z 96, presumably corresponding to a sulphate group with the ester bond, and, already observed in the other spectra, m/z 257. From these findings the molecular mass of the fragment giving the doubly charged ion of m/z 455 is 910, corresponding to the calculated molecular mass of a tetrasaccharide from HEP digestion with three sulphate groups that derives from the fragmentation of the penta-

sulphated tetrasaccharide in the front-collision region.

The CID spectra obtained from these ions are in agreement with the proposed interpretations in Fig. 6.

DISCUSSION

The chromatographic separations were performed on a reversed-phase (C_6) column instead of a more conventional ion-exchange column to avoid the use of the non-volatile buffers normally used with such columns. The counter ion, TPA, as already adopted by Linhardt *et al.* [14], was buffered for use with a silica-based stationary phase. A pH below 4.0 was chosen in order to minimize the chemical reactivity of TPA on the column and wetted parts of the HPLC system. Attempts to use a more usual stationary phase such as C_{18} lead to unacceptably high retention times especially for the highly sulphated HEP fragments. In this study, to allow the use of a membrane ion suppressor that specifically removes the TPA counter ions from the mobile phase, we performed the separation on an analytical column (4.6 mm I.D.); in fact, at present, a membrane ion suppressor for quaternary ammonium ion-pair reagents optimized with the low flow-rate of microbore columns is not commercially available. Comparable separations (data not reported) have been obtained using analytical or microbore columns packed with the same stationary phase (Spherisorb Hexyl silica, 5 μ m; Phase Separations).

The results obtained with purified disaccharides by enzymatic digestion of CS show that in the presence of ion-pair reagents their adducts with the whole molecules form the predominant ions; only with monosulphated disaccharides could molecular ions without TPA be observed. Interestingly, spontaneous fragmentations were not observed in the presence of the ion-pair reagent whereas without an ion-pair reagent fragmentations are evident mainly through the loss of the sulphate groups but also through the cleavage of the glycosidic bonds. Similar fragmentations have already been observed in studies performed on similar oligosaccharides using FAB [6,7], and therefore the use of ion-

pair reagents seems very important in facilitating the determination of the molecular masses of these oligosaccharides. The use of d_{28} TPA enabled us to confirm the spectral interpretations. Sodium adducts were frequently observed especially in the absence of an ion-pair reagent. Reported CID spectra were obtained from deprotonated molecular ions from samples analysed without an ion-pair reagent because no fragmentation could be obtained from adduct ions and also CID mass spectra from deprotonated molecular ions obtained in the presence of an ion-pair reagent were very weak. With molecules containing two or more sulphate moieties the most relevant daughter ions were derived from the loss of the sulphate groups; fragments corresponding to each hexose of the parent molecules can be observed with disaccharides containing one or no sulphate group. Generally the fragmentations observed under MS–MS conditions were similar to those observed in mass spectra acquired from samples in the absence of an ion-pair reagent. The daughter-ion spectra of mono- and disulphated disaccharides (Δ Di-4S, Δ Di-6S, Δ Di-diS_d and Δ Di-diS_e) showed interesting specific fragmentation patterns, depending on the position of the ester bonds, suggesting a possible role of MS–MS in discriminating positional isomers.

The results obtained with HEP were more complex to rationalize. Oligosaccharides from HEP have a very strong interaction with ion-pair reagents and therefore molecular ions cannot be observed when analysed under these conditions; moreover, in the absence of TPA or d_{28} TPA relevant fragmentations occur, giving spectra of complex interpretation. Only the combination of results obtained with TPA and d_{28} TPA permitted an unambiguous identification of the ions in these spectra and therefore the molecular masses of oligosaccharides can be determined accurately.

CID mass spectra of ions from oligosaccharides of HEP confirmed the preferential fragmentation at the ester bonds of the sulphate groups in comparison with the glycosidic bonds; in this study a specific evaluation of N–sulphate bond stability was not performed. Similar results were previously obtained on analysing sulphated oligosaccharides with FAB ionization. The use of

MS–MS with these samples, even if did not give detailed information on sequence, was useful for improving the interpretation of some ions (e.g., number of charges, presence of sulphate groups) obtained with the suppression of counter ions in the mobile phase, necessary to have effective fragmentation. The development of devices to remove quaternary ammonium counter ions from the mobile phase suitable for microbore HPLC will improve this technique; it is noteworthy that similar ion membrane suppressors are already available for applications to inorganic cations or anions (Dionex).

The sensitivity of the technique is interesting: 50 μ g were injected to obtain the reported spectra and therefore, considering a splitting ratio of >1:20, 2.5 μ g injected into a microbore column are sufficient to obtain clear scan spectra. In a previous study [9] we showed that, using single-ion monitoring, amounts of each oligosaccharide as low as 50 ng can be detected using a 1.0 mm I.D. column.

The use of the ionspray technique is one of the main reasons for the interesting results achieved in this study. Indeed, with this ionization method, no sample derivatization was required and on-line interfacing to an effective separative technique was easily achieved. The introduction of a counter-ion reagent, to obtain a good HPLC separation, was another unexpected and relevant improvement. In fact, highly sulphated oligosaccharides could be determined in complex mixtures, overcoming the previously observed problems of fragmentation and separation [7,10].

After this work using well known molecules, promising results have been already obtained by applying this HPLC–MS technique, in combination with enzymatic and chemical degradation, to characterize sulphated GAGs extracted from biological samples. These findings suggest a relevant role of this method in a “combined approach” [15] to elucidate the sequence of unknown GAGs.

REFERENCES

- 1 L.A. Fransson, in G.O. Aspinnall (Editor), *Mammalian Glycosaminoglycans*, Vol. 3, Academic Press, New York, 1985, p. 337.
- 2 E.A. Johnson, *Pharmacol. Res. Commun.*, 14 (1982) 289.

- 3 L. Thunberg, G. Backstrom and U. Lindahl, *Carbohydr. Res.*, 100 (1982) 393.
- 4 G. Torri, *Semin. Thromb. Hemost.*, 17, Suppl 1 (1991) 23.
- 5 J. Kovensky, J.A. Covian and A.F. Cirelli, *Carbohydr. Polym.*, 12 (1990) 307.
- 6 A. Dell, M.E. Rogers. and J.E. Thomas-Oates, *Carbohydr. Res.*, 179 (1988) 7.
- 7 L.M. Mallis, H.M. Wang, D. Loganathan and R.J. Linhardt, *Anal. Chem.*, 61 (1989) 1453.
- 8 P.A. Bruins, T.R. Covey and J.D. Henion, *Anal. Chem.*, 59 (1987) 2642.
- 9 L. Silvestro, I. Viano, A. Naggi, G. Torri, R. Da Col and C. Baiocchi, *J. Chromatogr.*, 591 (1992) 225.
- 10 K. Takagaki, K. Kojima, T. Majima, T. Nakamura, I. Kato and M. Endo, *Glycoconjugate J.*, 9 (1992) 174.
- 11 A. Linker and P. Hovingh, *Carbohydr. Res.*, 127 (1984) 75.
- 12 J.J. Conboy, J.D. Henion, M.W. Martin and J.A. Zweigenbaum, *Anal. Chem.*, 62 (1990) 800.
- 13 R.J. Linhardt, K.N. Gu, K.J. Rice, Y.S. Kim, D.L. Lohse, H.M. Wang and D. Loganathan, *Biochem. J.*, 254 (1988) 781.
- 14 R.J. Linhardt, K.N. Gu, D. Loganathan and S.R. Carter, *Anal. Biochem.*, 181 (1989) 288.
- 15 B. Casu, in D.A. Lane and U. Lindahl (Editors), *Heparin: Chemical and Biological Properties, Clinical Applications*, Vol. 2, Edward Arnold, London, 1989, p. 38.

CHROMSYMP. 2806

Rapid analysis of enzymatic digests of a bacterial protease of the subtilisin type and a “bio-engineered” variant by high-performance liquid chromatography–frit fast atom bombardment mass spectrometry

W.D. van Dongen* and C. Versluis

Bijvoet Centre for Biomolecular Research, Department of Mass Spectrometry, Utrecht University, Utrecht (Netherlands)

P.D. van Wassenaar

Unilever Research Laboratory, P.O. Box 114, 3130 Vlaardingen (Netherlands)

C.G. de Koster, W. Heerma and J. Haverkamp

Bijvoet Centre for Biomolecular Research, Department of Mass Spectrometry, Utrecht University, Utrecht (Netherlands)

ABSTRACT

Amino acid sequencing of a subtilisin-type bacterial protease and a bio-engineered variant was carried out by investigating various enzymatic digests using HPLC–frit fast atom bombardment MS methods. The fast atom bombardment mass spectral data allowed rapid identification of the enzymatically generated peptides and differentiation between both proteins. The feasibility of determining the positions and nature of mutations in the amino acid sequence depends mainly on the size of the peptides containing the modifications.

INTRODUCTION

Elucidating the amino acid sequence of proteins can be done either at the DNA level or at the protein level. DNA sequencing can be carried out relatively easily with considerable speed, but there are many situations in which this approach cannot be followed and sequencing must be done directly at the protein level. A commonly applied method for elucidating the primary structure of large proteins often includes proteolysis followed by chromatographic separation and structural analysis of the resulting

fragments. For the latter purpose classical Edman degradation is more and more being replaced by faster mass spectrometric methods.

Fast atom bombardment (FAB) is a very suitable ionization method for combined high-performance liquid chromatography–mass spectrometry (HPLC–MS) [1–5].

A frit FAB interface makes it possible to administer a flow of 2–10 $\mu\text{l}/\text{min}$ of column effluent to the ion source of the mass spectrometer under stable conditions. The bombarding xenon beam is directed to a fritted disc covering the exit of a thin fused-silica capillary that connects the HPLC system with the ion source [6].

In this study we used a conventional HPLC

* Corresponding author.

system coupled to a frit FAB interface and a sector mass spectrometer for the analysis of various protein digests. An advantage of FAB is that the mass spectra of peptides show not only the protonated molecules but also ions that are characteristic of the amino acid sequence in the peptide. Moreover, the behaviour of peptides under FAB conditions is well documented in the literature [7–10], so that not only is confirmation of the presence of expected peptides in mixtures possible, but also structural determination of unknowns is feasible.

The aim of this study was to identify specific mutations in the sequence of an enzyme variant (a subtilisin type of bacterial protease) produced by protein engineering. The strategy followed was to first subject the enzyme to specific cleavages by cyanogen bromide and trypsin and/or the less specific proteolysis procedures of pepsin, chymotrypsin and autolysis, followed by the analysis of the resulting peptides by HPLC–frit FAB-MS.

EXPERIMENTAL

Digestion of the proteases

Cyanogen bromide digestion. The bacterial protein and its bio-engineered variant (pre-treated with 0.1 M 2-mercaptoethanol at 37°C for 2 h) were dissolved to 10 mg/ml in 70% formic acid. A 50-fold molar excess over methionine of solid cyanogen bromide (Pierce) was added. After flushing with nitrogen the digest was stored in a dark room for 18 h, followed by addition of 10 ml of water and lyophilization.

Tryptic digestion. The resulting cyanogen bromide digests were further digested with 1-tosylamido-2-phenylethylchloromethyl (TPCK) treated trypsin (Worthington) for 16–20 h at 37°C with a substrate-to-enzyme ratio of 100:1 (w/w) in 0.1 M ammonium bicarbonate buffer solution at pH 8.5. The digest was then lyophilized and redissolved in the starting HPLC solvent A (see below) with an approximate sample concentration of 2 mg/ml.

Pepsin digestion. The bacterial protein and its bio-engineered variant were dissolved to 20 mg/ml in 99% formic acid. Pepsin dissolved in 1 M

hydrochloric acid (0.05 mg/ml) was added in a substrate-to-enzyme ratio of 50:1 (w/w). After flushing with nitrogen the digest was stored in a dark room for 18 h, followed by addition of 10 ml of water and lyophilization. The digest was then redissolved in the starting HPLC solvent A with an approximate sample concentration of 2 mg/ml.

Chymotrypsin digestion. The digestion procedure with chymotrypsin (Boehringer) was the same as for trypsin. After lyophilization the digestion solution was redissolved in the starting HPLC solvent A with a sample concentration of about 1–3 mg/ml.

Autolysis. The proteins were incubated at a protein concentration of 1 mg/ml at 60°C for 25 min in 0.1 M sodium hydrogencarbonate. Further autolysis was then stopped by addition of trifluoroacetic acid (TFA) (0.1 ml per ml of sample) and the samples were further stored at –20°C.

Liquid chromatography

Equipment. Binary gradient separation of the digests was carried out using two HPLC pumps (Shimadzu Model LC9A, Kyoto, Japan). Separated components were monitored at 214 nm with a Shimadzu SPD-6AV UV detector fitted with a standard 8- μ l flow cell. The injection valve (Model 7010) with a 50- μ l injection loop was obtained from Rheodyne (Berkeley, CA, USA).

LC separation. Solvent A: 0.06% TFA (v/v) (gradient grade for chromatography, Merck, Darmstadt, Germany) and 1% glycerol (v/v) (Jansen Chimica, Beerse, Belgium) to provide a FAB matrix in bidistilled water. Solvent B: 0.06% TFA (v/v) in acetonitrile–water (80:20, v/v) solution and 1% glycerol (v/v). The gradient used was 100% A, isocratic for 5 min, followed by a linear gradient to 70% B over the next 45 min, and finished with a linear gradient of 70–100% B for a further 5 min. A C₁₈ column, type 218TP54 (250 mm \times 4.0 mm) (Vydac, CA, USA) with a flow-rate of 1 ml/min, was used. A Jeol pneumatic splitter device (MS-PNS) maintained a constant flow-rate to the mass spectrometer of about 10 μ l/min, effectively using a split ratio of 100:1.

Mass spectrometry

Positive FAB mass spectra, first field-free region (1st FFR) and 3rd FFR B/E-linked scan spectra were obtained with a Jeol JMS-SX102/102A four-sector instrument of a B₁E₁-B₂E₂ geometry. HPLC-MS mass spectra were obtained with MS-1 operating at 3000 resolution (10% valley definition). The acceleration voltage was maintained at 6 kV and the magnet was scanned from 10 to 4000 u in 5 s. The most stable conditions were obtained with a source temperature of 85°C. The estimated probe tip temperature was 5–10°C less than that of the ion source block; the probe temperature cannot be controlled separately. On-line HPLC-B/E-linked scan spectra were obtained with MS-1 only. MS-MS mass spectra were acquired by selecting the desired precursor ion with MS-1, and colliding the ion of 6 keV translational energy in a collision cell at ground potential located in the 3rd FFR of the instrument [11,12]. The resulting fragment ions were determined by scanning MS-2. Linked scan spectra were recorded from a 50% attenuated main beam using air (1st FFR) and helium (3rd FFR) as collision gas. Xenon was used as the FAB gas; the gun was operated at 6 kV and a 5 mA discharge current.

RESULTS AND DISCUSSION

The amino acid sequence of the subtilisin-type (B) bacterial protease (269 amino acids, molecular mass 26 683, monoisotopically) is presented in Fig. 1 [13]. The variant protease (V) obtained by protein engineering has similar dimensions; the difference is caused by differences in a few amino acids.

For the HPLC-FAB-MS analysis it is necessary to hydrolyse the proteases into manageable fragments (preferably <3000 Da). As each protein has a unique character, defined by its sequence and higher order structure, the hydrolysis strategies used must be tailored to these proteases. Optimization procedures for hydrolysis are focused on obtaining maximum coverage of the sequence of the proteases, to be certain that all substitutions are traced. Thus, four complementary hydrolysis strategies were chosen: cyanogen bromide degradation followed

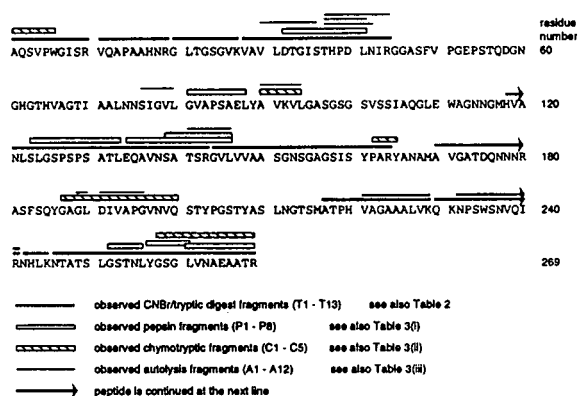


Fig. 1. Amino acid sequence of the bacterial protease (B) and the observed fragments from various hydrolysis strategies.

by tryptic cleavage, pepsin digestion, chymotrypsin digestion and autolysis. Table I gives the sites of cleavage and the specificity of the used processes. Cyanogen bromide tryptic treatment (Table II) cleaves highly specifically at sites well distributed in these proteases. Cyanogen bromide digestion preceding tryptic action is necessary for denaturation purposes; without cyanogen bromide treatment the HPLC-UV chromatograms of the digests showed no significant breakdown of the proteins. This procedure results in an easily predictable and limited number of peptides in the digest. The peptides of protease B (with known sequence) can be identified unequivocally on the basis of their MH⁺ ions. The MH⁺ ion chromatograms can be easily used for identification purposes. Important additional sequence information could be obtained by the less specific proteolysis strategies, using the characteristic series of sequence fragment ions of the various peptides (Table III).

In Tables II and III the identified and expected fragments (Table II only) are compiled together with their pseudomolecular masses and retention times for both proteins studied.

Fig. 2 shows the total ion current (TIC) chromatograms of the cyanogen bromide/tryptic digest peptide mixtures. The unique occurrence of the MH⁺ ions in the chromatographic time domain is demonstrated in the selected mass chromatograms (Fig. 3) and allowed an unambiguous identity assignment of the peaks in the

TABLE I
CLEAVAGE SITES OF THE HYDROLYSIS METHODS

Enzymatic digestion	Cleavage sites	Specificity
(i) Cyanogen bromide/trypsin	Cyanogen bromide: carboxyl site of Met (M) trypsin ^a : carboxyl site of Arg (R), Lys (K)	Relatively high Relatively high
(ii) Pepsin digestion ^{b,c}	On either site of Phe (F), Leu (L), Tyr (Y)	Relatively low
(iii) Chymotrypsin digestion ^{a,d}	Carboxy site of Phe (F), Trp (W), Tyr (Y), Leu (L), Met (M) ^e , His (H) ^e	Relatively low
(iv) Autolysis	Difficult to predict	Low

^a Peptide bonds involving Pro (P) relatively resistant.

^b Cleavage sites vary from one protein to another.

^c Peptide bonds involving Arg (R), Lys (K), Pro (P) and Ile (I) are not hydrolysed.

^d In order of decreasing susceptibility.

^e Peptides bonds sometimes involved in cleavage.

TABLE II
EXPECTED PEPTIDE FRAGMENTS AFTER CYANOGEN BROMIDE/TRYPIC DIGESTION

t_R = Retention time.

Peptide code	Residues	Peptide expected	MH ⁺	t_R (min)	Found B/V ^{a,b}
T1	242-245	NHLK	511.3	14	+/+
T2	170-180	AVGATDQNNNR	1159.6	15	+/+
T3	11-19	VQAPAAHNR	963.5	16	+/+
T4	20-27	GLTGSGVK	718.4	19	+/+
T5	221-229	VAGAALVK	799.5	22.2	+/+
T6 _B	217-229	ATPHVAGAAALVK	1205.7	23.5	+/-
T7	230-241	QKNPSWSNVQIR	1456.8	24.6	+/+
T8	232-241	NPSWSNVQIR	1200.6	25	+/+
T9	1-10	AQSPWGISR	1100.6	26.1	+/+
T10	144-164	GVLVVAASGNSGAGSISYPAR	1933.0	26.6	+/+
T11	246-269	NTATSLGSTNLYGSGLVNÁEAATR	2368.2	28	+/+
T12	28-44	VAVLDTGISTHPDLNIR	1821.0	29	+/+
T13	118-143	HVANLSLGSPSPSATLEQAVNSATSR	2594.3	30.5	+/+
Tu _V	?-?	unidentified	>4000?	32.5	-/+
-	230-231	QK	275.2	-	-/-
-	165-169	YANAm	539/521	-	-/-
-	93-117	VLGASGSGSVSSIAQGLEWAGNNGm ^c	2319/2301	-	-/-
-	181-216	AFSQYGAGLDIVAPGVNVQSTYPGST YASLNGTsm ^c	3580/3562	-	-/-
-	45-92	GGASFVPGEPTQDGNHGHGTHVAGTI AALNNSIGVLGVAPNAELYAVK	4588.3	-	-/-

^a B = Traced in bacterial protein; V = traced in variant.

^b + = Found; - = not found.

^c m = Homoserine or homoserine lactone.

TABLE III
IDENTIFIED PEPTIDE FRAGMENTS RESULTING FROM VARIOUS DIGESTS

Peptide code	Residues	Identity	MH ⁺	t _R (min)	B/V ^{a,b}
<i>(i) Pepsin digestion</i>					
P1	252–256	GSTNL	491.2	17.8	+/+
P2	257–261	YGSGL	496.2	21.1	+/+
P3	139–146	SATSRGVL	79.4 ^c	22.3	+/+
P4 _V	81–88	GVAPNAEL	770.4	23	-/+
P4 _B	81–88	GVAPSAEL	743.4	24	+/-
P5	134–146	EQAVNSATSRGVL	1331.7	24	+/+
P6	32–41	DTGISTHPDL	1055.5	25	+/+
P7	123–133	SLGSPSPSATL	1016.5	28.5	+/+
P8	261–269	LVNAEEATR	944.5	28.5	+/+
<i>(ii) Chymotrypsin digestion</i>					
C1	162–165	PARY	506.3 ^c	17	+/+
C2	258–269	GSGLVNAEEATR	1145.6	22.2	+/+
C3	90–94	AVKVL	529.3 ^c	24	+/+
C4	1–6	AQSVPW	687.3	27.2	+/+
C5	187–200	GAGLDIVAPGVNVQ	1309.6 ^c	28.8	+/+
<i>(iii) Autolysis</i>					
A1	189–190	GL	189.1	16.5	+/+
A2	37–42	THPDLN	696.3 ^c	18.1	+/+
A3	191–196	DIVAPG	571.3	21	+/+
A4	37–41	THPDL	582.3	21.5	+/+
A5	141–146	TSRGVL	632.4	22.4	+/+
A6	30–36	VLDTGIS	704.4 ^c	22.5	+/+
A7	90–94	AVKVL	529.3 ^c	24	+/+
A8	37–44	THPDLNIR	965.5	23.5	+/+
A9	76–80	SIGVL	488.3	27.5	+/+

^a B = Traced in bacterial protein; V = traced in variant.

^b + = Found; - = not found.

^c Identified from the unseparated mixture using 3rd FFR MS–MS spectra.

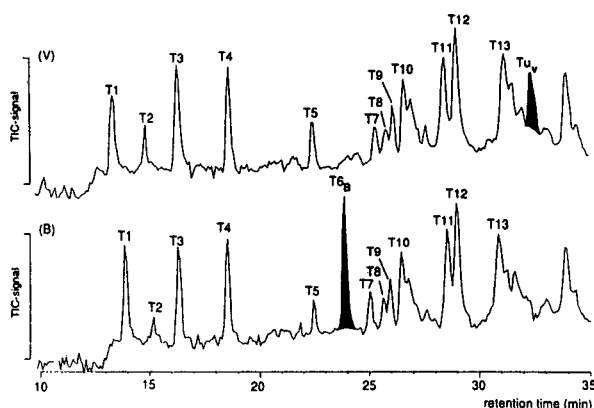


Fig. 2. Total ion current chromatograms of the bacterial protease (B) and the bio-engineered variant (V).

TIC chromatogram. The sequences of the various peptides were confirmed by their HPLC–FAB mass spectra.

Mass spectra of a reasonable quality even for the larger peptides could be obtained after separation by HPLC. As a typical example, the mass spectrum of the peptide T12 with assignment of sequence ions [14] is given in Fig. 4. In spite of the presence of a relatively strong background the spectrum allows confirmation of the expected peptide sequence.

From the obtained HPLC–FAB–MS data amino acid substitutions in variant V can be traced by carefully inspecting and comparing the TIC profiles of the digests and the MH⁺ mass

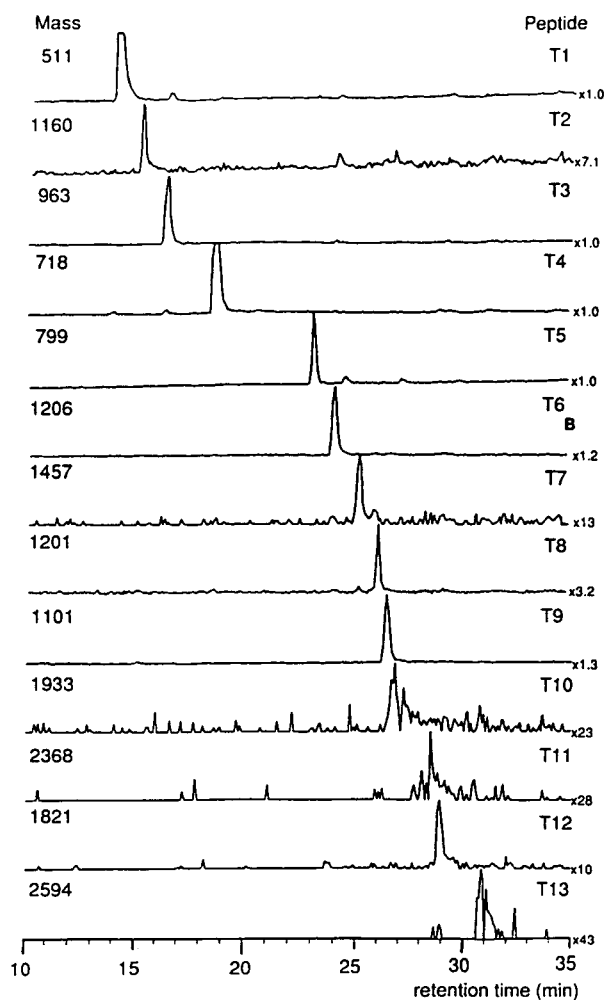


Fig. 3. Mass chromatograms of MH^+ ions in cyanogen bromide/tryptic digest peptide mixtures.

chromatograms of the individual peptides from the two proteases.

Some marked differences in the TIC chromatograms of the cyanogen bromide/tryptic digests were found. The marked peak in Fig. 2B could be traced only in the digest of protease B and is identified as peptide T6_B (positions 217–229, Table II). This peptide is a product of cleavage after a methionine and a C-terminal lysine residue. The marked peak in Fig. 2V is only present in the digest of protease V and is assigned as peptide Tu_V (Table II). The molecular mass of peptide Tu_V is apparently beyond the

scanning mass range at the chosen conditions, so that only a partial mass spectrum could be recorded. Based on some fragment ion peaks in the spectrum that can be assigned to A-, B- and a few Y"- type ions, the peptide probably represents the sequence fragment 181–229. Apparently cyanogen bromide scission in V is not occurring in this sequence part, which can be explained by assuming that the methionine residue at 216 present in protease B is replaced by another amino acid. Complete sequence analysis of Tu_V is in progress.

Comparison of the MH^+ mass chromatograms of the various components in both pepsin digests revealed another difference between the two proteases. The pepsin digests (Table III) contain different peptides, P4_B and P4_V, respectively. Owing to the low specificity of pepsin the peptide mixtures are highly complex and so are the mass spectra. Usually only the MH^+ ions outgrow the abundant chemical background, which obstructs full sequence analysis. If the normal FAB mass spectra (e.g. P4_V $MH^+ = m/z$ 770, Fig. 5A) show many interfering ions, 3rd FFR B/E-linked scanning of the MH^+ ion is the most obvious choice to eliminate background ions and to improve the quality of the resulting mass spectra. However, in a continuous-flow system, it is very difficult to select the desired precursor ion with MS-1 and tune MS-2, since the precursor ions are only present during about 1 min of the HPLC run. Moreover, its intensity is continuously changing during the elution of the component. Therefore, instead of using the "real" precursor ions, background ions have to be used for tuning procedures. Unfortunately, the intensity of the background ions at the mass of the precursor ion was not constant under continuous-flow conditions so that only poor-quality 3rd FFR spectra could be obtained. As an alternative, experimentally simpler 1st FFR B/E-linked scans of the MH^+ were performed. Thus better spectra with a relatively low chemical background, which could be easily interpreted, were obtained. A disadvantage of B/E-linked scan spectra compared with the normal mass spectra is the relatively strong ion intensity discrimination in the low-mass region as a result of the small translational energy of the low-mass

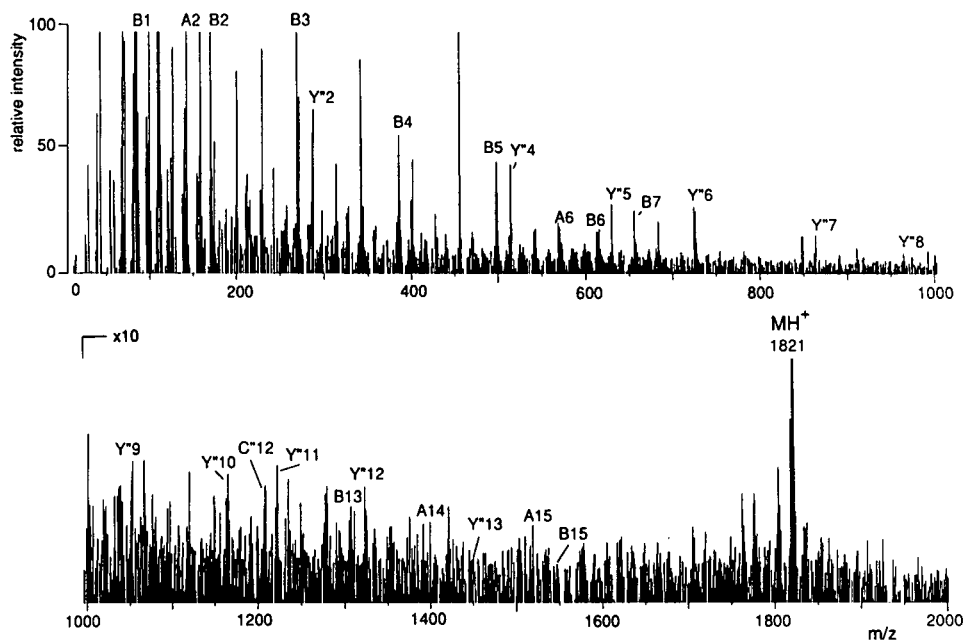


Fig. 4. Positive-ion FAB mass spectrum of a typical digest peptide VAVLDTGISTHPDLNIR (peptide T12); sequence ions are indicated.

fragment ions. Immonium ions are less than 20% of the precursor ion mass and will thus effectively be suppressed in B/E-linked scans (Fig. 5B and V). The 1st FFR B/E spectra of the protonated molecules of the peptides P4_B and P4_V show unequivocally the substitution of serine (S) at position 85 in B by asparagine (N) in V (Fig. 5B and V). Note that for both proteases B and V the Y₅' ions (at *m/z* 516 and 543, respectively) are very pronounced in the B/E-linked scan spectra. This relative abundance of the Y₅' ion is caused by a favourable fragmentation of the peptide bond between proline and its preceding amino acid leaving the charge at the C-terminal ion [15].

Chymotryptic and autolytic digestion also lead to a complex peptide fragment mixtures, resulting in the generation of several mass spectra in which only the MH⁺ can be identified. These spectra are not of high enough quality for sequencing purposes. The FAB mass spectra of the unseparated digests (B and V) exhibit a number of MH⁺ ions representing the more hydrophobic peptides. These ions occur at intensity sufficient

for 3rd FFR MS–MS analysis. The peptides of which the sequence could be confirmed from static FAB–MS–MS spectra are indicated in Table III.

The identified peptide fragments obtained by applying the four hydrolysis strategies have been matched to the relevant positions in the total protease sequences. As shown in Table I and Fig. 1 there is a considerable amount of redundancy in the data, as many of the peptides originate from overlapping sequences. Nevertheless approximately 72% of the sequence of the proteases could be assigned from the various identified peptides within a few days.

Work is in progress to develop an improved fragmentation strategy using a combination of proteases and advanced chromatographic methods resulting in easy-to-analyse peptide mixtures effectively covering the total sequence of this type of proteases. This HPLC–MS procedure should allow easy and rapid check of the sequence of novel subtilisin variants produced by site-directed or localized random protein engineering approaches.

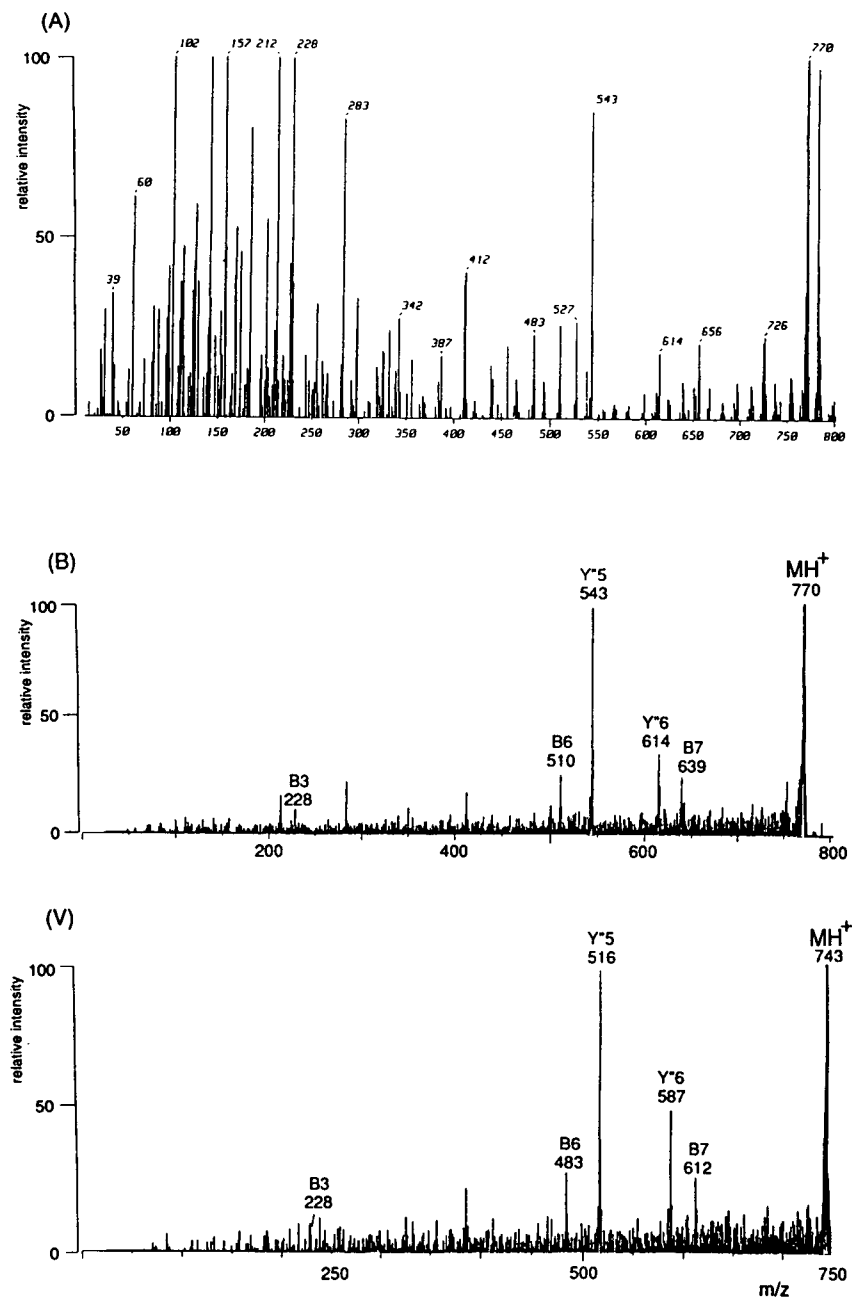


Fig. 5. (A) FAB-mass spectrum of the pepsin digest of protease V at $t_R = 23$ min. (V) B/E-linked scan of $m/z = 770$ of the pepsin digest of protease V at $t_R = 23$ min. (B) B/E-linked scan of $m/z = 743$ of the pepsin digest of protease B at $t_R = 24$ min.

REFERENCES

- 1 R.M. Caprioli, W.T. Moore, B. DaGue and M. Martin, *J. Chromatogr.*, 443 (1988) 355.
- 2 D.J. Bell, M.D. Brightwell, W.A. Neville and A. West, *Rapid Commun. Mass Spectrom.*, 4 (1990) 88.
- 3 D.J. Bell, M.D. Brightwell, W.A. Neville and A. West, *Org. Mass Spectrom.*, 4 (1991) 454.

- 4 W.J. Henzel, J.H. Bourell and J.T. Stults, *Anal. Biochem.*, 187 (1990) 228.
- 5 D.S. Jones, W. Heerma, P.D. van Wassenaar and J. Haverkamp, *Rapid Commun. Mass Spectrom.*, 5 (1991) 192.
- 6 Y. Ito, T. Takeuchi, D. Ishi and M. Goto, *J. Chromatogr.*, 346 (1985) 161.
- 7 S.A. Carr, G.D. Roberts and M.E. Hemling, in C.N. McEwen and B. Larsen (Editors), *Mass Spectrometry of Biological Materials*, Practical Spectroscopy Series, Vol. 8, Marcel Dekker, New York, 1990, p. 87.
- 8 K. Biemann, *Biomed. Mass Spectrom.*, 16 (1988) 9.
- 9 K. Biemann and S.A. Martin, *Mass Spectrom. Rev.*, 6 (1987) 1.
- 10 K. Biemann, *Annu. Rev. Biochem.*, 61 (1992) 977.
- 11 S.A. Martin, R.S. Johnson, C.E. Costello and K. Biemann, in C.J. McNeal (Editor), *The Analysis of Peptides and Proteins by Mass Spectrometry*, Wiley, New York, 1988, p. 135.
- 12 R.K. Boyd, *Int. J. Mass Spectrom. Ion Processes*, 75 (1987) 243.
- 13 C. Betzel, S. Klupsch, G. Papendorf, S. Hastrup, S. Branner and K.S. Wilson, *J. Mol. Biol.*, 223 (1992) 427.
- 14 P. Roepstorff and J. Fohlman, *Biomed. Mass Spectrom.*, 11 (1984) 601.
- 15 W. Heerma, C. Versluis, H. Lankhof, R.C.H.M. Oudejans, F.P. Kooiman and A.M.Th. Beenackers, *Anal. Chim. Acta*, 248 (1991) 553.

Application of liquid chromatography–thermospray mass spectrometry to the analysis of polyester oligomers

Alessandro Guarini*, Gianfranco Guglielmetti and Riccardo Po

Istituto Guido Donegani-Enichem, Via Fauser 4, 28100 Novara (Italy)

ABSTRACT

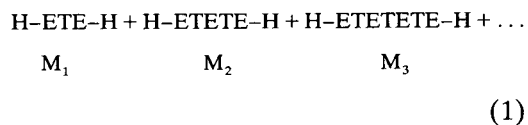
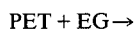
The products obtained by depolymerization of poly(ethylene terephthalate) (PET) with ethylene glycol were characterized by liquid chromatography–thermospray mass spectrometry (LC–TSP–MS). Discharge ionization produced intense negative ion mass spectra containing both acetate attachment and radical molecular anions of PET oligomers. Both full-scan and multiple ion detection modes were evaluated for the structural identification of the LC peaks. Improved performance of the LC–TSP–MS analysis could be obtained by derivatization of the depolymerization mixture with perfluoroanhydrides. This approach gave rise to a tenfold decrease in detection limits and allowed the identification of several additional components of the mixture. Major constituents of the glycolysis mixture were found to be linear and cyclic PET oligomers, diethylene glycol-containing oligomers and monoacetyl derivatives of linear oligomers.

INTRODUCTION

Recycling of plastics is a topic of growing interest, particularly with regard to poly(ethylene terephthalate) (PET) [1–3]. The recycling route consisting in depolymerizing PET from post-consumer soft drink bottles and re-using the so-formed monomer for making new polyester resin is attracting the attention of various chemical companies.

PET bottle scraps may be depolymerized by reaction with either methanol [4] or ethylene glycol (the latter process is referred to as glycolysis in the remainder of the paper) [3,5]. The latter is based on the process depicted in reaction 1. PET reacts with excess of ethylene glycol (EG) in the presence of an alkali or transition metal acetate as the catalyst to give bis(2-hydroxyethyl) terephthalate and homologous oligomers [5]. Among other by products are ethers

(mainly diethylene glycol and its terephthalate ester) and cyclic oligomers (macrocylic esters made up of ethylene terephthalate units) [3].



where $\text{PET} = -(\text{OC}-\text{C}_6\text{H}_4-\text{COO}-\text{CH}_2\text{CH}_2\text{O})_n-$,
 $\text{EG} = \text{HOCH}_2\text{CH}_2\text{OH}$, $\text{T} = -\text{CO}-\text{C}_6\text{H}_4-\text{CO}-$
and $\text{E} = -\text{OCH}_2\text{CH}_2\text{O}-$.

The simplest technique for the quantitative analysis of the mixture of glycolysis products of PET is reversed-phase HPLC with UV detection. However, the structural identification of all the LC peaks requires the employment of a more specific detector. Mass spectrometry has already been applied to the direct characterization of PET and related cyclic oligomers. Polyester oligomers in general have been analysed by fast atom bombardment mass spectrometry (MS)

* Corresponding author.

[6,7]. Electron impact or negative-ion chemical ionization have been used for the PET polymer (pyrolysis-MS) [8] or its cyclic oligomers [9]. Recently, the use of liquid chromatography-mass spectrometry (LC-MS) with a plasmaspray interface has been reported for the analysis of PET cyclic oligomers [10].

This paper describes the characterization of the glycolysis products of PET by means of LC-MS. The methods we have developed are based on the use of thermospray (TSP) as the LC-MS interface. The performances of both full-scan and multiple ion detection (MID) modes were evaluated. In order to enhance the sensitivity we also investigated the use of a suitable derivatization procedure for the PET glycolysis products with perfluoroanhydrides.

EXPERIMENTAL

Depolymerization of PET

A 96.0-g amount of PET bottle scraps and 124 g of ethylene glycol were refluxed for 6 h in the presence of 0.48 g of $\text{Mn}(\text{AcO})_4 \cdot 4\text{H}_2\text{O}$. The reaction mixture was poured into 1 l of hot distilled water. The suspension was cooled to room temperature and filtered, giving a solution and a solid residue. Suspension and filtration were repeated another six times on the solid portion isolated after each filtration. The final pale-green solid was dried under vacuum, constituting the analyte sample (27.9 g). A 15-mg amount of this sample was dissolved in 10 ml of tetrahydrofuran (THF) and used for subsequent LC-UV and LC-MS analyses.

Flow injection (FI)-TSP-MS, LC-UV and LC-TSP-MS

FI-TSP-MS analysis was performed using a Hewlett-Packard Model 1090 liquid chromatograph interfaced to a Finnigan TSQ700 triple quadrupole mass spectrometer equipped with a Finnigan TSP2 thermospray interface. A 10- μl volume of a THF solution of the sample was injected using a mobile phase of acetonitrile-0.05 M ammonium acetate (80:20) at a flow-rate of 1 ml/min. Negative-ion mass spectra were recorded by scanning the third quadrupole (Q3)

from m/z 100 to 900 in 1 s. For the thermospray conditions, see Results and Discussion.

LC separation was performed on the system described above. Sample injections of 5 μl were made on a Shandon Hypersil C_{18} column (250 mm \times 4.6 mm I.D.) using linear gradient elution from 30 to 90% B in 20 min (A = 0.05 M ammonium acetate; B = acetonitrile) at a flow-rate of 1.0 ml/min.

The LC eluent could be fed either to a Hewlett-Packard Model 1050 UV detector (242 nm) or to the TSP probe. The TSP conditions during LC-MS were the following: vaporizer temperature 70°C, source temperature 180°C, discharge voltage 800 V and repeller voltage -100 V. In the full-scan mode, Q3 was scanned from m/z 200 to 900 in 4 s. In the MID scan mode Q3 was scanned over mass windows 1.0 u wide and centred around m/z 254, 446, 488, 490, 576, 638, 682 and 830, with a total scan cycle time of 5 s.

Derivatization

A 1.0-ml volume of a THF solution of the sample was treated at room temperature with 100 μl of trifluoroacetic anhydride (TFA) or heptafluorobutyric anhydride (HFBA). After 30 min the mixture was dried under a stream of nitrogen, the residue was dissolved in 1.0 ml of THF and 100 μl of TFA or HFBA were added. The mixture was allowed to stand for 30 min, after which the solution was dried and the residue dissolved in 300 μl of acetonitrile. LC-MS analysis of the HFBA derivatives was performed by injecting 15 μl of the acetonitrile solution and using a linear gradient elution (from 80 to 90% B in 5 min; A and B as above). The vaporizer temperature was set at 65°C. Throughout the analysis Q3 was scanned from m/z 400 to 1500 in 4 s. All the other experimental conditions were as described for the underivatized sample. The derivatization yield was determined on the basis of LC-UV peak areas and was found to be almost quantitative (diderivatized/monoderivatized peak-area ratio = 100:1).

Detection limits were determined by flow injection (10 μl) of the appropriately diluted solutions of either the derivatized or the underivatized sample and operating Q3 in the single-

ion detection mode (window width 1 u, scan time 1 s).

Chemicals

HPLC-grade water, ammonium acetate, acetonitrile and THF were purchased from Merck. PET bottle scraps were obtained from Tecoplast (Ferrara, Italy). Analytical-reagent grade ethylene glycol was obtained from Carlo Erba. $\text{Mn}(\text{AcO})_4 \cdot 4\text{H}_2\text{O}$, TFA and HFBA were purchased from Aldrich. All chemicals were used as received.

RESULTS AND DISCUSSION

The search for the optimum TSP conditions was performed by flow injection (FI) analysis with a water–acetonitrile mobile phase containing ammonium acetate as the buffer. These preliminary experiments showed that by far the most intense signals were obtained by recording the negative-ion mass spectra produced by operating the TSP interface in the discharge ionization mode. A typical negative-ion FI–TSP mass spectrum of the glycolysis mixture is reported in Fig. 1. Most of the ions can be easily recognized as corresponding to two types of molecular ions of linear PET oligomers (from monomer M_1 to tetramer M_4 ; see reaction 1): odd-electron radical anions (M_n^-), presumably formed by electron attachment, and even-electron acetate attach-

ment ions $[(M_n + \text{AcO})^-]$. The ratio between the two molecular ions for each oligomer depends on the buffer content of the eluent. Other minor ions can be assigned to either fragment ions or molecular ions of additional components of the mixture.

Fine tuning of the TSP conditions was accomplished by systematically varying the experimental parameters over reasonable ranges of values. No significant effect was observed by changing the ion source temperature between 150 and 200°C. Lower temperatures were not tested to avoid source contamination and higher temperatures had a detrimental effect on the absolute ion intensities. The optimum discharge voltage was found to be 700–800 V; above this value a plateau was reached. Fig. 2a shows the influence of the vaporizer temperature on the intensities of different molecular ions. It can be seen that within the range 65–80°C radical anions are favoured at low temperatures, whereas the opposite is true for acetate attachment ions. Outside this range the intensities decreased dramatically. The effect of the repeller voltage on the intensity of molecular ions of various size is depicted in Fig. 2b. The voltage required for maximum intensity clearly depends on the size of the ion, and increases as the ion size is increased. A compromise was chosen by setting the repeller voltage at –100 V.

These optimum vaporizer and ion source temperatures are strikingly different from those reported previously [10] for the cyclic PET oligomers, which involved the use of temperatures up to 350°C. Therefore, we tested our “mild” TSP conditions with a pure sample of the cyclic PET trimer (cyclo- M_3). It turned out that the optimum experimental conditions for the cyclic trimer were identical with those found for the linear oligomers. Moreover, our conditions are consistent with the ion evaporation mechanism, which does not require the volatilization of the neutral analyte [11,12]. There seem to be no explanation for this marked disagreement other than differences in vaporizer and ion source design and the temperature control systems of the two TSP interfaces used.

The optimized TSP conditions were used in the subsequent LC–TSP–MS analysis of the

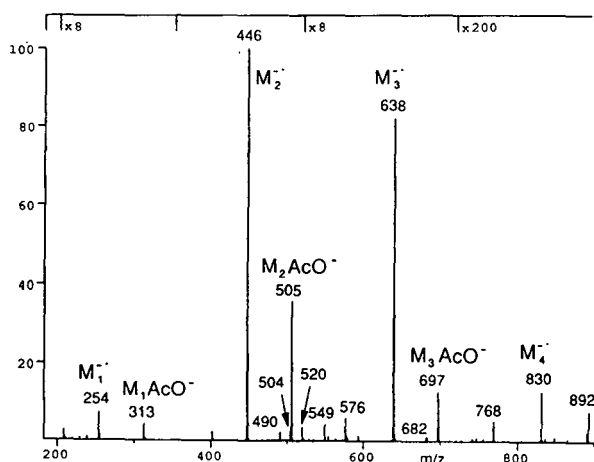


Fig. 1. FI–TSP mass spectrum of the mixture obtained by glycolysis of PET.

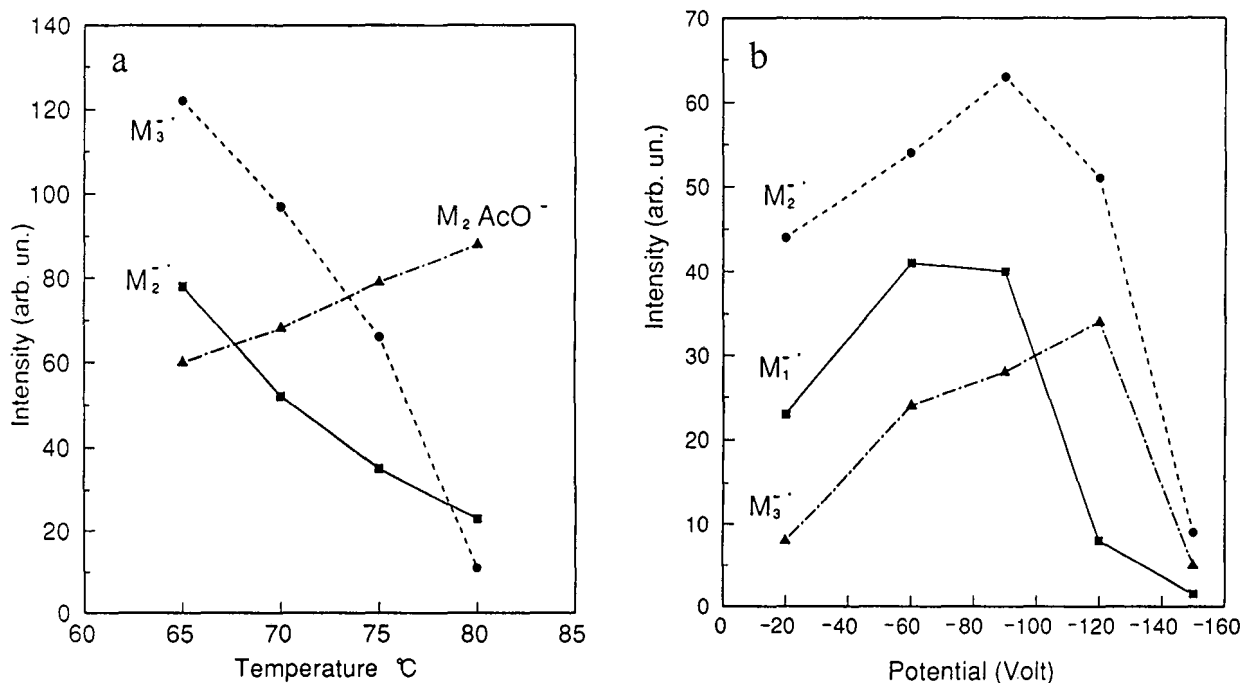


Fig. 2. Effects of (a) vaporizer temperature and (b) repeller voltage on the absolute ion intensities of different molecular ions.

mixture of the glycolysis products of PET. The chromatograms obtained with UV and full-scan MS detection are reported in Fig. 3. The MS trace is actually a reconstructed ion chromatogram made up only by the ion currents corresponding to the most abundant ions of the FI-TSP mass spectrum (Fig. 1). This data manipulation was necessary because the total ion current chromatogram was too noisy and mainly due to high-intensity background ions.

The comparison between the two traces reported in Fig. 3 clearly indicates that sensitivity in the TSP-MS mode is poorer than that in the UV mode. Peaks B and F are completely missing from the MS trace and peaks D and G are barely detectable.

The mass spectra of peaks C and E (Fig. 4) show both M^- and $[M + \text{AcO}]^-$ molecular ions of the linear PET dimer (m/z 446 and 505) and trimer (m/z 638 and 697), respectively. Fragment ions originated from the loss of 192 u, corresponding to the elimination of a repeating unit ($-\text{COC}_6\text{H}_4\text{COOC}_2\text{H}_4\text{O}-$). The mass spectrum taken on the left shoulder of peak C (Fig.

4) can be attributed to a linear PET dimer containing a diethylene glycol moiety instead of one of the three ethylene glycol groups (M^- at m/z 490 and $[M + \text{AcO}]^-$ at m/z 549), with a molecular mass 44 u higher than that of the normal dimer [13]. Similarly, peak A was the linear PET monomer (M^- at m/z 254 and $[M + \text{AcO}]^-$ at m/z 313). Unfortunately, the mass spectra of peaks D and G were too weak for unambiguous interpretation.

In the attempt to obtain at least the molecular mass of all the LC-UV peaks, we tried to use the mass analyser in the MID mode instead of the usual full-scan mode. The set of m/z values chosen for the MID scan included the most significant ions (that is, adduct ions were excluded) contained in the FI-TSP mass spectrum of the sample (see Fig. 1). The total ion chromatogram produced by the LC-TSP-MID analysis is reported in Fig. 5. All the peaks previously observed in the UV trace can be easily recognized in the MID trace. The ion responsible for each peak was tentatively considered to be the molecular ion of the corresponding component.

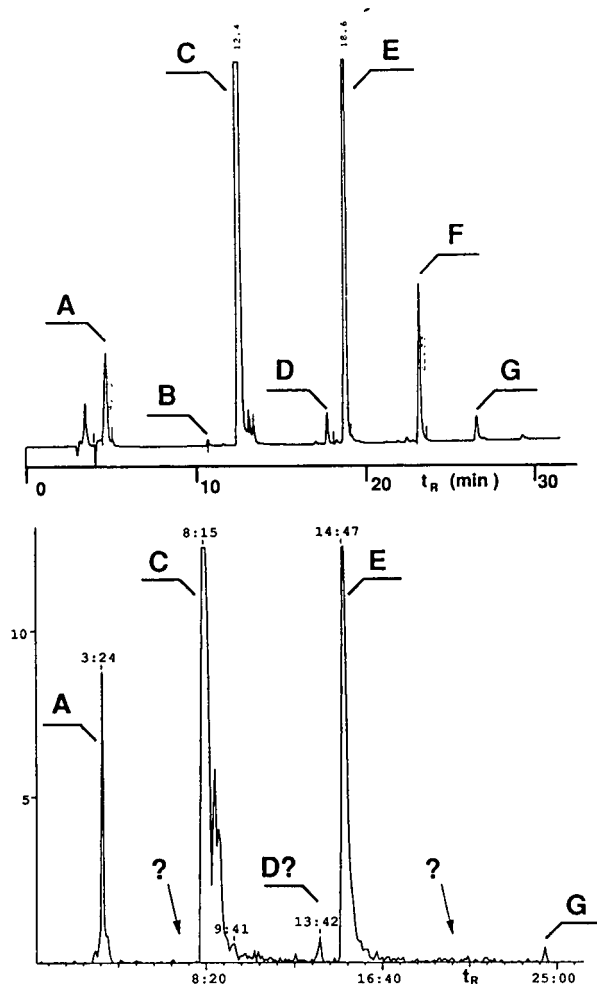


Fig. 3. LC-UV (top) and LC-TSP-MS (full-scan mode, bottom) traces for the glycolysis mixture of PET. The same amount of sample was injected in both instances. Time scales in min.

This assumption allowed the assignment of a tentative structure for peaks B, D, F and G. Peak B was an isomer of the diethylene glycol-containing dimer (m/z 490). Peak D was a mixture of the diethylene glycol-containing trimer (m/z 682) and the monoacetyl derivative of the linear PET dimer (m/z 488), the latter presumably formed by reaction between the oligomer and acetate from the catalyst. Peak F turned out to be the linear PET tetramer (m/z 830) and peak G could be assigned to the cyclic PET trimer (m/z 576). The results for the

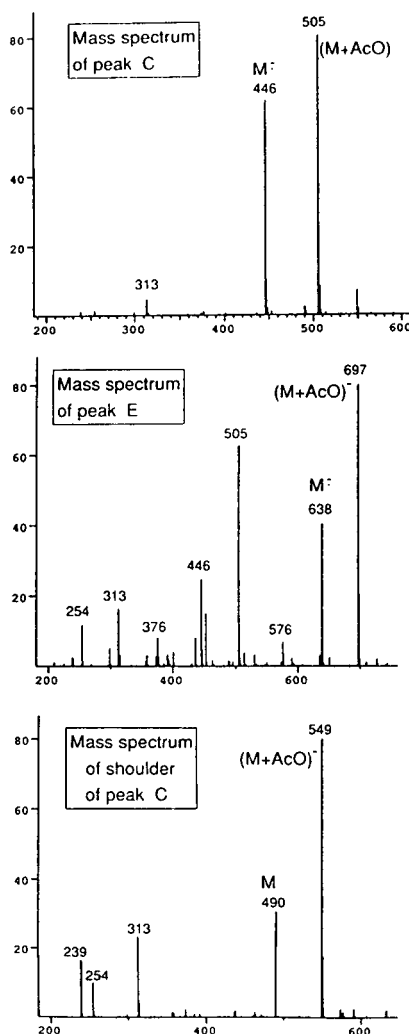


Fig. 4. TSP mass spectra of peak C (top), peak E (centre) and left shoulder of peak C (bottom) in the LC-TSP-MS trace in Fig. 3.

remaining peaks (A, C and E) were in agreement with the structural assignments obtained previously by LC-MS analysis in the full-scan mode.

It is worth noting that the proper use of the information derived from the FI-TSP mass spectrum allowed us to take advantage of the improved sensitivity typical of the MID mode (normally employed for target-compound analysis) for the characterization of an unknown mixture. On the other hand, the full-scan mode

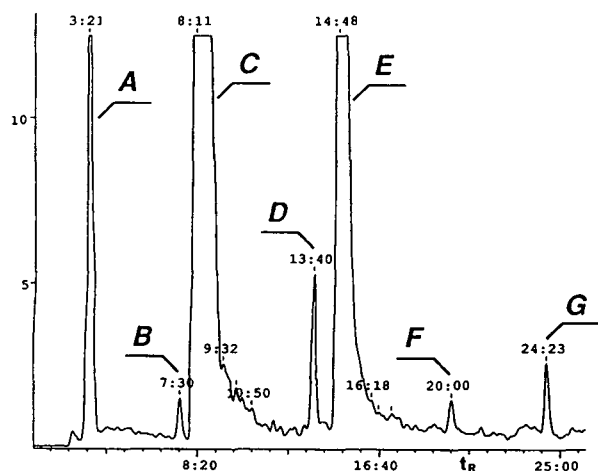


Fig. 5. LC-TSP-MS (MID mode) trace for the glycolysis mixture of PET. Time scale in min.

is certainly more reliable than the MID mode for the determination of the molecular mass of an unknown substance. However, mass spectra of minor components of the glycolysis mixture could not be recorded by LC-TSP-MS analysis, because the signal-to-noise ratio was too low. The causes of poor sensitivity could be (i) poor ionization efficiency, (ii) high-intensity background ions in the m/z range of interest and (iii) low volatility of the analytes. Another problem was the low solubility of the sample mixture. Maximum sample concentrations (about 1.5 mg/ml) could be obtained by using THF as the solvent. Unfortunately, the use of THF limited the injection volume to 5 μ l to avoid peak-splitting problems. Therefore, no more than about 7–8 μ g of the sample mixture could be injected.

Derivatization is usually employed in order to improve both the solubility and detectability of difficult analytes [14]. As one of the ionization mechanisms in the TSP-MS analysis of PET oligomers was electron attachment, we tried to enhance the ionization efficiency by derivatizing the terminal hydroxyl groups with perfluoroanhydrides. The derivatization procedure with either trifluoroacetic anhydride (TFA) or heptafluorobutyric anhydride (HFBA) was simple and gave rise to high conversion yields (>99%). The sole modification of the TSP parameters required by the derivatized samples was the lowering of

the vaporizer temperature to 65°C. The detection limits for the derivatized (with HFBA) and underivatized samples were determined under optimized TSP-MS conditions. On flow injection of 100 pg of the derivatized sample [which contains *ca.* 120 fmole of the HFBA derivative of the linear PET dimer (M_r 838), since this compound is by far the most abundant component of the sample mixture], a signal-to-noise ratio of 20 was obtained in the single-ion detection mode (m/z 838). A similar experiment with the underivatized sample required the injection of 300 pg (*ca.* 670 fmol of the linear dimer) to obtain a signal-to-noise ratio of 10. The resulting detection limit (signal-to-noise ratio \approx 3) for the derivatized dimer (about 20 fmol) turned out to be an order of magnitude lower than for the underivatized dimer (about 200 fmol). The results for the trimers were even better, as derivatization with HFBA resulted in a 30-fold increase in the signal-to-noise ratio, indicating that the derivatization reduced the discrimination against high-molecular-mass components, presumably because of the improved volatility of the perfluoroacyl derivatives.

Another advantage of the HFBA derivatives is that their solubility in the organic mobile phase (acetonitrile) is dramatically increased relative to that of the untreated sample. The use of acetonitrile instead of THF as the sample solvent allowed the injection of a much higher volume of a more concentrated solution. Fig. 6 shows the total ion chromatogram (unmanipulated data) obtained from the LC-TSP-MS analysis in full-scan mode of the sample derivatized with HFBA (50 μ g injected). The chromatogram reproduced fairly well the LC-UV trace of the same sample (not shown). Most of the negative-ion mass spectra contained the molecular radical anion only, but some of the minor peaks had mass spectra containing more than a single ion. The results and the structural assignments for all the LC-MS peaks are summarized in Table I. As can be seen from these data, the LC-TSP-MS analysis of the derivatized sample confirmed the results obtained from the underivatized mixture, but it was also able to reveal the presence of some additional components. Heptafluorobutyric acid (peak 1), the monoderivatized linear dimer

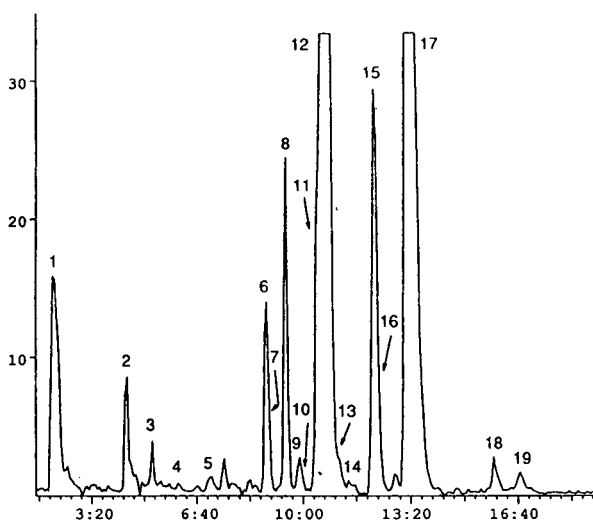


Fig. 6. LC-TSP-MS (full-scan mode) trace for the glycolysis mixture of PET derivatized with HFBA. Time scale in min.

(peak 3) and the linear dimer (peak 8) and trimer (peak 14) derivatized with a C_3F_7CO and a C_2F_5CO group (pentafluoropropionic anhydride is likely to be an impurity of HFBA) can be regarded as components originating from the derivatization step. The monoacetyl derivative of the linear trimer (peak 9) could not be detected in the underivatized sample. Unfortunately, it was not possible to assign a structure to the other impurities on the basis of the sole TSP mass spectrum. However, peaks 10 and 13 (although unresolved from adjacent peaks) could be recognized as the di-HFBA derivatives of two impurities that were observed in the FI-TSP mass spectrum of the sample (Fig. 1, m/z 504 and 520) but could not be found in the LC-TSP-MS chromatogram (Fig. 3, bottom). Therefore, the derivatization provided confirmation that these two ions were actually molecular anions of two

TABLE I

MASS SPECTRAL DATA FOR THE LC-MS PEAKS IN THE ANALYSIS OF THE HFBA-DERIVATIZED SAMPLE

Peak No.	m/z (relative abundance, %)	Structural assignment ^a	Proposed M_r for underivatized molecule
1	427 (100), 641 (20)	C_3F_7COOH	214
2	611 (100), 519 (50), 414 (50)	Unknown	?
3	642 (100), 701 (30)	$M_2(HFB)$	446
4	576 (100)	Cyclo- M_3	576(G) ^b
5	684 (100), 743 (30)	$M_2Ac(HFB)$	488(D)
6	646 (100)	$M_1(HFB)_2$	254(A)
7	541 (100), 522 (35), 502 (19), 462 (79), 460 (95)	Unknown	?
8	788 (100), 847 (12)	$M_2(HFB)(PFP)$	446
9	876 (100)	$M_3Ac(HFB)$	680
10	896 (100)	Unknown	504 ^c
11	882 (100), 941 (15)	$(M_2 + 44)(HFB)_2$	490(B)
12	838 (100), 897 (18)	$M_2(HFB)_2$	446(C)
13	912 (100), 971 (9)	Unknown	520 ^c
14	980 (100), 1039 (18)	$M_3(HFB)(PFP)$	638
15	613 (100), 594 (45), 574 (10), 534 (60), 532 (68)	Unknown	?
16	1074 (100), 1133 (20)	$(M_3 + 44)(HFB)_2$	682(D)
17	1030 (100), 1089 (7)	$M_3(HFB)_2$	638(E)
18	685 (100), 666 (40), 646 (16), 606 (57), 608 (61)	Unknown	?
19	838 (100), 1222 (25), 1030 (20)	$M_4(HFB)_2$	830(F)

^a HFB = heptafluorobutyl derivative; PFP = pentafluoropropionyl derivative; Ac = acetyl derivative; $(M_n + 44)$ = linear oligomer containing a diethylene glycol unit.

^b Peak labels used in Figs. 3a, 3b and 5.

^c Assumed on the basis of the FI-TSP mass spectrum of the underivatized sample (see text for explanation).

components of the glycolysis mixture. The mass spectra relative to peaks 7, 15 and 18 displayed exactly the same group of ions, with an overall increment of 72 u between each couple of adjacent spectra (see, for example, the doublets at m/z 460/462, 532/534 and 604/606 in Table I). This suggests that the peaks correspond to a set of three closely related substances. Further work is under way on the determination of the structure of the unknown components with the aid of other mass spectrometric techniques (e.g., MS–MS).

Three different LC–MS methods have been investigated. The first, involving full-scan acquisition, was the simplest as it did not require any previous knowledge about the sample and provided true mass spectra. The disadvantage was that the sensitivity was too low for the detection of several minor components.

The second approach was the MID mode analysis, which significantly reduced the detection limits but required a hypothesis to be formulated regarding the nature of the compounds analysed. In other words, given a set of expected molecular masses, e.g., those of a series of oligomers, the MID mode allowed the identification of the corresponding LC peaks in the chromatogram.

The third method, namely HFBA derivatization combined with full-scan analysis, was actually able to provide true mass spectra with sufficiently low detection limits. On the other hand, it required some additional effort (cost and time) for the preparation of the sample and, of course, it was effective only for those components which were converted into the derivative. Undesired derivatives (e.g., incompletely derivatized substances) were not a real problem as they could be easily recognized.

CONCLUSIONS

We have applied LC–TSP–MS to the characterization of the mixture obtained by glycolysis

of PET. Structural assignment was achieved for all the major constituents and several minor components could also be identified.

We believe that the use of the thermospray interface with discharge ionization in the negative ion mode can be successfully applied to the LC–MS analysis of the depolymerization products of various aromatic polyesters. The use of derivatization with perfluoroanhydrides, although adding some complexity to the analysis, should extend the range of application of discharge TSP ionization to aliphatic polyesters and, in general, to compounds containing hydroxyl groups.

REFERENCES

- 1 J. Milgrom, in R.J. Ehrig (Editor), *Plastic Recycling*, Hanser, Munich, 1992, Ch. 3.
- 2 W.De Winter, A. Marien, W. Heirbaut and J. Verheijen, *Makromol. Chem., Macromol. Symp.*, 57 (1992) 253.
- 3 D. Gintis, *Makromol. Chem., Macromol. Symp.*, 57 (1992) 185.
- 4 A.A. Naujokas and K.M. Ryan, to Eastman Kodak, *U.S. Pat.*, 5 051 528 (1991).
- 5 A. Fujita, M. Sato and M. Murakami, to Toray Industries, *U.S. Pat.*, 4 609 680 (1986).
- 6 G. Montaudo, *Rapid Commun. Mass Spectrom.*, 5 (1991) 95.
- 7 A. Ballistreri, D. Garozzo, M. Giuffrida and G. Montaudo, *Anal. Chem.*, 59 (1987) 2024.
- 8 R.E. Adams, *J. Polym. Sci., Polym. Chem. Ed.*, 20 (1982) 119.
- 9 S. Shiono, *J. Polym. Sci., Polym. Chem. Ed.*, 17 (1979) 4123.
- 10 H. Milon, *J. Chromatogr.*, 554 (1991) 305.
- 11 G. Schmelzeisen-Redeker, L. Butfering and F.W. Rollgen, *Int. J. Mass Spectrom. Ion Processes*, 90 (1989) 139.
- 12 V. Katta, A.L. Rockwood and M.L. Vestal, *Int. J. Mass Spectrom. Ion Processes*, 103 (1991) 129.
- 13 S.G. Hovenkamp and J.P. Munting, *J. Polym. Sci., Part A-1*, 8 (1970) 679.
- 14 K. Blau and G.S. King, *Handbook of Derivatives for Chromatography*, Heyden, London, 1977.

CHROMSYMP. 2854

Recent progress in high-performance anion-exchange chromatography–thermospray mass spectrometry of oligosaccharides

W.M.A. Niessen*, R.A.M. van der Hoeven and J. van der Greef

Division of Analytical Chemistry, Leiden/Amsterdam Center for Drug Research, P.O. Box 9502, 2300 RA Leiden (Netherlands)

H.A. Schols and A.G.J. Voragen

Wageningen Agricultural University, Department of Food Science, Bomenweg 2, 6703 HD Wageningen (Netherlands)

C. Bruggink

Dionex BV, P.O. Box 9338, 4801 LH Breda (Netherlands)

ABSTRACT

The on-line combination of high-performance anion-exchange chromatography and mass spectrometry via a thermospray interface has proved to be a powerful tool in the characterization of sugar oligomers obtained by enzymatic digestion of plant cell wall polysaccharides. The potential of the method can be improved by the use of a new column material, CarboPac PA100, which requires lower sodium acetate concentrations for the elution of large sugar oligomers. Further, the application of multiple-ion detection optimizes the information obtained from the analysis by improving both the signal-to-noise ratio and the conservation of the chromatographic resolution. Negative-ion instead of positive-ion detection results in significantly better signals, especially for the larger sugar oligomers.

INTRODUCTION

One of the major themes in the developments in on-line liquid chromatography–mass spectrometry (LC–MS) in the past few years has been its application in biochemistry. LC–MS has found wide application in the analysis of bio(macro)molecules, such as nucleosides and nucleotides [1] and peptides and proteins [2–5]. However, relatively little attention has been paid to the LC–MS analysis of sugar oligomers. Small oligosaccharides have frequently been used to establish the absence of thermal degradation in

LC–MS interfaces. In LC–MS studies of starch hydrolysates using a thermospray interface, thermally induced hydrolysis of oligosaccharides to monomeric units was observed [6–9]. Intact oligosaccharides have been studied by LC–MS using a moving-belt interface with fast atom bombardment ionization [10].

Recently, considerable progress has been made in the LC–MS analysis of oligosaccharides. Simpson *et al.* [11] demonstrated the possibility of direct coupling of high-performance anion-exchange chromatography (HPAEC) to MS by means of an anion micromembrane suppressor (AMMS). HPAEC can be considered to be one of the most powerful LC methods available for the separation of oligosaccharides [12]. Simpson

* Corresponding author.

et al. [11] demonstrated the analysis of monomeric and dimeric amino sugars using a thermospray interface. However, the protonated and ammoniated sugar dimer molecules analysed showed poor abundances, indicating thermal degradation in the thermospray interface.

One of the ways in which the thermal degradation of the sugar oligomers can be avoided is the application of the ionspray interface [13]. In contrast to the thermospray interface, no heat is used for the nebulization of the column effluent in the ionspray interface. On-line coupling of HPAEC and ionspray MS via an AMMS has been demonstrated by Conboy and co-workers [14,15]. The method was applied to the determination of high-mannose oligosaccharides that were obtained by the treatment of RNase B with endoglycosidase. Sugar oligomers of the type GlcNAc-(Man)_{*n*} with *n* = 5–9 were observed in these experiments [15].

Recently, we demonstrated that the thermal degradation of sugar oligomers in the thermospray interface is due to the presence of ammonium acetate in the solvent used and can be attributed to thermally induced ammoniolysis of the oligosaccharides to their monomeric units. However, with a mobile phase containing low concentrations of sodium acetate, intact sodiated molecules can be observed in the positive-ion mode for maltodextrins up to a degree of polymerization (*DP*) of 10, *e.g.*, after reversed-phase LC–MS [8,9]. This solvent system is also readily compatible with HPAEC in combination with an AMMS [16,17]. The HPAEC–MS system with the thermospray interface was applied to the analysis of oligosaccharides obtained by the enzymic degradation of plant cell wall polysaccharides. Sugar oligomers up to *DP* = 10 could be detected in these experiments [16,17].

The upper *DP* value achievable in HPAEC–MS is limited by two effects. First, larger sugar oligomers generally require higher sodium acetate concentrations for their elution. In our system, two AMMS in series are used to reduce the sodium concentration in the mobile phase to below 10⁻³ mol/l. This approach is successful as long as the sodium concentration in the mobile phase is kept below 0.4 mol/l. Sugar oligomers eluting at higher sodium concentrations are lost,

because the HPAEC system has to be disconnected from the LC–MS interface in order to avoid source contamination. Intense sodium acetate cluster ions are detected at higher sodium concentrations, resulting in signal instabilities and baseline noise [16,17]. Second, the response at higher *DP* values generally is significantly lower in thermospray MS under these conditions [17].

The studies described in this paper were aimed at the partial removal of these two limitations in order to extend the applicability of the approach. The discussion can be subdivided into two parts. The first part primarily describes improvements to the previously reported HPAEC–MS approach [16,17]. For instance, the use of a new commercially available column material, CarboPac PA100, which permits the elution of sugar oligomers at relatively lower sodium-acetate concentrations, has been tested in HPAEC–MS and the effects on the response of sugar oligomers are reported here. Further, a comparison is made between positive- and negative-ion detection of oligosaccharides under these conditions. Previously only positive-ion detection has been reported [16,17]. Negative-ion detection was investigated in order to improve the response, especially for the larger oligomers. In most experiments α -1,4-glucose oligomers (maltodextrins) were used as model compounds, but some results with other sugar oligomers are also described.

EXPERIMENTAL

The general experimental set-up was similar to that reported previously [16,17]. A Dionex (Sunnyvale, CA, USA) DX-300 modular ion chromatographic system, consisting of an EDM-2 solvent degassing unit, an AGP pump module, an LCM-3 chromatography module containing a Rheodyne (Cotati, CA, USA) Model 9126 all-PEEK injector with a 25- μ l loop, a pulsed electrochemical detector (PED) with a gold electrode and two AMMS-II in series, was coupled via a Kratos (Manchester, UK) Spectroflow 400 LC pump, which acted as a booster pump, to a Finnigan MAT (San Jose, CA, USA) thermospray interface fitted on to a Finnigan MAT

TSQ-70 tandem mass spectrometer equipped with a 20-kV conversion dynode detection system. Regeneration of the AMMS systems was performed by a continuous flow of 0.1 mol/l sulphuric acid at a flow-rate of *ca.* 15 ml/min through the system.

Two different columns (250 mm × 4 mm I.D.) were used in these experiments: a CarboPac PA1 column which had also been used in the earlier experiments [16,17] and the new CarboPac PA100 column, which is expected to give oligosaccharide elution at lower sodium acetate concentrations. Gradient elution was applied using two solvents: (A) 0.1 mol/l aqueous sodium hydroxide and (B) 1 mol/l sodium acetate in 0.1 mol/l aqueous sodium hydroxide. Each chromatographic run was followed by a washing and re-equilibration step (10 min at 100% solvent B and 10 min at 100% solvent A). A flow-rate of 1.0 ml/min was used. For maltodextrin analysis, a linear gradient from 0 to 30% solvent B in solvent A in either 20 or 30 min was used. At a T-piece between the AMMS and the booster pump 10^{-4} mol/l aqueous sodium acetate was added at 0.5 ml/min.

Typical operating conditions of the thermospray interface were block temperature 350°C, vaporizer temperature 80°C and repeller potential 50 V in the positive-ion mode and -50 V in the negative-ion mode. Mass spectra were acquired from *m/z* 150 to 1500 at 3–5 s per scan. In multiple ion detection (MID) 5–10 ions were selected per segment, *e.g.*, ions for *DP* = 1–5, ions for *DP* = 6–10. Switching from one segment to another was done at an appropriate moment during the run. The segments were acquired in 3–5 s.

Maltodextrin MD-25, a mixture of α -1,4-glucose oligomers, was obtained from Roquette (Lille, France).

RESULTS AND DISCUSSION

Improved response in HPAEC–MS over reversed-phase LC–MS

HPAEC is a very powerful tool in the analysis of oligosaccharides. The on-line coupling to thermospray mass spectrometry allows rapid molecular mass determination of the various

constituents of (complex) oligosaccharide samples. In Fig. 1a, the peak areas measured with reversed-phase LC–MS (data from ref. 9) and HPAEC–MS for various α -1,4-glucose oligomers are plotted as a function of the *DP* value. The peak areas were measured under comparable conditions in multiple-ion detection and were corrected for the difference in the amount injected. Depending on the *DP*, a 2–8-fold improvement in the response is achieved in HPAEC–MS. Therefore, despite the unfavourable mobile phase composition, the HPAEC–MS combination with the AMMS for suppression of the sodium ions results in considerably better ionization characteristics than reversed-phase LC–MS

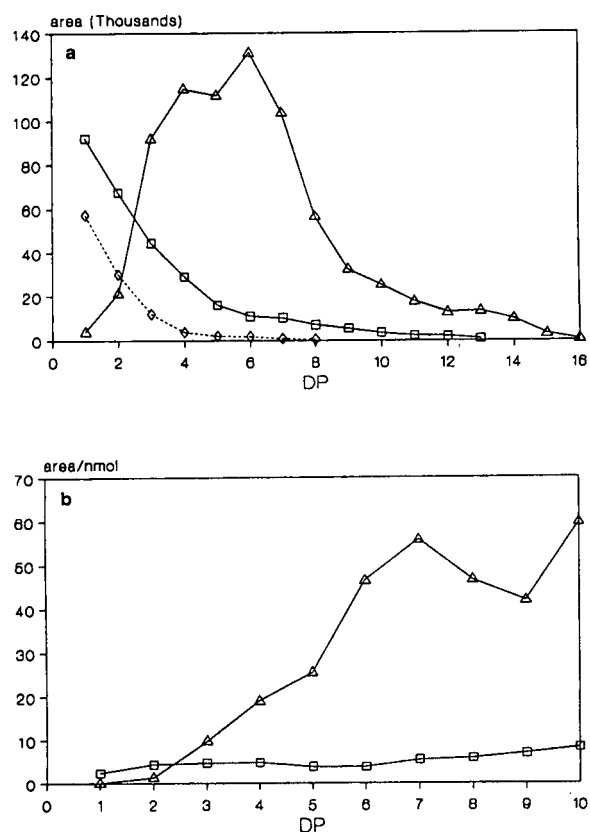


Fig. 1. Comparison of peak areas obtained by (\diamond) reversed-phase LC–MS, (\square) positive-ion HPAEC–MS and (Δ) negative-ion HPAEC–MS as a function of the degree of polymerization (*DP*) for α -1,4-glucose oligomers. (a) Absolute peak areas corrected for the difference in injected amount; (b) peak area per nmole of oligomers actually present in the injected amount. HPAEC–MS with a PA100 column. Peak areas in arbitrary units.

with 10^{-4} mol/l aqueous sodium acetate as the mobile phase.

Comparison of PA1 and PA100 columns

The high sodium acetate concentrations needed in HPAEC, especially in the analysis of larger sugar oligomers, present difficulties in the coupling to thermospray mass spectrometry. Therefore, the introduction of the CarboPac PA100 column material is expected to be advantageous for HPAEC–MS. The most important practical difference between the older CarboPac PA1 and the new CarboPac PA100 packing materials is that the latter allows the elution of oligosaccharides at lower sodium acetate concentrations. This can be explained by the smaller particle diameter, *i.e.*, $8.5\ \mu\text{m}$ for PA100 compared with $10\ \mu\text{m}$ for PA1, which enhances the ion exchange, and the lower capacity, *i.e.*, 90 $\mu\text{equiv.}$ for the PA100 compared with 100 $\mu\text{equiv.}$ for the PA1 column. In Fig. 2, the sodium acetate concentration required for the elution of a series of α -1,4-glucose oligomers is plotted as a function of *DP*. Significant lower sodium concentrations are required to elute most of the oligomers. As the sodium acetate concentration is a limiting factor in HPAEC–MS, sugar oligomers with higher *DP* values can be analysed. Whereas α -1,4-glucose oligomers up to *DP* = 6 could be detected with the PA1 column [17], oligomers up to *DP* = 12 were detected in

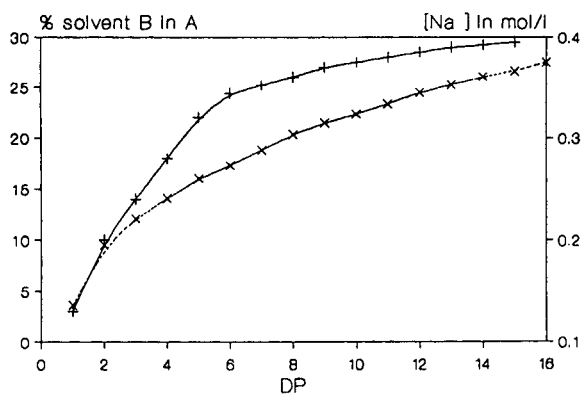


Fig. 2. Percentage of solvent B and corresponding sodium concentration in the mobile phase required for the elution of α -1,4-glucose oligomers as a function of the degree of polymerization (*DP*) for (+) CarboPac PA1 and (x) CarboPac PA100 columns.

experiments with the PA100 column (see also Fig. 1). With this particular sample, the detection of higher *DP* values is limited by the low concentration of these oligomers in the sample analysed [less than 1% (w/w) for *DP* > 10] and by the decrease in the signal at higher *DP* values. The response for α -1,4-glucose oligomers, expressed in peak area per nmole, is plotted as a function of the *DP* value in Fig. 1b. In practice, less than 0.2 nmol of *DP* = 10 is injected.

Improved resolution in HPAEC–MS by multiple-ion detection

In a previous report [16], it was claimed that the poor chromatographic peak shapes often observed at low sample concentrations in HPAEC–MS when operated in the full-scan mode would be significantly improved by the use of MID. In Fig. 3a, mass chromatograms from the HPAEC–MS analysis of an arabinogalactan digest are shown for Gal₂Ara obtained with both full-scan (upper trace) and MID acquisition (lower trace). Whereas from the full-scan mass chromatogram no conclusions can be drawn on the number of Gal₂Ara isomers present, three isomers are readily observed in the MID chromatogram.

With the same sample, it was observed that the separation in some instances is influenced by the amount of compound injected. In Fig. 3b, mass chromatograms are shown for Gal₂. A broad peak is observed in the upper trace, leading to the assumption that two components are present. When the sample is diluted tenfold and re-injected, these two components are well separated and apparently present in a *ca.* 1:15 ratio. With full-scan acquisition, the existence of two oligomers was not observed. The apparent column overloading with respect to the galactose dimers is used to permit the detection of minor components with higher *DP* values in the mixtures.

The presence of these galactose dimers is determined by the structure of the arabinogalactan and reveals the complex nature of this type of polysaccharide. Although one of the galactose dimers found originates from the linear β -1,4-linked galactan backbone, the second galactose

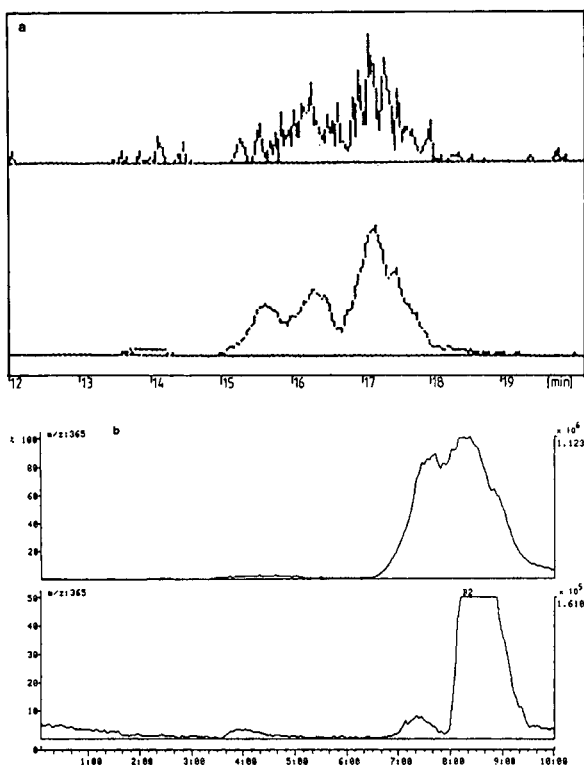


Fig. 3. Selected mass chromatograms from the HPAEC-MS analysis of arabinogalactan digests. (a) Comparison of full-scan (upper trace) and MID (lower trace) acquisition for Gal₂Ara. Estimated amount injected: ca. 100–200 ng per component. (b) Comparison of two sample concentrations, differing by a factor of 10, for Gal₂. CarboPac PA100 column. Estimated amount injected: ca. 150 ng for the major component.

dimer (present in minor amounts) suggests the presence of single-unit side-chains of galactose. This observation is confirmed by methylation analysis. Further results with the HPAEC-MS analysis of arabinogalactan digests are discussed in detail elsewhere [18].

As the application of MID leads to improvements in both signal-to-noise ratio and peak shape, our strategy in handling unknown samples has been changed. Initially, unknowns were only analysed with full-scan acquisition. Now, each sample is analysed twice. First, the sample is analysed with full-scan acquisition to detect major peaks and obtain a general view on the sample composition. Next, it is analysed using various appropriate segments of MID. The instrument control language (ICL) of our instru-

ment allows an automatic time-based or event-based switching between the various MID segments. In composing the MID segments, additional m/z values are taken into account for sugar oligomers differing by one or two units from the oligosaccharides already detected with full-scan acquisition. This strategy led to the acquisition of various pieces of new information, e.g., in the analysis of arabinogalactan oligomers [18]. Switching between the various MID segments must be done with care, considering the unpredictable elution order often observed in HPAEC-MS. The retention times of some peaks observed in a glucuronoarabinoxylan digest may serve as an example. The oligosaccharides in this sample consist of a linear β -1,4-xylose oligomer, branched with α -1,2- and α -1,3-arabinose units and a glucuronic or 4-O-methylglucuronic acid unit. Components with identical sugar composition but differing in the position of the arabinose units on the xylose backbone are found to give widely differing retention times; for instance, two GlcA-Pentose₅ isomers are detected at 21:23 and 27:16 min, whereas the latter peak almost co-elutes with a GlcA-Pentose₆ isomer eluting at 27:29 min. Sometimes a large time window is required in the MID segments. This example also indicates a current limitation of the HPAEC-MS approach: no structural information has yet been obtained. Therefore, the identity of the arabinoxylan isomers cannot be determined as arabinose and xylose are isomers. Obviously, on-line coupling of HPAEC and tandem mass spectrometry, permitting the determination of the sequence of monomeric units in the oligosaccharide, would be of great help, but at present little structural information has been obtained in attempts to fragment the sodiated sugar oligomers by collision-induced dissociation.

Negative-ion detection

In previous experiments only positive-ion detection was performed [16,17]. In order to investigate whether better signal-to-noise ratios can be obtained, some experiments were performed in the negative-ion mode. In principle, one would expect that optimization of the experimental conditions, especially the solvent

composition, would be required but these experiments were not performed. The solvent composition used in the negative-ion mode was identical with that used in the positive-ion mode. Possible improvement by optimization of the conditions is currently under investigation. Obviously, the present conditions ideally match the operation of HPAEC-MS.

The negative-ion mode was tested for α -1,4-glucose and arabinogalactose oligomers. The mass spectra obtained under these conditions are surprisingly complex. Typical negative-ion mass spectra for Glc_4 and Glc_8 are shown in Fig. 4.

For small α -1,4-glucose oligomers, *i.e.*, up to $DP = 4$, primarily three ions are detected in the negative-ion mode, *i.e.*, $[\text{M} - \text{H}]^-$ at $m/z = M_r - 1$, $[\text{M} + \text{OAc}]^-$ at $m/z = M_r + 59$ and $[\text{M} +$

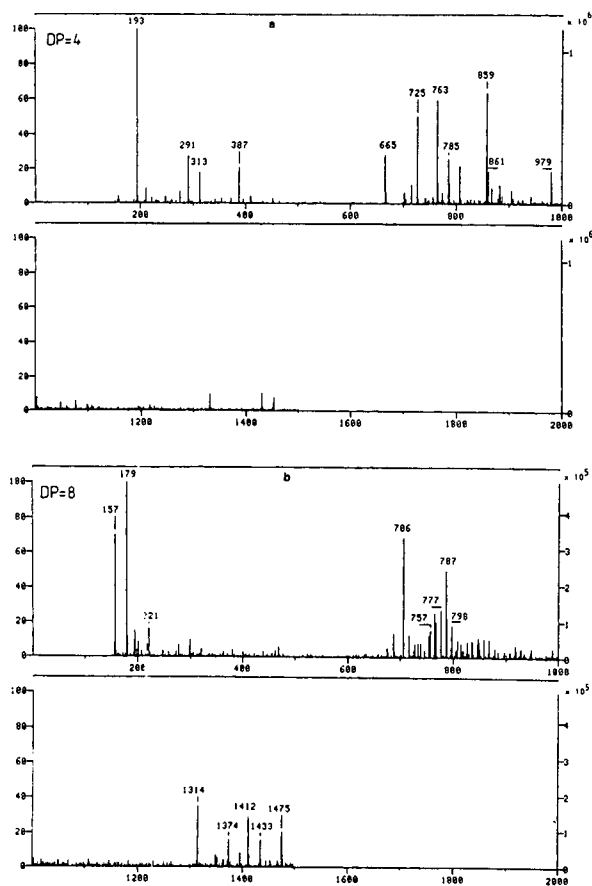


Fig. 4. Negative-ion thermospray mass spectra of α -1,4-glucose oligomers with (a) $DP = 4$ and (b) $DP = 8$ obtained by HPAEC-MS (*cf.*, Table I). For conditions, see text.

$\text{HSO}_4]^-$ at $m/z = M_r + 97$. The peak areas in the mass chromatograms for these ions as a function of DP are plotted in Fig. 5a. At $DP < 4$ the acetate or hydrogensulphate adducts are most abundant, whereas for DP between 5 and 7 the deprotonated molecule is most abundant, and at even higher DP values the doubly charged ions (see below) are most abundant. Further, some peaks due to dimers are detected, *e.g.*, $[\text{2M} - \text{H}]^-$ at m/z 359, 683, 1007 and 1331 and $[\text{2M} + \text{HOAc} + \text{OAc}]^-$ at m/z 479, 803, 1127 and 1451 for $DP = 1-4$, respectively. The relative abundance of these ions is generally below 25%. Frequently, additional adduct peaks are detected at $m/z + 120$, which are probably due to the

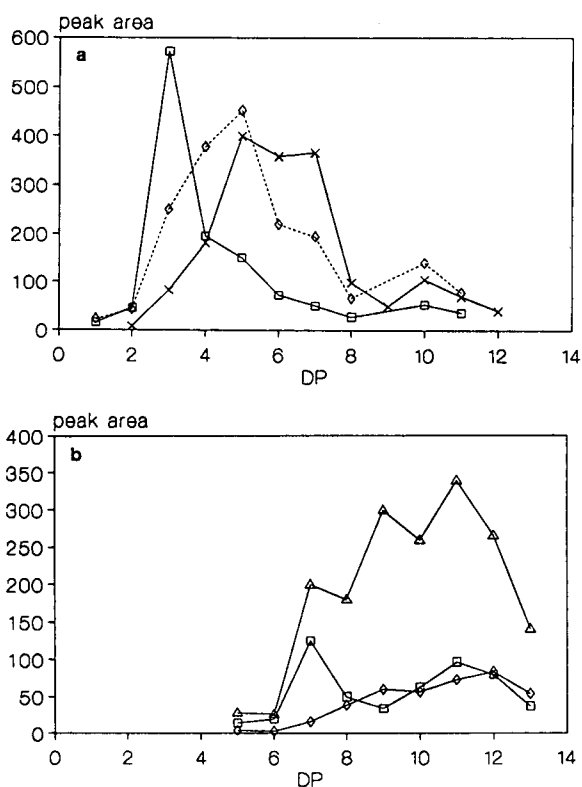


Fig. 5. Peak areas with negative-ion detection as a function of DP . (a) Peak areas for the singly charged ions, (\times) $[\text{M} - \text{H}]^-$ at $m/z = M_r - 1$, (\square) $[\text{M} + \text{OAc}]^-$ at $m/z = M_r + 59$ and (\diamond) $[\text{M} + \text{HSO}_4]^-$ at $m/z = M_r + 97$. (b) Peak areas for the doubly charged ions, (Δ) $[\text{M} + \text{SO}_4]^{2-}$ at $m/z = (M_r + 96)/2$, (\square) $[\text{M} - \text{H} + \text{OAc}]^{2-}$ or $[\text{M} + 2\text{OAc}]^{2-}$ at $m/z = (M_r + 58)/2$ and $(M_r + 118)/2$, respectively, and (\diamond) $[\text{M} + 2\text{HSO}_4]^{2-}$ or $[\text{M} - 2\text{H}]^{2-}$ at $m/z = (M_r + 194)/2$ and $(M_r - 2)/2$, respectively. Peak areas in arbitrary units. For further explanation, see text.

addition of two acetic acid molecules. The latter is also observed in the positive-ion mode.

For larger sugar oligomers, typically $DP > 5$, various doubly charged peaks are detected. The most abundant doubly charged peak is due to $[M + SO_4]^{2-}$, and doubly deprotonated ions and acetate and hydrogensulphate adducts are also observed. A summary of the various peaks detected and typical m/z values for α -1,4-glucose oligomers with $DP = 4$ and 8 is given in Table I. The peak areas in the mass chromatograms for these doubly charged ions as a function of DP are plotted in Fig. 5b and the peak areas for the singly charged ions in Fig. 5a. For clarity, the peak areas for only three types of ions are plotted in Fig. 5b. The peak areas of $[M - 2H]^{2-}$ and $[M + 2OAc]^{2-}$ are almost identical with those of $[M + 2HSO_4]^{2-}$ and $[M - H + OAc]^{2-}$, respectively. As in these experiments the mass spectrometer was scanning up to m/z 2000, the singly charged ions are only detected up to $DP = 12$. The relative abundance of the singly charged ions of the oligomers with high DP values may be underestimated as a result of the discrimination effects common to a quadrupole mass analyser.

Apparently, some fragmentation is also observed, especially to monomeric units, resulting in a peak at m/z 179 in the mass spectra for some of the DP values. In other mass spectra, other peaks are detected that are not readily explained, e.g., m/z 193 in the spectrum for $DP = 4$ (see Fig. 4a). The presence of glucuronic acid in this commercial sample is not expected. In general, little attention was paid to these not very reproducible peaks.

In general, the formation of (many) adduct ions is unfavourable to the sensitivity, because the ion intensity is spread over a number of peaks instead of being concentrated in only one peak. For quantification but also for molecular mass determination, as provided in this study, a single peak in the mass spectrum is preferred. However, in the present instance the observation of adduct ions is hardly a problem in that respect. The summed peak areas for $[M - H]^-$, $[M + OAc]^-$, $[M + HSO_4]^-$ and $[M + SO_4]^{2-}$ are plotted as a function of the DP value and compared with peak areas observed with positive-ion detection (see Fig. 1). It appears that a much better response is achieved in the negative- than in the positive-ion mode for most

TABLE I

TYPICAL IONS DETECTED FOR α -1,4-GLUCOSE OLIGOMERS IN THE NEGATIVE-ION MODE WITH HPAEC-MS USING A THERMOSPRAY INTERFACE

Charge	Ion identity	m/z value relative to M_r	m/z value for Glc ₄	m/z value for Glc ₈
-1	$[M - H]^-$	$M_r - 1$	665	1313
-1	$[M + OAc]^-$	$M_r + 59$	725	1373
-1	$[M + HSO_4]^-$	$M_r + 97$	763	1411
-1	$[M + NaSO_4]^-$	$M_r + 119$	785	1433
-1	$[M + HOAc + OAc]^-$	$M_r + 119$	785	1433
-1	$[2M - H]^-$	$2M_r - 1$	1331	n.d. ^a
-1	$[2M + HSO_4]^-$	$2M_r + 97$	1429	n.d.
-1	$[2M + HOAc + OAc]^-$	$2M_r + 119$	1451	n.d.
-1	$[2M + NaSO_4]^-$	$2M_r + 119$	1451	n.d.
-2	$[M - 2H]^{2-}$	$(M_r - 2)/2$	n.d.	656
-2	$[M - H + OAc]^{2-}$	$(M_r + 58)/2$	n.d.	686
-2	$[M + SO_4]^{2-}$	$(M_r + 96)/2$	n.d.	705
-2	$[M + 2OAc]^{2-}$	$(M_r + 118)/2$	n.d.	716
-2	$[M + 2HSO_4]^{2-}$	$(M_r + 194)/2$	n.d.	754

^a Not detected.

DP values, especially the higher values. This would also be the case when the peak areas for only one specific *m/z* value, e.g. only for the $[M + SO_4]^{2-}$ ion, per *DP* value was used in the comparison (data not shown). In order to appreciate fully the comparison in Fig. 1, it must be pointed out that the peak areas in the negative-ion mode were obtained from data acquisition in the scanning mode (scan range 150–2000), whereas in the positive-ion mode multiple-ion detection on singly and doubly charged sodiated molecules was performed. In general, multiple-ion detection results in at least a tenfold better response than that obtained in the scanning mode. Hence the negative-ion mode appears to be preferred over the positive-ion mode for the characterization of oligosaccharides. Further study, especially directed at the optimization of the experimental conditions and application to a wider variety of samples, e.g., acidic oligosaccharides, is required. Negative-ion detection may be especially helpful in more advanced studies directed at structure elucidation, i.e., determination of sugar type, linkage type and position, as from the literature it appears that the deprotonated molecules are more readily fragmented by collision activation in a triple quadrupole instrument than the sodiated molecules observed in the positive-ion mode. Further research along these lines is in progress.

An interesting topic is the origin of the various ions detected. The observation of deprotonated ions and acetate adduct ions is not very surprising. As a result of the removal of sodium ions by the AMMS, the solvent entering the mass spectrometer is acetic acid with concentrations following the sodium acetate gradient. Sodium acetate is converted into acetic acid in the AMMS. The observation of hydrogensulphate and sulphate adduct ions indicates leakage through the membrane of the sulphuric acid that is used for regeneration of the AMMS. As the membrane system was functioning properly and was not ruptured, which may be concluded from the fact that the introduction of sodium acetate in the range 0.1–0.3 mol/l within a few minutes results in complete contamination of the thermospray ion source and complete loss of signal, it must be concluded that some sulphuric acid is

diffusing through the membrane. This was already known from previous studies, as protonated sulphuric acid and water adducts thereof have previously been detected at too high sulphuric acid concentrations of the regenerant solvent [16]. Obviously, limited diffusion of sulphuric acid through the membrane significantly influences the ionization conditions in the thermospray source. To our knowledge, the addition of sulphuric acid to the solvent for thermospray has not been reported previously. It might also prove useful in the negative-ion detection of other compounds.

CONCLUSIONS

Significant progress in the method development for oligosaccharide characterization by HPAEC–MS has been made. Higher oligomers can be detected as a result of the lower sodium acetate concentration needed for oligosaccharide elution on the new CarboPac PA100 column. The use of multiple-ion detection in addition to the scanning mode results in improved chromatographic peak shapes in MS detection. As a result, more information on the samples analysed is obtained. The use of negative-ion detection in HPAEC–MS with a thermospray interface looks promising, especially because of the improved response for oligosaccharides with larger *DP* values.

ACKNOWLEDGEMENTS

Marian Verbruggen (Wageningen Agricultural University) is thanked for the glucuronoarabinoxylan sample. Dionex (Breda) are thanked for the loan of the HPAEC apparatus used in this work.

REFERENCES

- 1 J.A. McCloskey and P.F. Crain, *Int. J. Mass Spectrom. Ion Processes*, 118/119 (1992) 593.
- 2 J.B. Fenn, M. Mann, C.K. Meng, S.F. Wong and C.M. Whitehouse, *Science*, 246 (1989) 64.
- 3 R.D. Smith, J.A. Loo, C.G. Edmonds, C.J. Barinaga and H.R. Udseth, *Anal. Chem.*, 62 (1990) 882.
- 4 M. Mann, *Org. Mass Spectrom.*, 25 (1990) 575.

- 5 R.D. Smith, J.A. Loo, R.R. Ogorzalek Loo, M. Busman and H.R. Udseth, *Mass Spectrom. Rev.*, 10 (1991) 359.
- 6 E. Rajakylä, *J. Chromatogr.*, 353 (1986) 1.
- 7 P.J. Arpino, *Mass Spectrom. Rev.*, 9 (1990) 631.
- 8 W.M.A. Niessen, R.A.M. van der Hoeven and J. van der Greef, *Org. Mass Spectrom.*, 27 (1992) 341.
- 9 W.M.A. Niessen, R.A.M. van der Hoeven, J. van der Greef, H.A. Schols and A.G.J. Voragen, *Rapid Commun. Mass Spectrom.*, 6 (1992) 197.
- 10 S. Santikarn, G.R. Her and V.N. Reinhold, *J. Carbohydr. Chem.*, 6 (1987) 141.
- 11 R.C. Simpson, C.C. Fenselau, M.R. Hardy, R.R. Townsend, Y.C. Lee and R.J. Cotter, *Anal. Chem.*, 62 (1990) 248.
- 12 Y.C. Lee, *Anal. Biochem.*, 189 (1990) 151.
- 13 A.P. Bruins, T.R. Covey and J.D. Henion, *Anal. Chem.*, 59 (1987) 2642.
- 14 J.J. Conboy, J.D. Henion, M.W. Martin and J.A. Zweigenbaum, *Anal. Chem.*, 62 (1990) 800.
- 15 J.J. Conboy and J.D. Henion, *Biol. Mass Spectrom.*, 21 (1992) 397.
- 16 W.M.A. Niessen, R.A.M. van der Hoeven, J. van der Greef, H.A. Schols, G. Lucas-Lokhorst, A.G.J. Voragen and C. Bruggink, *Rapid Commun. Mass Spectrom.*, 6 (1992) 474.
- 17 R.A.M. van der Hoeven, W.M.A. Niessen, J. van der Greef, H.A. Schols, A.G.J. Voragen and C. Bruggink, *J. Chromatogr.*, 627 (1992) 63.
- 18 W.M.A. Niessen, H.A. Schols, R.A.M. van der Hoeven, A.G.J. Voragen and J. van der Greef, in preparation.

Fast screening method for eight phenoxyacid herbicides and bentazone in water

Optimization procedures for flow-injection analysis–thermospray tandem mass spectrometry

René B. Geerdink* and Paul G.M. Kienhuis

RIZA, P.O. Box 17, 8200 AA Leylstad (Netherlands)

Udo A.Th. Brinkman

Department of Analytical Chemistry, Free University, De Boelelaan 1083, 1081 HV Amsterdam (Netherlands)

ABSTRACT

The development of a screening method for the rapid screening of water samples for phenoxyacid herbicides and bentazone with flow-injection analysis–thermospray tandem mass spectrometry is described. A two-step optimization procedure was used to determine the optimum instrumental parameters. First, introducing the analytes of interest continuously, the vaporizer temperature, discharge voltage and repeller voltage were changed stepwise over a wide range under computer control. With different solvent mixtures and source block temperatures, the carrier stream with which the highest molecular (parent) ion intensities were obtained in the single scan Q3-MS scan mode was selected. This turned out to be 0.1 M aqueous ammonium acetate–acetonitrile (90:10, v/v). For phenoxyacid herbicides and bentazone negative ionization with buffer-assisted ion evaporation (ammonium acetate) gave the most intense parent ions. The discharge voltage had little influence on the signal intensities and a low repeller voltage turned out to be the best for all analytes. Next, the optimum collision gas pressure and collision offset voltage were determined. The most intense daughter ions were derived with a collision gas pressure (argon) of 3–4 mTorr (1 Torr = 133.322 Pa) and a collision offset voltage of 18 eV for phenoxyacid herbicides and 22 eV for bentazone. In order to obtain maximum sensitivity, a multiple reaction monitoring method was used in which two parent ion–daughter ion pairs were monitored for each phenoxyacid herbicide and one parent ion and three daughter ions for bentazone. Without sample concentration all eight phenoxyacid herbicides and bentazone can be determined at the low $\mu\text{g/l}$ level. The method is fully automated; with a 5-ml loop injection and the subsequent cleaning runs the analysis time is 10 min. The detection limit is *ca.* 1 $\mu\text{g/l}$ with linear calibration graphs up to 50 $\mu\text{g/l}$. The method was used to confirm the presence of bentazone and the absence of the phenoxyacid herbicides in a surface water sample.

INTRODUCTION

Phenoxyacid herbicides and bentazone are widely used in agriculture. They are toxic and environmentally persistent for several months.

These compounds are readily soluble in water and their runoff from cropland into rivers and lakes is considerable. Allowable concentration levels in Dutch inland waters depend on the type of compound and are between 0.1 and 11 $\mu\text{g/l}$ for phenoxyacid herbicides [1]. As surface water is used for the production of drinking water there is a need for continuous monitoring. The

* Corresponding author.

European Community (EC) has set the maximum allowable concentration for individual pesticides at 0.1 $\mu\text{g/l}$ for drinking water [2]. In our institute (RIZA), the chlorophenoxy carboxylic acid herbicides 4-chloro-2-methylphenoxyacetic acid (MCPA), (2,4-dichlorophenoxy)acetic acid (2,4-D), 2-(4-chloro-2-methylphenoxy)propionic acid (MCPP), 2-(2,4-dichlorophenoxy)propionic acid (2,4-DP), (2,4,5-trichlorophenoxy)acetic acid (2,4,5-T), 4-(2,4-dichlorophenoxy)butyric acid (2,4-DB), 4-(4-chloro-2-methylphenoxy)butyric acid (MCPB) and (2,4,5-trichlorophenoxy)propionic acid (2,4,5-TP) and bentazone are determined in surface and waste waters with a previously described fully automated liquid chromatographic (LC) method with UV detection [3,4].

With mass spectrometric (MS) detection, phenoxyacid herbicides can be determined with direct liquid introduction [5], particle beam [6,7] or with a thermospray interface in the negative-ion mode using filament-off, filament-on or discharge ionization modes [8–13]. In an attempt to provide additional structural information, chloroacetonitrile is added to the eluent [8,12,14].

The use of tandem mass spectrometry (MS–MS) permits rapid analyses for specific compounds [15]. The sensitivity levels obtained are generally *ca.* 100 pg [16] without the need for the chromatographic separation [17–19]. Although environmentally important compounds have been studied [13,16–24], few data on the (LC)–MS–MS of pesticides or polar hydrophilic compounds in aqueous samples have been published.

To achieve the lowest possible detection limits for a targeted compound with (LC)–MS–MS, single reaction monitoring (SRM) should be performed [25]. If a larger number of compounds need to be determined, the MS–MS conditions must be of “general” adjustment or they must be continuously changed to obtain optimum results for each compound.

In this study, it was our aim to develop a rapid screening method, preferably at the 0.1 $\mu\text{g/l}$ level, for phenoxyacid herbicides and bentazone in aqueous samples. Optimization procedures for flow-injection analysis–thermospray tandem mass spectrometry (FIA–TSP–MS–MS) were written for a Finnigan TSQ-70 instrument includ-

ing a TSP-2 interface. Most of the parameters were adjusted by the software and, except for the collision gas and the source block temperature, parameters such as the collision offset voltage, repeller voltage, discharge voltage and vaporizer temperature could be instantaneously (μs –s) changed by the data system.

EXPERIMENTAL

Reagents

Water was obtained from a Milli-Q system (Millipore, Bedford, MA, USA). HPLC-grade acetonitrile, formic acid, trifluoroacetic acid (used as tuning solvent) and ammonium acetate were obtained from J.T. Baker (Deventer, Netherlands). Ammonium formate was obtained from Sigma (St. Louis, MO, USA). All chlorophenoxy carboxylic acids were obtained from Riedel-de Haën (Hannover, Germany) and bentazone from Promochem (Wesel, Germany).

Apparatus

An LKB (Bromma, Sweden) Model 2150 pump was used to deliver the FIA carrier stream at a flow-rate of 1.5 ml/min.

For Procedures I and II (see below) the analytes were dissolved in the appropriate solvent mixture at concentrations of 500 or 50 $\mu\text{g/l}$ and continuously introduced into the MS–MS system.

An ASPEC (Gilson, Villiers-le-Bel, France) was used to inject samples with a 3- or 5-ml loop into the carrier stream. After each injection, an injection with pure water and an injection with acetonitrile were made to ensure complete cleaning of the total system including the thermospray interface. Also, the optimum repeller voltage in the single MS scan mode (Q3-MS) with regard to the intensity and mass assignment of the parent ions was checked daily by injecting a 50 $\mu\text{g/l}$ standard solution in 0.1 *M* aqueous ammonium acetate–acetonitrile (90:10, v/v).

A Finnigan TSQ-70 mass spectrometer (Finnigan Mat, San Jose, CA, USA) equipped with a Finnigan thermospray interface (TSP-2) was used. The conversion dynode was set at 15 kV, the electron multiplier at 1.5–2.0 kV and the electrometer amplifier gain at 10^{-8} . Argon was

used as the collision gas. All optimization procedures were written in Finnigan's instrument control language.

Sample handling

Stock solutions of the phenoxyacid herbicides and bentazone were prepared by dissolving *ca.* 25 mg of each compound in 50 ml of acetonitrile. From these solutions a mixed standard solution was prepared and diluted with Milli-Q-purified water, 0.1 M ammonium acetate, 0.1 M ammonium formate or 0.1 M formic acid (in Milli-Q-purified water) to obtain a series of solutions that contained 10 vol.% of acetonitrile and 500, 50, 5, 1, 0.5, 0.25, 0.125 or 0.1 $\mu\text{g/l}$ of each analyte.

Optimization procedures

Two stepwise optimization procedures were used to determine the optimum instrumental parameters. First (Procedure I, Fig. 1), introducing the analytes of interest continuously, the vaporizer temperature, discharge and repeller voltage were changed stepwise over a wide range under computer control with different solvent mixtures and source block temperatures in the single-scan Q3-MS scan mode.

From the data obtained, the conditions that gave the highest molecular ion $[M - 1]^-$ intensities were selected and used in Procedure II. For the phenoxyacid herbicides the parent ion masses were m/z 199, 213, 219, 227, 233, 247, 253 and 267 and for bentazone m/z 239.

Second (Procedure II), the optimum collision offset voltage that gave the highest daughter ions was selected at different collision gas pressures for the selected molecular ions in the daughter-ion scan mode. For the monochloro phenoxyacid herbicides the daughter ion mass was m/z , 141, for the dichloro phenoxyacid herbicides m/z 161, for the trichloro phenoxyacid herbicides m/z 195 and for bentazone m/z 132, 133 and 197.

In Procedure I the vaporizer temperature is increased stepwise (5°C per step) from 75 to 130°C . At every adjustment the discharge voltage goes stepwise from 0 to 2000 V at 250 V per step and during every adjustment of the discharge voltage the repeller voltage goes stepwise from 0 to -200 V at 20 V per step. The scantime was 2 s and the scan range m/z 90–350. The complete cycle takes *ca.* 40 min and produces *ca.* 1100 data. Procedure I was carried out for source block temperatures of 100, 150, 200 and 250°C and for all solvent mixtures.

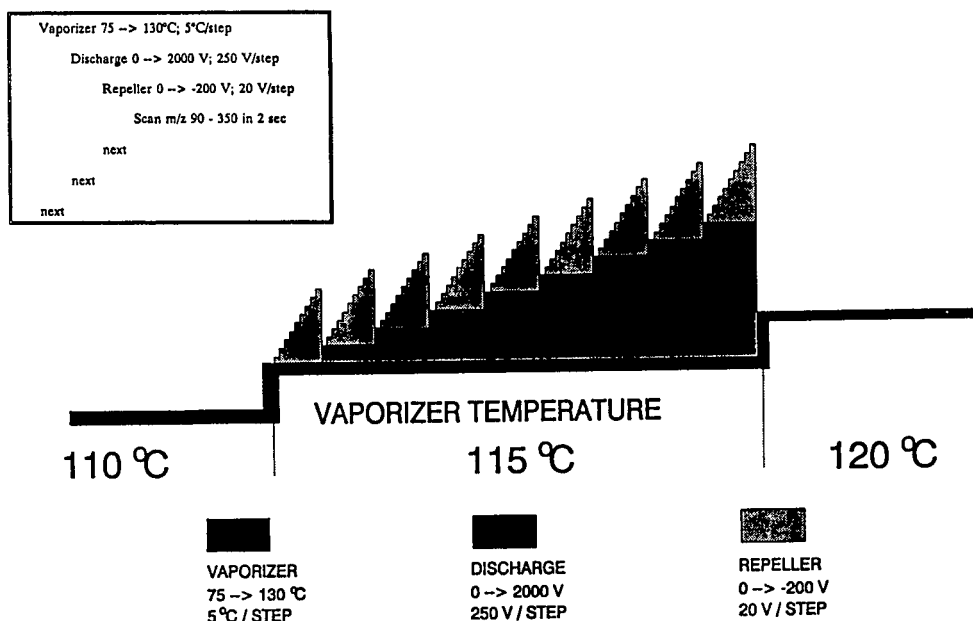


Fig. 1. Illustration of optimization Procedure I; for details, see Experimental.

In Procedure II the collision offset voltage is determined at different collision gas pressures to acquire daughter ion signals of the parent ions selected with Procedure I. In this procedure the collision offset voltage is increased stepwise at 2 eV per step from 0 to 50 eV, using collision gas (argon) pressures of 1, 2, 3, 4 and 5 mTorr (1 Torr = 133.322 Pa). From the data obtained the collision gas pressure, collision offset voltage and daughter ions are selected.

RESULTS AND DISCUSSION

With MS–MS, selected (single or multiple) reaction monitoring (SRM or MRM, respectively) is often used in trace analysis in which a limited number of parent ion–daughter ion pairs are monitored for each analyte to give maximum sensitivity [26]. MS–MS methods can be used to detect and confirm amounts of analytes as low as 100 pg [16,27]. In order to do so, it is desirable that the primary ionization conditions give an abundant high-mass ion preferably indicative of the molecular mass in the first mass analyser. Collisionally activated dissociation (CAD) with neutral gas molecules then produces characteristic fragments that can be identified in the second

mass analyser. The yield of these so-called daughter ions determines the analytical sensitivity and therefore the detection limit of the MS–MS procedure. Unfortunately, optimum conditions for the operating parameters are different for every class of compound and, often, even for every individual analyte within a certain class.

The optimization procedures presented here were written to select optimum conditions in terms of sample solution, source block and vaporizer temperature, discharge and repeller voltage, collision offset voltage and collision gas pressure.

Sample solution, source and vaporizer temperature

The sample solutions used in the experiments were 90:10 (v/v) mixtures of water, 0.1 M formic acid, 0.1 M ammonium acetate or 0.1 M ammonium formate and acetonitrile.

In Table I the results are given that were obtained using Procedure I (see Experimental). The data in each column of Table I were obtained from one spectrum. A source block temperature of 200°C, a sample solution containing 0.1 M ammonium acetate and a vaporizer temperature of 105–110°C gave the most intense

TABLE I

INTENSITIES ($\times 10^6$) OF MOLECULAR IONS OF PHENOXYACID HERBICIDES AND BENTAZONE IN VARIOUS SAMPLE SOLUTIONS AT DIFFERENT SOURCE BLOCK TEMPERATURES USING OPTIMIZATION PROCEDURE I

The sample solutions used in the experiments were 90:10 (v/v) mixtures of water, 0.1 M formic acid, 0.1 M ammonium acetate or 0.1 M ammonium formate and acetonitrile. A source block temperature of 100°C gave unstable vaporizer temperatures and are not reported; a source block temperature of 250°C was not measured for all solvents.

Analyte	m/z^a	Water			Formic acid		Ammonium acetate			Ammonium formate	
		150°C	200°C	250°C	150°C	200°C	150°C	200°C	250°C	150°C	200°C
MCPA	199	3.8	3.3	4.8	11.9	11.5	13.9	14.9	14.9	11.4	11.2
MCPB	213	4.5	6.3	6.1	11.9	9.4	12.8	14.0	13.3	11.6	11.2
2,4-D	219	9.2	1.3	2.7	9.2	6.4	6.9	9.5	9.0	7.1	5.8
MCPB	227	2.0	1.7	1.1	4.3	2.3	10.4	9.4	6.4	3.3	2.9
2,4-DP	233	8.2	2.8	4.7	8.2	8.6	9.6	11.5	7.4	7.0	6.1
Bentazone	239	0.82	0.65	0.58	2.0	1.6	14.6	13.4	12.3	13.1	10.7
2,4-DB	247	0.68	0.57	0.39	7.3	4.0	5.4	5.6	2.7	5.2	3.5
2,4,5-T	253	0.7	0.6	0.7	3.5	3.0	3.6	4.8	2.1	4.8	3.2
2,4,5-TP	267	1.5	1.6	1.6	8.3	5.6	8.7	9.5	5.7	9.5	7.4

^a $m/z = [M - 1]^-$

molecular ions for all compounds. Vaporizer temperatures higher than 115°C gave, with all solutions and at all source block temperatures, increased fragmentation of the molecular ion to low m/z fragments (see Fig. 2; scan 820–1100), while vaporizer temperatures below 100°C (Fig. 2; scan 0–460) gave less intense signals of the molecular ions. During optimization it turned out that a source block temperature of 100°C was too low to give stable vaporizer temperatures. The results obtained with a source block temperature of 250°C were similar to those at 200°C. Therefore, some sets of data obtained at the former temperatures have not been included in Table I.

Using Procedure I, for all four sample solutions and pure water, background signals of solvent adducts were recorded at a source block temperature of 200°C in order to detect whether any interfering peaks would show up. No such interferences with the parent scan masses were observed.

Solvent adducts with the molecular ion were absent with water as sample solvent but with the other solutions signals at $[M + \text{CH}_3\text{COO}]^-$ for ammonium acetate (relative abundance 5%) and $[M + \text{HCOO}]^-$ for formic acid (relative abundance 10–20%) and ammonium formate (rela-

tive abundance <50%) were observed. In the literature [8,10,12], these adducts are sometimes reported as the base peaks.

Discharge and repeller voltage

Fig. 3 shows an expansion of part of the data generated in Procedure I, *viz.*, for vaporizer temperatures of 105, 110 and partly 115°C. Low repeller voltages give intense signals whereas higher repeller voltages give only uniform effects. At 110°C the discharge voltage is much more irregular than at 105°C, while at 115°C the signals are strongly decreased, as explained above. Note the m/z 40 which is the vaporizer temperature and the starting point of a cycle at a new vaporizer temperature (see also legend Fig. 3). From this scan number the repeller voltage value and the discharge voltage value can be easily determined in the cycle, which has nine discharge steps and ten repeller steps.

With ammonium acetate as additive to the sample solution and with the other additives a discharge voltage of 1500–2000 V was found to favour the ionization process. From these results we conclude that a repeller voltage of –20 V and a discharge voltage of 1750 V with ammonium acetate (see also the asterisk in Fig. 3) as sample solution give the best results and should be used

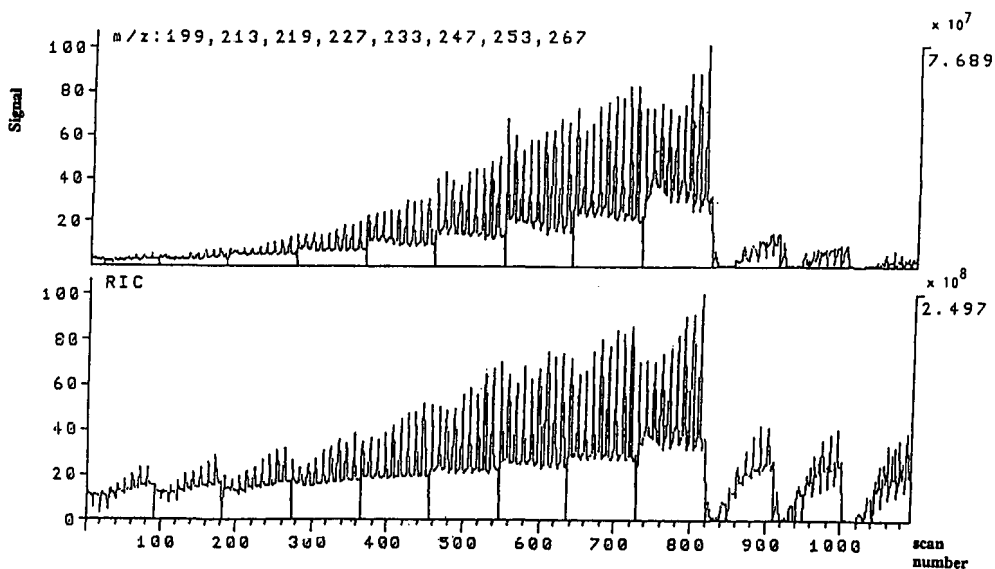


Fig. 2. The RIC and combined mass trace of 0.1 M ammonium acetate–acetonitrile (90:10, v/v) at a source block temperature of 200°C, recorded with Procedure I in the Q3-MS mode; for details, see Experimental.

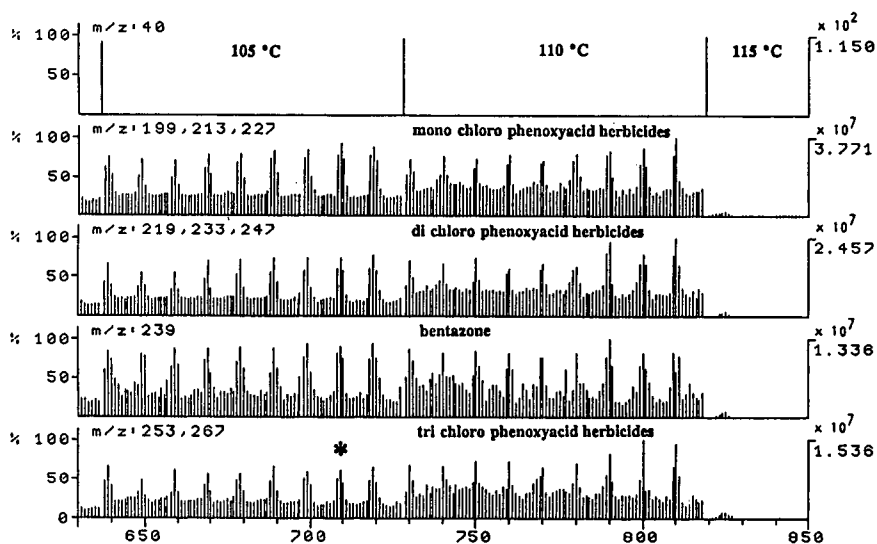


Fig. 3. Expansion of part of the data generated in Procedure I, viz., for vaporizer temperatures of 105, 110 and partly 115°C. The m/z 40 trace represents the vaporizer temperature. After every adjustment of the vaporizer temperature the actual source block temperature, aerosol temperature and vaporizer temperature are read out and put as m/z 20, 30 and 40, respectively, in the data file for convenient interpretation of the RIC and mass traces. The m/z 199, 213, 227 trace represents the combined parent scan masses of MCPA, MCPP and MCPB, respectively. The m/z 219, 233, 247 trace represents the combined parent scan masses of 2,4-D, 2,4-DP and 2,4-DB, respectively. The m/z 253, 267 trace represents the combined parent scan masses of 2,4,5-T and 2,4,5-TP, respectively. The m/z 239 trace represents the parent scan mass of bentazone.

during further optimization according to Procedure II. As an example, a typical result with ammonium acetate is depicted in Fig. 4, selected at a discharge voltage of 1750 V and a repeller voltage of -20 V. As explained under Experimental, the optimum repeller voltage is checked daily.

Collision offset voltage and collision gas pressure

Phenoxyacid herbicides show only slight fragmentation into intense daughter ions. To confirm the identity of the compounds, at least two, and preferably more, ions must be determined, according to mass spectrometric criteria [28]. We therefore decided to select the Cl-35 and Cl-37 isotopes of the molecular ion as the parent scan masses and the Cl-35 and Cl-37 isotopes of the most characteristic fragment as the daughter scan masses. With parent scan mass m/z 239 bentazone gave various fragments from which we chose m/z 132, 133 and 197 as daughter ion masses.

In Table II the intensities of the daughter ions produced during Procedure II and reported. The results show that at a gas pressure of 3–4 mTorr the daughter-ion signals have the highest intensity. Moreover, for the phenoxyacid herbicides, the measured isotope ratio is good in most instances, which is important for compounds having only one intense fragment and recognition must be based on two data points and their ratio.

At an argon pressure of 3 mTorr the collision offset voltage was, again, increased stepwise from 0 to 30 eV at 1 eV per step. For all phenoxyacid herbicides 18 ± 1 eV turned out to be optimum for producing intense daughter ions, whereas for bentazone 22 ± 1 eV was the optimum value.

In order to obtain maximum sensitivity, the combined results of Procedures I and II were used in a multiple reaction monitoring (MRM) method in which two parent ion–daughter ion pairs were monitored for each analyte except for bentazone, for which one parent ion and three

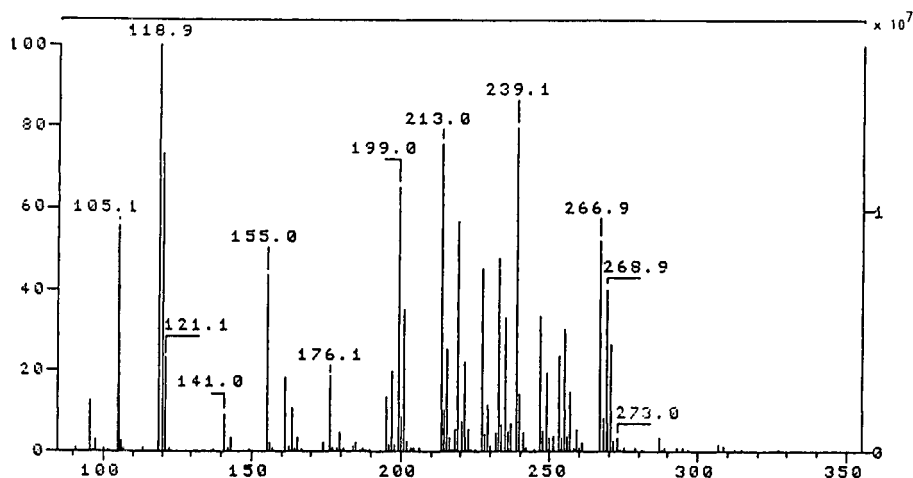


Fig. 4. Spectrum derived from Fig. 3 (see asterisk in Fig. 3) under optimum conditions of Procedure I in the Q3-MS mode. Vaporizer temperature 105°C, discharge voltage 1750 V and repeller voltage -20 V with 0.1 M ammonium acetate-acetonitrile (90:10, v/v) at a source block temperature of 200°C.

TABLE II

INTENSITIES ($\times 10^6$) OF DAUGHTER IONS OF PHENOXYACID HERBICIDES AND BENTAZONE

Sample solution, 0.1 M ammonium acetate-acetonitrile (90:10, v/v); source block temperature, 200°C; Vaporizer temperature, 105°C; discharge voltage, 1750 V; repeller voltage, -20 V; Flow-rate, 1.5 ml/min; concentration, 50 $\mu\text{g/l}$ of each analyte.

Analyte	Parent ion mass	Daughter ion mass	Intensity				
			1 mTorr	2 mTorr	3 mTorr	4 mTorr	5 mTorr
MCPA	199	141	1.1	3.0	3.2	3.2	2.6
	201	143	0.4	0.9	1.0	1.0	0.9
MCPP	213	141	1.4	2.7	3.2	3.5	2.9
	215	143	0.5	0.8	1.2	1.2	0.9
2,4-D	219	161	0.6	1.3	1.3	1.4	1.4
	221	163	0.4	0.8	1.1	1.1	0.9
MCPB	227	141	0.9	1.4	1.4	1.7	1.2
	229	143	0.3	0.7	0.5	0.6	0.4
2,4-DP	233	161	0.9	1.4	1.5	1.4	1.3
	235	163	0.5	0.9	1.0	1.0	0.8
2,4-DB	247	161	0.4	0.5	0.5	0.5	0.4
	249	163	0.3	0.3	0.3	0.3	0.2
2,4,5-T	253	195	0.3	0.4	0.5	0.5	0.4
	255	197	0.2	0.4	0.5	0.4	0.4
2,4,5-TP	267	195	0.5	0.8	1.1	1.1	0.9
	269	197	0.5	0.8	0.9	0.9	0.8
Bentazone	239	132	0.2	0.8	1.1	1.5	1.2
		133	0.07	0.3	0.4	0.6	0.4
		197	0.08	0.5	0.5	0.7	0.6

TABLE III

SCHEMATIC REPRESENTATION OF MRM PROCEDURE FOR PHENOXYACID HERBICIDES AND BENTAZONE IN MS–MS MODE

collision offset voltage = 18	
psm 199; go 141; psm 201; go 143; stop	#MCPA
psm 213; go 141; psm 215; go 143; stop	#MCPD
psm 219; go 161; psm 221; go 163; stop	#2,4-D
psm 227; go 141; psm 229; go 143; stop	#MCPB
psm 233; go 161; psm 235; go 163; stop	#2,4-DP
psm 247; go 161; psm 249; go 163; stop	#2,4-DB
psm 253; go 195; psm 255; go 197; stop	#2,4,5-T
psm 267; go 195; psm 269; go 197; stop	#2,4,5-TP
collision offset voltage = 22	
psm 239; go 132; go 133; go 197; stop	#Bentazone

daughter ions were selected. This final procedure takes *ca.* 20 s for a complete cycle with a scan time of 1 s for a daughter ion of a selected parent scan mass. This run program is briefly explained in Table III.

Application

First, calibration graphs were constructed using standard solutions in a 0.1 M ammonium acetate–acetonitrile (90:10, (v/v) containing 0.125–50 µg/l of each analyte. The results in Table IV show that, without trace enrichment, all phenoxyacid herbicides and bentazone can be determined down to *ca.* 1 µg/l in aqueous standard solutions. The calibration graphs show good linearity over the two orders of magnitude studied. For real drinking and surface water samples, the analytical results will no doubt be less good and trace enrichment of the analytes will have to be performed in order to meet the

TABLE IV

CALIBRATION GRAPH RESULTS OF PHENOXYACID HERBICIDES AND BENTAZONE IN MILLI-Q-PURIFIED WATER

Analyte	Daughter ion mass	r^2	$y = bx + c^a$	Detection limit (3σ) (µg/l)
Bentazone	132.0	0.99994	$y = 4.145x - 0.371$	0.5
	133.0	0.99982	$y = 2.191x - 0.670$	1.0
	197.0	0.99961	$y = 3.542x - 1.334$	1.4
MCPA	141.0	0.99977	$y = 6.367x + 2.026$	1.0
	143.0	0.99996	$y = 2.398x + 0.099$	0.5
MCPD	141.0	0.99850	$y = 7.621x + 3.956$	2.6
	143.0	0.99992	$y = 2.790x - 0.588$	0.7
MCPB	141.0	0.99991	$y = 2.211x + 0.530$	0.7
	143.0	0.99978	$y = 0.784x + 0.009$	1.1
2,4-D	161.0	0.99989	$y = 3.790x + 0.417$	0.7
	163.0	0.99933	$y = 2.611x - 0.792$	1.9
2,4-DP	161.0	0.99991	$y = 5.683x - 0.119$	0.6
	163.0	0.99976	$y = 3.507x - 0.533$	1.2
2,4-DB	161.0	0.99998	$y = 2.303x - 0.179$	0.3
	163.0	0.99988	$y = 1.470x - 0.543$	1.0
2,4,5-T	195.0	0.99981	$y = 2.154x + 0.203$	0.8
	197.0	0.99957	$y = 1.957x + 0.048$	1.4
2,4,5-TP	195.0	0.99999	$y = 6.177x + 0.199$	0.2
	197.0	0.99991	$y = 6.344x - 0.384$	0.6

^a x = concentration in µg/l; y = intensity ($\times 1000$).

EC drinking water regulations, which require a detection limit of $0.1 \mu\text{g/l}$ for individual pesticides. This can be achieved by an off-line solid-phase extraction of at least 100 ml of sample, desorption with 1 ml of acetonitrile and dilution to 10 ml with 0.1 M ammonium acetate. The final sample solution will then have the same composition as the samples in the optimization procedure.

In order to demonstrate the practicability of the present procedure, a surface water sample that contained *ca.* $300 \mu\text{g/l}$ of bentazone and no phenoxyacid herbicides, as determined by means of LC–UV detection according to a previously described method [3,4], was analysed. After

tenfold dilution with Milli-Q-purified water, addition of 10% of acetonitrile and sufficient ammonium acetate to give a 0.1 M concentration, the sample was subjected to FIA–TSP–MS–MS. The reconstructed ion chromatogram (RIC) and *m/z* 197 and 132 mass traces in Fig. 5A (standard) and B (surface water sample) show that, with a single 5-ml loop injection, up to 6–8 analysis cycles (scans 60–140) are generated with signals of at least 70% relative intensity which can be used for determination. It can also be seen that the daughter ion of *m/z* 197 (from 2,4,5-T, 2,4,5-TP and bentazone; see also Table III) is present three times in the standard solution and only once (from bentazone) in the

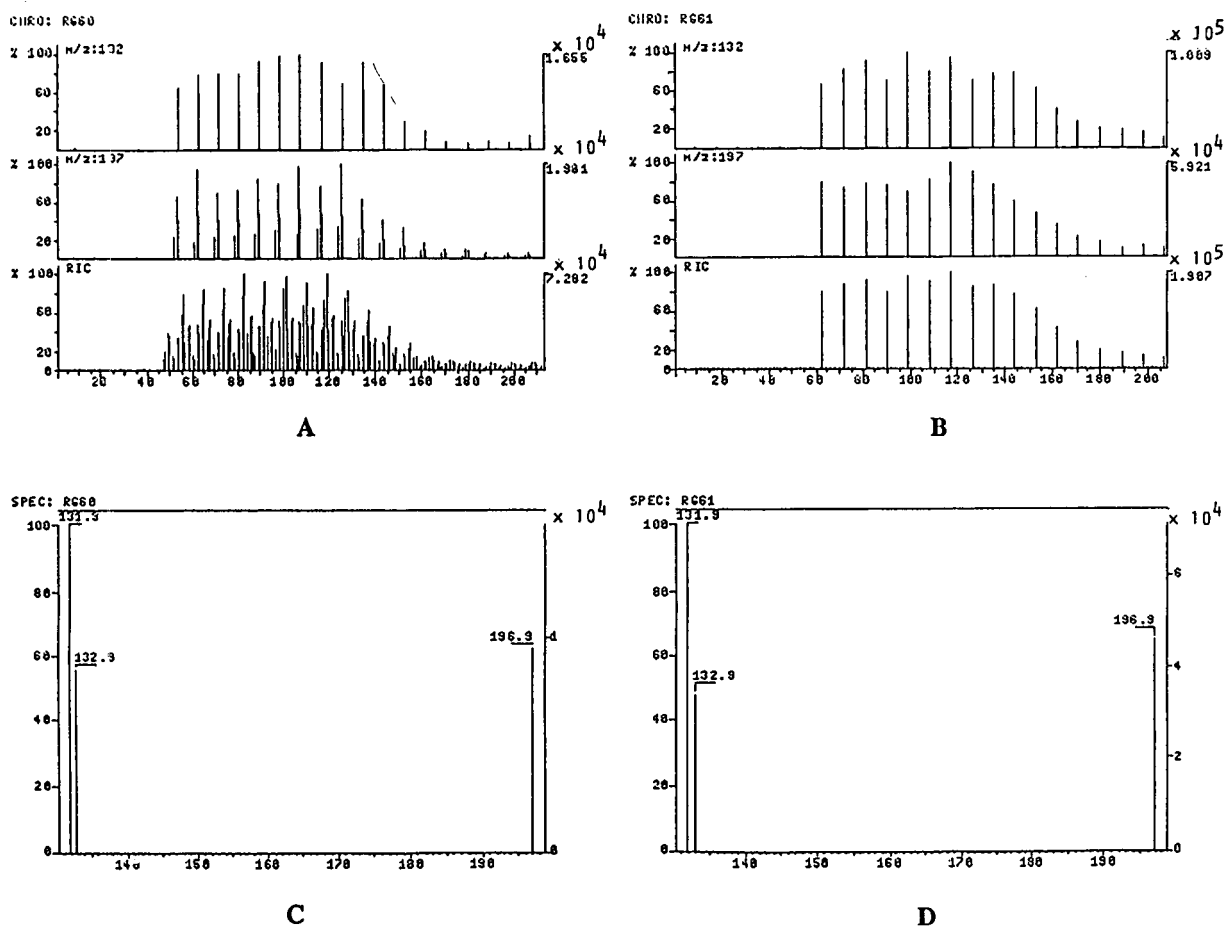


Fig. 5. Chromatogram and spectrum of a 5-ml loop injection of (A and C) a standard sample containing eight phenoxyacid herbicides and bentazone at $5 \mu\text{g/l}$ and (B and D) a surface water sample after tenfold dilution with MRM procedure (see Table III). Conditions as in Fig. 4.

surface water sample. Fig. 5C (standard) and D (surface water sample) show the resulting mass spectra from the standard and the sample. From their signal intensities the bentazone concentration in the sample was calculated to be 275 $\mu\text{g/l}$, which agrees satisfactorily with the value quoted above. In addition, as none of the daughter ion masses of the phenoxyacid herbicides were recorded, it can be concluded that, at the low $\mu\text{g/l}$ level, no such herbicides were present. Again, this is in agreement with the LC–UV data quoted above.

CONCLUSIONS

A rapid screening method based on FIA–TSP–MS–MS was developed to detect the presence of phenoxyacid herbicides and bentazone in aqueous samples. With a scan time of 1 s for the daughter ion mass of a selected parent ion mass, a cycle takes 20 s. With a 5-ml loop injection, the total time of analysis, which includes two cleaning steps, is 10 min. Using a multiple reaction monitoring (MRM) method, which is the result of several optimization procedures, one can determine the pesticides at levels down to 1 $\mu\text{g/l}$ in standard solutions without any trace enrichment. For a number of compounds mentioned in the Third National Policy Document on Water Management [1], such detection limits will be good enough. If divergent types of real water samples have to be analysed and the detection limits have to be as low as 0.1 $\mu\text{g/l}$ for individual pesticides, off-line trace enrichment by means of solid-phase extraction with subsequent dilution with a small volume of acetonitrile and appropriate dilution with water may well provide a solution.

The practicability of the proposed method was demonstrated by re-analysing a surface water sample that had already been subjected to LC–UV analysis. In actual practice, however, FIA–TSP–MS–MS will be used for a first rapid screening, with further analysis of suspected samples only by LC-based methods. This approach will considerably increase the speed of analysis and reduce costs.

With a Finnigan TSQ-70 or another, similar, MS–MS instrument the present technique can be

used for a broad range of compounds, provided that they can all be analysed at approximately the same source block temperature and collision gas pressure. The more important parameters such as vaporizer temperature, repeller voltage and collision offset voltage can, however, be rapidly adjusted by means of the data system.

REFERENCES

- 1 *Water in The Netherlands: a Time for Action. Third National Policy Document on Water Management*, Ministry of Transport and Public Works, The Hague, 1989.
- 2 *EEC Drinking Water Guideline 80/778/EEC, EEC N.L.*, 229 (1980) 11.
- 3 R.B. Geerdink, C.A.A. van Balkom and H.-J. Brouwer, *J. Chromatogr.*, 481 (1989) 275–285.
- 4 B.B. Geerdink, A.M.B.C. Graumans and J. Viveen, *J. Chromatogr.*, 547 (1991) 478–483.
- 5 R.B. Geerdink, F.A. Maris, G.J. de Jong, R.W. Frei and U.A.Th. Brinkman, *J. Chromatogr.*, 394 (1987) 51–64.
- 6 M.A. Brown, R.D. Stephens and I.S. Kim, *Trends Anal. Chem.*, 10 (1991) 330–336.
- 7 I.S. Kim, F.I. Sasinis, R.B. Stephens, J. Wang and M.A. Brown, *Anal. Chem.*, 63 (1991) 819–823.
- 8 D. Barcelo, G. Durand, R.J. Vreeken, G.J. De Jong, H. Lingeman and U.A.Th. Brinkman, *J. Chromatogr.*, 553 (1991) 311–328.
- 9 D. Barcelo, *Org. Mass Spectrom.*, 24 (1989) 219–224.
- 10 D. Barcelo, *Org. Mass Spectrom.*, 24 (1989) 898–902.
- 11 R.D. Voyksner, W.H. McFadden and S.A. Lammert, in J.D. Rosen (Editor), *Applications of New Mass Spectrometry Techniques in Pesticide Chemistry*, Wiley, New York, 1987, Ch. 17.
- 12 D. Barcelo, in M.A. Brown (Editor), *Liquid Chromatography/Mass Spectrometry—Applications in Agricultural, Pharmaceutical and Environmental Chemistry (ACS Symposium Series, No. 420)*, American Chemical Society, Washington, DC, 1990, pp. 48–61.
- 13 T.L. Jones, L.D. Betowski and J. Yinon, in M.A. Brown (Editor), *Liquid Chromatography/Mass Spectrometry—Applications in Agricultural, Pharmaceutical and Environmental Chemistry (ACS Symposium Series, No. 420)*, American Chemical Society, Washington, DC, 1990, pp. 62–74.
- 14 R.J. Vreeken, U.A.Th. Brinkman, G.J. de Jong and D. Barcelo, *Biomed. Environ. Mass Spectrom.*, 19 (1990) 481–492.
- 15 F.W. McLafferty, in J.F.J. Todd (Editor), *Advances in Mass Spectrometry*, Wiley, New York, 1986, p. 493.
- 16 T. Cairns and E.G. Siegmund, in M.A. Brown (Editor), *Liquid Chromatography/Mass Spectrometry—Applications in Agricultural, Pharmaceutical and Environmental Chemistry (ACS Symposium Series, No. 420)*, American Chemical Society, Washington, DC, 1990, pp. 40–47.
- 17 K.S. Chiu, A. Van Langenhove and C. Tanaka, *Biomed. Environ. Mass Spectrom.*, 18 (1989) 200–206.

- 18 L.D. Betowski and T.L. Jones, *Environ. Sci. Technol.*, 22 (1988) 1430–1434.
- 19 H.F. Schröder, *J. Chromatogr.*, 554 (1991) 251–266.
- 20 S.V. Hummel and R.A. Yost, *Org. Mass Spectrom.*, 21 (1986) 785–791.
- 21 H.F. Schröder, *Water Sci. Technol.*, 23 (1991) 339–347.
- 22 H.F. Schröder, *Wasser*, 73 (1989) 111–136.
- 23 D.F. Hunt, *Anal. Chem.*, 57 (1985) 525–537.
- 24 L.D. Betowski, S.M. Pyle, J.M. Ballard and G.M. Shaul, *Biomed. Environ. Mass Spectrom.*, 18 (1987) 343–354.
- 25 K.L. Busch, G.L. Glish and S.A. McLuckey (Editors), *Mass Spectrometry/Mass Spectrometry, Techniques and Applications of Tandem Mass Spectrometry*, VCH, New York, 1988.
- 26 J.V. Johnson and R.A. Yost, *Anal. Chem.*, 57 (1985) 758A–768A.
- 27 S.D. Menacherry and J.B. Justice, Jr., *Anal. Chem.*, 62 (1990) 597–601.
- 28 *Off. J. Eur. Commun.*, L223 (1987) 26.

CHROMSYMP. 2775

Determination of chlorinated pesticides by capillary supercritical fluid chromatography–mass spectrometry with positive- and negative-ion detection

Anja Jablonska and Marianne Hansen

Department of Chemistry, University of Oslo, P.O. Box 1033 Blindern, N-0315 Oslo (Norway)

Dag Ekeberg

Department of Biotechnological Science, Agricultural University of Norway, P.O. Box 40, N-1432 Ås (Norway)

Elsa Lundanes*

Department of Chemistry, University of Oslo, P.O. Box 1033 Blindern, N-0315 Oslo (Norway)

ABSTRACT

An interface between a capillary supercritical fluid chromatograph and a double-focusing mass spectrometer was developed. Modification of the standard electron ionization (EI)–chemical ionization (CI) combination ion source was necessary to obtain useful mass spectra with negative-ion detection. A detection limit in the lower nanogram range of the chlorinated pesticides (DDT and dieldrin) was found irrespective of the mode of detection. Positive-ion methane CI resulted in a relatively abundant $[M + H]^+$ ion, whereas positive-ion isobutane and ammonia CI appeared not to be amenable to the detection of chlorinated pesticides. The EI–charge exchange mass spectra of the investigated pesticides generally did not match the library mass spectra. In the negative-ion mode, CO_2 was an efficient moderating gas giving relatively large amounts of M^{-*} , in addition to some fragment ions. More fragmentation was observed when N_2O replaced CO_2 as the mobile phase. No major effects on the mass spectra, obtained by using pure mobile phase, were observed on adding methane, isobutane or ammonia.

INTRODUCTION

Gas chromatography–mass spectrometry (GC–MS) has become an extremely useful technique for the detection and identification of pesticides. Negative-ion chemical ionization (NICI) has great potential because of its selectivity for materials containing electronegative atoms, a property common to most pesticides. Recently, supercritical fluid chromatography–mass spectrometry (SFC–MS) also has been

employed for pesticide analysis in both positive- [1,2] and negative-ion [3,4] modes.

Unlike GC, SFC is not restricted by compound volatility or lability, from which some pesticides such as acid and carbamate types suffer. SFC–MS is a relatively new technique. Nevertheless, a wide range of applications has already been demonstrated [5].

One of the main drawbacks of SFC–MS as compared with GC–MS is that library searchable electron ionization (EI) mass spectra are not readily obtained. However, the charge exchange (CE) mass spectra obtained have been reported to resemble the EI mass spectra [2,6]. The

* Corresponding author.

detection limit in the positive-ion EI mode has been reported to be in the lower nanogram range [3], whereas those in SFC–CI–MS are in the range of tens of picograms in the full-scan mode and comparable to those found in GC–MS analysis [7].

The main aim of this study was to retrofit an interface for capillary SFC to a JEOL double-focusing mass spectrometer. The interface and the necessary instrument modifications are described. Another aim of our study was to investigate the possibility of using the SFC–MS system for pesticide analysis. Hexachlorocyclopentadiene and chlorodiphenylmethane derivatives were used as model substances to investigate the effect of different mobile phases (carbon dioxide and nitrous oxide) and different reagent and moderating gases on the limit of detection (LOD) and mass spectra in both positive- and negative-ion modes.

Even though CO₂ and N₂O have been shown to have nearly identical properties as mobile phases [8], it was of interest to examine their possible difference in behaviour with respect to the mass spectrometric detection of chlorinated pesticides. For negative-ion detection, modifications of the standard ion source were necessary. The influence on the mass spectra using CO₂ as the mobile phase in negative-ion MS was investigated by varying the ion source temperature, amount of mobile phase CO₂ and different CI reagent gases. The results demonstrate that CO₂ acts as a moderating gas.

EXPERIMENTAL

Materials

SFC-grade liquid CO₂ and N₂O were obtained from Scott Speciality Gases (Plumsteadville, PA, USA) and methane, isobutane and ammonia from AGA Norgas (Oslo, Norway). The standards used were obtained from different commercial sources. The compounds were dissolved in HPLC-grade chloroform, dichloromethane or carbon disulphide (Rathburn, Walkerburn, UK).

Columns and restrictors

A 5 m × 50 μm I.D. (375 μm O.D.) SB-phenyl-5 (0.25-μm film thickness) column that

was purchased from Lee Scientific (Salt Lake City, UT, USA) was used throughout. Integral restrictors [9] made of 50 μm I.D. (375 μm O.D.) fused silica (Polymicro Technologies, Phoenix, AZ, USA) and 50 μm I.D. frit restrictors (Lee Scientific) were used. Linear restrictors of 10–25 μm I.D. fused silica (Polymicro Technologies) were used for the dynamic splitting.

Instrumentation

A Model 602 SFC system (Lee Scientific) was used. This instrument is equipped with a C14W injector (Valco) with a 200-nl loop, which can be operated with timed split injection. In addition, a 500 μm I.D. dynamic splitter [10] was installed inside the oven. Injections were performed at or slightly above ambient temperature, while dynamic splitting occurred under supercritical conditions. The column was installed in the dynamic splitter at a position 2–3 mm below the injector rotor. The split restrictor was heated by an extra heating unit (copper block) with temperature control (Eurotherm, Worthing., UK). The heating unit was located outside the oven.

The column and the restrictor were connected by a 400 μm I.D. butt connector (Lee Scientific) between the oven and the MS instrument. An oven temperature of 100°C was used and, if not mentioned otherwise, a linear pressure programme from 100 to 250 bar.

A 3-kV JMS-DX 303 double-focusing mass spectrometer (JEOL), of EB geometry, equipped with a 10-kV post-acceleration conversion dynode detector was used for detection. An electron ionization–chemical ionization (EI–CI), an LC ion source and a modified version of the LC ion source were used. The LC ion source was also a dual EI–CI ion source (Fig. 1).

A thoriated iridium filament (Interion, Manchester, UK) replaced the original rhenium filament. This filament cannot be easily welded, therefore the filament holder was modified to allow for attachment by two screws (all new parts were made of stainless steel 316). The filament current limit had to be increased compared with that used for rhenium filaments in order to obtain a satisfactory emission from the thoriated iridium filament.

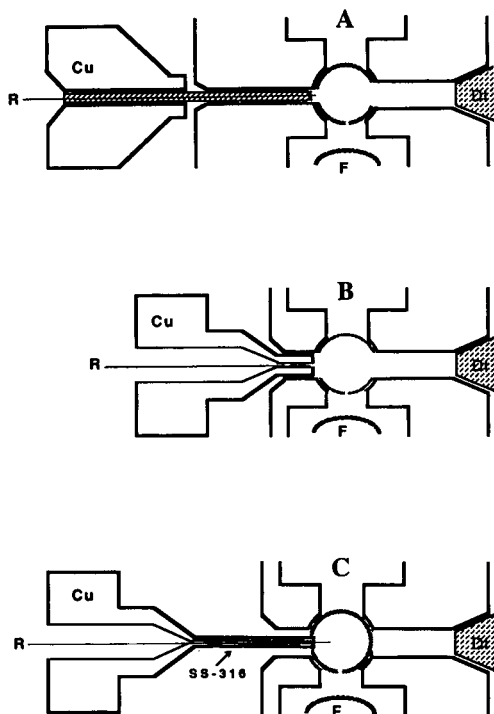


Fig. 1. (A) EI–CI ion source with restrictor heating unit (not to scale). The heating zone is $4\text{ cm} \times 0.8\text{ mm}$ I.D. (stainless steel). (B) LC ion source with restrictor heating unit (not to scale). The heating zone is $5\text{ mm} \times 0.5\text{ mm}$ I.D. (copper). (C) Modified LC ion source with restrictor heating unit (not to scale). The heating zone is $2\text{ cm} \times 0.5\text{ mm}$ I.D. (stainless steel). The EI–CI and LC ion sources can be operated in the EI mode (without the inner circle) and in the CI mode, whereas the modified ion source can be operated in the CI mode only. R = Restrictor (the approximate restrictor outlet position is indicated in the drawings); Cu = copper heating block; DI = direct insertion probe (closing the outlet); F = thoriated iridium filament; SS-316 = stainless steel.

The restrictor was connected to the mass spectrometer through the GC–MS entrance of the ion source housing through a 1/4 in. O.D. glass tube (1 in. = 2.54 cm). The restrictor changing procedure requires that the ion-source housing is exposed to atmospheric pressure. However, the complete procedure usually requires less than 20 min, including heating to the operating conditions. Different restrictor heating designs (Fig. 1) were investigated, depending on the choice of ion source. In all instances the LC interface controller of the MS supplied the electric current for the heaters and temperature monitoring. The approximate restrictor positions

used are indicated in Fig. 1. Fine adjustment of the restrictor position was performed depending on the flow-rates and operating temperatures. A restrictor heater temperature of 300°C was used if not mentioned otherwise. The transfer line between the SFC and MS systems can be heated to constant temperature, using the heating unit of the GC–MS interface. However, heating of the transfer line was not necessary for the compounds investigated in this study.

In order to use high CO_2 flow-rates, the apparent CO_2 pressure could be reduced by introducing liquid nitrogen into the liquid nitrogen trap of the mass spectrometer. For a linear flow-rate of about 1.7 cm/s of supercritical CO_2 at 100 bar, a pressure of about $2 \cdot 10^{-5}$ Torr (1 Torr = 133.322 Pa) was measured in the ion source housing. When liquid nitrogen was introduced into the trap, less than $2 \cdot 10^{-6}$ Torr was measured. Cryotrapping of CO_2 and N_2O allowed the use of flow-rates higher than 3 cm/s also in the CI mode. No noticeable difference in LODs and mass spectra were observed with or without cryotrapping.

The mass spectrometer was operated with electron multiplier voltages of about 1.5 kV and an ionization current of $100\ \mu\text{A}$ throughout. EI–CE mass spectra were obtained using an electron energy of 70 or 22 eV and CI mass spectra were obtained using 230 eV in both the positive- and negative-ion modes. All data were recorded with a mass resolution of 500.

RESULTS AND DISCUSSION

Filament

A substantial background signal in the mass range m/z 180–270 was observed on introduction of CO_2 into the ion source in the EI–CE mode when using a rhenium filament. The background level increased slightly with increasing mobile phase flow-rate and was strongly enhanced when solutes entered the ion source. The effect was most pronounced for oxygen-containing compounds such as alcohols and carboxylic acids, less for polyaromatic hydrocarbons and alkanes. The background signal was caused by thermochemical reactions with the hot rhenium filament, as was evident by the presence of several

rhodium oxide species [11] in the background mass spectra. A similar effect was observed with a tungsten filament. Installation of a thermo-spray-type thoriated iridium filament eliminated this problem. This filament was also used with N_2O as mobile phase without any background problem. The thoriated iridium filament has therefore been used throughout this study, and as the filament lifetime was observed to be >400 h, we can recommend this type of filament.

Positive-ion MS

EI-charge exchange. It has been argued that when CO_2 is used as a mobile phase and the ionization potential of the sample molecule is lower than the recombination energy of CO_2^+ (13.8 eV), CE ionization is achieved [12]. However, it has also been pointed out that ionization by the CE mechanism requires the use of a higher ion source pressure (0.5–1 Torr) and a higher electron energy (200–500 eV) [3]. It is not possible to measure the actual pressure in the ion source of this mass spectrometer. The ion sources are relatively open in the EI mode, and this implies that the pressure in the ion source may be close to the measured pressure in the ion source housing in this mode (without cryotrapping), whereas the pressure in a more closed CI ion source is much higher. The maximum ionization energy was 70 eV in the EI mode. However, it was observed that a reduced electron energy resulted in improved signal-to-noise ratio, mainly owing to a reduced background signal level in the low-mass range (m/z 50–100). The larger amount of background fragment ions using 70-eV electrons may be caused by the exothermicity of EI and not the CE mechanism. As it is difficult to establish whether the ionization of our sample molecules is due to EI, CE or a dual EI-CE mechanism, we have used the notation EI-CE ionization when the instrument was operated in the EI mode.

Detection limits, calculated as amount injected on to the column giving a signal-to-noise ratio of 3 in the full-scan mode, were investigated for different types of compounds in addition to the chlorinated pesticides. A detection limit in the lower nanogram range was found for polycyclic

aromatic hydrocarbons, fatty acid ethyl esters and polystyrenes. The detection limits for different chlorinated pesticides were in the range 2–4 ng. As large variations in injector loop size have been reported [13], and the dynamic splitting ratio may be difficult to control, only approximate values are reported. These detection limits are in the same range as reported in the literature [3].

In the mass spectrum of DDT the main process observed is loss of HCl and CCl_3 and molecular ion M^+ has a low abundance. This is different from the results of Houben *et al.* [2] and the library mass spectrum of DDT, where $M - CCl_3^+$ yields the base peak. However, the main fragment ion observed of DDD was $M - CHCl_2$, and a relatively smaller amount of $M - CHCl$. The mass spectrum of dieldrin was complex, and compared with the EI library mass spectrum less fragmentation was observed. However, the mass spectrum of aldrin resembled the EI library mass spectrum. Therefore, as EI-like mass spectra were not obtained in all of our experiments, the identification of chlorinated pesticides using library mass spectra is not feasible.

CI with methane as reagent gas. The LODs for dieldrin and DDT are in the range 1–4 ng using

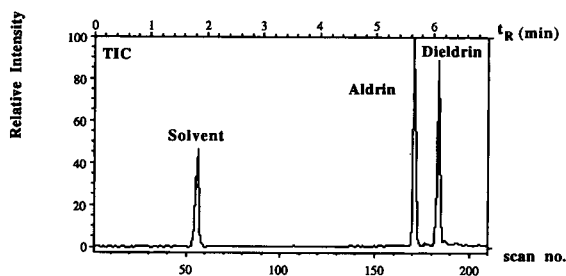


Fig. 2. Total ion current chromatogram of aldrin and dieldrin obtained with positive-ion methane CI using the modified LC ion source. A 0.5 mg/ml (in CS_2) solution and a 1:12 splitting ratio result in about 8 ng of each compound being injected on to the column. SFC conditions: column temperature 100°C and pressure programming: 100 bar (2 min), then increased from 100 to 250 bar at 20 bar/min (linear gradient). MS conditions: restrictor heating temperature 300°C, ion-source temperature 135°C and scanning from m/z 100 to 600 at 2.0 s per scan. The solvent peak is due to clusters of CS_2 .

both CO_2 and N_2O as mobile phases. In the chromatogram shown in Fig. 2 about 8 ng of each compound were injected. A slightly lower LOD and a relatively larger amount of $[\text{M} + \text{H}]^+$ were obtained using the modified ion source (Fig. 1C) than with the standard EI–CI ion source (Fig. 1A) than with the standard EI–CI ion source. The mass spectra of these compounds are shown in Fig. 3A and B.

Compared with the reported methane CI mass spectra of dieldrin and aldrin [14], a relatively

larger amount of $[\text{M} + \text{H}]^+$ was found in this work. This may be explained by better conditions for ion–neutral reactions and hence an increase in stabilized ions.

CI with isobutane as reagent gas. When isobutane replaced methane as the reagent gas a less favourable LOD (6–10 ng) was obtained for the chlorinated pesticides using CO_2 as mobile phase. The detection limit was >30 ng using N_2O as mobile phase, so no further experiments

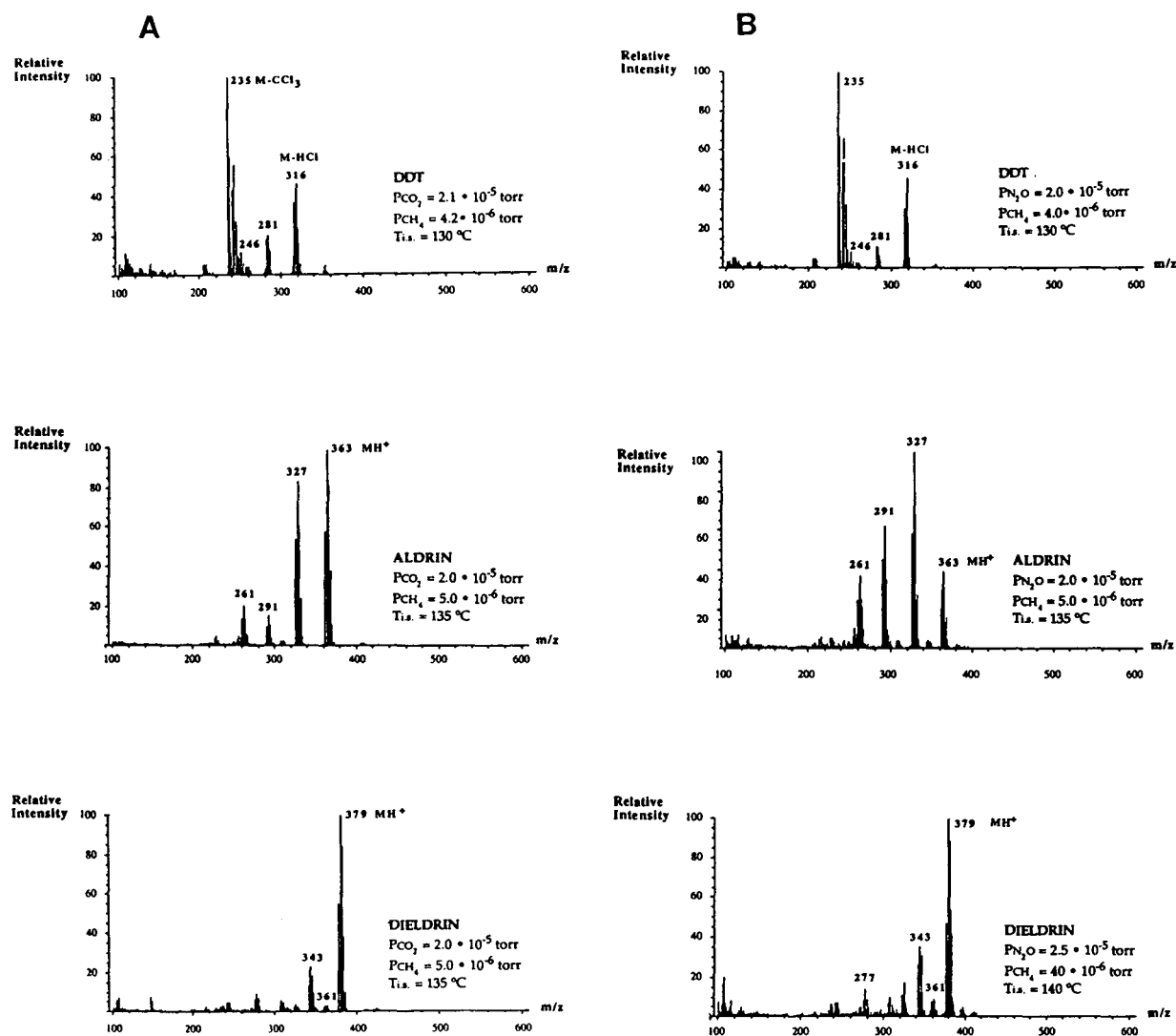


Fig. 3. Positive-ion methane CI mass spectra of dieldrin, aldrin and DDT using (A) supercritical CO_2 and (B) supercritical N_2O as mobile phase. The EI–CI ion source (Fig. 1A) was used. Ion-source pressure is given as $P_{\text{CO}_2} + P_{\text{CH}_4}$ and ion-source temperature as $T_{\text{i.s.}}$.

were carried out with this combination of mobile phase and reagent gas.

However, the LOD for anthracene and chlorinated anthracene was in the lower nanogram range using both CO_2 and N_2O as mobile phase, and $[\text{M} + \text{H}]^+$ were the main ions. Isobutane alone has been reported to give useful mass spectra of chlorinated pesticides in both positive- and negative-ion modes [15]. The major ions in each of the reported mass spectra may be accounted for by dissociative proton transfer and hydride and chloride abstraction involving C_4H_9^+ . Our results indicate that the proton affinity of the investigated compounds is less than that of isobutane as protonated molecular ions are absent.

CI with ammonia as reagent gas. Ammonia has been used as the reagent gas [5,16–21] for a great variety of compounds in positive-ion CI. When CO_2 and ammonia were used as mobile phase and reagent gas, respectively, the chlorinated pesticides could be detected as peaks (LOD ca. 2–4 ng) in the chromatogram, but the mass spectra did not give any structural information. The mass spectra were dominated by the fragment ion at m/z 130 that was present at a constant level throughout the chromatogram, but increased when compounds and the solvent CS_2 were eluted. Similar effects have been observed by others [22] using ammonia as reagent gas. No $[\text{M} + \text{H}]^+$, $[\text{M} + \text{NH}_4]^+$ or any sample-containing ions were observed for compounds with large electron-capture cross-sections. The m/z 130 ion found in our work may originate from a $[(\text{CO}_2)(\text{NH}_3)_5\text{H}]^+$ cluster. The ammonia pressure used was about $4.0 \cdot 10^{-6}$ Torr. From the negative-ion MS experiments we know that the CO_3^- ions are present in the ion source, and may neutralize m/z 130 ions. Hence, if compounds introduced into the ion source are ionized by the CO_3^- ions, fewer of the CO_3^- ions will be available for the m/z 130 neutralization. Hence an increase in the m/z 130 level may be observed.

Negative-ion MS

Electron-capture and ion–neutral reactions are the two main ionization techniques that are used in this mode [23]. The soft nature of these

processes is an advantage when molecular ions are wanted. For the electron-capture process, the choice of moderating gas, among other parameters, is considered as an important factor for the yield of M^- .

The results obtained in the negative-ion mode using the original EI–CI ion source was very discouraging; both high LODs and extensive fragmentation were observed. However, successful SFC–negative-ion MS has been reported by others also on chlorinated pesticides [3,4].

The reason for the high ratio of fragmentation in our experiments is the low pressure in the ion source, which implies a smaller amount of thermalized electrons. We therefore modified the ion source (LC version) to obtain a higher pressure in the ion source. This modified ion source was used throughout our experiments in negative-ion MS.

It soon became apparent that an ion-source temperature lower than 220–300°C (which is normally used in SFC–positive-ion CI–MS [7]) improved the mass spectra. Temperatures above 200°C, as used by Huang *et al.* [4], led to extensive fragmentation and a high LOD of dieldrin. Thus, in most of the reported experiments, a temperature of about 150°C was used. Even better results with respect to LOD and reduced fragmentation were obtained in our experiments when the temperature was lowered to about 70°C. However, this temperature could not be used over a long period of time, owing to the heat supported by the filament and restrictor heater. The possibility of cooling the ion source thus appears to be a necessary requirement. An ion-source temperature of about 140°C was used by Roach *et al.* [24], who also pointed out the necessity of using lower temperatures in negative-ion MS.

A repeller potential of 0 V was used throughout all the negative-ion mode experiments, as this potential will increase the residence time of molecular ions and electrons, and hence increase the collision probability with the moderating gas molecules (third-body collisions). Such conditions are necessary to obtain collisional stabilization of excited ions.

CO₂ as moderating gas. CO_2 is considered to be a slightly more efficient moderating gas than

isobutane, which in turn is more efficient than methane [23]. The use of CO_2 as moderating gas has also been reported to give relatively simple mass spectra, usually without unexpected ions [23]. The observation of a fragment ion of m/z 60 throughout our experiments may be explained by fragmentation of CO_2 clusters [25].

When CO_2 is used as the mobile phase it may also act as a moderating gas. Fig. 4 shows the mass spectra obtained for endrin using CO_2 as mobile phase and moderating gas. An apparent

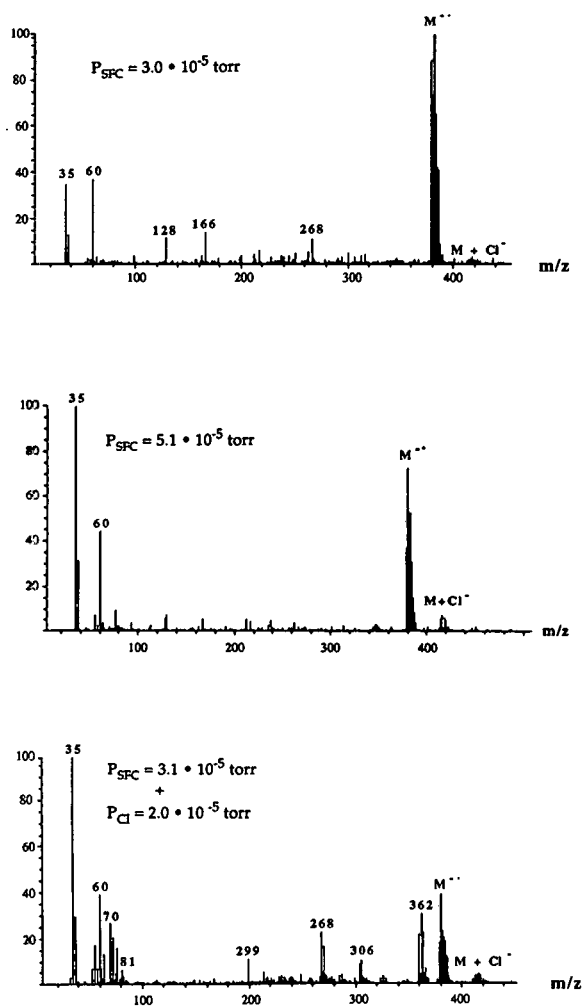


Fig. 4. Negative-ion mass spectra of endrin using CO_2 as a moderating gas. The ion source pressure caused by the mobile phase CO_2 is denoted by P_{SFC} . P_{CI} refers to the pressure of the CO_2 gas introduced through the CI reagent gas transfer line. The ion source temperature was 70°C and the modified LC ion source was used.

difference in mass spectra is observed. When mobile phase CO_2 is the only source of CO_2 , very little fragmentation occurs and $\text{M}^{\bullet-}$ dominates the mass spectrum. This is thought to be caused by a more efficient production of thermalized electrons. Adiabatic cooling cause a moderating gas with a lower thermal energy compared with the buffer gas introduced via the CI inlet system. The lower thermal energy of mobile phase CO_2 gas molecules results in a higher efficiency of primary electron quenching and hence in an increased loss of energy of the latter [26]. Secondary electrons are thermalized electrons which may have an energy of about 0.1 eV, which is wanted for resonance electron capture. The reduced thermal energy of the buffer gas is caused by the formation of neutral clusters, as a consequence of adiabatic expansion. The cluster production will give a relatively high local density in the thermalization area and hence a higher thermalization efficiency of the electrons. The consequence of the factors mentioned above is a decreasing exothermicity of the ionization process, which in turn implies an increased amount of molecular ions. The use of an electron energy lower than 230 eV of the primary electrons did give a slight improvement with respect to detection limits.

The negative-ion mass spectrum of dieldrin, using CO_2 as moderating gas, is shown in Fig. 5A. The $\text{M}^{\bullet-}$ ion is also present for this compound, but other fragment ions dominate the mass spectrum. This mass spectrum was obtained using a higher temperature than that used for endrin. The limit of detection for the investigated pesticides was about 2–4 ng. If the measured pressure became higher than $2.5 \cdot 10^{-5}$ Torr, quenching of the signal and thus higher LODs were observed.

N_2O as moderating/reagent gas. The mass spectrum obtained for dieldrin using N_2O as mobile phase with no additional reagent gas is shown in Fig. 5B. A smaller amount of $\text{M}^{\bullet-}$ is found than when CO_2 was used as the mobile phase (Fig. 5A). The main differences in the mass spectra utilizing CO_2 and N_2O as mobile phase are due to the ionization process. When N_2O is used, the main ionization process is caused by CI, which is a more energetic reaction

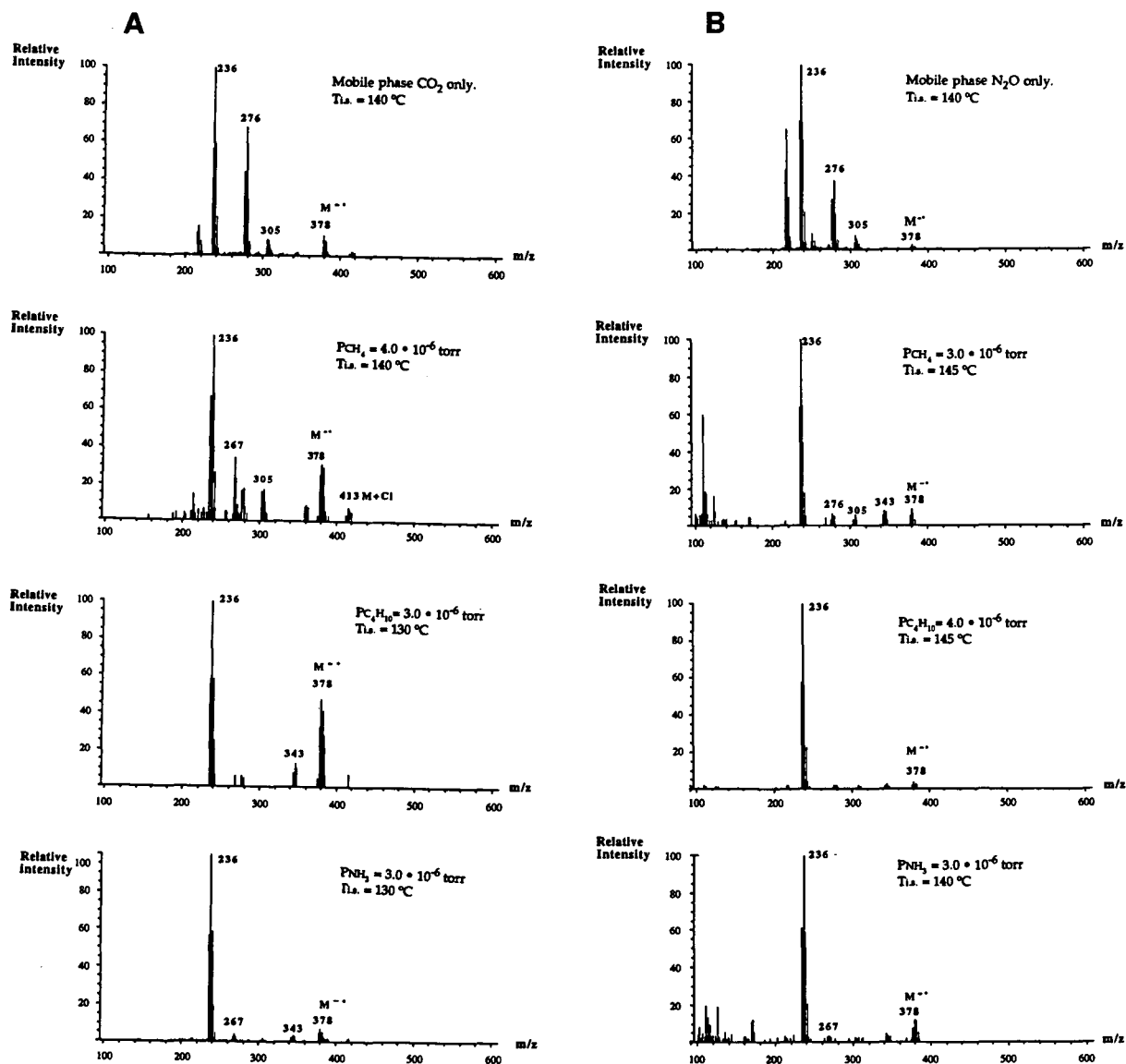


Fig. 5. Negative-ion mass spectra of dieldrin using (A) supercritical CO₂ and (B) supercritical N₂O as mobile phases. Ion-source temperatures and pressure of the added gases are given. The modified LC ion source was used. The ion-source pressure due to mobile phase only was about $2 \cdot 10^{-5}$ Torr when dieldrin was eluted using a pressure programme from 100 to 250 bar.

than electron attachment by thermalized electrons.

The main conclusion to be drawn from these experiments is that CO₂ is preferred when electron attachment is wanted and N₂O when reagent ions [23] are required for CI. The LODs were in the range 2–4 ng.

Methane as moderating/reagent gas. Methane is also classified as a moderating gas in negative-ion MS [23]. However, in combination with N₂O, the reagent ion OH⁻ will be present. The mass spectra of dieldrin shown in Fig. 5 indicate that the combination of CO₂ or N₂O with methane results in ionization caused by an elec-

tron-capture mechanism also. Compared with the negative-ion methane mass spectrum of dieldrin [27], several differences are observed. The reported $[M + Cl]^-$ and $[M + O - Cl]^-$ ions cannot be observed in Fig. 5B. However, the abundant fragment ion at m/z 236 which is the dominant fragment in Fig. 5B was not revealed in the reported mass spectrum. The ion of m/z 236 may be due to $C_5Cl_5^-$. The LODs were in the range 2–4 ng.

Isobutane as moderating/reagent gas. Isobutane itself is reported to be a better moderating gas than methane, and may give reagent ions in mixtures with N_2O [23]. The mass spectra of dieldrin obtained with isobutane as reagent gas are also shown in Fig. 5. The m/z 236 fragment is the dominant fragment using both CO_2 and N_2O as mobile phase.

Relatively more of $M^{\bullet-}$ is preserved when using CO_2 as mobile phase, as is the case using mobile phase alone. These results indicate that both the mobile phases and the added gas function as moderating gases in these experiments. The LODs were in the range 2–4 ng.

Ammonia as reagent/moderating gas. The mass spectra of dieldrin obtained using ammonia as an additional reagent gas (Fig. 5) resembled those obtained using the other gases, with only minor differences in the relative intensities of the fragment ions. Thus, in our experiments, ammonia seems to function as a moderating gas only. It has been reported [4] that pesticides and herbicides gave essentially the same mass spectra using neat CO_2 , $CO_2 + CH_4$ and $CO_2 + NH_3$. However, both $M^{\bullet-}$ and MH^- were observed in polyisocyanate mass spectra using CO_2 and ammonia [28]. The LODs in our study were in the range 2–4 ng.

CONCLUSIONS

The interfacing of capillary SFC with a JEOL double-focusing mass spectrometer equipped with GC and LC interfaces was fairly simple. A thoriated iridium filament had to be used instead of a rhenium filament, which gave a severe background of rhenium oxides.

The detection limits obtained, measured as nanograms of sample injected on-column and

with full-scan detection, were in the lower nanogram range, irrespective of the mode of detection, *i.e.*, positive-ion EI-CE, positive-ion CI or negative-ion detection. This is not in accordance with other reports on detection limits. Our results using negative-ion detection are inferior to those observed by others [4] using double-focusing MS. The discrepancies in reported LODs may be caused by the different instrumental designs. Modification of the standard ion source was necessary to obtain useful mass spectra in the negative-ion mode, and further modifications are necessary to improve the LOD.

The EI-CE mass spectra of the investigated chlorinated pesticides did not all match the EI library mass spectra, thus making identification without the use of standards difficult. A relatively abundant $[M + H]^+$ ions was found in the positive-ion methane CI mass spectra, whereas isobutane and ammonia CI were not suitable for the detection of chlorinated pesticides.

In the negative-ion mode, CO_2 was shown to be an efficient moderating gas, giving relatively large amounts of $M^{\bullet-}$. The mobile phase CO_2 cooled by adiabatic expansion was more effective than CO_2 added through the CI reagent gas transfer line in producing thermalized electrons.

Apparently, the mobile phase N_2O also functions as a moderating gas, as the same fragment ions were observed as with CO_2 . However, the differences in intensity are pronounced. Addition of methane, isobutane or ammonia did not dramatically change the mass spectra obtained using CO_2 or N_2O alone as mobile phase. Hence electron capture seem to be the dominant mechanism with all the investigated combinations of gases. The possibility of obtaining both $M^{\bullet-}$ and fragment ions is most useful for the identification of chlorinated pesticides.

This work demonstrates that capillary SFC-MS may be a valuable tool in analyses for chlorinated pesticides, offering the possibility of both positive- and negative-ion modes of detection. The detection limits in the low nanogram range may not be a restriction compared with GC-MS analysis, as other injection techniques in which larger volumes may be introduced can be used [29].

REFERENCES

- 1 H.T. Kalinoski, B.W. Wright and R.D. Smith, *Biomed. Environ. Mass Spectrom.*, 13 (1986) 33.
- 2 R.J. Houben, P.A. Leclercq and C.A. Cramers, *J. Chromatogr.*, 554 (1991) 351.
- 3 E.C. Huang, B.J. Jackson, K.E. Markides and M.L. Lee, *Anal. Chem.*, 60 (1988) 2715.
- 4 E.C. Huang, B.J. Jackson, K.E. Markides and M.L. Lee, *J. Microcol. Sep.*, 2 (1990) 88.
- 5 R.D. Smith, H.T. Kalinoski and H.R. Udseth, *Mass Spectrom. Rev.*, 6 (1987) 445.
- 6 E.D. Lee, S.-H. Hsu and J.D. Henion, *Anal. Chem.*, 60 (1988) 1990.
- 7 S.V. Olesik, *J. High Resolut. Chromatogr.*, 14 (1991) 5.
- 8 M.B. Baastoe and E. Lundanes, *J. Chromatogr.*, 558 (1991) 458.
- 9 E.J. Guthrie and H.E. Schwartz, *J. Chromatogr. Sci.*, 24 (1986) 236.
- 10 M.L. Lee, B. Xu, E.C. Huang, N.M. Djordjevic, H.-C.K. Chang and K.E. Markides, *J. Microcol. Sep.*, 1 (1989) 7.
- 11 G. Ramendik, J. Verlinden and R. Gijbels, in F. Adams, R. Gijbels, R. van Grieken (Editors), *Inorganic Mass Spectrometry*, Wiley, New York, 1988, p. 30.
- 12 E.C. Huang, B.J. Jackson, K.E. Markides and M.L. Lee, *Chromatographia*, 25 (1988) 51.
- 13 T. Greibrokk, B.E. Berg and H. Johansen, in M. Perrut (Editor), *Proceedings of the International Symposium on Supercritical Fluids, Nice, October 1988*, Vol. 1, Société Française de Chimie, Paris, 1988, p. 425.
- 14 F.J. Biros, R.C. Dougherty and J. Dalton, *Org. Mass Spectrom.*, 6 (1972) 1161.
- 15 R.C. Dougherty, J.D. Roberts and F.J. Biros, *Anal. Chem.*, 47 (1975) 54.
- 16 T.L. Chester, J.D. Pinkston, D.P. Innis and D.J. Bowling, *J. Microcol. Sep.*, 1 (1989) 182.
- 17 J.D. Pinkston, D.J. Bowling and T.E. Delaney, *J. Chromatogr.*, 474 (1989) 97.
- 18 J.D. Pinkston and D.J. Bowling, *J. Microcol. Sep.*, 4 (1992) 295.
- 19 H.T. Kalinoski and R.D. Smith, *Anal. Chem.*, 60 (1988) 529.
- 20 V.N. Reinhold, D.M. Sheely, J. Kuei and G.-R. Her, *Anal. Chem.*, 60 (1988) 2719.
- 21 P.J. Arpino, D. Dilettato, K. Nguyen and A. Bruchet, *J. High Resolut. Chromatogr.*, 13 (1990) 5.
- 22 P. Rudewicz, T.-M. Feng, K. Blom and B. Munson, *Anal. Chem.*, 56 (1984) 2610.
- 23 H. Budzikiewicz, *Mass Spectrom. Rev.*, 5 (1986) 345.
- 24 J.A.G. Roach, J.A. Sphon, J.A. Easterling and E.M. Calvey, *Biomed. Environ. Mass Spectrom.*, 18 (1989) 64.
- 25 C.E. Clots and R.N. Compton, *J. Phys. Chem.*, 69 (1978) 1636.
- 26 L.J. Sears and E.P. Grimsrud, *Anal. Chem.*, 61 (1989) 2523.
- 27 R.C. Dougherty, J. Dalton and F.J. Biros, *Org. Mass Spectrom.*, 6 (1972) 1171.
- 28 W. Blum, P. Ramstein and H.-J. Grether, *J. High Resolut. Chromatogr.*, 13 (1990) 290.
- 29 B.E. Berg, A.M. Flaaten, J. Paus and T. Greibrokk, *J. Microcol. Sep.*, 4 (1992) 227.

CHROMSYMP. 2782

Packed-column supercritical fluid chromatography coupled with electrospray ionization mass spectrometry

Freddy Sadoun and Henry Virelizier

Commissariat à l'Énergie Atomique, Centre d'Étude de Saclay, SPEA/SAIS, 91190 Gif-sur-Yvette (France)

Patrick J. Arpino*

Laboratoire de Chimie Analytique, Institut National Agronomique, 75231 Paris 05 (France)

ABSTRACT

A new approach to combined supercritical fluid chromatography–mass spectrometry (SFC–MS) was explored using a two-pump supercritical fluid chromatograph, and a packed column with the outlet directly interfaced to an electrospray (ES) ion source attached to a single quadrupole mass spectrometer. The experimental set-up is described and preliminary results are reported for mobile phase flow-rates in the range 0.15–1 ml/min, using CO₂ modified by the addition of 1–30% (v/v) of a polar organic solvent. The combined system has a greater potential for the analysis of polar molecules by MS than earlier SFC–MS instruments that utilized capillary column SFC directly coupled to the ion source of a chemical ionization mass spectrometer. A liquid-phase ionization process was utilized for solute ion formation, and it could be applied to the determination of high-mass and polar molecules separated by packed column SFC; however, the MS response is dependent on the mobile phase composition and the SFC–ES–MS instrument is still limited to the determination of low-mass samples owing to cold trapping on some critical surfaces.

INTRODUCTION

Several methods have been devised during the last decade to provide an effective coupling of supercritical fluid chromatography with mass spectrometry (SFC–MS). Nevertheless, the results have not convinced MS instrument manufacturers to promote any of these methods strongly, and SFC–MS users have to custom-build their machines. As a consequence, the number of instruments in routine use remains low. In a previous paper [1], the reasons for this particular situation were discussed, and it is now clear that SFC–MS coupling is not as easy to conceive as was thought in the early 1980s. In particular, the method referred to as direct

coupling or direct fluid interfacing, consisting of directly connecting a capillary SFC column to the ion source of a chemical ionization mass spectrometer, has been plagued by inherent limitations, the most severe one being the poor MS response with high-mass molecules when the supercritical fluid pressure is varied over a wide interval, and with ionization produced by charge exchange with CO₂^{+•} primary ions.

In contrast, the situation of combined liquid chromatography–mass spectrometry (LC–MS) is brighter today. After many years of progression at a moderate rate [2], LC–MS has progressed rapidly in recent years because it has benefited from the explosive development of atmospheric pressure MS sources utilizing electrospray (ES) ionization [3] (no distinction is made here between electrospray and its pneumatically assisted variant called ionspray). Because LC–MS and

* Corresponding author.

SFC–MS have often followed similar routes, it is not surprising that the atmospheric pressure ion source (API) has been considered for potential use in a combined SFC–MS instrument, although the number of reports of this union is still low.

With one exception in which cationization with lithium primary ions was used for solute ionization [4], other reports on SFC–MS with an API source have described the production of sample ions from supercritical solutions by gas-phase ionization in a corona discharge, following total solution vaporization. Because of the gas-phase nature of the ionization process, the restrictor at the column end was generally set at temperatures well above 200°C. For example, gas-phase ionization by corona discharge was used together with packed column SFC, eluted with either neat CO₂ or CO₂ modified by the addition of a few percent of a polar organic solvent, for the determination of steroids in biological matrices [5], polyaromatic hydrocarbons in coal tar and sand oil extracts [6] and various synthetic mixtures including polyethylene glycol and polystyrene oligomers and vitamins [7].

We have assembled an instrument that is similar to those described by others [5–7], with the notable exception that the corona needle electrode was omitted. Supercritical solutions of polar basic solutes in CO₂ modified with organic solvents were introduced at mobile phase flow-rates compatible with the use of packed columns, *i.e.*, 150–1000 μl/min. We observed that by maintaining the restrictor at a low temperature, and by establishing an electrical potential of a few kilovolts between the restrictor end and the MS sampling orifice, both solvent and sample ions were produced. The conditions appeared to be identical with those existing in conventional electrospray ionization, a liquid-phase ionization process that is known to require the presence of charged liquid droplets. Such charged liquid droplets can be transiently obtained during decompression and cooling of the expanding subcritical jet at the restrictor outlet, thus allowing solvent-derived cluster ions and preformed sample ions to escape from the charged droplets into the gas phase, and be mass analysed. The light-scattering detector modified for SFC monitoring

[8] is another case of an SFC detector that similarly utilizes liquid droplets transiently formed in the decompressed SFC fluid. In this paper we describe the experimental set-up, report preliminary results and discuss possibilities and limitations of electrospray ionization applied to SFC–MS coupling.

EXPERIMENTAL

Chemicals

HPLC-grade solvents were obtained from Merck. Atrazine was obtained from Cluzeau Info Labo (Sainte-Foy-la-Grande, France) and 1-chloro-2-amino pyridine ($M_r = 128$) and 1-chloro-2-(*N*-*tert.*-butylcarbamate)pyridine ($M_r = 228$) were provided by the Biochemistry Department of the CEA in Saclay (France). In this text, the mass 128 and 228 pyridine derivatives are referred to as Py-I and Py-II, respectively.

Supercritical fluid chromatography (Fig. 1)

High-purity (grade N48) liquid carbon dioxide supplied in cylinders with a dip tube (Air Liquide, Le-Plessis-Robinson, France) was introduced directly into a Gilson (Villiers-le-Bel, France) Model 305 single-piston reciprocating pump, fitted with a Model 10SC pump head, and modified for SFC operation. The polar solvent modifier was pumped by a Gilson Model 307 pump equipped with a Model 5SC pump head.

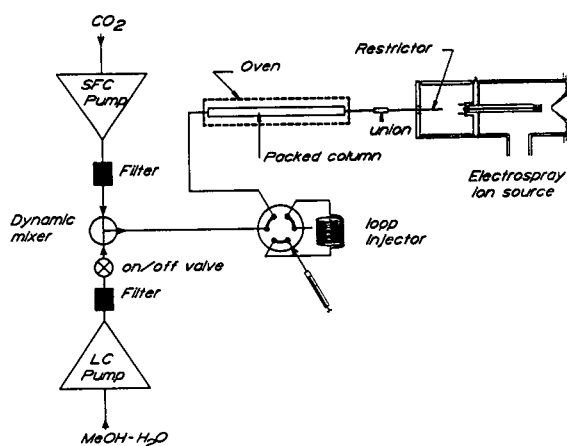


Fig. 1. Schematic diagram of the packed column SFC system utilizing gradient elution of a polar modifier in CO₂.

Both effluents were combined using a Gilson Model 811C dynamic mixer. The sample injector was either a Rheodyne Model 7520 fitted with a 5.0- μ l sample loop or a Valco Model LC206 with a 1- μ l internal loop, depending on the analytical SFC column diameter. Columns were either 150 mm \times 2.1 mm I.D. 5- μ m Zorbax Rx-C₁₈ or 150 mm \times 1 mm I.D. 5- μ m Hypersil C₈. The column temperature was maintained constant in the range 40–100°C by an HPLC-type column heater and controller (Model Croco-Cil, Cluzeau Info Labo). Higher column temperatures, up to 200°C, were obtained by placing the column inside the oven of a gas chromatograph. The restrictor was attached at one end to the analytical column by a zero-dead-volume connector (Valco, part number CEF 1.5). The other end was positioned directly in the electrospray ion source, as described below. Valco and Rheodyne equipment and analytical columns were purchased from Touzart et Matignon (Vitry-sur-Seine, France).

SFC–MS interface (Fig. 2)

The end tip of the restrictor was located at *ca.* 5 cm and in direct line of sight with the ion sampling aperture. Linear restrictors were generally used and were made of 25–30 cm long fused-silica tubing (SGE, Villeneuve-St-George, France) of 60 and 25 μ m I.D. when coupled to 2.1 and 1 mm I.D. columns, respectively. Proper electrospray ionization requires that the nebulizer be electrically conducting, to avoid disturbing charge build-up. Consequently, the polyim-

ide coating of the fused-silica tube was covered with an electrically conducting layer of nickel-doped polyurethane paint (Aero 7465 antistatic paint; MAP, Pamiers, France) over a length of *ca.* 10 cm. In general, the restrictor end was kept at ground potential, and was only warmed by the surrounding nitrogen bath at 80°C in the atmospheric pressure ion source.

Another restrictor type was used occasionally and consisted of a stainless-steel tube (30 cm \times 1 mm I.D.) crimped at the terminal end, such that a pressure drop of 100 bar was measured when the mobile phase flow-rate was 1 ml/min of CO₂. The restrictor end in the API source was heated at temperatures up to 300°C by a coil of resistance wire (Thermocoax, Suresnes, France).

Mass spectrometry (Fig. 2)

The mass spectrometer was a Nermag Model R1010C (Quad Service, Argenteuil, France) single-quadrupole instrument equipped with an Analytica (Branford, CT, USA) electrospray source and a Spectral-30, version 3.70, data system (P2A Système, Vincennes, France). With the exception of the above sample-introduction device, the Analytica electrospray source was used without modification, and typical operating voltages are listed in Fig. 2. A stream of dry nitrogen, at a flow-rate of 9 l/min and a temperature of 80°C, built a small positive pressure into the ES source that prevented the introduction of contaminants from the laboratory atmosphere, assisted solution vaporization and broke heavy ion clusters prior to MS analysis.

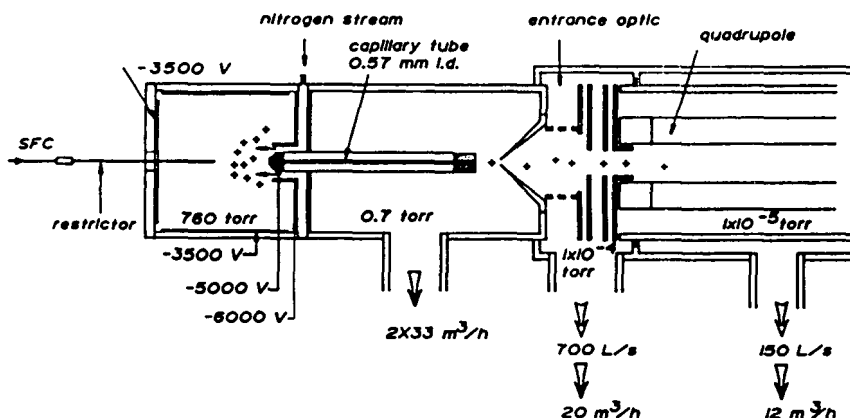


Fig. 2. Schematic diagram of the SFC–MS interface and electrospray ion source.

RESULTS AND DISCUSSION

Fluid temperature conditions

Both solvent cluster ions and solute-derived ions are observed using the described instrument when the supercritical fluid temperature is kept within a given range of temperature conditions, for a given flow-rate of the mobile phase. The temperature was varied either by changing the column oven temperature, up to 200°C, with the metallized fused-silica restrictor end only warmed by the nitrogen bath at 80°C into the ES source, or alternatively by keeping the column oven at 80°C and by varying the pinched metal restrictor temperature up to 300°C, using the resistor wire. Both conditions produce the same effects. Constant ion production is observed over a large temperature interval (typically 40–100°C) and is followed by a regularly decreasing ion signal at higher temperatures. As an example (Fig. 3), using a 25 μm I.D. fused-silica restrictor, the 1 mm I.D. SFC column and a fluid flow-rate of 250 $\mu\text{l}/\text{min}$, the plot of the MH^+ ion abundance for atrazine ($\text{MH}^+ = 216$) as a function of the column oven temperature declines regularly above 120°C and vanishes above 200°C. The regular ion current decrease for tempera-

tures above 120°C also affects the ion currents (not shown) for solvent-derived clusters at low masses, and no total ion current is observed above 200°C. A similar trend was observed when the column oven temperature was kept constant at 80°C and the pinched metal restrictor tip was heated, causing the disappearance of any ion current at restrictor temperatures above 200°C. The workable temperature range at a nearly constant solute response is large enough to encompass common SFC requirements. Nevertheless, reducing the fluid flow-rate narrowed the operating temperature interval, thus showing that heat power to the vaporizing fluid is the relevant experimental factor.

This general SFC–ES–MS trend is similar to the decrease in solvent and solute ions in a thermospray experiment when heat power to the capillary nebulizer exceeds some upper temperature limits [9]. It is now established that optimum ion production in thermospray MS occurs when nearly complete vaporization of the liquid solution is achieved, with a mist of small droplets emerging from the capillary nebulizer. There is much evidence that electrospray ionization can occur in a conventional thermospray ion source, but the process is frequently obscured by gas-

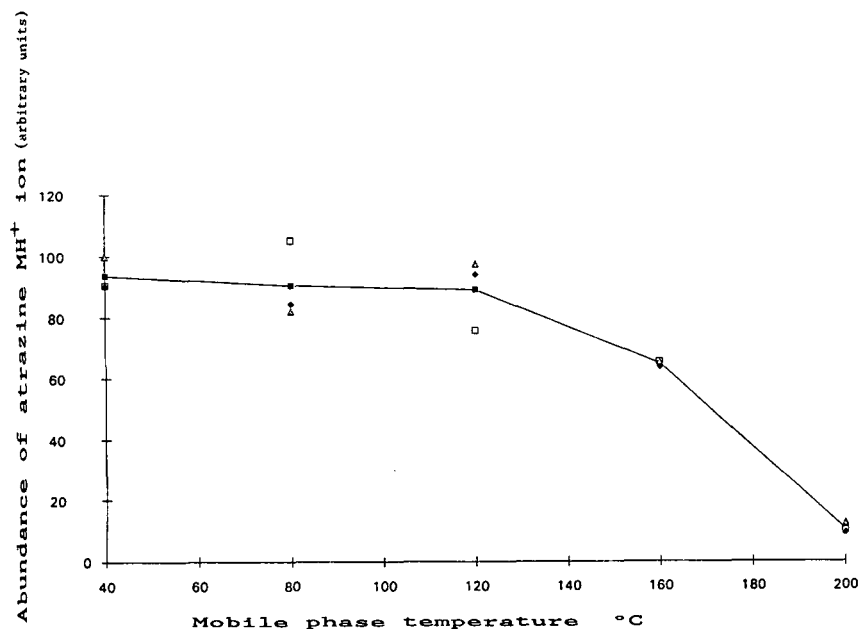


Fig. 3. Effect of the mobile phase temperature on the intensity of the atrazine MH^+ ion. Linear metallized fused-silica restrictor, 25 cm \times 25 μm I.D.; 1 mm I.D. SFC column; mobile phase composition, 8% MeOH–H₂O (95:5, v/v) in 250 $\mu\text{l}/\text{min}$ of CO₂. Data from three sets of experiments with the plot joining mean values.

phase CI reactions. Too high a heat power applied to the vaporizing fluid causes total evaporation inside the capillary, a condition that is known to be undesirable, and in particular, excessive heat is at the origin of thermally induced dissociations frequently observed in thermospray mass spectra of fragile solute molecules [10].

We believe that a same limitation exists with our system. Fluid decompression and cooling produce liquid droplets that are charged by the electrical field beyond the nebulizer end tip. This droplet formation makes possible electrospray ionization in our API source. When excessive heat power is applied prior to fluid decompression, a dry gaseous jet is formed at the nebulizer tip and no ion current is produced.

It should be noted that, under our experimental conditions, low-mass volatile samples can also be ionized by gas-phase CI reactions induced by methanol-derived clusters. During SFC-MS analysis of some low-mass compounds, *e.g.*, Py-I, a decreasing abundance of the solvent cluster ions was recorded when the solute eluted, thus producing an inverted chromatographic elution profile. Such a reactant ion behaviour generally proves the occurrence of gas-phase CI reactions.

SFC mobile phase composition

Solvent and sample ion generation strongly

depends on the mobile phase composition. Pure CO_2 produced no ion for any investigated fluid temperature and flow-rate and API source voltage conditions. The similarity with the absence of ions when non-polar solvents are used in thermospray experiments is also notable [10]. On the other hand, solvent- and solute-derived ions were present when a minimum amount of a polar solvent was added to the mobile phase. Currents for solvent ions (Figs. 4 and 5) and protonated sample molecules (Fig. 6) were recorded when the percentage of a polar mixture of methanol, containing 5% of water, was varied at a constant CO_2 flow rate of 1 ml/min. The observed solvent-derived ions and clusters (Fig. 4) correspond to H_3O^+ (m/z 19), $(\text{CH}_3\text{OH})_n\text{H}^+$ with $n = 1, 2$ (m/z 33, 65), and a mixed cluster $(\text{H}_2\text{O})(\text{CH}_3\text{OH})\text{H}^+$ (m/z 51). The presence of an ion at m/z 61 is more difficult to explain, unless one postulates a reaction involving CO_2 and MeOH that would lead to $\text{CH}_3\text{COOH}_2^+$; this would be the only visible ion arising from CO_2 . Other frequently observed ions in SFC-MS studies using pure CO_2 and a CI source, *e.g.*, $\text{CO}_2^+\bullet$ and higher cluster ions [11], are totally absent here. The ion current trace of the atrazine MH^+ ion (not shown) exhibits a behaviour identical with the total solvent ion response (Fig. 5), with the same maximum when 2–3% of polar modifier is added to CO_2 . The presence of 5% of

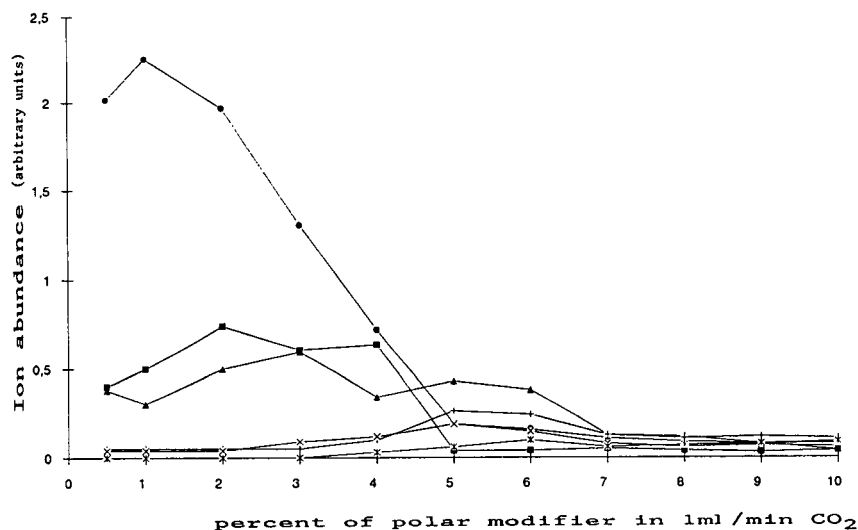


Fig. 4. Effect of the mobile phase composition on solvent-derived ion abundances. Oven temperature, 80°C; linear metallized fused-silica restrictor, 25 cm × 60 μm I.D.; 2.1 mm I.D. SFC column eluted with CO_2 at 1 ml/min and modified with MeOH- H_2O (95:5, v/v). m/z ratio of recorded ions: ▲ = 19; ● = 33; + = 51; × = 61; ■ = 65; * = 83.

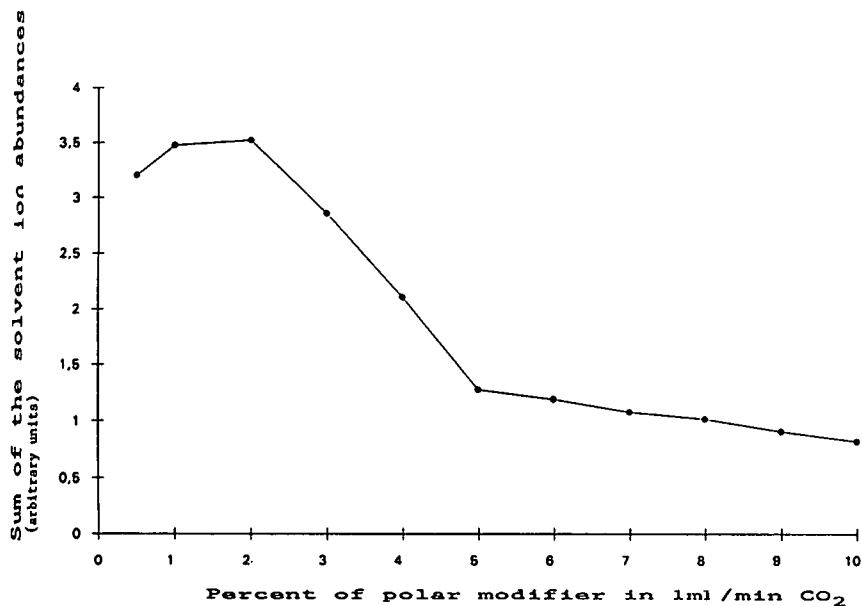


Fig. 5. Sum of solvent ion intensities as a function of the mobile phase composition. Experimental conditions as in Fig. 4.

water in the polar liquid additive was not found to be essential, because similar curves, with a weak signal at m/z 19 and no visible ion at m/z 51, but with intense methanol-derived ions and protonated solute ions, were obtained regularly in later experiments with pure methanol added to CO₂.

Whereas CO₂ does not appear to play any direct role in the ion formation, because of the lack of any abundant CO₂-derived primary ions (with the possible exception of the m/z 61 ion), the methanol- and solute-derived ion currents remain a function of the total mobile phase flow-rate. For example, the plot of the intensity

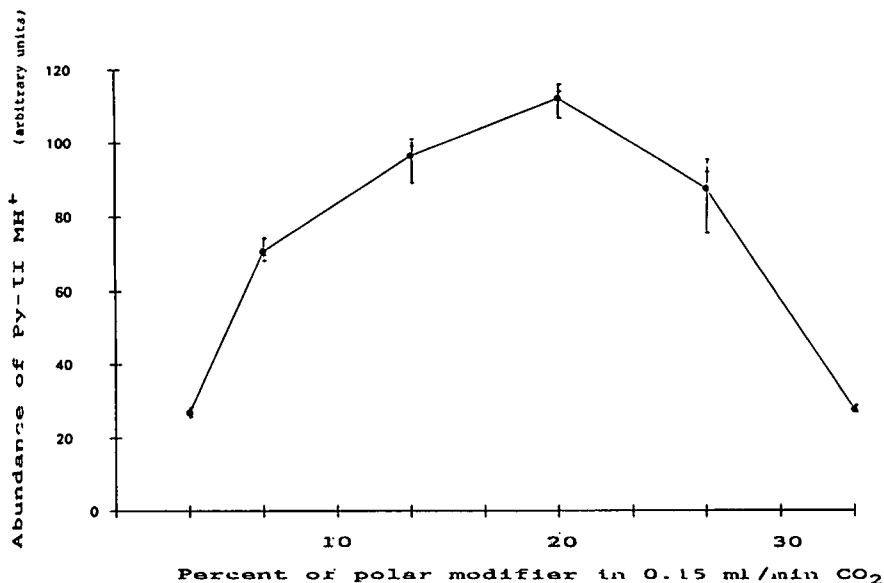


Fig. 6. MH⁺ ion intensity for Py-II, at m/z 229, as a function of the mobile phase composition. Experimental conditions as in Fig. 3, except mobile phase temperature and flow-rate, 120°C and 150 μ l/min, respectively. Added polar modifier: MeOH-H₂O (95:5, v/v).

of the MH^+ ion for Py-II at m/z 229 as a function of the mobile phase composition showed a maximum at a different solvent composition (Fig. 6) when the 1 mm I.D. column was eluted with 150 $\mu\text{l}/\text{min}$ of mobile phase. The total ion current trace for solvent ions (not presented) shows a similar curve. For both curves, the ion formation optimum is shifted to 20% of polar modifier, compared with the 2–3% values observed when the mobile phase flow-rate is 1 ml/min. Despite the apparently different experimental conditions, it should be noted that 20% of a 150 $\mu\text{l}/\text{min}$ flow and 2–3% of a 1 ml/min flow provide roughly the same 20–30 $\mu\text{l}/\text{min}$ of polar modifier to the electrospray region. A strong effect of the CO_2 flow-rate on this sample ion was also observed (Fig. 7) when a 25 $\mu\text{l}/\text{min}$ constant flow-rate of polar modifier and a variable flow-rate of CO_2 in the interval 50–350 $\mu\text{l}/\text{min}$ flowed through the column, while monitoring the Py-II MH^+ ion during sample elution. We cannot fully explain such a strong influence for different CO_2 flow-rates.

A problem will arise when planning to achieve real SFC–ES–MS separations with a gradient of mobile phase composition, because constant ion

formation appears not to be possible. Methods to overcome this limitation, probably by the use of post-column addition of a suitable solvent additive, will be needed. The second consequence is the preferable choice of the 1 mm I.D. column over the 2.1 mm I.D. column for SFC–MS because it allows a wider interval of possible solvent composition. On the other hand, the use of supercritical fluid mixtures with 1–10% of polar modifier at very low CO_2 flow-rates (less than 100 $\mu\text{l}/\text{min}$) was found to be experimentally difficult to achieve reproducibly. The use of very narrow packed SFC columns, of I.D. less than 1 mm, was precluded for this reason.

Nevertheless, there is at least one very important positive influence of the presence of CO_2 , namely the increase in the tolerable input of mobile phase flow-rate into the API source. The basic Analytica ES source is limited to very small liquid flow-rate inputs, below 5 $\mu\text{l}/\text{min}$ [12]. Much higher flow-rates were possible in our experiments, because the decompressing CO_2 acts as a nebulizer gas. We believe that CO_2 has the same beneficial influence on the tolerable fluid input as the added gas in an ionspray experiment [13].

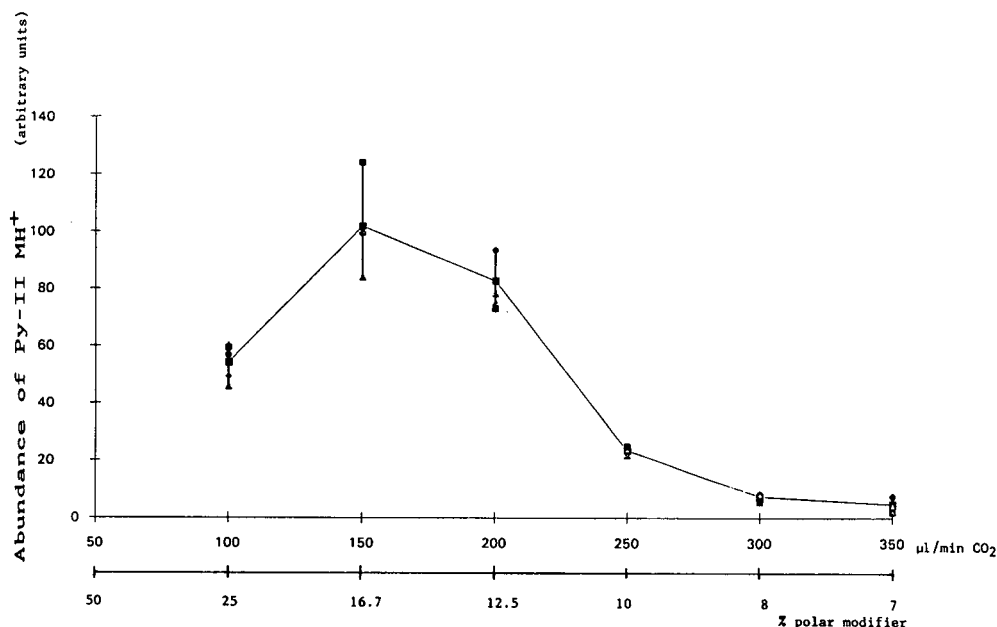


Fig. 7. MH^+ ion intensity for Py-II, at m/z 229, as a function of CO_2 flow-rate. Experimental conditions as in Fig. 3, except, oven temperature, 40°C; constant addition of 25 $\mu\text{l}/\text{min}$ of MeO– H_2O (95:5, v/v) in a variable flow-rate of CO_2 .

Limit of detection and response curve for model compounds

The optimum operating conditions derived from the data in Fig. 4 were selected for the response study of the atrazine MH^+ ion as a function of the injected sample amount, except that the column oven temperature was 80°C . Under these conditions, atrazine is poorly retained and elutes with k' close to 0. The response curve (Fig. 8) is similar to those often produced on electrospray ionization, with a lower detection limit in the low picogram range (Fig. 9), and a rapid signal saturation when nanogram amounts of sample are injected. Although this could be a source of difficulty when analysing real sample mixtures, the observed response curve is different from that in similar SFC–MS studies with gas-phase ionization using a corona discharge [5]. Corona discharge ionization generally exhibits a wider dynamic range of response, and the observed difference is further proof of the liquid-phase ionization mechanism believed to exist under our experimental conditions.

Application to a simple mixture and limitations of the system

The separation of a mixture of four herbicides, containing basic nitrogen functions, was reported previously [1], and was an example of the good sensitivity of the instrument to this class of compounds. Another SFC–MS example, corre-

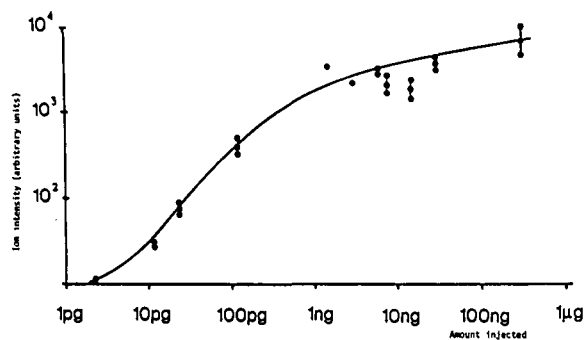


Fig. 8. Atrazine MH^+ ion intensity as a function of the amount injected. Instrument conditions as in Fig. 4, except for a constant solvent composition of 3% of polar additive in CO_2 .

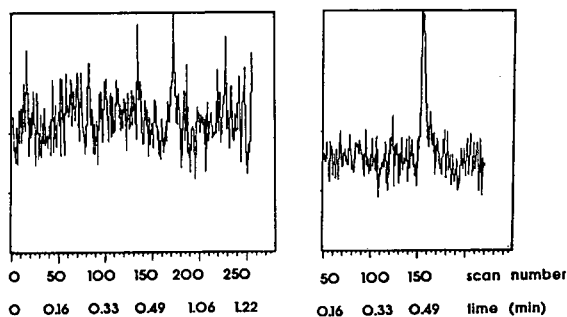


Fig. 9. Detection limit of atrazine MH^+ ion with signal-to-noise ratio = 2 (left) and 5 (right). Conditions as in Fig. 8. Sample concentration, (left) 2 and (right) 10 nmol/l; sample amount deposited on column, (left) 10.4 fmol or 2.2 pg and (right) 52 fmol or 11 pg.

sponding to the separation of the two pyridine derivatives Py-I and Py-II (Fig. 10), illustrates the major difficulty to be overcome in future experiments. The total ion current and selected ion current profiles for solute MH^+ ions were recorded using the 1 mm I.D. column. The poor peak shape of the second peak is notable and was frequently observed for heavier compounds. Intact molecule-derived ions were obtained for many organic compounds, including mixtures of polyethylene oligomers with molecular masses above 1000, but the eluting peaks were generally useless owing to excessive tailing. We believe that peak asymmetry is due to cold trapping at the nebulizer tip. The peak asymmetry was reduced when the restrictor or the mobile phase was heated, but this also decreased the ion currents (Fig. 3), hence the operating temperature was often a compromise between conservation of chromatographic peak integrity and good MS sensitivity. We expect to improve the situation by the design of an optimized nebulizer, rather than the crude system used in this work. We have observed that most of the trapped sample is retained on the outer surface of the capillary nebulizer end, and a liquid sheet of methanol, or another suitable polar solvent, could continuously wash this surface. Post-SFC column addition of the polar additive would also provide ES ionization more independent of the chromatographic requirements of the mobile phase composition.

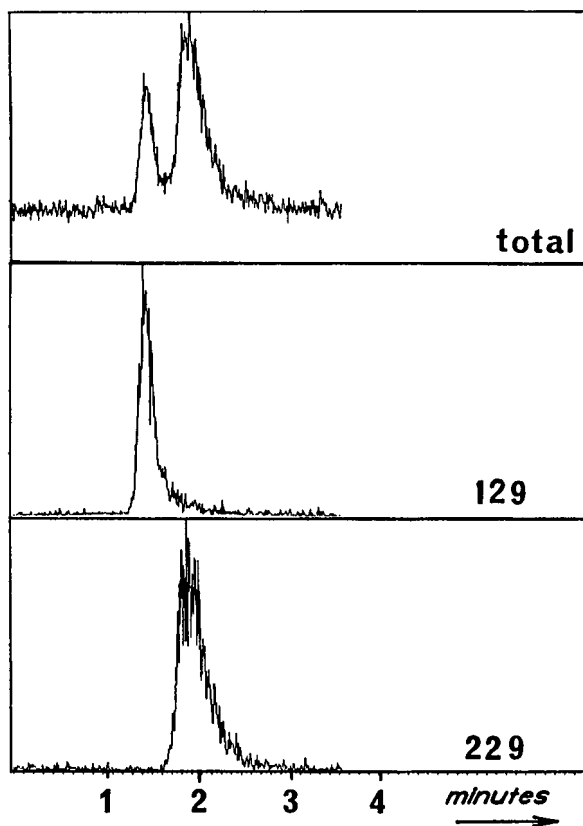


Fig. 10. SFC–MS analysis of a mixture of two pyridine derivatives. Top trace: total ion current recording for ions with $m/z > 100$. Middle and bottom traces: selected ion current profiles for solute MH^+ ions (m/z 129 and 229). Instrument conditions as in Fig. 3, except oven temperature, 50°C, and a constant fluid composition of 3% of polar modifier in CO_2 .

CONCLUSIONS

The possibility of producing solute ions from a packed SFC column in the absence of a corona discharge has been demonstrated, using a stan-

dard electrospray ion source of the type normally designed for liquid solution sampling. A polar modifier must be present for the production of sample ions. Some of the polar additive could be added postcolumn to provide SFC–ES–MS conditions more independent of the chromatographic requirements, especially when using a gradient of mobile phase composition. At present the potential application of the liquid-phase ionization process involved in the ion formation mechanism to the determination of high-mass and polar samples is not fully exploited, because our required mild nebulizing conditions are still too disturbing to the conservation of chromatographic peak integrity.

REFERENCES

- 1 P.J. Arpino, F. Sadoun and H. Virelizier, *Chromatographia*, 37 (1993) 1.
- 2 P. Arpino, *J. Chromatogr.*, 323 (1985) 3.
- 3 J.B. Fenn, M. Mann, C.K. Meng, S.F. Wong and C.M. Whitehouse, *Mass. Spectrom. Rev.*, 9 (1990) 37.
- 4 T. Fujii, *Anal. Chem.*, 64 (1992) 775.
- 5 E. Huang, J. Henion and T.R. Covey, *J. Chromatogr.*, 511 (1990) 257.
- 6 F. Anacleto, L. Ramaley, R.K. Boyd, S. Pleasance, M.A. Quilliam, P.G. Sim and F.M. Benoit, *Rapid Commun. Mass Spectrom.*, 5 (1991) 149.
- 7 K. Matsumoto, S. Nagata, H. Hattori and S. Tsuge, *J. Chromatogr.*, 605 (1992) 87.
- 8 D. Nizery, D. Thiebaut, M. Caude, R. Rosset, M. Lafosse and M. Dreux, *J. Chromatogr.*, 467 (1989) 49.
- 9 M.L. Vestal and G.J. Fergusson, *Anal. Chem.*, 57 (1985) 2373.
- 10 P. Arpino, *Mass Spectrom. Rev.*, 9 (1990) 13.
- 11 J. Cousin and P. Arpino, *J. Chromatogr.*, 398 (1987) 125.
- 12 C.M. Whitehouse, R.N. Dreyers and J.B. Fenn, *Anal. Chem.*, 57 (1985) 675.
- 13 T.R. Covey, R.F. Bonner, B.I. Shushan and J.D. Henion, *Rapid Commun. Mass Spectrom.*, 2 (1988) 249.

CHROMSYMP. 2790

Capillary zone electrophoresis–ionspray mass spectrometry of a synthetic drug–protein conjugate mixture

R. Kostiainen[☆], E.J.F. Franssen and A.P. Bruins*

University Centre for Pharmacy, Antonius Deusinglaan 2, 9713 AW Groningen (Netherlands)

ABSTRACT

Low-molecular-mass proteins, such as lysozyme, may be suitable carriers to target drugs to the kidney. Naproxen, an anti-inflammatory drug, has been conjugated with lysozyme via a covalent amide bond formed between the carboxylic acid function of naproxen and the amino group of one of the lysines in lysozyme. The reaction products were analysed by capillary electrophoresis–ionspray mass spectrometry. Native lysozyme and its conjugates with one, two and three naproxen molecules were separated and their identities were confirmed by mass spectrometry. The ion current profiles of the individual conjugates showed pH-dependent tailing and adsorption–desorption phenomena in the capillary electrophoresis column not observed in the total ion current profiles and not observable by UV detection.

INTRODUCTION

Research on new drugs requires well characterized materials. The combination of an efficient separation method with a mass spectrometer can be used for quality control of pure drugs and for the structure elucidation of individual components in a reaction mixture obtained in drug synthesis.

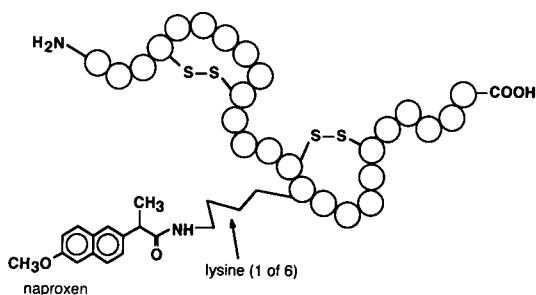
One-line gas chromatography–mass spectrometry (GC–MS) is used routinely in biomedical research. Liquid chromatography–mass spectrometry (LC–MS) has matured over the past 10 years and is now indispensable in the investigation of drug synthesis and drug metabolism. The obvious benefits of GC–MS and LC–MS have

spurred the development of capillary electrophoresis–mass spectrometry (CE–MS). CE–electrospray MS and CE–ionspray MS have been shown to be powerful techniques in the separation and analysis of large proteins [1,2]. The recently introduced LC–MS interfaces, continuous-flow fast atom bombardment (CF–FAB) [3], electrospray [4,5] and ionspray [6] (pneumatically assisted electrospray), are suitable techniques for the combination of CE with MS [7,8,9]. However, FAB is not a suitable ionization technique for large biomolecules, whereas molecules of $M_r > 100\,000$ can be analysed using the electrospray technique [10].

Low-molecular-mass proteins, such as lysozyme, may be suitable carriers to target drugs to the kidney. Naproxen, an anti-inflammatory drug, has been conjugated with lysozyme via a covalent amide bond formed between the carboxylic acid function of naproxen and the amino group of one of the lysines in lysozyme, and the pharmacokinetics of the conjugate have been

* Corresponding author.

* On temporary leave from the Food and Environmental Laboratory of Helsinki, Helsinginkatu 24, 00530 Helsinki, Finland.



studied [11,12]. The synthetic 1:1 conjugate was purified by preparative ion-exchange fast protein liquid chromatography (FPLC). Under the conditions chosen for preparative FPLC, native lysozyme was separated from the 1:1 conjugate. Higher conjugates of naproxen with lysozyme (2:1, 3:1, etc.) were expected but not observed. In this study we apply CE-ionspray MS to the identification of the conjugates.

EXPERIMENTAL

Naproxen (Sigma) was coupled to lysozyme (Sigma) by the N-hydroxysuccinimide method described in detail previously [11,12]. The raw product (1 mg) was dissolved in the buffer (1 ml) used in CE. Injections were made with a Prince (Lauerlabs, Emmen, Netherlands) microprocessor-controlled injector using electrokinetic injection at 30 kV for 9 s. The electrophoresis voltage of 30 kV was provided by a Glassman (Whitehouse Station, NJ, USA) EH30R00.5-22 power supply controlled by the Prince. The fused-silica capillary (deactivated, 60 cm \times 50 μ m I.D., part No. 062804) was obtained from SGE (Melbourne, Australia). Unfortunately, the manufacturer does not provide information about the nature of the deactivation. The buffer solution used was 100 mM ammonium acetate in water purified using a Milli-Q system (Millipore) and the pH was adjusted to 4.6 and 5.6 with acetic acid.

The fused-silica capillary was inserted into a coaxial ionspray interface (Fig. 1). A voltage of 3 kV was applied to the stainless-steel tube (10 cm \times 0.4 mm I.D.). The nebulizing gas (99.9% nitrogen) pressure was 3 bar. A make-up flow (5 μ l/min) was provided by a Micro Gradient

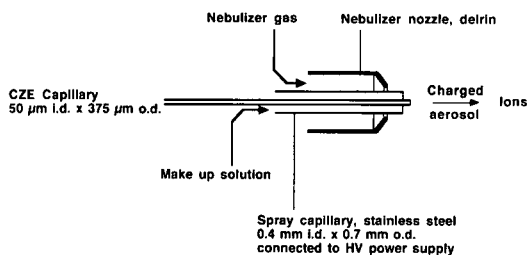


Fig. 1. Schematic illustration of the coaxial interface for combined capillary electrophoresis-ionspray mass spectrometry. HV = High voltage.

System syringe pump (ABI/Brownlee, Santa Clara, CA, USA). The make-up solution was water-methanol-acetic acid (40:60:1, v/v/v).

The mass spectrometer was a Nermag R 3010 (Delsi-Nermag, Argenteuil, France) equipped with a custom-built prototype atmospheric pressure ionization (API) source described previously [13]. Nitrogen (99.9%) was used as a curtain gas. The spectra were recorded in the positive-ion mode with a nozzle-skimmer voltage difference of 120 V. The mass spectrometer was scanned from m/z 1200 to 2000 with a cycle time of 1.5 s per scan. Interface and ion source tuning was done by means of the Prince by continuous pressure feed (50 mbar) of a sample solution via the CE capillary. The sample solution flow was combined with a make-up flow in the coaxial CE-MS interface. Accurate mass measurements on the sample mixture were made in the profile mode of the data system, under the same sample and make-up flow conditions as used for source and interface tuning.

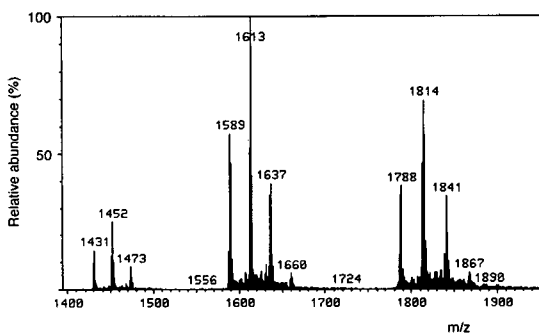


Fig. 2. Ionspray mass spectrum obtained by continuous pressure feed via a CE capillary of the reaction mixture obtained from the synthesis of conjugates of naproxen (M_r 230) with lysozyme (M_r 14 305).

RESULTS AND DISCUSSION

Fig. 2 shows the ionspray spectrum obtained by continuous pressure feed of the sample solution (in buffer of pH 4.6) via the CE capillary, combined with a make-up flow of water–methanol–acetic acid (40:60:1, v/v/v). The spectrum shows ions of charge state 8, 9 and 10 at m/z 1786–1890, 1587–1662 and 1429–1496, respectively. The ion series at m/z 1431, 1589 and 1788 corresponds to lysozyme carrying ten, nine and eight protons, respectively. The reaction products give rise to the series m/z 1452, 1613, 1814, to the series 1473, 1637, 1841 and to the series 1494, 1660 and 1867. Accurate m/z values were measured separately in the profile mode. The molecular masses can be determined from the measured m/z values using a simple algorithm presented previously [14]. The determined average molecular masses are 14 303.7, 14 516.0, 14 728.7 and 14 938.9. These values correspond to native lysozyme and 1:1, 2:1 and 3:1 naproxen–lysozyme conjugates, for which the calculated average molecular masses are 14 305.2, 14 517.4, 14 729.6, 14 941.8, respectively. The determined values are slightly below the calculated values, but the error is only 1 in 10^4 and the results confirm the presence of the naproxen conjugates in the sample. The calculated increment for the covalent bond between naproxen and one of the lysines in lysozyme through formation of an amide is 212 u. If complexation had taken place via non-covalent bonds, the observed mass increment for a naproxen molecule bound to lysozyme would have been 230 u, which is not observed and clearly not the case in the reaction product.

Next, the conjugates were separated and identified by on-line CE–MS. A commercially available deactivated column was used to minimize the adsorption of lysozyme and its conjugates. Basic proteins such as lysozyme have been reported to adsorb on the walls of undeactivated bare fused-silica CE capillaries [2,15]. Figs. 3 and 4 show the separation of lysozyme and its three naproxen conjugates (1:1, 2:1 and 3:1) at pH 4.6 and 5.6, respectively. Lysozyme and its conjugates can just be separated at pH 4.6 (Fig. 3). The spectra recorded for each compound

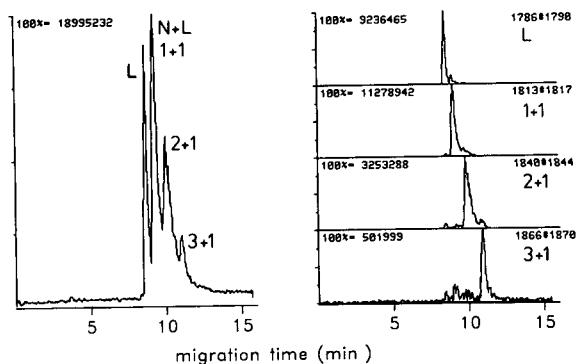


Fig. 3. Total ion current trace and ion current traces of individual components obtained by CE–MS at pH 4.6.

confirm the presence of native lysozyme and 1:1, 2:1 and 3:1 naproxen–lysozyme conjugates. The ion current profiles of the individual components with eight charges show some residual tailing due to sample adsorption. At pH 5.6 (Fig. 4) the separation is seemingly improved in the total ion current trace. However, the ion current profiles of the individual components show that lysozyme is apparently adsorbed on the column, but displaced and released when the 1:1 conjugate elutes. At pH 4.6 the averaged mass spectrum of the 1:1 conjugate recorded in scans 253–264 (Fig. 5, top) and the averaged mass spectrum of the 2:1 conjugate recorded in scans 277–279 (Fig. 5, bottom) contain minor contributions of earlier eluting components at m/z 1788 (top) and at m/z 1816 (bottom). The peak at m/z 1788, due to native lysozyme (indicated with an arrow) in the mass spectrum of the 1:1 conjugate re-

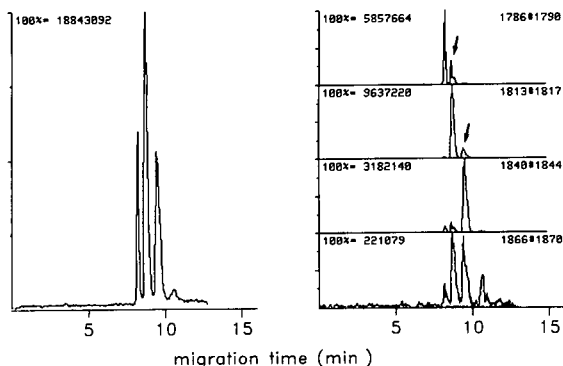


Fig. 4. Total ion current trace and ion current traces of individual components obtained by CE–MS at pH 5.6.

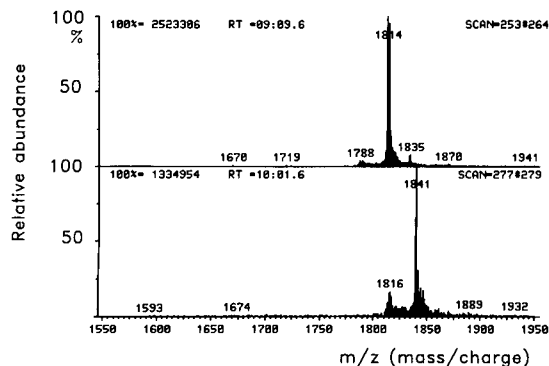


Fig. 5. Ionspray mass spectra of the 1:1 and 2:1 naproxen-lysozyme conjugates obtained by CE-MS at pH 4.6.

corded in scans 243–246 (Fig. 6, top) and the peak at m/z 1816 due to the 1:1 conjugate in the mass spectrum of the 2:1 conjugate recorded in scans 263–272 (Fig. 6, bottom) demonstrate that interference from earlier eluting components is stronger at pH 5.6. Explaining the inference noted above by adsorption and displacement may seem speculative. A more thorough discussion would require knowledge of the modification of the capillary wall. Unfortunately, such information is not available as the CE capillary is deactivated by a proprietary process. Mass spectrometric fragmentation of sample ions with loss of naproxen under the conditions chosen in this study can be ruled out. First, the ion source and ion transport conditions were mild enough to prevent fragmentation. Second, the interference problem observed is clearly pH dependent. Frag-

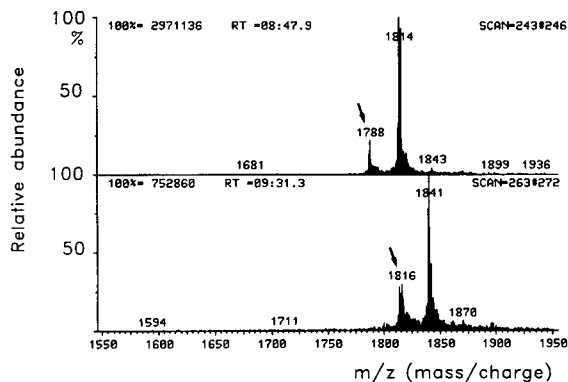


Fig. 6. Ionspray mass spectra of the (top) 1:1 and (bottom) 2:1 naproxen-lysozyme conjugates obtained by CE-MS at pH 5.6. The arrows point to co-eluting native lysozyme (m/z 1788) and 1:1 naproxen-lysozyme (m/z 1816).

mentation by collision-induced dissociation inside the mass spectrometer would be entirely dependent on the voltage settings of ion optics elements, which were kept the same in all experiments.

The 3:1 conjugate, which is a minor component in the mixture, was split into four peaks, in particular at pH 5.6 as shown in Fig. 4. Protein adsorption alone cannot account for the observation made here. We assume that relatively large amounts of lysozyme and its 1:1 and 2:1 conjugates apparently carry small amounts of the 3:1 conjugate in their zones. The problems observed in our experiments cannot be detected by non-specific detectors such as a UV detector. This highlights one of the advantages of the use of a mass spectrometer as a detector in CE.

The peak areas of the individual compounds in the ion current profiles in Fig. 3 show that the relative amounts of the native lysozyme and the 1:1, 2:1 and 3:1 conjugates are about 70, 100, 40 and 5%, respectively. These relative amounts correspond well to the relative abundances of the native lysozyme and its conjugates in the spectrum recorded without separation by continuous pressure feed of the sample solution (Fig. 2).

The spectra recorded by continuous pressure feed showed ions of charge states 10, 9 and 8. In contrast, the spectra recorded with CE-MS showed only ions of charge state 8. As the mass range of our instrument is limited to m/z 2000, we cannot observe the expected ions of charge states 7 and 6. The shift to lower charge states also takes place when the high voltage (30 kV) is applied to the front end of the CE capillary during continuous pressure feed of the sample. These results show that the electrophoretic transport of ions in the CE capillary influences the electrospray ionization process. For unknown reasons, lysozyme and its conjugates appear to collect fewer protons when +30 kV is applied to the front end of the CE capillary. This phenomenon will be studied further in the future.

ACKNOWLEDGEMENT

The authors thank H.H. Lauer (Lauerlabs) for the loan of the Prince injector and Glassman power supply.

REFERENCES

- 1 R.D. Smith, H.R. Udseth, C.J. Barinaga and C.G. Edmonds, *J. Chromatogr.*, 559 (1991) 197.
- 2 P. Thibault, C. Paris and S. Pleasance, *Rapid Commun. Mass Spectrom.*, 5 (1991) 484.
- 3 R.M. Caprioli (Editor), *Continuous-Flow Fast Atom Bombardment Mass Spectrometry*, Wiley, New York, 1990.
- 4 H. Yamashita and J.B. Fenn, *J. Phys. Chem.*, 88 (1984) 4451.
- 5 M.L. Aleksandrov, L.N. Gall, N.V. Krasnov, V.I. Nikolaev and V.A. Shkurov, *Zh. Anal. Khim.*, 40 (1984) 1570.
- 6 A.P. Bruins, T.R. Covey and J.D. Henion, *Anal. Chem.*, 59 (1987) 2642.
- 7 M.A. Moseley, L.J. Deterding, K.B. Tomer and J.W. Jorgenson, *J. Chromatogr.*, 480 (1989) 197.
- 8 R.D. Smith, C. Barinaga and H.R. Udseth, *Anal. Chem.*, 60 (1988) 1948.
- 9 E.D. Lee, W. Mück, J.D. Henion and T.R. Covey, *Biomed. Environ. Mass Spectrom.*, 18 (1989) 844.
- 10 J.B. Fenn, M. Mann, C.K. Meng, S.F. Wong and C.M. Whitehouse, *Science*, 246 (1989) 64.
- 11 E.J.F. Franssen, R.G.M. van Amsterdam, J. Visser, F. Moolenaar, D. de Zeeuw and D.K.F. Meijer, *Pharm. Res.*, 8 (1991) 1223.
- 12 E.J.F. Franssen, J. Koiter, C.A.M. Kuipers, A.P. Bruins, F. Moolenaar, D. de Zeeuw, W.H. Kruizinga, R.M. Kellogg and D.K.F. Meijer, *J. Med. Chem.*, 35 (1992) 1246.
- 13 A. Raffaelli and A.P. Bruins, *Rapid Commun. Mass Spectrom.*, 5 (1991) 269.
- 14 M. Mann, C.K. Meng and J.B. Fenn, *Anal. Chem.*, 61 (1989) 1702.
- 15 H.H. Lauer and D. McManigill, *Anal. Chem.*, 58 (1986) 166.

CHROMSYMP. 2794

Off-line coupling of capillary electrophoresis with matrix-assisted laser desorption mass spectrometry

P.A. van Veelen and U.R. Tjaden*

Division of Analytical Chemistry, Leiden-Amsterdam Center for Drug Research, P.O. Box 9502, 2300 RA Leiden (Netherlands)

J. van der Greef

Division of Analytical Chemistry, Leiden-Amsterdam Center for Drug Research, P.O. Box 9502, 2300 RA Leiden (Netherlands) and Department of Structure Elucidation and Instrumental Analysis, HVV-TNO, P.O. Box 360, 3700 AJ Zeist (Netherlands)

A. Ingendoh and F. Hillenkamp

Institute for Medical Physics and Biophysics, University of Münster, W-4400 Münster (Germany)

ABSTRACT

Capillary electrophoresis was coupled off-line with matrix-assisted laser desorption mass spectrometry. Special attention was paid to minimizing loss of the achieved electrophoretic resolution, which was realized by appropriate voltage programming during the sampling of the analytes migrating out of the capillary. Different modes of coupling these techniques are discussed in terms of resolution, sensitivity and ease of handling.

INTRODUCTION

Capillary electrophoresis (CE) has since 1981 grown into a separation technique characterized by speed, high efficiencies and small sample volumes [1]. Detection usually takes place on-capillary using UV absorbance or laser-induced fluorescence (LIF), or, more recently, by on-line coupling to a mass spectrometer equipped with a continuous-flow fast atom bombardment (FAB) or electrospray (ES) interface.

Matrix-assisted laser desorption ionization mass spectrometry (MALDI-MS) has since 1988 rapidly developed into a very sensitive and fast

MS technique capable of analysing high molecular masses, up to 300 000, by irradiation of small sample spots.

The characteristics of both methods makes coupling in principle very attractive. On-line coupling is not as easy to achieve as, for example, with ES-MS, which, as a liquid introduction system, is easily coupled. Therefore, the off-line coupling of CE and MALDI-MS has been investigated, with the obvious advantage that both techniques can be optimized separately. On-line LC-laser desorption MS of some small compounds ($M_r < 300$) without use of a matrix was reported in 1984 [3]. Until now the off-line coupling of CE with desorption MS methods, such as plasma desorption (PD) MS and MALDI-MS, has been achieved by fraction collection of peptides and proteins, using a porous glass

* Corresponding author.

joint to complete the electrical circuit at the cathodic end of the column [4,5].

We here report the off-line coupling of CE and MALDI-MS by collecting the effluent on a moving belt-like system, after which the trace is subsequently scanned by the laser beam. The main objective of the study was to investigate whether the high resolution obtained in the CE system could be maintained using this off-line coupling procedure. The various aspects of this approach will be discussed in terms of resolution, sensitivity and ease of use. The results using this approach are compared with those achieved with fraction collection.

EXPERIMENTAL

Chemicals

All chemicals, unless otherwise stated, were purchased from Merck (Darmstadt, Germany). The buffers used (sodium phosphate, ammonium phosphate, ammonium acetate and ammonium hydrogencarbonate) were all at 7 mM concentration and pH 8.5. The β -endorphins were a gift from Organon (Oss, Netherlands), and used without further purification.

Capillary electrophoresis

CE was performed in untreated fused-silica capillaries with an internal diameter of 75 μm (SGE, Milton Keynes, UK). The capillary length was 1 m in all cases. The on-capillary UV detection was realized by creating a window made by burning off the coating of the capillary over a length of 5 mm, at a distance of 54 cm from the anodic end of the capillary. Effluent collection at the end of the capillary was done by appropriate timing. Before starting an electrophoresis run, the capillary was flushed with the buffer solution for 30 mins.

The samples were injected using a PRINCE (PRogrammable INjector for CE) purchased from Lauerlabs (Emmen, Netherlands). Injections were made hydrodynamically by applying a pressure of 10 mbar for 10 s (8 nl) in most cases. In some cases larger volumes of up to 48 nl were injected (60 mbar for 10 s). The PRINCE system allows easy and fast switching between several voltages and/or pressures in a well-defined way,

which makes the collection and deposition procedures very reproducible.

The high-voltage power supply (up to 30 kV) was obtained from Lauerlabs, and was set at 30 kV during the CE separations, with a resultant current of 15 μA , which was measured post capillary using a Model 8062 A multimeter (Fluke, Tilburg, Netherlands). Deposition of the effluent took place directly on a laser desorption target, made of stainless steel, which acted as the cathode. During the analyte collection and deposition, normally 5 kV were applied.

Addition of a sheath flow was accomplished by a Model 22 syringe infusion pump (Harvard Apparatus, South Natick, MA, USA), with the following assembly. The cathodic end of the separation capillary was inserted into a 300 μm I.D. fused-silica capillary via a T-piece. The matrix solution was added through the annular space between both capillaries at a flow-rate of 0.3 $\mu\text{l}/\text{min}$.

UV detection was done using a Kratos 757 Spectroflow absorbance detector (ABI, Maarsse, Netherlands), in which a home-made detection cell with an illuminated volume of about 7 nl was installed.

Mass spectrometry

The mass spectrometer used was a VISION 2000 reflector-type time-of-flight laser desorption instrument (Finnigan MAT, Bremen, Germany) equipped with a Q-switched (5 ns) frequency-tripled Nd-YAG laser (Speser 600, Spektrum, Berlin, Germany), operating at a wavelength of 355 nm. The laser beam was focused at the sample surface to a spot diameter of 70 μm with irradiances between 10^6 and 10^7 W/cm^2 , close to the threshold for obtaining ions in all cases. The ions generated were accelerated to a potential of 5 kV in the ion source and post-accelerated to a potential of 10 kV for detection with a secondary electron multiplier. Registration of the analogue signal was performed with a transient recorder (LeCroy 9450) with a 5 ns per channel resolution. The acquired spectra consisted of the sum of twenty single acquisitions. They were internally calibrated using the known masses of the matrix peaks.

The VISION 2000 offers the opportunity to

observe the sample by a camera mounted on the end of a microscope with a lateral resolution of approximately 10 μm . Thus control of the sample and selection of different sites of it during the measurement is possible. Every spot on the target can be reached for irradiation by means of an x - y manipulator.

The matrix used was 2,5-dihydroxybenzoic acid (DHB) at a concentration of 10 g/l in water [6]. It was added in an approximately 1000-fold molar excess to the analytes. After deposition on a stainless-steel target, it was air dried and introduced into the mass spectrometer.

RESULTS AND DISCUSSION

The molecular masses of the three investigated β -endorphins are listed in Table I. As a first step, the detection limit of the compounds was determined by using the normal preparation, *i.e.* by dripping a dilute solution, both in water and in buffer solution, onto the target and adding some matrix solution [6]. The detection limits were determined in a mixture, since suppression effects do not play a significant role in MALDI-MS. The detection limits for all compounds of interest were 10 fmol, determined from a pure water solution as well as from the buffer solution. A spectrum is shown in Fig. 1. As can be seen, only the sodium and potassium cationized molecules were detected. Apparently, the peptides have a great affinity for these cations. The absolute amount of 10 fmol was loaded on the target in a 0.5- μl droplet, corresponding to a concentration of 20 pmol/ml. When capillary electrophoresis is used as a separation system it must be considered, owing to the very small

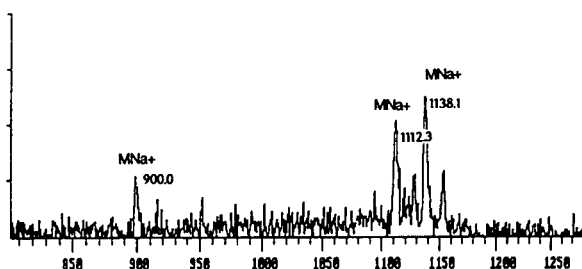


Fig. 1. Matrix-assisted laser desorption mass spectrum obtained from 10 fmol per component of the β -endorphin mixture using DHB as a matrix. The concentration of the loaded sample solution was $2 \cdot 10^{-9}$ M.

injection volumes of about 10–50 nl, that the above-mentioned concentration corresponds to an absolute amount of material between 200 and 1000 amol, which is far below the detection limit. This means that higher concentrations are necessary to obtain any signal.

We used MALDI-MS for qualitative determination, *i.e.* to reveal the identity of the analyte.

A typical electropherogram of three β -endorphins using on-capillary UV detection is shown in Fig. 2. The plate numbers of the different peaks are between 100 000 and 150 000. This electropherogram was recorded using a 7 mM sodium phosphate buffer (pH 8.5). This relatively high pH was used to prevent analyte adsorption to the wall since at this pH both the wall and the analytes have a negative charge.

Since this buffer is not very suitable for combination with MS, several other buffers containing ammonium acetate, ammonium hydrogencarbonate and ammonium phosphate were studied. The separations based on ammonium hydrogencarbonate appeared to be rather poor, while

TABLE I

LIST OF THE AMINO ACID SEQUENCES AND THE MOLECULAR MASSES OF THE THREE β -ENDORPHIN FRAGMENTS USED

Peptide	Amino acid sequence	Average mass (MH^+)	Average mass (MNa^+)	Average mass (MK^+)
β -End 8–17	EKSQTPLVTL	1116.3	1138.3	1154.3
β -End 6–15	TSEKSQTPLV	1090.2	1112.2	1128.2
β -End 6–13	TSEKSQTP	877.9	899.9	915.9

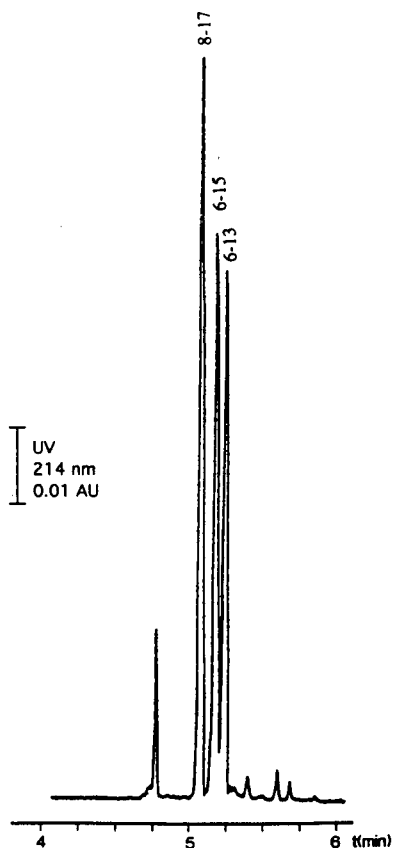


Fig. 2. On-capillary UV detection trace of the separation of three β -endorphins. $V_{inj} = 8$ nl; $[C] = 300 \mu\text{g/ml}$; $L_{cap} = 1$ m (54 cm to detector), $I.D._{cap} = 75 \mu\text{m}$; Buffer = 7 mM ammonium phosphate. Plate numbers are between 100 000 and 150 000.

with ammonium phosphate the same results as with sodium phosphate could be obtained.

In the case of PD-MS, buffers which have ammonium as a cation are not troublesome [7], even if they are not volatile. This is in contrast with ES-MS, in which non-volatile buffers can contaminate the source. Since in PD-MS and MALDI-MS only a negligible fraction of the sample is consumed, the enormous excess of non-volatile material does not cause contamination problems. Therefore, it was decided to continue with the ammonium phosphate buffer.

Off-line coupling of the CE-separated analytes with MALDI-MS was first studied using fraction collection, which can take place in several ways. The use of a porous glass joint close to the end of the capillary, which serves to decouple the

high voltage from the capillary outlet [4,5], enables the collection of fractions without disturbing the CE process. The fractions can subsequently be analysed by mass spectrometry.

Our first approach was to perform the electrophoresis until the separated analytes reached the very end of the capillary, then switch off the high voltage and subsequently apply a pressure to the anodic end of the capillary, thereby pushing out the separated fractions for fraction collection.

The result is depicted in Fig. 3 for different pressures. The situation at the cathodic end of the capillary is mimicked by performing the analogous experiment in front of the UV window. It can be seen that the resolution was strongly reduced when pressures between 60 and 30 mbar were applied, because of the laminar-flow profile generated in the capillary. At 20 mbar, and especially at 10 mbar, there is hardly any loss of resolution. The high voltage only

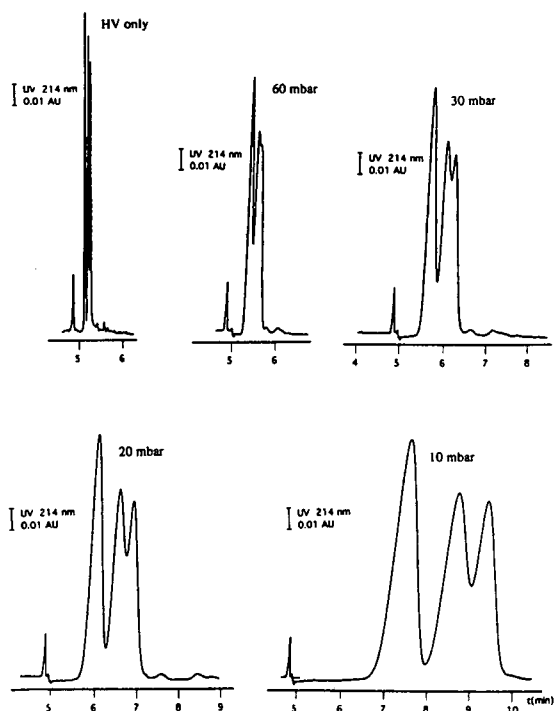


Fig. 3. The effect of pressures applied, for pushing out the effluent at the capillary outlet, after switching the high voltage off, is shown for several pressures. The high voltage-only picture is the reference electropherogram run under pure CE conditions.

electropherogram, *i.e.* without pressure, has been added as a reference electropherogram in the figure. An additional helpful effect of the application of low pressure is the very low flow-rate in the capillary, leading to an expanded time-scale, which is favourable for collecting such very close peaks. The volumes of the various peaks remain the same, and are difficult to handle. The various fractions were therefore collected in small vials containing 1 μ l of matrix solution. This solution was subsequently loaded onto a MALDI-MS target for further analysis. A major disadvantage of this fraction collection procedure is the dilution factor, which is approximately 5.

Using this method, the resolution is not seriously affected when the low pressure is applied for only several minutes. When the porous glass joint approach [4,5] is used, the analytes move out of the capillary after passing the electrical decoupling point in a laminar-flow mode. When 30 kV is applied over the separation capillary, an electroosmotic flow is generated similar to a hydrodynamic flow obtained with a pressure drop of 90 mbar (see Table II). This implies that during electrophoresis in the post-porous joint part of the capillary a laminar flow is induced, which causes a dramatic loss of resolution (see also Fig. 3). The required resolution for our problem and for all closely separated compounds will therefore be lost and the method in such cases will be less useful.

TABLE II

ELUENT FLOW THROUGH THE SEPARATION CAPILLARY AS A RESULT OF THE APPLIED ELECTRICAL FIELD OR AS A RESULT OF DIFFERENT APPLIED PRESSURES AT THE ANODIC END OF THE CAPILLARY

Pressure (mbar)	Voltage (kV)	Flow (nl/s)
0	30	7.3
10	0	0.8
20	0	1.6
30	0	2.3
50	0	3.9
60	0	4.7
90	0	7.0

Another way of maintaining resolution during fraction collection is by lowering the high voltage from, for example, 30 to 5 kV, when the analytes have reached the capillary outlet. In principle, the contact to the target, which is at earth potential, should be maintained all the time. However, it appeared in practice this is not necessary when the applied high voltage does not exceed 10 kV. The contact could be interrupted several times, for changing the collection vials, without disturbing the resolution of the electrophoresis. Collection in this way is quite convenient, although still very small volumes must be handled. The time scale can be elongated to any desired size, analogous to the case in which small pressures are applied.

The last method investigated was deposition of the effluent on a moving belt-like system, followed by scanning the deposited electropherogram with the laser beam in the ion source of the mass spectrometer. Deposition of CE effluents on a moving belt system has been reported [8,9]. In this case the effluent is deposited on a blotting membrane and further analysed by protein chemical methods. In our case the moving belt-like system was a moveable laser desorption target, which was part of the electrical circuit.

Deposition of the effluent can be done in a continuous as well as in a stepwise manner, when either pressure or a lowered high voltage is applied, as described above. It appeared that application of a high voltage yields the best results. Therefore, this method was used in combination with the moveable target system.

Continuous deposition of the effluent on a moving target is in principle the best way of maintaining resolution. By appropriate tuning of the target speed, the total electropherogram can be transferred to the target without loss of resolution. Care must be taken not to dilute the analytes over a too large surface area.

In practice, it is easier to deposit the effluent by moving the belt in a stepwise manner, and break the contact at every step for a very short period. As discussed above, the procedure does not cause the electrophoresis performance to deteriorate, and can be tuned just as well as in case of continuous deposition. Since the time-scale can be optimized as desired by choosing the

appropriate voltage, as in the case of fraction collection, this stepwise mode is similar to the continuous mode. An advantage of stepwise deposition is the resulting higher surface density of the collected analytes, which is favourable for MALDI-MS. A severe problem that also occurs in direct deposition onto a laser desorption target is the tiny amount of effluent (approximately 1 nl/s at 5 kV). This problem has been solved by application of a sheath flow-at a rate of 0.3 $\mu\text{l}/\text{min}$. This sheath flow contained the matrix needed for MALDI-MS. Depositing new droplets every 30 s yielded drops of about 180 nl. After drying the droplets, nice crystals were observed through the camera mounted on the

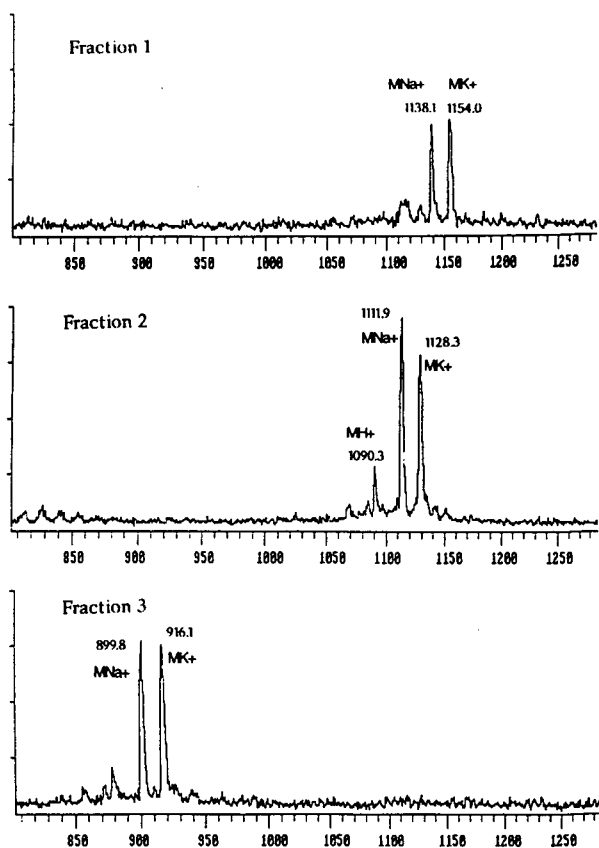


Fig. 4. Mass spectra of the separated compounds collected on the moveable target system, after changing the high voltage from 30 to 5 kV. As can be seen, the several fractions are not contaminated with components of other fractions. $V_{\text{inj}} = 8 \text{ nl}$, $[C] = 300 \mu\text{g}/\text{ml}$, corresponding to 2.4 pmol per component. The corresponding electropherogram is shown in Fig. 2.

laser desorption instrument. This way of applying the sample to the target yields the same results as after the normal preparation, in which usually larger drops are deposited, and more time is available for mixing of analyte and matrix, and also for good crystallization. Using even smaller sheath flows, down to 0.1 $\mu\text{l}/\text{min}$, yielded very small droplets. However, crystals of poor quality were obtained, with consequently poor signals in the MALDI-MS experiments.

The results of the stepwise deposition method are presented in Figs. 4 and 5. Absolute amounts of 2.4 pmol and 144 fmol per analyte were injected into the CE capillary. The corresponding electropherograms are also shown (see

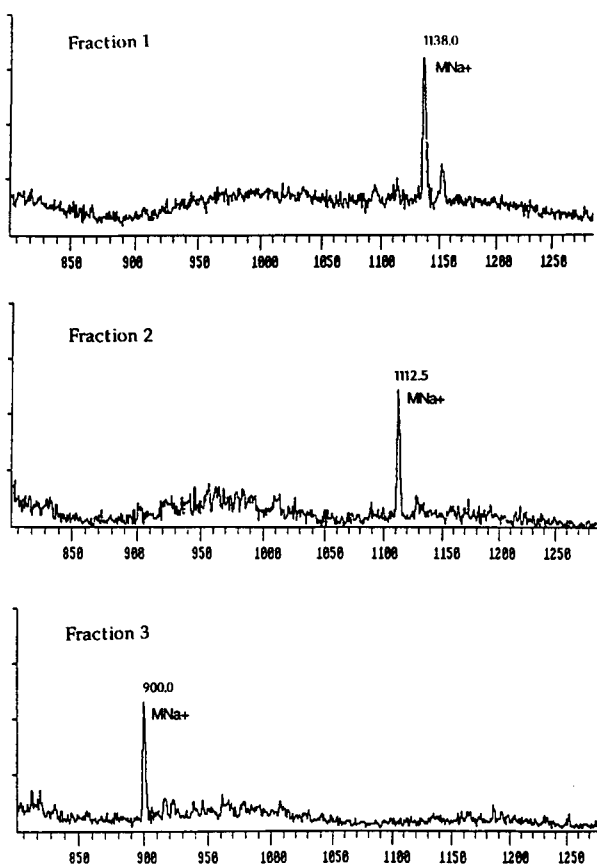


Fig. 5. Mass spectra of the separated compounds collected on the moveable target system, after changing the high voltage from 30 to 5 kV. As can be seen, the several fractions are not contaminated with components of other fractions. $V_{\text{inj}} = 48 \text{ nl}$, $[C] = 3 \mu\text{g}/\text{ml}$, corresponding to 144 fmol per component. The corresponding UV electropherogram is shown in Fig. 6.

Figs. 2 and 6). The absolute amounts injected corresponds to concentrations of 3000 $\mu\text{g/ml}$ (8 nl injected) and 3 $\mu\text{g/ml}$ (48 nl injected), respectively. As can be seen, an injection of 48 nl already decreases the resolution in the electropherogram. Higher injection volumes cannot therefore be used when maximum resolution is needed. At lower analyte concentrations (see Figs. 1 and 5) only the sodium adducts are observed and not the potassium adducts, although the same buffer is used. So far, we cannot explain this phenomenon.

The results for the 300 and 30 $\mu\text{g/ml}$ solutions could be easily obtained, while for the 3 $\mu\text{g/ml}$ solutions some problems were met. In this concentration range obtaining the MALDI mass spectra was more difficult, but successful in every case, mainly because the sample could be observed in the mass spectrometer and because of the possibility of selecting different sites during operation.

As can be seen from the electropherograms, the limit for UV detection is almost reached for the lowest concentrations used. Comparison of the data shows that MALDI-MS offers about the same detection limits as UV detection.

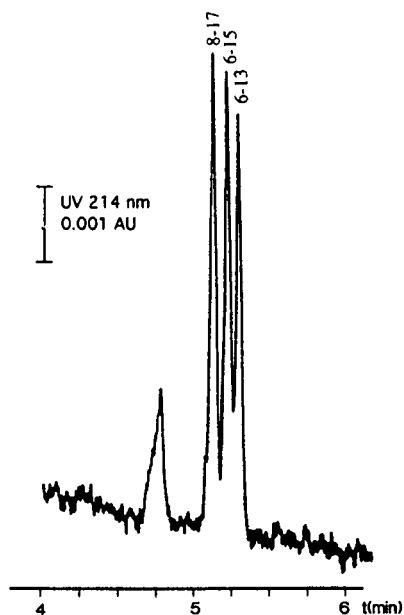


Fig. 6. On-capillary UV detection trace of the separation of three β -endorphins. $V_{inj} = 48$ nl; $[C] = 3$ $\mu\text{g/ml}$. The corresponding mass spectral are depicted in Fig. 5.

Future research will be devoted to improving detection limits as well as to applying our findings to analyse more intricate electrophoretic separations by MALDI-MS.

CONCLUSIONS

Several modes of performing off-line CE-MALDI-MS have been investigated. Deposition of the effluent on a moving belt-like system in a stepwise manner, using a sheath flow of matrix solution and subsequent scanning of the laser desorption target yielded the best results in terms of resolution, detection limit and ease of handling. Absolute detection limits are of the order of 100 fmol for some β -endorphins, corresponding to low $\mu\text{g/ml}$ concentrations.

It has been shown that the high separation efficiency obtained in CE can be maintained easily in the off-line MALDI-MS detection system. MALDI-MS is shown to yield detection limits of the same order of magnitude as UV detection.

ACKNOWLEDGEMENTS

We thank N.J. Reinhoud for many helpful discussions and practical advice. We wish to thank Professor S. Hjertén for the fruitful discussions on this topic. These investigations were supported by the Netherlands Foundation for Chemical Research (SON) with financial aid from the Netherlands Technology Foundation (STW).

REFERENCES

- 1 J.W. Jörgenson and K.D. Lukacs, *J. Chromatogr.*, 218 (1981) 209.
- 2 M. Karas and F. Hillenkamp, *Anal. Chem.*, 60, (1988) 2299.
- 3 T.P. Fan, E.D. Hardin and M.L. Vestal, *Anal. Chem.*, 56 (1984) 1870.
- 4 R. Takigiku, T. Keough, M.P. Lacey and R.E. Schneider, *Rapid Commun. Mass Spectrom.*, 4 (1990) 24.
- 5 T. Keough, R. Takigiku, M.P. Lacey and M. Purdon, *Anal. Chem.*, 64 (1992) 1594.
- 6 K. Strupat, M. Karas and F. Hillenkamp, *Int. J. Mass Spectrom. Ion Process.*, 111 (1991) 89.
- 7 M. Mann, H. Rahbek-Hielsen and P. Roepstorff, in A.

Hedin and B.U.R. Sundqvist (Editors), *Ion Formation from Organic Solids V, Proceedings of the 5th IFOS Conference, Lövånger, Sweden, June 18–21, 1989*, Wiley, Chichester, 1990, p. 47.

8 K.-O. Eriksson, A. Palm and S. Hjertén, *Anal. Biochem.*, 201 (1992) 211.

9 M. Albin, S.M. Chen, A. Louie, C. Pairaud, J. Colburn and J. Wiktorowicz, *Anal. Biochem.*, 206 (1992) 382.

Pseudo-electrochromatography–negative-ion electrospray mass spectrometry of aromatic glucuronides and food colours

M. Hugener, A.P. Tinke, W.M.A. Niessen*, U.R. Tjaden and J. van der Greef

Division of Analytical Chemistry, Leiden Amsterdam Center for Drug Research, P.O. Box 9502, 2300 RA Leiden (Netherlands)

ABSTRACT

Pseudo-electrochromatography is a combination of liquid chromatography and an electromigration technique, especially directed at the separation of ionic compounds prior to mass spectrometric detection with a mobile phase composition compatible with mass spectrometry. The application of pseudo-electrochromatography to the separation of food colours and aromatic glucuronides is described. An example of selectivity tuning by applying voltages of differing polarity during the chromatographic run is given. The coupling of pseudo-electrochromatography with electrospray mass spectrometry is demonstrated. Differences in the effects of the axial potential over the column between silica-based and polymeric packing materials are discussed.

INTRODUCTION

Pseudo-electrochromatography (PEC) [1] was introduced to combine the benefits of conventional liquid chromatography and electromigration methods such as capillary electrophoresis (CE) and electrochromatography (EC). The technique consists of a pressure-driven liquid flow through a packed bed with an axial potential difference. In a recent review on electrochromatography by Tsuda [2] pseudo-electrochromatography was also covered.

In pure electrochromatography as described by Knox and Grant [3], the mobile phase is driven through a packed capillary of 50–300 μm I.D. by applying a potential gradient of 10–50 kV/m. In fused silica the walls bear a fixed negative charge caused by deprotonated silanol and adsorbed hydroxyl groups, whereas the liquid in contact forms a thin layer (*ca.* 10 nm) of positive charge to compensate for the negative

charge. This sheath of positive charge encloses the rest of the neutral solvent and takes it along in the direction of the negative electrode as soon as a potential is applied. This so-called electroosmotic flow (EOF) is the only driving force of the mobile phase in EC and has a flow profile approaching a perfect plug [3]. In pressure-driven chromatography the flow has a parabolic profile. This is the reason for the lower efficiency of LC than electromigration methods such as electrochromatography. Neutral compounds are separated in EC by the interaction with the stationary phase whereas the migration of charged compounds is additionally dependent on their electrophoretic mobility, which is a function of the field strength and the size and charge of the ion [4].

Unfortunately, the EOF is very sensitive to pH, electrolyte concentration and organic modifier content of the mobile phase [5]. A serious problem in EC is Joule heating through high currents in the capillary resulting in peak dispersion and bubble formation [6]. Therefore, small column diameters (<300 μm) and low

* Corresponding author.

buffer concentrations (<20 mM) have to be used in EC. The combination of EC and LC by superposing a pressure-driven flow supplied by an HPLC pump was first described by Tsuda [7], originally used to suppress bubble formation. Verheij *et al.* [1] named this pressure-assisted method pseudo-electrochromatography (PEC), to distinguish it from pure electrically driven electrochromatography. The advantages of pseudo-electrochromatography are higher flow-rates, shorter analysis times and the loss of the limitations on pH and buffer composition, because the EOF is no longer important. On the other hand, the flow profile is approaching LC and therefore the efficiency of PEC lies between those of LC and EC, depending on the ratio of pump flow and EOF. This is probably a reason why PEC has not yet become a common analytical technique. The separation of ionic compounds is more readily accomplished with the use of ion pairs and buffer gradients, where the usual HPLC equipment can be used. However, if a mass spectrometer is used as a detector, most ion-pairing agents and many buffers cannot be used, because of the rapid contamination of the ion source.

Experiments have been made to replace non-volatile ion-pair reagents by volatile compounds such as di- or trialkylamines for anions and perfluorinated sulphonic acids for cations [8].

As mentioned before, the retention time of ionic compounds can easily be influenced with the help of a high voltage. Continuing the work of Verheij *et al.* [1], new classes of compounds such as aromatic glucuronides and food colours (sulphonated azo dyes) were investigated. The possibility of changing the polarity of the voltage during the analysis to obtain both acceleration and retardation of compounds in the same run was of special interest. Polymer packing material was used for the first time in PEC and compared with the normally used octadecylsilanized (ODS) stationary phases.

For the coupling of PEC and mass spectrometry, continuous-flow fast atom bombardment (FAB) and electrospray or ionspray are most promising, because of the low flow-rate of only a few microlitres per minute used in PEC. Verheij *et al.* [1] showed the possibility of cou-

pling PEC with FAB-MS. In this work the coupling of PEC with electrospray MS is described.

EXPERIMENTAL

Chemicals and solid phases

Methanol, 2-propanol (Baker, Deventer, Netherlands) and acetonitrile (Rathburn, Walkern, UK) were of HPLC grade. Water was purified with a Milli-Q apparatus (Millipore, Bedford, MA, USA). Phenyl- β -D-glucuronide (PG), *o*-aminophenyl- β -D-glucuronide (APG), *p*-nitrophenyl- β -D-glucuronide (NPG) and α -naphthyl- β -D-glucuronide (NAG) were supplied by Sigma (Brussels, Belgium), the food colours (>85% pure) E102 [Colour Index (CI) Food Yellow 4, Acid Yellow 23], E110 (CI Food Yellow 3), E122 (CI Food Red 3, Acid Red 14), E123 (CI Food Red 9, Acid Red 27) and E124 (CI Food Red 7, Acid Red 18) by Morton (Amersfoort, Netherlands) and ammonium acetate (reinst) by Merck (Darmstadt, Germany). The column packings were Nucleosil 100-5C₁₈, Nucleogel RP100-5/150 (Macherey-Nagel, Düren, Germany) and 12-20- μ m PRP-1 (Hamilton, Reno, NV, USA).

Instrumentation

The PEC-MS system is outlined in Fig. 1. A Phoenix 20 CU syringe pump (Carlo Erba, Rodano, Italy) was used to deliver the solvent. A Swagelock tee (Crawford Fitting, Solon, OH, USA) with a 40 cm \times 50 μ m I.D. fused-silica capillary was used to split the mobile phase in a ratio of about 1:50 to 1:100 in order to obtain a flow-rate between 0.5 and 2 μ l/min. A 10-mm guard column (Chrompack, Bergen op Zoom, Netherlands) filled with Nucleosil 100-5C₁₈ was placed between the pump and the preinjector split to retain small impurities of the solvent. It has been found that the usual solvent filters at the pump inlet were not sufficient for microcolumns. Even when the solvent was filtered before use through 0.2- μ m filters, the columns became clogged in less than 24 h. The microcolumns were laboratory prepared and packed (see below) and directly connected to a Valco CI4W internal volume (60/150 nl) micro-

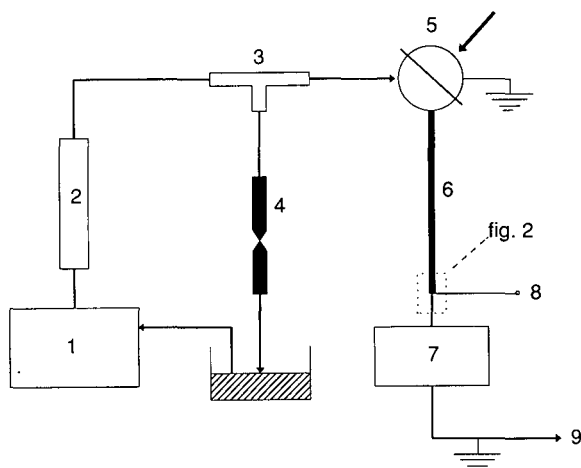


Fig. 1. Scheme of the PEC system. 1 = Syringe pump; 2 = 1-cm guard column filled with 5- μm ODS stationary phase; 3 = preinjector split; 4 = restrictor; 5 = 150-nl microinjector; 6 = microcolumn; 7 = UV detector; 8 = high voltage; 9 = electro spray mass spectrometer.

injector (Valco Instruments, Houston, TX, USA). A window of 10 mm length was burned in the polyimide coating of the 50 μm I.D. fused-silica outlet capillary, which was placed in a modified UV cell of a Spectroflow 757 UV detector (Kratos Analytical, Ramsey, NJ, USA). Signals were registered on a BD41 multi-range recorder (Kipp & Zonen, Delft, Netherlands). The high voltage was delivered from a switchable 0 to ± 30 kV Spellman CZE 1000R power supply (Spellman High Voltage Electronics, Plainview, NY, USA) and connected to the Valco union at the end of the column. The injector was set to ground potential.

PEC-electrospray coupling

The mass spectrometer used was a Finnigan MAT (San Jose, CA, USA) TSQ 70 triply quadrupole instrument equipped with a Finnigan MAT electro spray interface. The system was operated in the negative-ion mode. A sheath flow consisting of 10% water in 2-propanol (1–2 $\mu\text{l}/\text{min}$) was delivered by a Model 2400 syringe pump (Harvard Apparatus, Edenbridge, UK). A 40 μm I.D. fused-silica capillary was inserted in the sheath-flow needle of the electro spray interface. The capillary was connected to the outlet of the UV detector by a Valco zero dead volume

union, which lies at earth potential. If no UV detector is used, the capillary is directly connected to the column outlet.

Column preparation

The capillary columns were made of 220 μm I.D. fused-silica capillary tubing (SGE, Melbourne, Australia) or 250 μm I.D., 1/16 in. O.D. (1 in. = 2.54 cm) polyether ether ketone (PEEK) tubing (Jour Research, Onsala, Sweden). To make the connection of the fused-silica capillary easier, they were glued in a 0.5 mm I.D., 1/16 in. O.D. PEEK tube with a two-component epoxy glue (Torr Seal, Varian, Lexington, MA, USA), so that the fused-silica capillary protruded a few centimeters. The space between the fused-silica and PEEK tubing has to be carefully filled to avoid dead volumes. After the glue had hardened the protruding ends were cut with a sharp knife and the remaining glue removed from the PEEK capillary. In this way fused-silica columns could be connected with the usual 1/16 in. Valco stainless-steel ferrules or PEEK fingertight fittings. To keep the packing inside the column, 1/16 in., 2 μm metal screen filters (Valco) or 3 μm Fluoropore filters, cut with a hand-made 1/16 in. disc cutter from commercial Fluoropore filters (Millipore), were placed on both ends of the column. This is much simpler than making sintered frits [9] or using a plug of quartz-wool [1,10]. Further, the filters always have the same thickness and pore size, which is very important when making microcolumns of reproducible quality. The column end with the filter was connected to a Valco zero dead volume union, which also served as electric contact for the high voltage (Fig. 2). Although the bore of the zero dead volume union is 250 μm , the separation is not improved by using a through union.

Different packing procedures have been described [11]; acetonitrile is the most common solvent for the packing of ODS stationary phases. According to Cappiello *et al.* [12], other conditions are necessary to pack a PEEK column, because of repulsive forces between the particles themselves and the internal column walls. They developed a method called soap packing, with a solution of 1% aqueous sodium

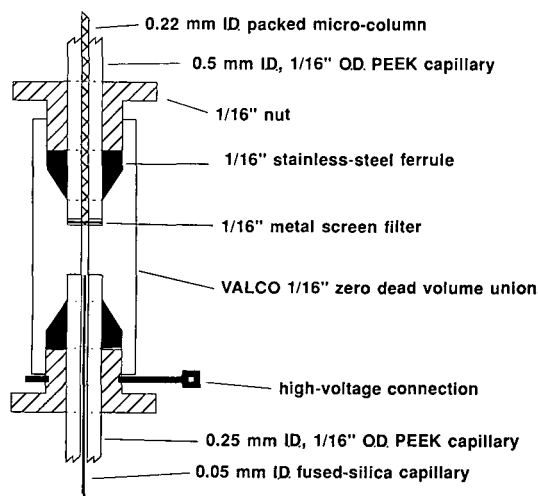


Fig. 2. Connection between microcolumn and detector. " = Inch.

laurylsulphate as packing solvent. However, this method gave poor results with our packing apparatus, which was different from that described in their paper. The same packing conditions as for the fused-silica columns were used for the preparation of the PEEK columns. The efficiency of PEEK columns was *ca.* 30% lower than that of silica columns, but can probably be optimized. For polymer packing material (Nucleogel RP100-5/150 and Hamilton PRP-1) methanol–water (6:4) proved to be superior to acetonitrile.

The following packing procedure was used for a 20 cm \times 220 μ m I.D. fused-silica capillary column. A Brownlee micro gradient system (Brownlee Labs., Santa Clara, CA, USA) dual-syringe pump was used to pack the columns, which were connected to a 1.5-ml laboratory-made high-pressure mixing chamber, equipped with a magnetic stirrer. A slurry of 8 mg of Nucleosil 100-5C₁₈ in 1 ml of acetonitrile was homogenized for 5 min in an ultrasonic bath and then transferred with a syringe into the mixing chamber. The microcolumn was directly connected to the mixing chamber with the end of the column pointing upwards. The magnetic stirrer was activated and the programme of the pump (initial pressure 30 bar, maximum pressure 300 bar, flow-rate 100 μ l/min) was started. When all the air had been flushed out of the column, the

whole installation was turned through 180°, so that the end of the column was pointing downwards. The maximum pressure was reached in about 15 min and maintained for about 1 h. Thereafter, the flow was stopped and the column was removed after the depressurization was complete (1–2 h). For the polymer packings Nucleogel and PRP-1 the slurry concentration was 4 mg/ml in methanol–water (4:6) and a maximum pressure of 200 bar was used. In addition, the column was rinsed afterwards with water for at least 20 h, giving better baseline stability, perhaps owing to impurities in the polymer packing. The column performance was tested with a set of three parabenes [methanol–water (4:6) with silica-based and acetonitrile–water (1:1) with polymer stationary phases].

RESULTS AND DISCUSSION

Separation of food colours

Five water-soluble food colours (E102, E110, E122, E123 and E124) were chosen as model compounds for multiply charged ions to investigate the influence of the high voltage on retention time and peak shape. The dyestuffs, which have two or three sulphonic acid groups and, for E102, also a carboxylic acid group, were separated on a capillary column filled with 5- μ m ODS particles with 10 mM ammonium acetate–methanol (8:2) as mobile phase.

At high pH the acidic groups are fully deprotonated, forming doubly and triply negatively charged ions. The triply charged dyes (E102, E123, E124) are eluted first, followed by the doubly charged E110 and E122 (Fig. 3a). Without a modifier gradient the analysis time of E122 is very long (240 min, extrapolated from Fig. 3b) and the peak is too broad for detection. Applying a positive voltage over the column shortens the retention time dramatically (Fig. 3). For example, the retention time of E122 is a few hours without a voltage and 33 min at 2 kV, but at 8 kV it is less than 5 min. At the same time, the peak becomes narrower and higher, resulting in improved detection limits.

However, at high voltage joule heating becomes a severe problem, leading to gas bubble formation, which can irreversibly destroy the

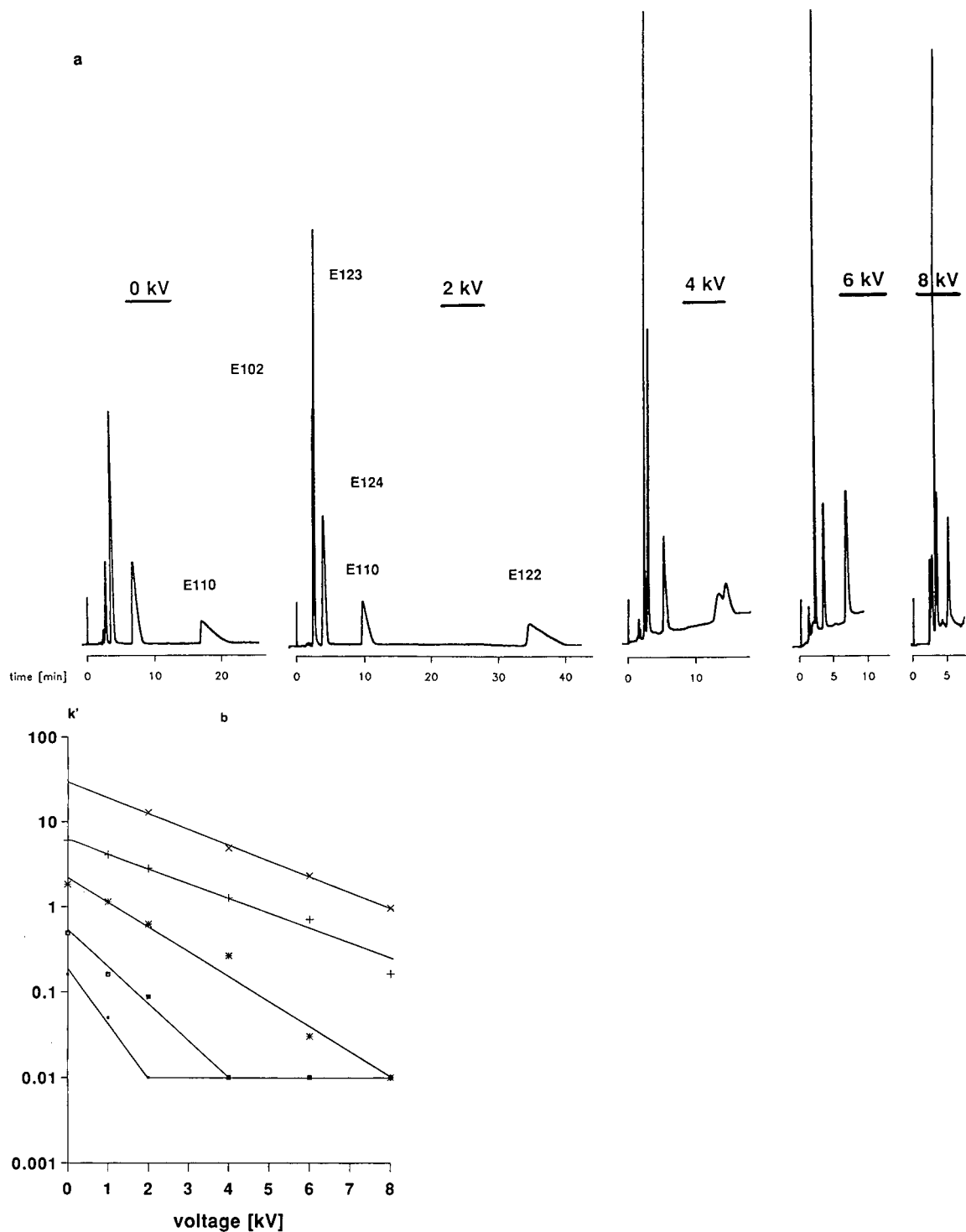


Fig. 3. Separation of food colours. Column, 20 cm \times 250 μ m I.D. PEEK column packed with Nucleosil 100-5C₁₈; mobile phase, 10 mM ammonium acetate (pH 8.5)–methanol (8:2); sample concentration, 0.5 mg/ml each in water. (a) Chromatograms with UV detection at 220 nm with different voltages; (b) plot of k' vs. voltage.

packed bed of the column. It is interesting that bubbles are formed more easily in fused-silica than in PEEK capillaries, perhaps because of sharper edges at the column end. Decreasing the buffer concentration reduces the current and therefore also the joule heating in the capillary, but the stability of the system also decreases, leading to less reproducible results. In addition, at lower ammonium acetate concentrations the retention time is also reduced because ammonium acts with anions as an ion-pair reagent.

The structure of E123 and the corresponding mass spectrum in the negative-ion mode are shown in Fig. 4. All sodium ions are exchanged by protons already in solution. Therefore, only signals of the free sulphonic acid (= M) are present. The base peak is the triply charged ion at m/z 178, followed by the doubly charged ion at m/z 268. The single charged $[M - H]^-$ ion can hardly be distinguished from the background. The ion at m/z 597 is probably an adduct with $[M + OAc]^-$. The electrospray (ESP) mass spectra of these azo dyes are almost identical with the ionspray spectra obtained by Edlund *et al.* [13], who also did not observe fragmentation. In

negative-ion thermospray (TSP) the doubly charged ion was the base peak in neutral solution [14], whereas in positive-ion TSP (repeller on) the loss of $NaSO_3$ has been reported [15].

Separation of aromatic glucuronides

Glucuronides are important metabolites of many biologically active compounds found in urine. The applicability of PEC-ESP-MS to some aromatic glucuronides as model compounds was investigated. Stefansson and Westerlund [16] studied the influence of the stationary phases, pH and counter ions in the separation of these aromatic glucuronides by ion-pair chromatography. The best results were obtained with a mobile phase consisting of 20 mM dodecylamine and a zwitterionic 2-(N-morpholino)ethanesulphonic acid (MES) buffer. These mobile phase conditions are clearly not compatible with MS conditions.

The chromatogram of the four glucuronides without the use of an ion pair is shown in Fig. 5a. The three structurally similar phenyl glucuronides are eluted first, NAG coming much later as a broad peak. At 0 kV PG and APG

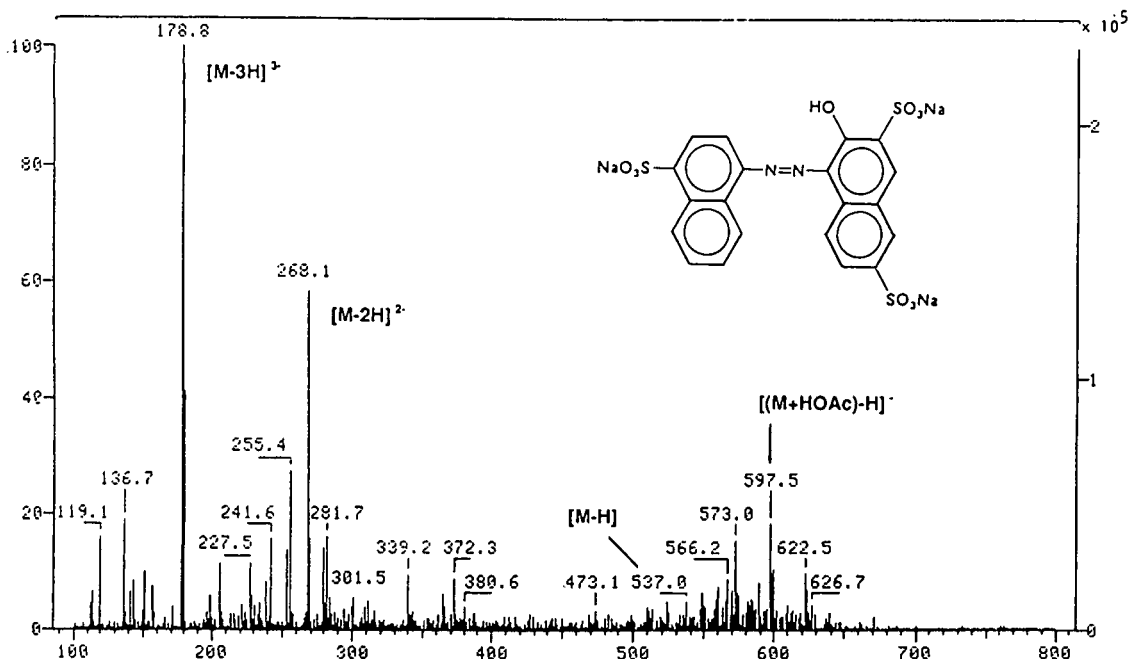


Fig. 4. Mass spectrum of food colour E123 in the negative-ion mode (M is the free acid). Constant infusion ($1 \mu\text{l}/\text{min}$) of $100 \mu\text{g}/\text{ml}$ in 2 mM ammonium acetate; sheath flow $2 \mu\text{l}/\text{min}$ of 2-propanol– 2 mM ammonium acetate (9:1).

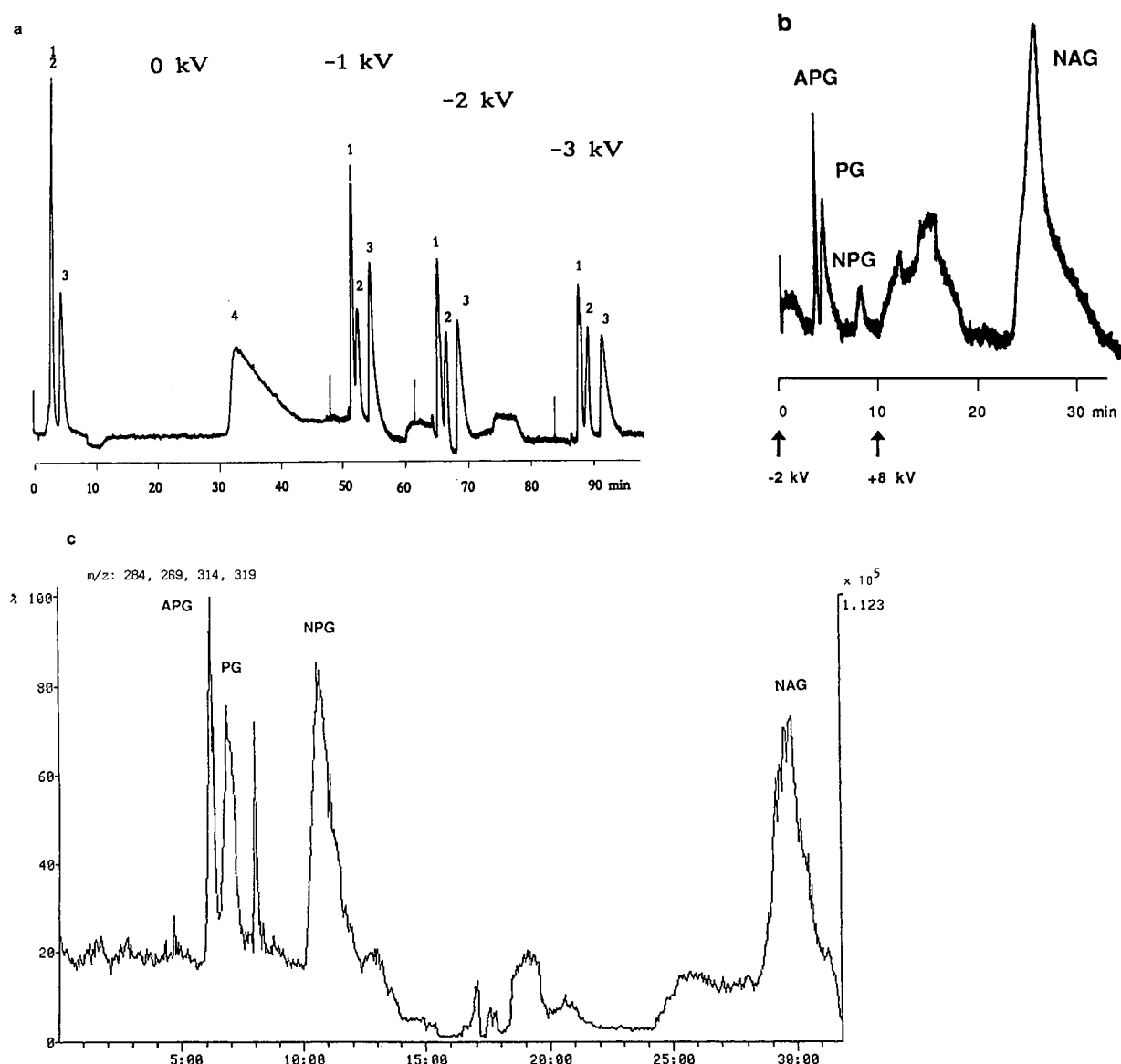


Fig. 5. Separation of aromatic glucuronides on a 20 cm \times 220 μ m I.D. fused-silica column packed with PRP-1 (12–20 μ m). Mobile phase, 2 mM ammonium acetate (pH 7)–acetonitrile (95:5). (a) Influence of voltage on the retention time (1 = PG, 2 = APG, 3 = NPH, 4 = NAG; UV detection at 220 nm); (b) UV and (c) mass chromatogram of the four glucuronides; concentration, 100 μ g/ml in water.

elute together, but if a negative voltage is applied to increase the retention time, the resolution of the three glucuronides becomes better with higher voltage (Fig. 5a). At –3 kV almost baseline separation is obtained. Unfortunately, NAG is retained in the same way, resulting in a very long analysis time. In Fig. 5b and c the

advantage of PEC over ion pairs is demonstrated: to shorten the analysis time of NAG the voltage was changed from –2 to +8 kV after the elution of the third compound, whereby NAG was now accelerated instead of delayed.

However, as can be seen, after the change in the voltage, the baseline is disturbed, resulting

from a redistribution of the acetate buffer. Acetate anions are now accelerated while ammonium is retarded. This phenomenon can also be seen by simply changing the voltage without injection. Tsuda [17] already described that after applying a voltage to a packed capillary, an equilibration time of around 20 min was necessary before the retention time became constant. The same happened when the voltage was switched off. This phenomenon was explained by a change in the surface and with release or saturation of adsorptive materials from or to the surface of the column support, originally present in the mobile phase.

A closer investigation of this problem shows that this equilibration time is dependent on different factors such as mobile phase composition, flow-rate and especially the nature of the packing material. In order to obtain more information about this equilibration time the following experiment, also described by Tsuda [2], was carried out. Repeated injections of a solution of E124 were made every 3 min on to a column filled with Nucleogel RP100-5/150 and with E110 on to a column of Nucleosil 100-5C₁₈ (Fig. 6a) under identical conditions. Different compounds have to be used in order to obtain peaks with comparable retention times, because of the different polarities of the two stationary phases. A voltage of +3 kV was applied 16 min after the first injection and switched off after 41 min. For the polymer packing no equilibration time was observed. The first injection, after the voltage had been applied (at 18 min), already shows the same retention time as the samples injected later (Fig. 6b). The injections at 12 and 9 min are different, because these compounds were already in the column when the voltage was switched on. The sample injected at 9 min shows a peak that is much broader than the preceding peaks and with a retention time that is longer, instead of being shorter as expected (Fig. 6a). There is no good explanation for this observation, but the change in the buffer concentration in the column, caused by the high voltage, is certainly one factor contributing to this phenomenon. When the voltage is switched off, the retention time returns to the initial value as in the beginning of the experiment.

With the ODS stationary phase an equilibrium time of *ca.* 8 min is measured after the voltage has been applied. Again the first compound which is in the column when the voltage is changed has a longer retention time than without a voltage. When the voltage is switched off, ODS material needs a very long time to regain the original surface properties, which is measured by the retention time of the food colour. Even 1 h after the voltage has been switched off, the retention time is still shorter (400 s) than at the beginning (444 s). This remains in contradiction with the observations of Tsuda [2], who described an equilibrium time of 20 min when the voltage was applied, but only 10 min when the voltage was switched off. It is obvious that the nature of the ODS stationary phase, in contrast to the polymer phase, is changed on applying a voltage. This must be ascribed to the presence of free hydroxyl groups still present in silica-based supports and the easier adsorption of polar compounds by these groups.

The mass spectrum with continuous-flow injection of the four glucuronides in the positive- and negative-ion modes is shown in Fig. 7. The intensities of the $[M - H]^-$ ions are almost identical in the negative-ion mode and the spectrum shows no other ions except for some addition clusters of two glucuronides $[M_1 + M_2 - H]^-$ between m/z 500 and 600 with low intensity. In the positive-ion mode, $[M + Na]^+$ ions are formed and APG as the only compound forms a very intense $[M + H]^+$ ion (100%). The relative intensity of the ions reflects the electron affinity and the pK_a of the aglycone. This is also observed in the FAB mass spectra of aromatic glucuronides, where the sensitivity for NPG is 100 times lower than for 8-hydroxyisoquinoline glucuronide [18]. No fragmentation was observed and the base peak was $[M + H]^+$ or $[M + NH_4]^+$, again depending on the basicity of the aglycone.

Whereas molecular ions of glucuronides cannot be detected with a particle beam interface in either the electron impact or chemical ionization mode [19], the best results in TSP are obtained with the filament on and buffer ionization in the negative-ion mode [20]. In positive-ion TSP with buffer ionization only the ammonium adduct

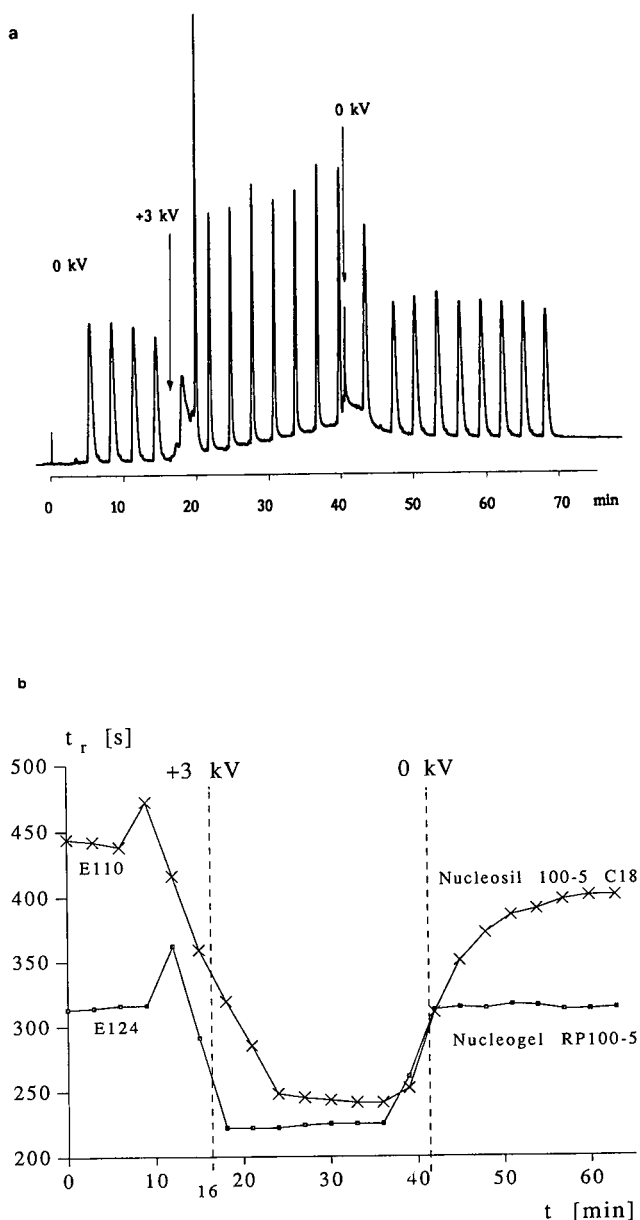


Fig. 6. Repeated injection of food colours. Mobile phase, 10 mM ammonium acetate (pH 7)–methanol (7:3); column, 20 cm \times 250 μ m I.D. PEEK column packed with polymer Nucleogel RP100-5/150 and silica-based Nucleosil 100-5C₁₈; UV detection at 220 nm. (a) Diagram of retention time with and without applied voltage; (b) multiple injection chromatogram of E124 on polymer support.

$[M + NH_4]^+$ was registered, whereas Liberato *et al.* [21] observed significant fragmentation in the filament-off mode, with the sugar fragments at m/z 194 or 177 as base peaks. Watson *et al.* [22,23] analysed steroid glucuronides and

monosulphates in negative-ion TSP and obtained almost only the deprotonated anions without fragmentation in LC-MS, using a water–acetonitrile gradient without any ammonium acetate.

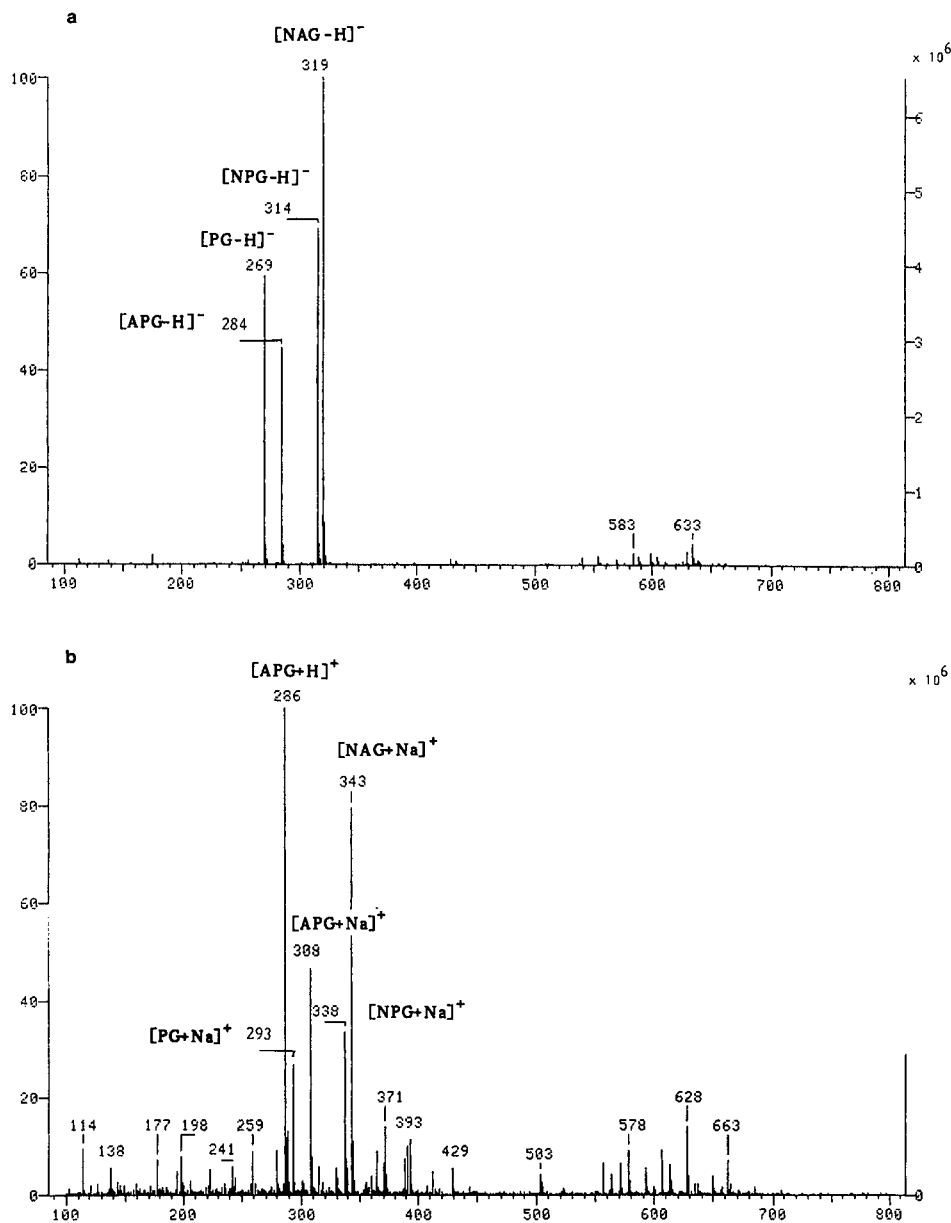


Fig. 7. Mass spectra of a mixture of four aromatic glucuronides. Constant infusion of 100 $\mu\text{g/ml}$ of each compound in 2 mM ammonium acetate (pH 8.5) (2 $\mu\text{l/min}$). (a) Negative-ion mode; sheath flow, 2 $\mu\text{l/min}$ of 2-propanol–2 mM ammonium acetate (pH 8.5) (9:1); (b) positive-ion mode; sheath flow, 2 $\mu\text{l/min}$ of 1% acetic acid in 2-propanol–water (9:1).

CONCLUSIONS

It was shown that charged compounds can be both accelerated and retarded by changing the sign of the high voltage in the same run. This attractive feature was applied to some food

colours (sulphonated azo dyes) and aromatic glucuronides in the on-line combination of PEC and MS. The coupling of electrospray mass spectrometry and PEC does not lead to more problems than with micro-LC. To prevent the high voltage from affecting the spray, a con-

nection to ground has to be placed in front of the electrospray interface. In addition, the capillary has to be narrow and not too short, otherwise the current passing through it is too high. Another possibility is to connect the injector to the high voltage and the outlet of the column to ground. In this case no zero dead volume union has to be placed between the column and electrospray interface. For security reasons, an automatic injector has to be used in that event. PEC-ESP-MS has been demonstrated to be a useful tool for the separation of charged compounds.

The interest in micro-LC is still growing because of the advantages of low solvent consumption and the smaller amount of packing material needed, which is an important factor when expensive supports are used, especially in separations using chiral phases. Here, PEC offers an alternative to microgradient systems, where the technique is still in development.

REFERENCES

- 1 E.R. Verheij, U.R. Tjaden, W.M.A. Niessen and J. van der Greef, *J. Chromatogr.*, 554 (1991) 339.
- 2 T. Tsuda, *LC · GC Int.*, 5, No. 9 (1992) 26.
- 3 J.H. Knox and I.H. Grant, *Chromatographia*, 24 (1987) 135.
- 4 J.T. Edward, *Adv. Chromatogr.*, 2a (1966) 63.
- 5 T. Tsuda, K. Nomura and G. Nakagawa, *J. Chromatogr.*, 248 (1982) 241.
- 6 H. Knox, *Chromatographia*, 26 (1988) 329.
- 7 T. Tsuda, *Anal. Chem.*, 59 (1987) 521.
- 8 R.G. van Leuken and G.T.C. Kwakenbos, *J. Chromatogr.*, in press.
- 9 H. Yamamoto, J. Baumann and F. Erni, *J. Chromatogr.*, 593 (1992) 313.
- 10 T. Takeuchi and D. Ishii, *J. Chromatogr.*, 213 (1981) 25.
- 11 T. Hirata, *J. Microcol. Sep.*, 2 (1990) 214.
- 12 A. Cappiello, P. Palma and F. Mangani, *Chromatographia*, 32 (1991) 389.
- 13 P.O. Edlund, E.D. Lee, J.D. Henion and W.L. Budde, *Biomed. Environ. Mass Spectrom.*, 18 (1989) 233.
- 14 D.A. Flory, M.M. McLean, M.L. Vestal and L.D. Betowski, *Rapid Commun. Mass Spectrom.*, 1 (1987) 48.
- 15 J. Yinon, T.L. Jones and L.D. Betowski, *Biomed. Environ. Mass Spectrom.*, 18 (1989) 445.
- 16 M. Stefansson and D. Westerlund, *J. Chromatogr.*, 499 (1990) 411.
- 17 T. Tsuda, *Anal. Chem.*, 60 (1988) 1677.
- 18 C. Fenselau, D.J. Liberato, J.A. Yergey and R.J. Cotter, *Anal. Chem.*, 56 (1984) 2759.
- 19 F.R. Brown and W.M. Draper, in M.A. Brown (Editor), *Liquid Chromatography/Mass Spectrometry. Applications in Agricultural, Pharmaceutical and Environmental Chemistry (ACS Symposium Series, Vol. 420)*, American Chemical Society, Washington, DC, 1990, p. 232.
- 20 W.M. Draper, F.R. Brown, R. Bethem and M.J. Miille, *Biomed. Environ. Mass Spectrom.*, 18 (1989) 767.
- 21 D.J. Liberato, C.C. Fenselau, M.L. Vestal and A.L. Yergey, *Anal. Chem.*, 55 (1983) 1741.
- 22 D. Watson, G.W. Taylor and S. Murray, *Biomed. Mass Spectrom.*, 12 (1985) 610.
- 23 D. Watson, G.W. Taylor and S. Murray, *Biomed. Environ. Mass Spectrom.*, 13 (1986) 65.

Author Index

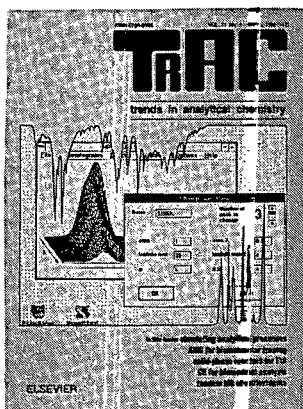
- Alcalde, P., see Ventura, R. 647(1993)203
Alexander, J.N., IV and Quinn, C.J.
Organic acid analysis by ion chromatography-particle beam mass spectrometry 647(1993)95
Arpino, P.J., see Sadoun, F. 647(1993)351
Bagheri, H., Brouwer, E.R., Ghijsen, R.T. and Brinkman, U.A.Th.
On-line low-level screening of polar pesticides in drinking and surface waters by liquid chromatography-thermospray mass spectrometry 647(1993)121
Baiocchi, C., see Da Col, R. 647(1993)289
Barceló, D., Durand, G. and Vreeken, R.J.
Determination of quaternary amine pesticides by thermospray mass spectrometry 647(1993)271
Bean, K., see Hopfgartner, G. 647(1993)51
Bertrand, M.J., see Gagné, J.P. 647(1993)13
Bertrand, M.J., see Gagné, J.P. 647(1993)21
Biancone, L., see Silvestro, L. 647(1993)261
Brinkman, U.A.Th., see Bagheri, H. 647(1993)121
Brinkman, U.A.Th., see Geerdink, R.B. 647(1993)329
Brouwer, E.R., see Bagheri, H. 647(1993)121
Bruggink, C., see Niessen, W.M.A. 647(1993)319
Bruins, A.P., see Kostianen, R. 647(1993)361
Camussi, G., see Silvestro, L. 647(1993)261
Careri, M., Mangia, A., Manini, P., Predieri, G., Raverdino, V., Tsoupras, G. and Sappa, E.
Particle beam liquid chromatography-mass spectrometry behaviour of polynuclear metal carbonyl compounds 647(1993)79
Carrier, A., see Gagné, J.P. 647(1993)13
Carrier, A., see Gagné, J.P. 647(1993)21
Cedro, A., see Da Col, R. 647(1993)289
Da Col, R., Silvestro, L., Naggi, A., Torri, G., Baiocchi, C., Moltrasio, D., Cedro, A. and Viano, I.
Characterization of the chemical structure of sulphated glycosaminoglycans after enzymatic digestion.
Application of liquid chromatography-mass spectrometry with an atmospheric pressure interface 647(1993)289
Da Col, R., see Silvestro, L. 647(1993)261
De Boer, J., see Genuit, W.J.L. 647(1993)73
De Koster, C.G., see Van Dongen, W.D. 647(1993)301
Devaux, P., see Legrand, R. 647(1993)3
Duchateau, A.L.L., see Van Leuken, R.G.J. 647(1993)131
Durand, G., see Barceló, D. 647(1993)271
Ekeberg, D., see Jablonska, A. 647(1993)341
Esmans, E.L., see Lemièrre, F. 647(1993)211
Falconnet, J.-B., see Legrand, R. 647(1993)3
Franssen, E.J.F., see Kostianen, R. 647(1993)361
Gagné, J.P., Carrier, A., Varfalvy, L. and Bertrand, M.J.
Evaluation of the performance of capillary liquid chromatography-fast atom bombardment mass spectrometry systems with precolumn addition of glycerol as a viscous matrix 647(1993)13
Gagné, J.P., Carrier, A., Varfalvy, L. and Bertrand, M.J.
Origin of the decrease in chromatographic resolution induced by the addition of viscous matrices in liquid chromatography-fast atom bombardment mass spectrometric systems 647(1993)21
Geerdink, R.B., Kienhuis, P.G.M. and Brinkman, U.A.Th.
Fast screening method for eight phenoxyacid herbicides and bentazone in water. Optimization procedures for flow-injection analysis-thermospray tandem mass spectrometry 647(1993)329
Genuit, W.J.L. and De Boer, J.
Applications of dual-beam thermospray liquid chromatography-mass spectrometry 647(1993)73
Ghijsen, R.T., see Bagheri, H. 647(1993)121
Grossi, P., see Rossato, P. 647(1993)155
Guarini, A., Guglielmetti, G. and Po, R.
Application of liquid chromatography-thermospray mass spectrometry to the analysis of polyester oligomers 647(1993)311
Guglielmetti, G., see Guarini, A. 647(1993)311
Hansen, M., see Jablonska, A. 647(1993)341
Haverkamp, J., see Van Dongen, W.D. 647(1993)301
Heerma, W., see Van Dongen, W.D. 647(1993)301
Henion, J., see Hopfgartner, G. 647(1993)51
Henry, R., see Hopfgartner, G. 647(1993)51
Hillenkamp, F., see Van Veelen, P.A. 647(1993)367
Hopfgartner, G., Bean, K., Henion, J. and Henry, R.
Ion spray mass spectrometric detection for liquid chromatography: a concentration- or a mass-flow-sensitive device? 647(1993)51
Hostettmann, K., see Maillard, M.P. 647(1993)137
Hostettmann, K., see Maillard, M.P. 647(1993)147
Hostettmann, K., see Wolfender, J.L. 647(1993)183
Hostettmann, K., see Wolfender, J.L. 647(1993)191
Hugener, M., Tinke, A.P., Niessen, W.M.A., Tjaden, U.R. and Van der Greef, J.
Pseudo-electrochromatography-negative-ion electrospray mass spectrometry of aromatic glucuronides and food colours 647(1993)375
Ingendoh, A., see Van Veelen, P.A. 647(1993)367
Jablonska, A., Hansen, M., Ekeberg, D. and Lundanes, E.
Determination of chlorinated pesticides by capillary supercritical fluid chromatography-mass spectrometry with positive- and negative-ion detection 647(1993)341
Karlsson, K.-E.
Deuterium oxide as a reagent for the modification of mass spectra in electrospray microcolumn liquid chromatography-mass spectrometry 647(1993)31
Kienhuis, P.G.M.
Radiofrequency-only daughter scan mode to provide more spectral information in liquid chromatography-thermospray tandem mass spectrometry 647(1993)39
Kienhuis, P.G.M., see Geerdink, R.B. 647(1993)329
Koivisto, P., see Kostianen, R. 647(1993)91
Kostianen, R., Franssen, E.J.F. and Bruins, A.P.
Capillary zone electrophoresis-ionspray mass spectrometry of a synthetic drug-protein conjugate mixture 647(1993)361
Kostianen, R., Koivisto, P. and Peltonen, K.
Characterization of the products formed in the reaction between 1,3-butadienemonoxide and 2'-deoxyadenosine by liquid chromatography-continuous-flow fast atom bombardment mass spectrometry 647(1993)91

- Kwakkenbos, G.T.C., see Van Leuken, R.G.J. 647(1993)131
- Legrand, R., Falconnet, J.-B., Prevost, D., Schoot, B. and Devaux, P.
Peptide mapping of recombinant human interferon- γ by reversed-phase liquid chromatography with on-line identification by thermospray mass spectrometry and UV absorption spectrometry 647(1993)3
- Lemière, F., Esmans, E.L., Van Dongen, W., Van den Eeckhout, E. and Van Onckelen, H.
Evaluation of liquid chromatography-thermospray mass spectrometry in the determination of some phenylglycidyl ether-2'-deoxynucleoside adducts 647(1993)211
- Levsen, K., see Volmer, D. 647(1993)235
- Libertucci, D., see Silvestro, L. 647(1993)261
- Lundanes, E., see Jablonska, A. 647(1993)341
- Maillard, M.P. and Hostettmann, K.
Determination of saponins in crude plant extracts by liquid chromatography-thermospray mass spectrometry 647(1993)137
- Maillard, M.P., Wolfender, J.-L. and Hostettmann, K.
Use of liquid chromatography-thermospray mass spectrometry in phytochemical analysis of crude plant extracts 647(1993)147
- Maillard, M., see Wolfender, J.L. 647(1993)183
- Mangia, A., see Careri, M. 647(1993)79
- Manini, P., see Careri, M. 647(1993)79
- McCarney, C.C., see Niessen, W.M.A. 647(1993)107
- Moltrasio, D., see Da Col, R. 647(1993)289
- Moult, P.E.G., see Niessen, W.M.A. 647(1993)107
- Nadal, T., see Ventura, R. 647(1993)203
- Naggi, A., see Da Col, R. 647(1993)289
- Niessen, W.M.A., Van der Hoeven, R.A.M., Van der Greef, J., Schols, H.A., Voragen, A.G.J. and Bruggink, C.
Recent progress in high-performance anion-exchange chromatography-thermospray mass spectrometry of oligosaccharides 647(1993)319
- Niessen, W.M.A., see Hugener, M. 647(1993)375
- Niessen, W.M.A., see Tinke, A.P. 647(1993)63
- Niessen, W.M.A., see Tinke, A.P. 647(1993)279
- Niessen, W.M.A., McCarney, C.C., Moult, P.E.G., Tjaden, U.R. and Van der Greef, J.
Liquid chromatography-mass spectrometry for the identification of minor components in benzothiazole derivatives 647(1993)107
- Peltonen, K., see Kostianen, R. 647(1993)91
- Po, R., see Guarini, A. 647(1993)311
- Predieri, G., see Careri, M. 647(1993)79
- Preiss, A., see Volmer, D. 647(1993)235
- Prevost, D., see Legrand, R. 647(1993)3
- Quinn, C.J., see Alexander, J.N., IV 647(1993)95
- Raverdino, V., see Careri, M. 647(1993)79
- Rossato, P., Scandola, M. and Grossi, P.
Investigation into lacidipine and related metabolites by high-performance liquid chromatography-mass spectrometry 647(1993)155
- Sadoun, F., Virelizier, H. and Arpino, P.J.
Packed-column supercritical fluid chromatography coupled with electrospray ionization mass spectrometry 647(1993)351
- Sappa, E., see Careri, M. 647(1993)79
- Scandola, M., see Rossato, P. 647(1993)155
- Scappaticci, E., see Silvestro, L. 647(1993)261
- Schols, H.A., see Niessen, W.M.A. 647(1993)319
- Schols, H.A., see Tinke, A.P. 647(1993)279
- Schoot, B., see Legrand, R. 647(1993)3
- Schröder, H.F.
Surfactants: non-biodegradable, significant pollutants in sewage treatment plant effluents. Separation, identification and quantification by liquid chromatography, flow-injection analysis-mass spectrometry and tandem mass spectrometry 647(1993)219
- Segura, J., see Ventura, R. 647(1993)203
- Silvestro, L., Da Col, R., Scappaticci, E., Libertucci, D., Biancone, L. and Camussi, G.
Development of a high-performance liquid chromatographic-mass spectrometric technique, with an ionspray interface, for the determination of platelet-activating factor (PAF) and lyso-PAF in biological samples 647(1993)261
- Silvestro, L., see Da Col, R. 647(1993)289
- Straub, R.F. and Voyksner, R.D.
Determination of penicillin G, ampicillin, amoxicillin, cloxacillin and cephapirin by high-performance liquid chromatography-electrospray mass spectrometry 647(1993)167
- Tiller, P.R.
Application of particle-beam mass spectrometry to drugs. An examination of the parameters affecting sensitivity 647(1993)101
- Tinke, A.P., Van der Hoeven, R.A.M., Niessen, W.M.A., Tjaden, U.R. and Van der Greef, J.
New ionization strategies in particle-beam liquid chromatography-mass spectrometry based on the principle of surface ionization 647(1993)63
- Tinke, A.P., see Hugener, M. 647(1993)375
- Tinke, A.P., Van der Hoeven, R.A.M., Niessen, W.M.A., Van der Greef, J., Vincken, J.-P. and Schols, H.A.
Electrospray mass spectrometry of neutral and acidic oligosaccharides: methylated cyclodextrins and identification of unknowns derived from fruit material 647(1993)279
- Tjaden, U.R., see Hugener, M. 647(1993)375
- Tjaden, U.R., see Niessen, W.M.A. 647(1993)107
- Tjaden, U.R., see Tinke, A.P. 647(1993)63
- Tjaden, U.R., see Van Veelen, P.A. 647(1993)367
- Torri, G., see Da Col, R. 647(1993)289
- Tsoupras, G., see Careri, M. 647(1993)79
- Van den Eeckhout, E., see Lemière, F. 647(1993)211
- Van der Greef, J.
Foreword 647(1993)1
- Van der Greef, J., see Hugener, M. 647(1993)375
- Van der Greef, J., see Niessen, W.M.A. 647(1993)107
- Van der Greef, J., see Niessen, W.M.A. 647(1993)319
- Van der Greef, J., see Tinke, A.P. 647(1993)63
- Van der Greef, J., see Tinke, A.P. 647(1993)279
- Van der Greef, J., see Van Veelen, P.A. 647(1993)367
- Van der Hoeven, R.A.M., see Niessen, W.M.A. 647(1993)319
- Van der Hoeven, R.A.M., see Tinke, A.P. 647(1993)63
- Van der Hoeven, R.A.M., see Tinke, A.P. 647(1993)279

- Van Dongen, W.D., Versluis, C., Van Wassenaar, P.D., De Koster, C.G., Heerma, W. and Haverkamp, J.
Rapid analysis of enzymatic digests of a bacterial protease of the subtilisin type and a "bio-engineered" variant by high-performance liquid chromatography-frit fast atom bombardment mass spectrometry 647(1993)301
- Van Dongen, W., see Lemière, F. 647(1993)211
- Van Leuken, R.G.J., Kwakkenbos, G.T.C. and Duchateau, A.L.L.
Volatile ion-pairing agents for liquid chromatographic-thermospray mass spectrometric determination of amino acids and amino acid amides 647(1993)131
- Van Onckelen, H., see Lemière, F. 647(1993)211
- Van Veelen, P.A., Tjaden, U.R., Van der Greef, J., Ingendoh, A. and Hillenkamp, F.
Off-line coupling of capillary electrophoresis with matrix-assisted laser desorption mass spectrometry 647(1993)367
- Van Wassenaar, P.D., see Van Dongen, W.D. 647(1993)301
- Varfalvy, L., see Gagné, J.P. 647(1993)13
- Varfalvy, L., see Gagné, J.P. 647(1993)21
- Ventura, R., Nadal, T., Alcalde, P. and Segura, J.
Determination of mesocarb metabolites by high-performance liquid chromatography with UV detection and with mass spectrometry using a particle-beam interface 647(1993)203
- Versluis, C., see Van Dongen, W.D. 647(1993)301
- Viano, I., see Da Col, R. 647(1993)289
- Vincken, J.-P., see Tinke, A.P. 647(1993)279
- Virelizier, H., see Sadoun, F. 647(1993)351
- Volmer, D., Preiss, A., Levsen, K. and Wünsch, G.
Thermospray mass spectral studies of pesticides. Temperature and salt concentration effects on the ion abundances in thermospray mass spectra 647(1993)235
- Voragen, A.G.J., see Niessen, W.M.A. 647(1993)319
- Voyksner, R.D., see Straub, R.F. 647(1993)167
- Vreeken, R.J., see Barceló, D. 647(1993)271
- Wolfender, J.L. and Hostettmann, K.
Liquid chromatographic-UV detection and liquid chromatographic-thermospray mass spectrometric analysis of *Chironia* (Gentianaceae) species. A rapid method for the screening of polyphenols in crude plant extracts 647(1993)191
- Wolfender, J.L., Maillard, M. and Hostettmann, K.
Thermospray liquid chromatographic-mass spectrometric analysis of crude plant extracts containing phenolic and terpene glycosides 647(1993)183
- Wolfender, J.-L., see Maillard, M.P. 647(1993)147
- Wünsch, G., see Volmer, D. 647(1993)235

Having problems keeping up-to-date with the latest developments in analytical methods and instrumentation?

The obvious solution



TRAC

trends in analytical chemistry

CONSULTING EDITORS:

Y. Gohshi, Tokyo, Japan
J.F.K. Huber, Vienna, Austria
A. Townshend, Hull, UK

CONTRIBUTING EDITORS:

D. Barceló, Barcelona, Spain
U.A.Th. Brinkman, Amsterdam, The Netherlands
A.E. Bruno, Basel, Switzerland
A.L. Burlingame, San Francisco, CA, USA
P. Van Espen, Wilrijk, Belgium
P.K. Gallagher, Columbus, OH, USA
G. Gauglitz, Tübingen, Germany
G. Görög, Budapest, Hungary
M. Grasserbauer, Vienna, Austria
P.R. Haddad, Hobart, Australia
K. Jinno, Toyohashi, Japan
I.S. Krull, Boston, MA, USA
D.L. Massart, Brussels, Belgium
M. Munowitz, Naperville, IL, USA
R.W.A. Oliver, Salford, UK
Y. Umezawa, Tokyo, Japan
K.K. Unger, Mainz, Germany
M. Valcarcel, Cordoba, Spain
A.P. Wade, Vancouver, Canada
S.G. Weber, Pittsburgh, PA, USA
J.E. Wiktorowicz, Foster City, CA, USA
P.J. Worsfold, Plymouth, UK

The articles in TRAC are concise overviews of new developments in analytical chemistry, aimed at helping both analytical chemists and users of analytical techniques to explore and orient themselves in fields outside of their particular specialization(s). The reviews form an excellent introduction to topics of interest in numerous fields including biochemistry, biotechnology, clinical chemistry, environmental monitoring, instrumentation, forensic science, laboratory automation, materials science and pharmaceutical chemistry.

Issues contain:

- ❖ news
- ❖ meeting reports
- ❖ a computer corner presenting useful tips for getting the most out of a lab computer
- ❖ short, critical invited review articles aimed at an interdisciplinary readership
- ❖ book and software reviews
- ❖ meeting announcements.

SUBSCRIPTION INFORMATION

Personal Edition 1993: Volume 12 (in 10 issues)
Dfl. 199.00 / US \$ 110.50 (including postage)
ISSN 0165-9936
for individuals only, not available to libraries or documentation centers

Library Edition 1993: Volume 12
+ Hardcover reference book
Dfl. 915.00 / US \$ 508.25 (including postage)
ISSN 0167-2940



Elsevier Science Publishers
Attn. Brenda Campbell
P.O. Box 330, 1000 AH Amsterdam
The Netherlands
Fax: (+31-20) 5862 845
In the USA & Canada
Attn. Judy Weislogel
P.O. Box 945, Madison Square Station
New York, NY 10160-0757, USA
Fax: (212) 633 3880

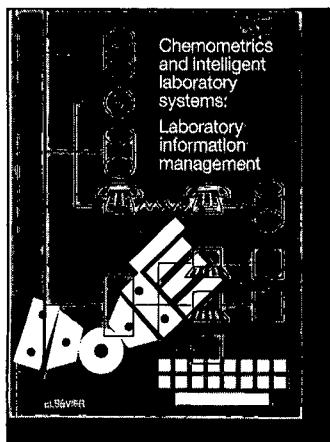
CHROM

- I would like a Free Sample Copy of TrAC
 Instructions to Authors.
 to enter a Library subscription for 1993.
Send me a Proforma Invoice.
 to enter a Personal subscription for 1993.

Name _____

Address _____

The Dutch Guilder price (Dfl.) is definitive. US\$ prices are for your convenience only and are subject to exchange rate fluctuations. Customers in the European Community should add the appropriate VAT rate applicable in their country to the price(s).



Audience

Chemists, pharmacists, computer scientists and managers working in academic, clinical, industrial and government laboratories.



Elsevier Science Publishers

Attn. Carla G.C. Stokman
P.O. Box 330, 1000 AH Amsterdam
The Netherlands

Fax: (+31-20) 5862 845

In the USA & Canada

Attn. Judy Weislogel
P.O. Box 945, Madison Square Station
New York, NY 10160-0757, USA
Fax: (212) 633 3880

LABORATORY INFORMATION MANAGEMENT

Section of CHEMOMETRICS AND INTELLIGENT LABORATORY SYSTEMS

Editor:

R.D. McDowall, *The Wellcome Research Laboratories, Beckenham, Kent, UK*

Coordinating Editor:

D.L. Massart, *University of Brussels, Brussels, Belgium*

Editor for North America:

R.R. Mahaffey, *Eastman Chemical Company, Kingsport, TN, USA*

Associate Editor:

R.E. Dessy, *Virginia Polytechnic Institute, Blacksburg, VA, USA*

AIMS AND SCOPE

The journal covers all aspects of information management in a laboratory environment, such as information technology, storage, processing and flow of data. The following topics are covered:

- ❖ **Laboratory Information Management Systems (LIMS):** Systems architecture, database design, novel aspects of interfacing, methods of data acquisition and integration with other computer applications and instruments.
- ❖ **Means of integrating and merging laboratory information:** Document preparation using chemical structures, spectra, results and text; corporate communication.
- ❖ **Networks:** Novel technology for the dissemination, storage and retrieval of information.
- ❖ **Regulatory Aspects:** Development and implementation of governmental guidelines and regulations and industry standards, and their effect on information management.
- ❖ **Electronic Laboratory Notebooks.**
- ❖ **Human aspects of laboratory automation:** The application of chemometrics and expert systems to handle laboratory information is within the scope of the journal. The application of robotics or dedicated automation systems is of interest where these systems form part of an integrated solution for information management. The journal aims to cover micro-, mini-, and mainframe applications and systems, both those designed in-house or available commercially.

The journal publishes five types of papers: **Original research papers, Tutorial articles, Case studies, State-of-the-art review articles, and Short communications.** A **Monitor Section** provides news on meetings, book and software reviews, a calendar of forthcoming events, etc.

ABSTRACTED/INDEXED IN: ASCA, Analytical Abstracts, BioSciences Information Service, Cambridge Scientific Abstracts, Chromatography Abstracts, Current Contents, Current Index to Statistics, Excerpta Medica, INSPEC, SCISEARCH.

1993: SUBSCRIPTION INFORMATION

Volume 21 In 3 Issues

Dfl. 448.00 / US \$ 256.00 (including postage) ISSN 0925-5281

CHROM

- I would like a free sample copy of Laboratory Information Management.
- Instructions to Authors.
- to enter a subscription for 1993.
Please send me a Proforma Invoice.

Name _____

Address _____

The Dutch Guilder price (Dfl.) is definitive. US\$ prices are for your convenience only and are subject to exchange fluctuations. Customers in the European Community should add the appropriate VAT rate applicable in their country to the price(s).

PUBLICATION SCHEDULE FOR THE 1993 SUBSCRIPTION

Journal of Chromatography and *Journal of Chromatography, Biomedical Applications*

MONTH	1992	J-A	M	J	J	A	S	O	N	D	1994
Journal of Chromatography	Vols. 623-627	Vols. 628-636	637/1 637/2 638/1 638/2	639/1 639/2 640/1 + 2	641/1 641/2 642/1 + 2 643/1 + 2 644/1	644/2 645/1 645/2 646/1	646/2 647/1 647/2	648/1 648/2			
Cumulative Indexes, Vols. 601-650											651/1 + 2
Bibliography Section		649/1		649/2			650/1			650/2	
Biomedical Applications		Vols. 612, 613 and 614/1	614/2 615/1	615/2 616/1	616/2 617/1	617/2 618/1 + 2	619/1 619/2	620/1 620/2	621/1 621/2	622/1 622/2	

INFORMATION FOR AUTHORS

(Detailed *Instructions to Authors* were published in Vol. 609, pp. 437-443. A free reprint can be obtained by application to the publisher, Elsevier Science Publishers B.V., P.O. Box 330, 1000 AH Amsterdam, Netherlands.)

Types of Contributions. The following types of papers are published in the *Journal of Chromatography* and the section on *Biomedical Applications*: Regular research papers (Full-length papers), Review articles, Short Communications and Discussions. Short Communications are usually descriptions of short investigations, or they can report minor technical improvements of previously published procedures; they reflect the same quality of research as Full-length papers, but should preferably not exceed five printed pages. Discussions (one or two pages) should explain, amplify, correct or otherwise comment substantively upon an article recently published in the journal. For Review articles, see inside front cover under Submission of Papers.

Submission. Every paper must be accompanied by a letter from the senior author, stating that he/she is submitting the paper for publication in the *Journal of Chromatography*.

Manuscripts. Manuscripts should be typed in **double spacing** on consecutively numbered pages of uniform size. The manuscript should be preceded by a sheet of manuscript paper carrying the title of the paper and the name and full postal address of the person to whom the proofs are to be sent. As a rule, papers should be divided into sections, headed by a caption (e.g., Abstract, Introduction, Experimental, Results, Discussion, etc.) All illustrations, photographs, tables, etc., should be on separate sheets.

Abstract. All articles should have an abstract of 50-100 words which clearly and briefly indicates what is new, different and significant. No references should be given.

Introduction. Every paper must have a concise introduction mentioning what has been done before on the topic described, and stating clearly what is new in the paper now submitted.

Illustrations. The figures should be submitted in a form suitable for reproduction, drawn in Indian ink on drawing or tracing paper. Each illustration should have a legend, all the legends being typed (with double spacing) together on a *separate sheet*. If structures are given in the text, the original drawings should be supplied. Coloured illustrations are reproduced at the author's expense, the cost being determined by the number of pages and by the number of colours needed. The written permission of the author and publisher must be obtained for the use of any figure already published. Its source must be indicated in the legend.

References. References should be numbered in the order in which they are cited in the text, and listed in numerical sequence on a separate sheet at the end of the article. Please check a recent issue for the layout of the reference list. Abbreviations for the titles of journals should follow the system used by *Chemical Abstracts*. Articles not yet published should be given as "in press" (journal should be specified), "submitted for publication" (journal should be specified), "in preparation" or "personal communication".

Dispatch. Before sending the manuscript to the Editor please check that the envelope contains four copies of the paper complete with references, legends and figures. One of the sets of figures must be the originals suitable for direct reproduction. Please also ensure that permission to publish has been obtained from your institute.

Proofs. One set of proofs will be sent to the author to be carefully checked for printer's errors. Corrections must be restricted to instances in which the proof is at variance with the manuscript. "Extra corrections" will be inserted at the author's expense.

Reprints. Fifty reprints will be supplied free of charge. Additional reprints can be ordered by the authors. An order form containing price quotations will be sent to the authors together with the proofs of their article.

Advertisements. The Editors of the journal accept no responsibility for the contents of the advertisements. Advertisement rates are available on request. Advertising orders and enquiries can be sent to the Advertising Manager, Elsevier Science Publishers B.V., Advertising Department, P.O. Box 211, 1000 AE Amsterdam, Netherlands; courier shipments to: Van de Sande Bakhuyzenstraat 4, 1061 AG Amsterdam, Netherlands; Tel. (+31-20) 515 3220/515 3222, Telefax (+31-20) 6833 041, Telex 16479 els vi nl. UK: T.G. Scott & Son Ltd., Tim Blake, Portland House, 21 Narborough Road, Cosby, Leics. LE9 5TA, UK; Tel. (+44-533) 753 333, Telefax (+44-533) 750 522. USA and Canada: Weston Media Associates, Daniel S. Lipner, P.O. Box 1110, Greens Farms, CT 06436-1110, USA; Tel. (+1-203) 261 2500, Telefax (+1-203) 261 0101.

BIOAFFINITY CHROMATOGRAPHY

By **J. Turková**, Czechoslovak Academy of Sciences, Institute of Organic Chemistry and Biochemistry, Prague, Czech Republic

Journal of Chromatography Library Volume 55

Bioaffinity chromatography is now the preferred choice for the purification, determination or removal of many biologically active substances. The book includes information on biologically active substances with their affinants, solid supports and methods of coupling, summarized in tables covering classical, high-performance liquid and large-scale bioaffinity chromatography.

Optimization of the preparation and the use of highly active and stable biospecific adsorbents is discussed in several chapters. Following a chapter dealing with the choice of affinity ligands, affinity-sorbent bonding is described in detail. Other chapters give information on solid supports, the most common coupling procedures and a general discussion of sorption and elution. Several applications of bioaffinity chromatography are described, e.g. quantitative evaluation of biospecific complexes and many applications in medicine and in the biotechnology industry.

Contents:

1. Introduction.
2. The principle, history and use of bioaffinity chromatography.
3. Choice of affinity ligands (affinants).
4. General considerations on affinant - sorbent bonding.
5. Solid matrix supports.
6. Survey of the most common coupling procedures.
7. Characterization of supports and immobilized affinity ligands.
8. General considerations on sorption, elution and non-specific binding.
9. Bioaffinity chromatography in the isolation, determination or removal of biologically active substances.
10. Immobilization of enzymes by biospecific adsorption to immobilized monoclonal or polyclonal antibodies.

11. Study of the modification, mechanism of action and structure of biologically active substances using bioaffinity chromatography.
 12. Solid-phase immunoassay and enzyme-linked lectin assay.
 13. Several examples of the application of biospecific adsorption in medicine.
 14. Application of bioaffinity chromatography to the quantitative evaluation of specific complexes.
 15. Theory of bioaffinity chromatography.
- Subject Index.

© 1993 819 pages Hardbound
Price: Dfl. 495.00 / US \$ 282.75
ISBN 0-444-89030-0

ORDER INFORMATION

For USA and Canada
ELSEVIER SCIENCE PUBLISHERS
Judy Weislogel, P.O. Box 945
Madison Square Station
New York, NY 10160-0757
Fax: (212) 633 3880

In all other countries
ELSEVIER SCIENCE PUBLISHERS
P.O. Box 330
1000 AH Amsterdam
The Netherlands
Fax: (+31-20) 5862 845

US\$ prices are valid only for the USA & Canada and are subject to exchange rate fluctuations; in all other countries the Dutch guilder price (Dfl.) is definitive. Customers in the European-Community should add the appropriate VAT rate applicable in their country to the price(s). Books are sent postfree if prepaid.



ELSEVIER
SCIENCE PUBLISHERS



0021-9673(19930924)647:2:1